

The background of the entire page is a stylized American flag, with the stars and stripes visible. The stars are white on a blue field, and the stripes are red and white.

SANDIA REPORT

SAND99-1976

Unlimited Release

Printed October 1999

SLIMHOLE HANDBOOK: Procedures and Recommendations for Slimhole Drilling and Testing in Geothermal Exploration

John Finger, Ron Jacobson, Charles Hickox, Jim Combs, Gene Polk and Colin Goranson

Prepared by

Sandia National Laboratories

Albuquerque, New Mexico 87185 and Livermore, California 94550

Sandia is a multiprogram laboratory operated by Sandia Corporation,
a Lockheed Martin Company, for the United States Department of
Energy under Contract DE-AC04-94AL85000.

Approved for public release; further dissemination unlimited.



Sandia National Laboratories

Issued by Sandia National Laboratories, operated for the United States Department of Energy by Sandia Corporation.

NOTICE: This report was prepared as an account of work sponsored by an agency of the United States Government. Neither the United States Government, nor any agency thereof, nor any of their employees, nor any of their contractors, subcontractors, or their employees, make any warranty, express or implied, or assume any legal liability or responsibility for the accuracy, completeness, or usefulness of any information, apparatus, product, or process disclosed, or represent that its use would not infringe privately owned rights. Reference herein to any specific commercial product, process, or service by trade name, trademark, manufacturer, or otherwise, does not necessarily constitute or imply its endorsement, recommendation, or favoring by the United States Government, any agency thereof, or any of their contractors or subcontractors. The views and opinions expressed herein do not necessarily state or reflect those of the United States Government, any agency thereof, or any of their contractors.

Printed in the United States of America. This report has been reproduced directly from the best available copy.

Available to DOE and DOE contractors from
Office of Scientific and Technical Information
P.O. Box 62
Oak Ridge, TN 37831

Prices available from (703) 605-6000
Web site: <http://www.ntis.gov/ordering.htm>

Available to the public from
National Technical Information Service
U.S. Department of Commerce
5285 Port Royal Rd
Springfield, VA 22161

NTIS price codes
Printed copy: A08
Microfiche copy: A01



SAND99-1976
Unlimited Release
Printed August 1999

SLIMHOLE HANDBOOK:
Procedures and Recommendations
for
Slimhole Drilling and Testing
in
Geothermal Exploration

John Finger
Ron Jacobson
Geothermal Research Department

Charles Hickox
Engineering Sciences Center

Sandia National Laboratories
PO Box 5800
Albuquerque, NM 87185-1033

Jim Combs
Geo Hills Associates
Reno, NV

Gene Polk
Baroid Drilling Fluids
Albuquerque, NM

Colin Goranson
Consultant
Richmond, CA

ABSTRACT

This Handbook documents R&D projects completed in-house and third-party R&D sponsored by Sandia National Laboratories in the Slimhole Drilling Program. It comprises: narrative accounts of field drilling projects, compilation of test data from Sandia projects and synopsis of data from Japanese boreholes, descriptions of in-house and other analyses of the data set, descriptions of drilling and logging equipment available for slimholes, and guidelines for drilling and testing geothermal slimholes.

CONTENTS

I. Overview

II. Equipment

- a. Comparison of rotary and core-drilling II-1
- b. Drill rigs II-3
- c. Downhole logging tools II-4
- d. Surface instrumentation and test equipment II-7

III. Case histories

- a. Steamboat Hills, Nevada III-1
- b. Vale, Oregon III-8
- c. Newberry Crater, Oregon III-17
- d. Fort Bliss, Texas III-27
- e. Other slimhole experience III-39
- f. Japanese experience III-42

IV. Analysis

- a. Transmissivity estimates by pressure-transient analysis IV-2
- b. Comparison of field data with wellbore simulators IV-8
- c. Description of various wellbore simulators IV-13
- d. Planning flow tests IV-14
- e. Summary of Japanese data; correlation of productivity/injectivity IV-16

V. Guidelines

- a. Typical slimhole problems V-1
- b. Recommendations on well design V-3
- c. Recommendations on drilling practice V-5
- d. Recommendations on drilling fluids V-9
- e. Recommendations on lost circulation V-21
- f. Recommendations on flow testing procedures and equipment V-23
- g. Recommendations on data analysis V-30

VI. Glossary

I. OVERVIEW

There are two major reasons for pursuing the concept of slimholes for geothermal projects: exploration and small power plants. The following is an overview of each.

Geothermal Exploration: Drilling costs associated with exploration and reservoir assessment are a major barrier limiting expansion of proven geothermal reserves. The geothermal industry (utilities and geothermal operators) needs to reduce exploration and reservoir assessment costs to be competitive in meeting the growing Western requirements for environmentally benign, alternative energy sources. Typical geothermal exploration comprises drilling a large-diameter, production-size well and, if it shows the presence of fluid and high temperature, producing steam or brine from it while measuring the fluid temperature and, ideally, downhole pressure. These flow tests, which usually last for days to weeks, directly evaluate the energy or enthalpy output of the well and indicate whether the reservoir is drawn down significantly over the course of the test. From this, potential power-plant output and reservoir life can be estimated.

This method has major disadvantages: it is very expensive (\$1-3M per well); there is significant environmental impact from the roads, large drill sites, and fluid-handling requirements; and if the operator hopes to turn an exploration well into a production well, it may be located at the fringe of the resource, where it is not convenient for eventual construction of a power plant.

Drilling production-size holes for geothermal exploration also puts a large expense at the beginning of the project, and thus requires a long period of debt service before those costs can be recaptured from power sales. If a reservoir is defined and proved with slimholes, production well drilling can be delayed until the power plant is under construction, saving years of interest payments. High exploration costs also limit the number of potential new resource areas which can be evaluated, preventing significant expansion in the nation's proven geothermal reserves.

Traditionally, diamond-cored "slimholes" (usually 3" to 4" in diameter) have been used to measure temperature gradients while selecting sites for production-size exploratory geothermal wells. If it can be shown, however, that improved testing in slimholes reliably predicts productivity and identifies a useful geothermal resource, this could eliminate or greatly reduce the need for large-diameter exploration wells. The cost savings and reduced environmental impact of this approach, compared to drilling production-size holes, are compelling incentives to use slimhole technology.

Drilling is cheaper for slimholes than for production wells because the rigs, casing and cementing, crews, locations, and drilling fluid requirements are all smaller; because site preparation and road construction in remote areas is significantly reduced, up to and including the use of helicopter-portable rigs; and because it isn't necessary to repair lost-circulation zones before drilling ahead. For comparison, a 3.9" slimhole drilled in 1993 (see Section III-a), including all testing and overhead, cost approximately \$150/foot while a neighboring production well (12-1/4" production diameter) cost \$377/foot to its total depth of 740 feet. Although the slimhole's greater total depth reduced its overall cost per foot, the intermediate cost of drilling the slimhole to the same depth as the large well was less than 60% of the large well's total cost. Similarly, another slimhole drilled to the same depth as, and within two miles of, a rotary-drilled exploration hole showed that the rotary hole cost approximately 40% more (see Section III-b.)

Sandia began an investigation to establish the basic feasibility of slimhole exploration with in-house analysis and, later, field experiments on existing geothermal coreholes. At the same time, there was an extensive survey of the geothermal industry to define its needs and priorities. Drilling costs associated with exploration and reservoir assessment are a major factor affecting future geothermal development. Industry contacts specified lower-cost exploration as a high priority, and were generally enthusiastic over the slimhole idea. For this to be a valid exploration method, however, it is necessary to demonstrate that slimholes produce data that provide a prediction of reservoir productivity equivalent to results from full-size wells. Because of the different flow characteristics in slimholes, there was some doubt among industry representatives about the validity of slimhole testing, or even that slimholes could be made to discharge. Experience in the U. S. and Japan shows conclusively that slimhole flow tests are practical, but early in the program their predictive value was less clear.

In considering the flow of fluid through the formation and into the wellbore, there is friction loss both in the formation and in the wellbore. In a low-permeability reservoir, the mass-flow rate is limited by the friction loss in the formation, so wellbore size has little effect on the total flow. In high-permeability reservoirs, which are of most interest, the restriction of the wellbore may be the factor that limits flow from the well. Slimholes have a higher (circumference)/(area) ratio than larger wells, so friction losses are more significant in slimholes. Demonstrating, through analysis, modeling, and field data, that flow in a slimhole can be accurately extrapolated to predict production in a large well has been one of the principal thrusts of Sandia's slimhole research and development.

Although the vast majority of drilling technology used in the geothermal industry is derived from the oil and gas industry, geothermal requirements are qualitatively different. There are hard, abrasive, and fractured rocks; high temperatures; and underpressured formations, frequently containing corrosive fluids. All these factors create a harsher environment than normally found in oil and gas drilling. The service and drilling tool industries have little incentive to address these problems, since the number of geothermal wells drilled in a year is about 0.1% of the corresponding number for oil and gas. This lack of commercial R&D is the primary rationale for DOE's support of geothermal technology development. Once demonstrated, slimhole drilling technology will have application to geothermal exploration and reservoir assessment in both the U. S. and international markets.

Small Power Plants: A huge shift in world energy demand is under way. According to at least one scenario¹, the *growth* in energy consumption in developing countries between 2000 and 2010 will be greater than today's consumption in Western Europe, and more electrical generating capacity will be built in the next 25 years than was built in the previous century. Worldwide, the market for new power generation facilities over the next 10 to 12 years has been estimated^{2,3} at 900,000 MW. Geothermal resources, indigenous and environmentally benign, now meet a part of this growing demand but it is primarily through large power plants which do not serve the market niche considered here.

The conventional notion of geothermally-produced electricity involves large, multi-megawatt (MW) power plants. The World Bank⁴ currently considers 5MW plants as "mini-geothermal," but there is a significant market niche for much smaller units - down to the 100-1000kW range. Pritchett's analyses^{5,6} indicate that holes as small as 3" diameter can drive a 100kW generator,

and somewhat larger holes (but still "slimholes" because they are not greater than our arbitrary limit of 6" diameter) can produce well over 1000kW. In remote areas, far from the utility grid, third-world villages and facilities such as hospitals, pumps for potable water, and long-term mining operations can replace their diesel generators with small-scale geothermal power plants (SGPP) drawing hot fluids from slimhole wells. The cost of getting fuel to remote diesel generators drives those electricity prices above 50¢/kWh, but Entingh *et al.*⁷ have estimated that an SGPP – for example, a 300-kW unit using 120°C brine – can produce electricity for about 11¢/kWh, even without the cost savings from slimhole drilling. In addition to the advantage of price, SGPP are far more environmentally benign than fossil-burning plants, which is crucial in view of current climate-change concerns and burgeoning electricity demand in the less-developed countries. It thus appears that a significant market opportunity exists for slimhole drilling in support of small geothermal power plants.

Handbook Outline: This Handbook documents work done and sponsored by Sandia National Laboratories in the Slimhole Drilling Program. It comprises: narrative accounts of field drilling projects, compilation of test data from Sandia projects and synopsis of data from Japanese wells, descriptions of in-house and other analyses of the data set, descriptions of drilling and logging equipment available for slimholes, and guidelines for drilling and testing geothermal slimholes. These topics are organized in sections as shown below, with appropriate references cited in each section collected at the end of that section.

<u>Section</u>	<u>Contents</u>
II.	Equipment -- Description of drill rigs, including minerals-type core rigs, small rotary rigs, and hybrids; description of slimhole logging tools available from industry and under development at Sandia; description of surface instrumentation for drilling/testing and other hardware for flow testing; comparison of core-drilling and rotary technology.
III.	Case histories -- Narratives of Sandia-sponsored drilling projects; brief descriptions of other slimhole drilling by industry; extensive description of Japanese borehole data.
IV.	Analysis -- Sample data from Sandia-sponsored slimholes and comparison with wellbore models; summary of Japanese slimhole and production-well data, with conclusions relevant to productivity/injectivity correlations; description of wellbore simulators.
V.	Guidelines -- Recommendations for drilling practice, well design, surface instrumentation, drilling fluids, logging, testing, and data collection.

Acknowledgments: The authors appreciate the review and valuable input of Larry Pisto (Tonto Drilling), Ken Williams (Boart Longyear), Dave Glowka (former Manager, Geothermal Research Department, Sandia National Laboratories), Sabodh Garg and John Pritchett (Maxwell Technologies) and others who have generously contributed their time and knowledge.

-
1. Carr, E., "Energy: The new prize"; *The Economist*, June 18, 1994
 2. U. S. Department of Energy; "Geothermal Fact Sheet"; April, 1994
 3. National Geothermal Association, Brochure entitled "*Geothermal Energy in Developing Countries*", February, 1993
 4. Oak Ridge National Laboratory, "Environmental Screening for the Renewable Energy Component of the Indonesian Second Rural Electrification Project"; *Geothermal Resources Council Bulletin.*, May, 1994
 5. Pritchett, J. W., "Preliminary Estimates of Electrical Generating Capacity of Slim Holes - A Theoretical Approach"; *Proc. Twentieth Workshop on Geothermal Reservoir Engineering*, Stanford, California, January, 1995
 6. Pritchett, J. W., "A Study of Electrical Generating Capacity of Self-discharging Slim Holes"; *Proc. Twenty-First Workshop on Geothermal Reservoir Engineering*, Stanford, California, January, 1996
 7. Entingh, D. J.; Easwaran, E.; McLarty, L., "Small Geothermal Electric Systems for Remote Powering"; *Proceedings of DOE Geothermal Review XII*, San Francisco, CA, April, 1994.

II. EQUIPMENT

a. Comparison of Rotary and Core Drilling

This preliminary description explains some of the differences between conventional rotary drilling and minerals-type core drilling, and especially points out how those differences affect operations for holes where one rig does both types of drilling.

Typical large rotary drill rigs, mostly used for exploration and production of fossil-fuels and for geothermal production, use full diameter bits to drill holes between 6 to 26 inches in diameter to depths sometimes more than 20,000 feet. The drill string comprises the bit, the drill pipe, and an often complex bottom-hole assembly (BHA) made up of drill collars, stabilizers, reamers, crossovers, and other special tools. The string is turned by a top drive or a rotary table which applies torque to the string while allowing it to travel downward under its own weight. Weight on bit is controlled by holding back a portion of the drill string weight. Coring can be done with this kind of rig, using diamond or roller-cone bits, but the complete drill string must be tripped to retrieve the core sample. Bits for this type of coring cut a much wider kerf than those in minerals rigs, so drilling fluid returns must be maintained to remove cuttings from the hole.

Core rigs, most often used by the minerals industry to explore for ore bodies, use diamond bits which cut a thin cylindrical kerf in the rock, leaving a core sample protruding up the center of the drill string inside a separate tube usually called the inner barrel. Hole diameters are from 2 to 6 inches with corresponding core diameters of 1 to 4 inches. After drilling through an interval the length of the inner barrel (usually 5 to 20 feet), rotation is stopped and the drill string is raised, breaking off the core just behind the bit. A wireline is then run down inside the drill string to retrieve the core in its inner barrel, thus avoiding the necessity for tripping the drill string to get the core sample. The drill string is turned either by a top drive, which uses a hydraulic motor to rotate the entire drilling assembly from its topmost connection, or by a chuck, which grips the outside diameter of the drill rod and rotates it. Weight on bit or rate of penetration is precisely controlled by a hydraulic feed cylinder. Because the cuttings produced by the diamond bits are very fine and make up a smaller fraction of the hole volume than in rotary-rig coring, minerals-type core drilling can continue without drilling fluid returns.

This ability to drill “blind” makes the core drill popular for temperature-gradient geothermal exploration holes. If the temperatures and rock properties look encouraging, an exploratory production well is drilled with a large rotary rig and is then flow tested to evaluate the potential reservoir. With improved flow testing and well construction, however, the gradient hole can also be used to evaluate the permeability and productivity of a potential reservoir.

There are tradeoffs between the two kinds of drilling but, in Sandia's geothermal slimhole program, the small hole sizes have favored the use of core rigs. These rigs may not be cost-effective in oil and gas exploration because in many sedimentary formations rotary drilling has much faster penetration and can therefore drill those intervals more cheaply, but the advantage of being able to drill through lost circulation zones in geothermal formations can offset slower penetration. In either kind of drilling, there will be substantial savings in a smaller hole because

of reduced requirements for casing and cementing. Configurations and relative sizes of the two kinds of rigs are shown in Figure II-1 below. The core rig is a Boart-Longyear HD600 and the rotary rig is a conventional production-well rig drilling in The Geysers.

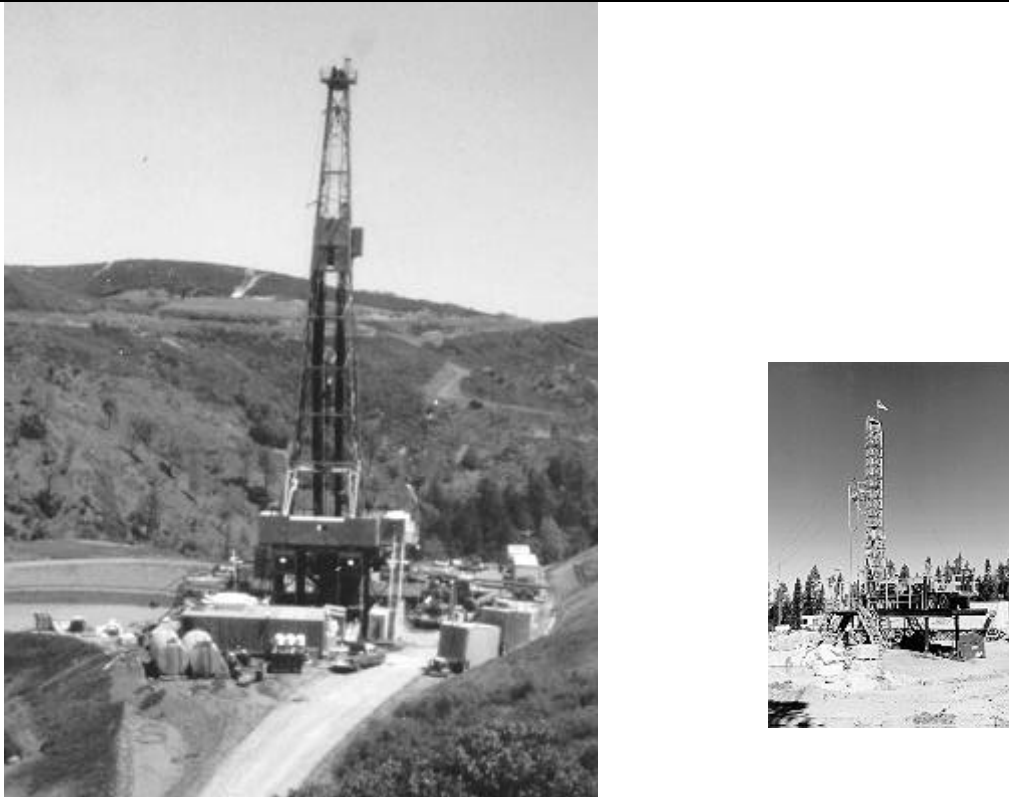


Figure II-1 Conventional rotary rig (left) at The Geysers and core rig (right) at Newberry Crater. Photos are scaled to show relative sizes of rigs. Note also the amount of auxiliary equipment and size of the drilling sump for the rotary rig, compared to the core rig, which has a very small sump (foreground) and is essentially self-contained.

There are considerable advantages in the ability to do both rotary and core drilling with the same rig: This is highly attractive for the applications common to slimhole geothermal exploration, where there may be relatively soft, easily drilled overburden above the hard, fractured geothermal source rocks. Some drill rigs, such as the UDR5000 (see Section II-b) and its smaller version the UDR1500, are designed to be used for both types of drilling - UDR is an acronym for "Universal Drill Rig" - and almost all core rigs have at least a limited rotary-drilling capability. Although these rigs can do both kinds of drilling, they are far more often used to drill and retrieve core, and that predominant use is reflected in the tools and procedures normally used in operating these drills. The effect of this on hybrid drilling is described in more detail in Section V-b, "Recommendations on drilling practice".

Another option becoming more common is an accessory top-drive which can be attached to a conventional drill rig. Oil-field top-drives usually can't rotate fast enough for diamond core drilling, but commercial top-drives for coring (e.g., Tonto Drilling) are available and a coring

package designed for scientific drilling is described below. A comparison of some typical rotary and core rig properties is given below.

	Rotary drill	Core drill
Crew:	5 plus toolpusher	2 or 3 with or w/o pusher
Mud logger:	yes	no
Mud engineer:	yes	sometimes
Consultant/ company man:	yes	sometimes
Drill site:	400' by 250' large pits (1200 bbl) and sumps	200' by 150' or smaller small pits (25 bbl) and sumps
Rig:	150' high 40 truck-loads 30' high base (large BOPE, flowlines) big mud pumps (600 gpm/3000 psi)	60' high 2 to 5 loads 11' high base (smaller stacks) small pumps (45 gpm/1100 psi)

b. Drill Rigs

Drill rigs used in cost-shared Sandia/industry drilling projects have been supplied by Tonto Drilling Services and Boart-Longyear companies, two of the principal contractors in the domestic core-drilling industry. Detailed information on these drills can be obtained from the companies^{1,2}. Other suppliers of core drills are available, and some "compact" rotary rigs, as described by Hutter³, may also be suitable of slimhole exploratory drilling. Several of these compact rigs exist only as designs, and others are just entering field service, so it is premature to evaluate their performance now. Summary details of the core rigs used on Sandia projects are given below.

Tonto UDR5000: The drill rig used for Vale Exploratory hole (see Section III-b) was a Tonto Drilling UDR5000 top-drive coring rig. This is a trailer-mounted derrick which can pull 40' stands of pipe and has a depth rating of 9700' with CHD101 coring tools.

During the rotary drilling part of the operation, the drillstring comprised CHD134 core rods (5" OD) connected with a cross-over sub to a conventional bottom-hole assembly (BHA) with stabilizers, drill collars, and roller-cone bits. During the rotary drilling in this hole, a rental mud system with a large triplex pump was used, since the drill rig's pumps normally used for coring are rated at 40 gpm/1000 psi, which is not sufficient volume delivery for the designed rotary bit hydraulics. After 4-1/2" casing was set to 3111', rig pumps were used and the hole was core-drilled to 5825' with HQ (hole diameter 3.85", core diameter 2.5", rod diameter 3.5") drill rods and diamond-impregnated bits.

Longyear HD 602: The drill rig used for the Steamboat Hills, Fort Bliss, and Newberry Exploratory holes (see Sections III-a, III-c, and III-d) was a Longyear truck-mounted Model HD602, with a 60' mast, capable of pulling 40' stands of pipe, and a hoist rated at 60,000 pounds. The drill string is rotated by a chuck which grips the outside of the drill rods; rotary drilling was done with CHD101 drill rods connected by a crossover sub to a conventional

BHA. The rig was supported on a hydraulic jack-up substructure which provided approximately 8' clearance between the bottom of the substructure and ground level. Two mud pumps were available; a Gardner-Denver duplex (150 gpm @ 260 psi) for rotary drilling and reaming, and an FMC Model M12 triplex (100 gpm @ 1000 psi) for coring. A 40' parts trailer contained tools, bits, spare parts, and a welder.

This particular rig has a depth capability of approximately 8200' with HCQ rods, and approximately 5340' with CHD101 drill rods (approximately 4" diameter); it can reach below 8400' with CHD76 rods (approximately 3" diameter), enabling slimhole exploration in most known geothermal areas.

DHCS: An auxiliary coring package built for scientific drilling was used for Phase III drilling at the Long Valley Exploratory Well. This hydraulically-powered unit, which includes a hydraulic power package, top-drive, 23-foot-stroke feed cylinder, mud pumps, power tongs, wireline winch, parts and shop van, and control console, was attached to the very large (177' to crown) Nabors drill rig which has stood at this location since 1989. (See Figure II-2)

The DHCS (DOSECC Hybrid Coring System) provided the power to rotate the drill string and to control the feed rate and weight on bit, while the big rig drawworks were used to trip pipe in 90' stands. It used a composite drill string with 4" Hydril tubing in the upper part and CHD101/HMQ coring tools below, which gave a depth capability approaching 14,000 feet. Although this particular package was built for DOSECC (Drilling, Observation and Sampling of the Earth's Continental Crust) to drill a scientific hole in Hawaii, a very similar unit was extensively used by Tonto Drilling for geothermal exploration in Indonesia.



Figure II-2 – DHCS mounted in Nabors Rig

c. Downhole Logging Tools

The most fundamental properties in geothermal exploration are the temperature and the permeability of the reservoir rocks. Evaluation of these properties is usually carried out through measurement of temperature in the wellbore and by analysis of transient downhole pressures after flow into and/or from the zone of potential production. Although space limitations require

the descriptions to be brief, the principal types of tools for making these measurements are discussed below.

Surface read-out pressure/temperature tools: These tools collect data in the wellbore and transmit it electrically up a wireline, which is a steel cable containing one or more electrical conductors. If the wireline has multiple conductors (usually 4 or 7) then the signals can be processed and transmitted uphole without having heat-sensitive electronics in the downhole package. During the Sandia-sponsored drilling projects described in Section III, many temperature logs were taken with Sandia's platinum-resistance-thermometer (PRT) tool and a Sandia logging truck. This instrument uses a simple resistance bridge, with changes in resistance (caused by changes in temperature) measured from the surface through a four-conductor cable. Since there are no downhole electronics, temperature drift with time is negligible and PRT temperature measurements were considered the reference standard for these projects. The tradeoffs for multi-conductor cable are that it is more expensive, is more difficult to re-head, and is often the limiting factor when very hot ($>300^{\circ}\text{C}$) holes are to be logged.

Single-conductor wireline is most often used by the logging service companies, but this requires electronic multiplexing to get several channels of data up the wireline. The downhole electronic components are not only heat-sensitive in terms of sheer survival, but their readings can drift as their temperature increases. For these reasons, they are usually protected by an insulating shield, or "Dewar", which keeps the interior of the tool relatively cool for a period of several hours, the time depending on the downhole temperature.

For both surface-readout and memory tools, temperature and pressure transducers are usually combined into one tool, and spinner (which indicates the velocity of fluid flowing past the tool) is often added to surface-readout tools. Even though a Dewar increases the size of some tools, most of the PTS (pressure-temperature-spinner) tools available from service companies are less than 2" in diameter, thus fitting easily into a slimhole.

Electronic memory tools: As the name implies, these tools record data (generally pressure

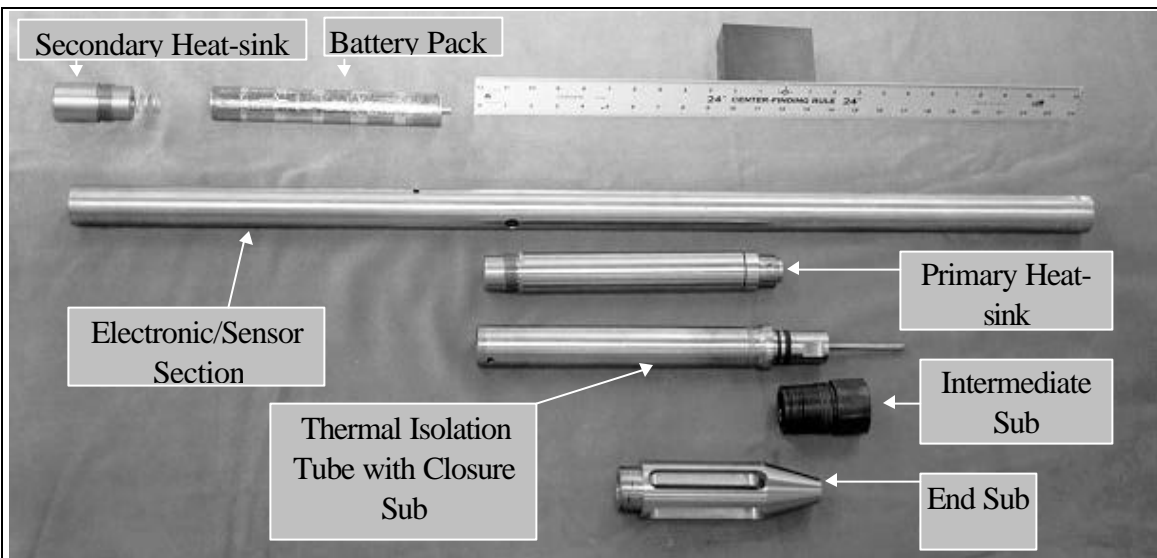


Figure II-3 Components of a typical pressure/temperature memory tool; complete tool is approximately 6' long by 2" diameter.

and temperature, sometimes gamma radiation) downhole and store it in an on-board electronic memory, which can be downloaded into a computer when the tool is retrieved to the surface. Components of a Deward, pressure/temperature logging tool⁴ are shown in Figure II-3. Memory tools have several advantages: 1) Because there is no conductor-carrying wireline, that is no longer a limitation on high-temperature logging; 2) A specialized logging truck is not needed, because the memory tool can be run into and out of the hole on the rig's sand line or with a simple "slickline" winch; 3) Assuming a relatively low first cost, an operator can own one of these tools and acquire temperature/pressure logs whenever it is desirable, without incurring expensive service-company logging operations. There are corresponding disadvantages associated with the delay in getting data and with the lack of any surface indication if the tool fails during a test, but this is a promising technology which deserves further development.

Mechanical tools: One of the earliest methods of acquiring downhole data, still frequently used, is with a "mechanical memory", generically called a Kuster tool. These contain a clockwork mechanism which rotates a cylinder inside the tool, with a scribe tracing a temperature or pressure line on it. Because the line traced on the cylinder relates a measured property to time, it is necessary to know the depth at given times, so that these can be combined to give a log of temperature or pressure versus depth.

Approximate downhole temperatures are often acquired with maximum-reading-thermometers (MRTs) attached to the core-retrieval wireline in core drilling or to the inclination-survey wireline in rotary drilling. These thermometers retain the maximum reading they have experienced downhole, but they require some residence time to have reasonable accuracy and there is no assurance that the maximum temperature is at the bottom of the hole.

Downhole pressures can be measured with capillary tubing. In this technique, a metal tube with small inside-diameter is inserted into the borehole and liquid is purged from the tubing, usually with high-pressure nitrogen, leaving it filled with gas. Once the purging gas is shut off, liquid will then rise inside the tubing until its pressure is balanced by the compressed gas, and that pressure can be read at the surface with an ordinary pressure gauge. This method is cheap and simple, particularly for long-term monitoring, but it is difficult to traverse the borehole for a pressure profile, and other logging cannot be done while the capillary tubing is in place.

Fiber-optic tools: A recently developed technology for acquiring downhole temperatures is the use of fiber optic strands suspended in the wellbore⁵. By directing a laser pulse down the fiber and measuring specific components of the back-scattered light, a continuous distribution of temperature with depth can be read. Although the surface equipment is expensive, the fiber itself is relatively cheap and the same surface unit can be used to read fibers in many different boreholes.

There is current development on an optical grating which can be applied to the fiber for measurement of pressure, thus giving this technology an equivalent to more conventional pressure-temperature tools. Although long-term fiber operation at high temperature has not been fully demonstrated, the ability to acquire a near-instantaneous log of the complete wellbore, and to do it as often as necessary, makes this concept extremely attractive for geothermal exploration.

Other downhole tools: Two other downhole measurements sometimes made in geothermal exploration are seismics and wellbore imaging. Downhole seismic receivers are often below the

near-surface rubble which causes acoustic mis-matches and signal degradation. These receivers can detect ground motion either from natural seismic events or from surface excitation by vibrator trucks, in either case giving better definition of the reservoir's large-scale structure.

Images of the wellbore wall can be developed either electrically (formation micro-scanner) or acoustically (borehole televiewer.) The micro-scanner has a series of conductive pads which contact the borehole wall and use changes in resistivity to identify fractures and formation changes. The televiewer has a rotating crystal which sweeps a continuous string of acoustic pulses around the wellbore wall and measures the intensity and time-of-flight of their return, thus measuring wellbore radius very accurately and identifying areas of low reflectivity (such as corrosion in casing, formation fractures, etc.) in the wellbore. Knowledge of the fractures' dip, frequency, and orientation is very valuable in evaluating the geometry and potential productivity of a geothermal reservoir.

d. Surface Instrumentation and Test Equipment

A great variety of surface instrumentation can be connected around the drill rig, depending on what data is considered necessary. As part of Sandia's ongoing Lost Circulation program, an extensive flow-measuring system was used on all the cost-shared drilling projects described in Section III. The rigs were instrumented with flow transducers to measure and record drilling fluid inflow rate and temperature, outflow rate and temperature, pump strokes and pressure, drillstring rotary speed, and depth. All these values were displayed on video monitors at the driller's station and in the Sandia mobile office. In addition to their designed function of detecting lost circulation and calibrating various flow measuring devices, these instruments were used to collect flow rate and surface pressure data during injection tests and also proved to be valuable for understanding drilling performance and the nature of the interval being drilled.

Some of the phenomena which can be identified with this instrumentation are the following:

- Lost (or gained) circulation: This was the original purpose of the measurement system. When non-transient outflow rate falls below inflow, then drilling fluid is being lost to the formation. Conversely, when outflow rate is higher, the formation is producing fluid into the wellbore.
- Drill-string washouts: Sudden drop in pump pressure at a constant flow rate frequently indicates a washout in the drillstring.
- Pump efficiency: If flow rate measured by non-intrusive flow sensors decreases relative to the calculated flow rate based on pump strokes, this indicates that pump efficiency is declining.
- Temperature difference between inflow and outflow: Bottomhole temperature cannot be inferred directly from an increase in flow line (outflow) temperature, because there are many different temperature gradients in the formation that will produce the same outflow temperature or ΔT between inflow and outflow, but rapid variations are a signal that something has changed downhole. For example, in a known lost circulation zone, where outflow is a variable fraction of inflow, a change in outflow temperature while the inflow temperature remains constant can mean that the wellbore has penetrated a producing formation with water hotter or colder than the drilling fluid.

- Drilling optimization: Having all readings available on one monitor makes it easier for the driller to optimize the combination of drilling parameters such as rotary speed and circulation rate.

In general, drilling contractors do not provide this much instrumentation with their rigs, but it is useful to discuss this before a job, so that both parties clearly understand what data will be available.

When the borehole reaches a zone with promising temperatures, it is also necessary to know the zone's permeability for an estimate of potential productivity. If the slimhole has a depth/temperature/permeability combination which allows it to produce fluid, this is by far the best way to predict large-diameter well productivity. If this is not possible, permeability-thickness product, denoted in most equations by kh , is usually evaluated by analyzing transient downhole pressures during and after an injection test. These subjects are treated in more detail in Section IV.

For a production flow test in any size borehole, flow rate and downhole enthalpy - principal measures of productivity - can be obtained with relatively simple, non-electronic equipment. The well is discharged through a James tube into a flash tank to separate the vapor from the liquid component of the flow, and the liquid flows into a weir box., which uses the height of the flowing liquid in a V-notch to measure the liquid flow rate. The James tube is a straight run of pipe from the wellhead to the flash tank, with a pressure gauge at the lip of the downstream end, where the tube discharges into the flash tank. Sizes of these items will vary with the expected borehole conditions, but at Steamboat Hills where the total flow rate was approximately 120 gallons/minute, the flash tank was 6' diameter by 7' high, the weir box was 3' by 3' by 5', and the James tube was 3" pipe by 4' long.

Flow rate and energy content (enthalpy) are calculated using two equations⁶ which relate the James tube lip pressure to the mass flow rate and the enthalpy,

$$(1) \quad \frac{\dot{m}h^{1.102}}{Ap_l^{0.96}} = 1680, \quad \text{and}$$

$$(2) \quad \dot{m} = \dot{m}_w \left[\frac{h'_{fg}}{h'_g - h} \right]$$

where \dot{m} = total mass flow rate and \dot{m}_w = water flow rate, kg/sec; h = enthalpy of flowing fluid, kJ/kg; A = flow area of James tube, cm²; p_l = lip pressure, Pa (absolute); h'_{fg} and h'_g are the enthalpies, kJ/kg, of vaporization and saturated vapor, respectively, evaluated at local atmospheric conditions; and the constant is not dimensionless. If the enthalpy is known (from a temperature log, for example) then (1) can be used directly to solve for flow rate, given lip pressure, or (2) can be used with the water flow rate from the weir box and with known values of enthalpy to get the flash correction factor, or the total mass flow rate. If the only data available is lip pressure and water flow rate, then (1) and (2) can be combined to give (3), which has a trial-and-error solution for enthalpy, after which that value can be used as before.

$$(3) \quad \frac{1680 p_l^{0.96} A}{h^{1.102}} = \dot{m}_w \left[\frac{h'_{fg}}{h'_g - h} \right]$$

These topics are covered in much more detail in Reference 6.

-
1. Tonto Drilling Services, 2200 South 4000 West, Salt Lake City, UT 84120
 2. Boart-Longyear Company, 32 Stokes Drive, Dayton, NV 89403
 3. G. W. Hutterer, "Technical and Economic Evaluation of Selected Compact Drill Rigs for Drilling 10,000 Foot Geothermal Production Wells"; Sandia Contractor Report SAND97-2872, Sandia National Laboratories, November 1997
 4. J. A. Henfling and R. A. Normann, "Precision Pressure/Temperature Logging Tool", Sandia Report SAND98-0165, January 1998
 5. S. Großwig, E. Hurtig, K. Kühn; "Fibre optic temperature sensing: A new tool for temperature measurements in boreholes"; *Geophysics*, Vol. 61, No. 4 (July-August 1996), p. 1065-1067
 6. M. A. Grant, I. G. Donaldson, P. F. Bixley; "Geothermal Reservoir Engineering"; Academic Press, New York, 1982

III. CASE HISTORIES

The following case histories are for slimholes that have either been reported in the literature or have been cost-shared between Sandia and an industrial partner.

III-a. Steamboat Hills, Nevada¹

a.1 Introduction and Background

Following an extensive survey of the geothermal industry, which specified lower-cost exploration as a high priority and was generally enthusiastic over the slimhole idea, Sandia carried out negotiations with Far West Capital, which operates the Steamboat Hills geothermal field. The result was an agreement to drill and test an exploratory slimhole on their lease. This exploratory hole (number SNLG 87-29), which was drilled during July-September 1993, was specifically designed for extensive production and injection tests so that those results could be compared with production and injection data from existing large-diameter wells in this developed field. The exploratory well is drilled approximately 30 feet from an existing, but unused, production well.

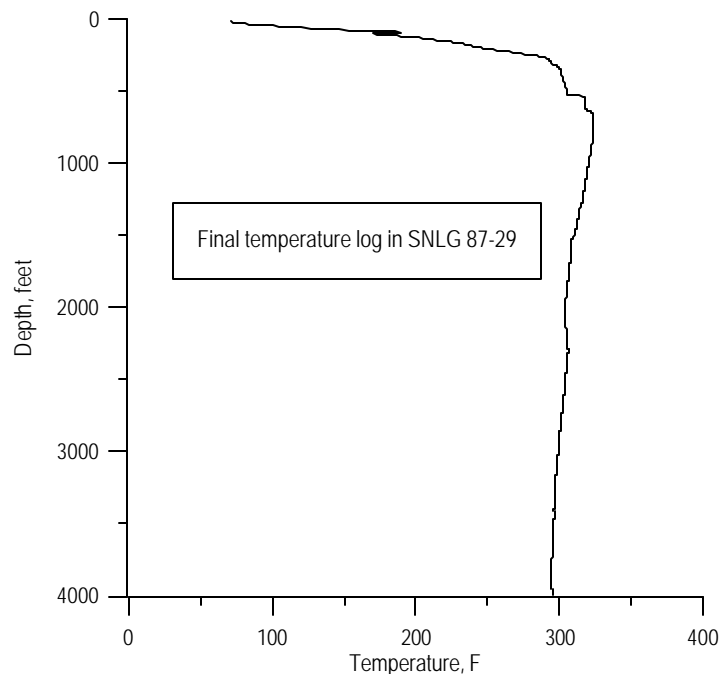


Figure III-1 - Temperature log from slimhole SNLG 87-29

Steamboat Hills geothermal area is located about eight miles south of Reno, Nevada, and currently supports two power plants with a rated total output of approximately 36 MWe. Production zones for the power-plant wells are typically shallow (less than 1000'), of moderate temperature (~325°F), characterized by large, well-connected fractures in granodiorite, and extremely permeable; test data indicate values of transmissivity exceeding 1,000 Da-ft. Boreholes previously drilled here showed temperature reversals, with the maximum temperature above 1000' (see Figure III-1), however, a nearby power plant on another operator's lease draws from a reservoir at approximately 420°F, indicating that a hotter resource might lie beneath the one currently produced for the Far West power plants. Extensive previous development in this field meant that drilling conditions were reasonably well-known, but because most of the existing wells are shallow, there was still an opportunity for slimhole exploration in search of a deeper, hotter reservoir.

The principal objectives for this exploratory slimhole were the following: development of slimhole testing methods, comparison of slimhole data with that from adjacent production-size wells, and definition of formation-temperature profiles below the existing wells. Although not all of these objectives were completely met, the exploratory well (which ended at a total depth of 4001') was generally successful in gathering a large amount of data useful to the slimhole development program and to the operator.

a.2 Summary of Operations

To meet our testing and data collection goals, this slimhole was designed to meet the following criteria:

- Recover continuous core from surface to TD.
- Obtain a competent cement job on all casing, to allow extended production testing.
- Maintain HQ hole diameter (3.89") as deep as possible, to allow setting packers for isolation of possible production/injection zones.

The borehole design (Figure III-2) has 7" casing to nominal 150' and 4-1/2" casing to nominal 500 feet. Since regulatory agencies require at least 10% of the total depth to be cased, this casing program allows a maximum well depth of 5000', even though the drilling permit was for 4000 feet. To minimize the amount of reaming necessary, while still collecting continuous core, the drilling program was to (1) core the first 150' with HQ, (2) ream to 8-1/2" with roller bit, (3) set 7" casing, (4) drill out of 7" casing with BSF™ core bit (6-1/4" hole by 4" core) to 500', (5) set 4-1/2" flush joint casing, and (6) drill to TD with HQ core tools. This plan was followed to a final depth of 4001 feet. Total project time, from spud through completion of testing, was 58 days.

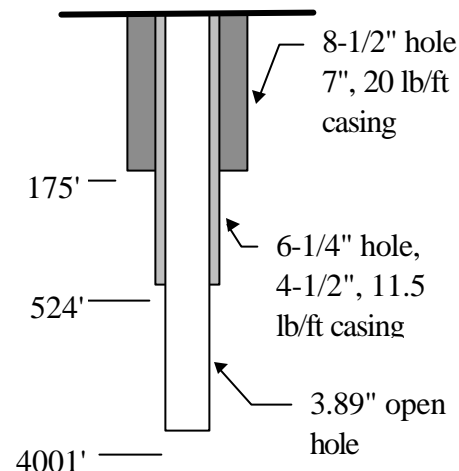


Figure III-2 - Borehole design for slimhole SNLG 87-29

During the project, drilling was suspended four times for a series of production and injection tests, each time taking downhole (pressure, temperature, spinner) and surface (wellhead pressure and temperature, James tube lip pressure, flow rate) data. These test series were done at well depths of 968, 1510, 2930, and 4000 feet. All discharge tests were initiated by air-lifting the fluid from a depth of approximately 250', at an air flow rate of approximately 150 scfm. In general, the surface data, including a comparison of different flow rate measurement techniques, were consistent and repeatable. Downhole data were more difficult to compare because of some malfunctions in the logging tools and because the two service companies which

took measurements used different tools and different calibrations. By comparing the downhole readings with the corresponding surface data, however, and by comparing the service companies' tools with Sandia temperature logs, most of the ambiguities in the downhole data were resolved.

a.3 Description of Test Equipment and Methods

The following descriptions cover the major pieces of equipment used during the project and, where applicable, explanations of their use.

Drill rig: The drill rig used for this slimhole was a Longyear truck-mounted Model HD602, which is described in detail in Section II-b.

Although the granodiorite which comprised more than 3500' of the drilled interval is hard (most of it about 6 on the Mohs hardness scale), bit life averaged over 200' after settling on a Series 7, impregnated diamond bit specifically designed for this formation. Core recovery was very good, more than 99% for the entire well. Because there were no returns after drilling through a major void at 815', the upper part of the drillstring ran dry afterward, causing intermittent drillstring vibrations. This problem was mitigated by liberal applications of powdered Teflon and bio-degradable rod grease to the core rods as they were tripped into the hole.

Wellhead: The wellhead was designed to not only provide conventional pressure control while drilling, but to allow discharge testing from the well with minimum changes. The wellhead assembly comprised, from the bottom up, a double-gate BOP, a flow tee, a 4" gate valve, and an annular BOP. The inside diameter of the flow tee was large enough to pass all the HQ tools, allowing the tee to remain in place during normal drilling so that there was no need to re-configure the wellhead for testing. The side leg of the flow tee fed, through another 4" valve, into a run of 4" pipe with a James tube (see Figure III-3

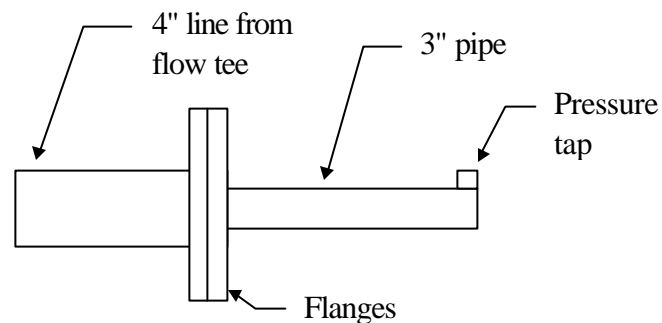


Figure III-3 - James tube design

for diagram of James tube) mounted at the end, and this exhausted into a flash tank. Use of the James tube is described in Section II-d.

Flash tank/weir box: The flash tank was an open-topped 6' diameter by 7' high steel tank, equipped with internal baffles, which received the flow from the well through a tangentially-directed opening in its side. The liquid portion of the flow then passed from the flash tank into a 3" line, through a magnetic flow meter, and into a 5' x 3' x 3' weir box. The weir box has a V-shaped notch in an internal partition, and the height of water flowing through this notch is a measure of the liquid flow rate. The liquid flow rate measured in the weir box was consistent with that indicated by the magnetic flow meter.

Surface instrumentation: Instrumentation at and near the wellhead comprised the following:

- Electronic pressure transducer (0-20 psi) for James tube lip pressure

- Pressure gauge (various) for James tube lip pressure (note: both James tube pressure measurements included approximately 1.2 psi from a water column above the transducer tee -- this water column prevented sub-atmospheric pressures at the transducers and damped pressure fluctuations.)
- Electronic pressure transducer (first 0-200, later 0-60 psi) in the wellhead flow tee
- Pressure gauge (0-100 psi) in the wellhead flow tee
- Electronic pressure transducer (0-200 psi) at the pump/drill rod connection (injection tests)
- Thermal well with thermocouple just downstream of the flow tee 4" valve
- Thermal wells with thermocouples in 3" line between flash tank and weir box and in injection line
- Magnetic flow meter in the 3" line between the flash tank and weir box
- Vortex flow meter in the water line from power plant (measure flow rates for injection)

All electrical transducers were connected to a signal-processing station at the drill rig and then, via a simple twisted-pair wire to the data-logging computer in the Sandia trailer. After each test was complete, data from the computer was down-loaded onto diskettes and distributed to other researchers.

Downhole instrumentation: Downhole data during production and injection tests were acquired using pressure/temperature/spinner (PTS) tools from two different service companies. Although details differed, all the commercial downhole instruments were designed to take data and to transmit that data uphole in real time, using a single-conductor wireline. All the instruments (each company used more than one) employed a dewar, or thermal flask, to protect the downhole electronics, but in spite of that, the internal tool temperature would rise significantly during the course of a normal test. If this effect is not compensated, heating the electronics will cause the signal output to drift, giving unreliable data. A properly calibrated tool accounts for the heating and provides accurately compensated data, but we were not always confident that this was the case with the instrumentation used in this project. This experience indicates that there is significant room for improvement in slimhole, high-temperature logging tools.

Numerous temperature logs were taken with Sandia's platinum-resistance-thermometer (PRT) tool which, along with a Sandia logging truck, remained on-site for the entire project. Static temperature logs (no flow in hole) were done with this tool before each series of production/injection tests.

Two other Sandia instruments were used briefly: the acoustic borehole televiewer (BHTV) yielded wellbore images down to 520'; and a Sandia memory tool gave pressure-temperature data for a shut-in test at the end of the project. Because no oriented core has been collected in this field, the televiewer images giving fracture direction were extremely informative, but the BHTV could not be used at greater depths because of its temperature limitations (~250°F). The memory tool, which does not use an electric wireline but stores data downhole in an on-board computer, has been used extensively on later projects but was still in development during this drilling and was only run at the end of the project.

Packers: Part of the injection testing used downhole packers for isolating various zones and evaluating their permeability. By running the packers into the hole on N-rod (2.75" OD), the

annulus was roughly the same cross-sectional area as the inside of the pipe. It was then possible to inject into either the zone above the packer or the one below, and compare the injectivity of those intervals.

The packers were manufactured by TAM International and were inflated by pumping into the drill pipe with a wire-line-retrievable standing valve seated in the packer. Once proper inflation pressure was reached, the pump pressure was bled (a check valve holding pressure in the packer) and the standing valve retrieved with the drill rig's wireline. This standing valve arrangement left a large enough ID in the packer for the PTS logging tools to pass through, so measurements were obtained below the packers while injecting.

a.4 Discussion, Conclusions, and Recommendations

Drilling is cheaper for slimholes than for production wells because the rigs, crews, locations, and drilling fluid requirements are all smaller; because site preparation and road construction in remote areas is significantly reduced, up to and including the use of helicopter-portable rigs; and because it isn't necessary to repair lost-circulation zones before drilling ahead. As a comparison, the Steamboat Hills slimhole, including all testing and overhead, cost approximately \$150/foot while the neighboring production well (Hot Air #4; 12-1/4" production diameter) cost \$377/foot. Although the slimhole's greater total depth reduced its overall cost per foot, the intermediate cost of drilling the slimhole to the same depth as the large well was less than 60% of the large well's total cost.

The field results appear to validate this testing strategy for this slimhole. Because drilling and testing conditions are so site-specific, the procedures used at Steamboat may not be a universal recipe, but this is a generally useful method for slimhole exploration. In particular, test measurements have been compared with wellbore models (see Section IV-b), and have made a convincing case for the ability to predict flow in this type of reservoir.

There are several conclusions from this project concerning slimhole testing; the last two are specific to the Steamboat Hills geothermal field and the others are more generic.

1. Slimholes can be flow-tested, with successful surface and downhole measurements. Relatively cheap and simple surface measurements (James tube and weir box) can give flow rate and enthalpy.
2. The internal flow in the wellbore greatly complicates the analysis of attempted pressure transient (build-up or fall-off) tests. This emphasizes the need for better definition of intra-wellbore flow.
3. The strategy used for these tests appears to have produced the necessary test data, taken with appropriate accuracy, to evaluate the commercial potential of a larger well at this location.
4. Numerical simulation of flow in the wellbore can yield a predictive curve of flow rate versus wellhead pressure, as shown in the slimhole data. Applied to a larger diameter well, this same simulation will give the same kind of production curve, giving a measure of the reservoir's commercial potential. Extrapolation from the slimhole data to the wellbore diameter of a near-by production well gave a reasonable estimate of the larger well's actual flow rate for a given wellhead pressure.

5. It is desirable to develop a coupled wellbore-reservoir simulator, and to extend this exploration strategy into other reservoir types, to validate the predictive capability of that model.
6. The deeper, hotter reservoir postulated in this location was not encountered down to 4000'. There is, however, significant permeability below the 815' production zone, implying that water hotter than 300°F can be pumped from deeper zones, or water from a power plant could be injected into these zones.
7. The existing reservoir is extremely permeable; calculations of transmissivity are probably lower bounds.

Although the test results here are encouraging, the highly fractured, highly permeable, reservoir may not be generally representative of other geothermal resources. It is important to do exploratory slimhole drilling and testing in reservoirs with different flow characteristics and to compare those results with production wells in those reservoirs.

A consequence of moving to other types of reservoirs will be the increasing need for better modeling capability, especially in terms of coupling a reservoir simulator to a wellbore simulator. As described in Section IV-c, the assortment of wellbore models used to date give reasonable predictions of flow behavior, but the codes' performance is enhanced, or perhaps even made possible, by the extreme transmissivity of this specific reservoir, which allows the assumption of a fixed pressure at the feedzone to be realistic. In other reservoirs, this may not be the case. A coupled reservoir-wellbore model would be a great aid to further analysis.

There are also areas in which the instrumentation and data-collection strategy used in these tests could be improved. An enhanced instrumentation development could be a collaborative effort between Sandia and industry, or could be stimulated in industry alone by increased commercial slimhole exploration. Specifically, the following concerns should be addressed:

- Spinner measurements should be made with a tool which can distinguish flow direction (up or down); this feature is presently available in some commercial logging services, but is not always used. Data from most spinner tools is probably only good when the tool is moving bow-on into the flow (logging down), so data acquired logging up (flow stern-on) should be disregarded. Logging at a slower line speed will increase the probability that flow is bow-on to the tool, but the lower relative velocity makes the spinner more likely to stick. Careful analysis of the internal flow seems to be more important for slimhole exploration than in conventional production-size well testing because of the increased emphasis on down-hole instrumentation in the slimhole testing.
- As an aid to interpretation of the internal flow, accurate static pressure-temperature logs should be run at regular intervals, particularly when drilling data or core indicate that new high-permeability zones have been penetrated. Examination of the points on these logs where deviation of the pressure gradient coincides with changes in the temperature gradient should reveal sources and sinks of intra-wellbore flow.
- Optimum logging speed should be established; most of the service companies run their tools at 50 to 100 feet/min, which may be too fast for the pressure and temperature resolution needed in comparison of modeling and field data.

- Data drift caused by internal heating of the downhole electronics became significant because of the distortion of the data and because of the limitation this placed on the time available to do certain tests, particularly pressure transients. If these tests are thought to be valuable, a different testing technique, perhaps capillary tubing from the surface, or the use of tools with longer high-temperature residence times may be necessary.
- During development of slimhole testing methodology, commercial PTS logging tools should do static temperature logs at the beginning and end of each test series. These temperature logs could then be compared with some reference standard, such as the Sandia temperature tool, to evaluate the drift in the tool during the tests.
- Static water level in the well should be measured at regular intervals, probably daily, to keep track of the formation pressure in the permeable intervals penetrated to date.

Finally, the experience during the Steamboat Hills project showed the value of real-time, on-site data analysis. Software which could have compared downhole data with a wellbore simulator during the test sequence would have indicated malfunctioning instrumentation, or reservoir anomalies, quickly enough to have either taken remedial action or have changed the testing methodology appropriately.

a.5 Brief Geologic Description (after reference 2)

The Steamboat Hills geothermal area, which covers approximately four square miles and includes active hot springs and fumaroles, has been studied for several decades. The oldest known rocks in this area are metamorphosed sedimentary and volcanic rocks, known collectively as the Peavine sequence. These rocks outcrop south and west of the drill site, and are believed to be of Triassic-Jurassic age.

The Peavine sequence is extensively intruded by Cretaceous-age plutonic rocks, of which granodiorite is the most abundant. There are also numerous outcrops of the granodiorite around the drill site. Next oldest are the Tertiary Alta and Kate Peak Formations. These formations primarily comprise volcanic flows, mud flow breccias, and sedimentary deposits. The Alta Formation is approximately 22 million years old (myo) and the Kate Peak is about 13 myo.

Youngest rocks are the Quaternary flows, domes, and sedimentary deposits, including the Steamboat Hills Rhyolite, believed to be associated with four small domes on a line that runs southwest to northeast of the drill site. A so-far-undetected shallow rhyolite intrusion is believed by some to be the heat source for the Steamboat Hills hydrothermal system.

All the different rocks in the Steamboat Hills geothermal area have been hydrothermally altered to a greater or lesser extent. Hydrogen sulfide rises, oxidizes to sulfuric acid and chemically attacks silicate minerals, replacing them with opal and cristobalite. Below the water table, silicate minerals are generally replaced by alunite and kaolinite.

Three principal lithologies were penetrated during drilling: Quaternary hot spring siliceous sinter deposits with intercalated alluvium; a series of Tertiary volcanic breccias and lahars; and an extensive Cretaceous-age granodioritic plutonic complex. Minor lithologic features include at least two andesite dikes, a probable ash fall or siltstone, pervasive calcite-chlorite veining, druzy quartz veins, stibnite, pyrite, and other sulfide mineral deposits, xenoliths, and possible plant fossils within the siliceous sinter.

Structurally, the pre-Cenozoic metamorphic rocks are intensely folded and faulted. Dips range from 45 to 90 degrees, while bedding strikes range from northeast to northwest. At least three systems of normal faults have been recognized in the Steamboat Hills. One set, which is still active, strikes northeast, parallel to the axis of the Hills. Another set strikes northwest, almost perpendicular to the first set. The third set of faults strikes nearly north and is prominent on the main terrace of hot springs. The Steamboat Hills hydrothermal system has been active, possibly intermittently, for approximately the last 2.5 million years, and faulting appears to be the principal structural control for fluid flow.

III-b. Vale, Oregon³

b.1 Introduction and Background

In April-May 1995, Sandia drilled a cost-shared exploratory slimhole with Trans-Pacific Geothermal Corporation (TGC), which owns leases in the Vale KGRA. In addition to possible discovery of a new geothermal resource, this situation offered an opportunity for direct cost comparison between an exploration slimhole drilled with "hybrid" techniques on a diamond-coring rig and a previous exploration well, which was conventionally drilled but would be considered a slimhole in that technology. TGC drilled this previous well, approximately two miles away, in early 1994, and completed it to roughly the same depth as that planned for this project.

The exploratory slimhole (number TGC 61-10) was specifically designed to evaluate the geothermal potential at this location, and to provide additional data on drilling practices, costs, and testing in slimholes. This report describes the drilling and testing operations, gives a preliminary summary and interpretation of the data, and makes a few recommendations for future projects.

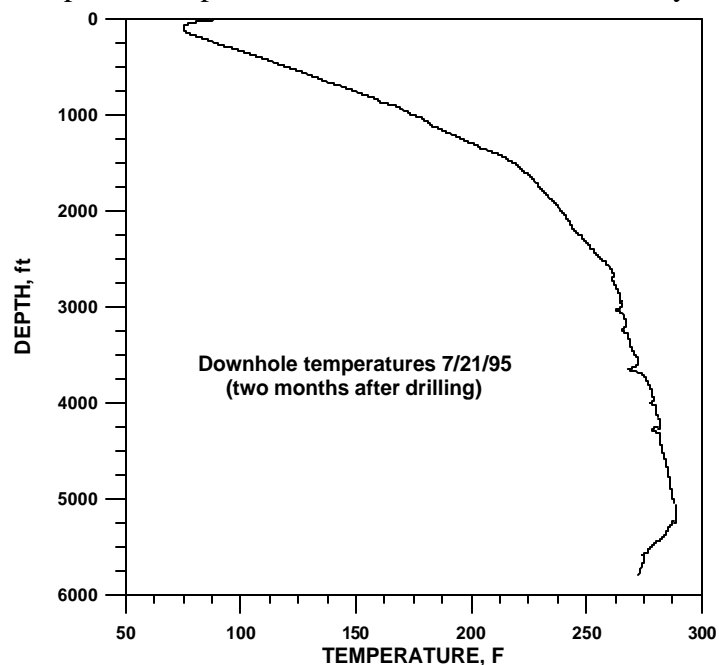


Figure III-4 - Temperature log in slimhole TGC 61-10

The principal objectives for this project were the following: development of slimhole drilling and testing methods, cost comparison with a recent, near-by, conventionally-drilled exploratory well, comparison of reservoir and performance data from this well with that from subsequent production-size wells, and evaluation of commercial geothermal potential at this location. Although formation temperatures were lower than expected (see Figure III-4), and it is unlikely that commercial development will take place in this location, the drilling and testing here successfully demonstrated slimhole technology and the principal objectives have been met.

b.2 Summary of Operations

To meet our testing and data collection goals for this slimhole, it was designed to satisfy the following criteria:

- Drill to TD at minimum cost consistent with necessary testing.
- Obtain a competent cement job on all casing, to allow extended production testing.
- Maintain HQ hole diameter (3.85") as deep as possible, to allow setting packers for isolation of possible production/injection zones.

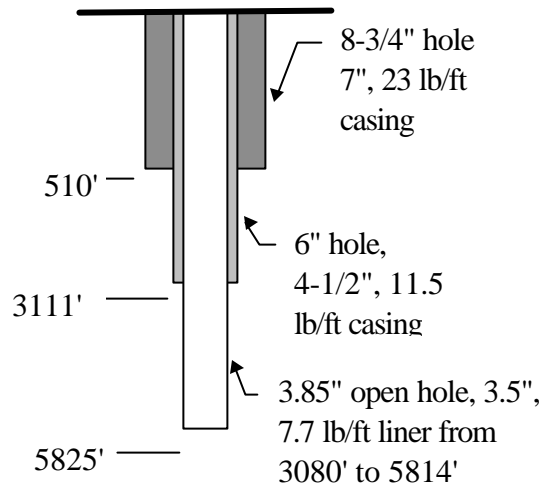


Figure III-5 - Design for slimhole TGC 61-10

The well design (Figure III-5) has 7" casing to 510' and 4-1/2" casing to 3111 feet. The drilling program used a core rig with conventional rotary tools to drill the top 3112 feet of hole and to then core the interval of interest from casing shoe to TD. This approach combined the cost savings of a slimhole drill rig, doing fast rotary drilling in the upper part of the hole, with the scientific and reservoir data obtained from core in the potential production zone.

Drilling was relatively continuous, with all testing (other than temperature logs) reserved until hole TD at 5825 feet. The following tests were then performed: wireline logs before casing; post-casing injection tests into the complete open hole section, with pressure shut-in data; bailing from the bottom 500' of the hole, which was isolated with an inflatable packer, and then measuring temperature change in that section; repeated temperature logs in the hole, following well completion with a 3-1/2" liner from 3080' to 5814'.

Since neither the tests performed just after drilling nor repeated temperature logs over the following four months indicated that this hole was in a promising geothermal resource, the hole was plugged and abandoned during September, 1995. The HQ liner was cut 100' below the casing shoe, the cut liner was pulled from the hole, a bridge plug was pushed down to the top of the remaining liner, and a cement plug was pumped from that point back up into the casing. The P&A configuration for the slimhole is shown in Figure III-6.

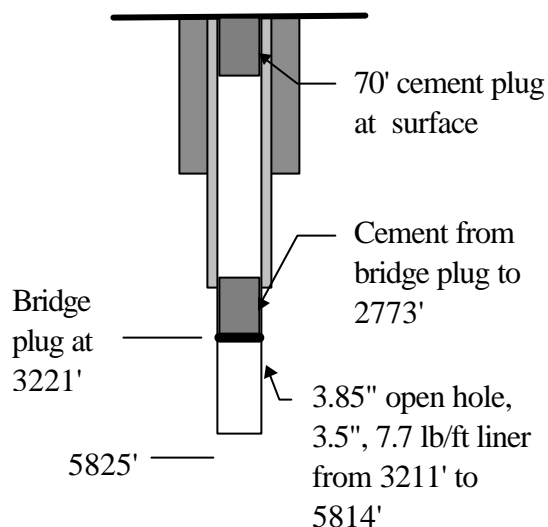


Figure III-6 - Abandonment design

b.3 Description of Test Equipment and Methods

This section covers the major items of equipment used in the drilling and testing, and, where appropriate, describes their operation.

Drill rig: The drill rig used for this hole was a Tonto Drilling UDR5000 top-drive coring rig, described in detail in Section II-b.

During the rotary drilling part of the operation, the drillstring comprised CHD134 core rods (5" OD) turning a conventional bottom-hole assembly (BHA) with stabilizers, drill collars, and roller-cone bits. During the rotary drilling, a rental mud system was also used, since the drill rig's pumps normally used for coring did not have sufficient volume delivery for the designed bit hydraulics.

After the 4-1/2" casing was set to 3111', the remainder of the hole was drilled with HQ (hole diameter 3.85", core diameter 2.5", rod diameter 3.5") drill rods and diamond-impregnated bits.

Surface flow instrumentation: As part of Sandia's ongoing Lost Circulation Program, the drill rig was instrumented with flow transducers which were used to measure and record drilling fluid inflow rate and temperature, outflow rate and temperature, pump strokes and pressure, drillstring rotary speed, and depth. All these values were displayed on video monitors at the driller's station and in the Sandia mobile office. Use of this surface instrumentation is described in more detail in Section II-d.

Downhole instrumentation: Numerous temperature logs were taken with Sandia's platinum-resistance-thermometer (PRT) tool which, along with a Sandia logging truck, remained on-site for the entire project. Static temperature logs (no flow in hole) were done with this tool when coring operations were suspended for bit trips, rig maintenance, or other time intervals that would permit the hole to warm up near its static temperature gradient.

After the hole reached TD, a pressure-temperature storage ("memory") tool was also used to compare temperature data with that previously taken by the PRT tool and to collect downhole pressure data during the injection and shut-in tests. This tool, part of Sandia's ongoing program in Instrumentation Development, has a Dewar flask around an electronic memory which stores data (approximately 10,000 data points total capacity) that can later be downloaded into a laptop computer. This tool's primary advantage is its ease of operation, since it can be run into the hole on the rig's wireline and specialized logging trucks are not required. As an experiment, the tool was also run into the hole inside a core-barrel "cage" while tripping the drillstring and gave good results.

A prototype temperature/spinner tool was also run during injection tests. The tool appeared to be collecting good data in the upper part of the hole, but as it entered the lower section, where the wellbore wall was heavily coated with rod grease, the impeller became clogged with grease and would not turn. The problem was probably not unique to this tool, since commercial spinner tools would likely have plugged in the same way. Grease plugging would have been eliminated or greatly reduced if we had first been able to do a production flow test, which would have cleaned the wellbore.

b.4 Discussion, Conclusions, and Recommendations

Test results: Analysis of the two injection tests performed at the exploratory slimhole site during May, 1995 yielded estimates for the permeability-thickness product (transmissivity) kh of 0.25 and 0.23 Da-ft, based on pressure fall off after injection (see Section IV-a). Using the pressure buildup for the second test, a transmissivity of 0.610 Da-ft was estimated. These estimates are approximately an order of magnitude smaller than the kh values estimated for the nearby A-Alt well which was tested in 1994. The model used to estimate kh is based on the Theis solution which assumes an infinite reservoir of constant thickness and permeability and a line source injection well. The reservoir tested is fractured and of finite extent, so the model used does not convey explicit information on the geothermal reservoir geometry or the distribution of fractures and feed zones. The estimated value for kh is, however, useful for comparing reservoirs and for identifying potentially productive reservoirs. It is generally assumed that the kh value must be at least 10 Da-ft for a potentially productive reservoir, so the low kh values measured for this well are indicative of a very tight reservoir which is unlikely to be an economically viable geothermal resource.

Drilling technology: Although the UDR5000 drill used for this hole is considered a "hybrid" rig, capable of either conventional rotary drilling or minerals-type core drilling, it is used far more often for coring, and there are significant differences in the two kinds of drilling. These differences affect the equipment required for the job, the logistics of handling the equipment around the rig, and the training that the drill crews should have to successfully do both kinds of drilling. See Section V-b for more discussion of this topic.

Cost comparison: A major objective of the slimhole program is to demonstrate not only that the smaller wells give sufficient data to evaluate a reservoir, but that they do it more cheaply than conventionally-drilled large holes. The Vale slimhole presented an ideal situation for cost comparison because a rotary-drilled exploration hole had been completed less than two miles away, to approximately the same depth, in February 1994. The table below gives a breakdown of costs for both wells, and helps to define where major cost differences occur.

Well Name:	A-Alt	TGC 61-10
Depth	5757'	5825'
Completion	14" line pipe to 62' 9-5/8" casing to 506' 7" casing to 3010' 5" slotted liner, 2902'-5723'	10" line pipe to 29' 7" casing to 510' 4-1/2" casing to 3111' 3-1/2" H-rod, 3080'-5814'
Rig days	31 + 5 standby	40

WELL	A-Alt	TGC 61-10
Rig Charges (day rate, footage, crew per-diem)	184,955	254,837
Rig mobilization and de-mob	87,860	43,560
Site construction and maintenance	57,700	29,998
Mud logging	26,040	13,490
Bits and downhole tools	67,279	27,978
Directional	37,374	0
Fishing	3,200	1,695
Rentals	28,090	20,182
Fuel and water	10,350	5,570
Drilling fluids	48,421	48,468
Casing, casing crews, and cement	172,817	107,076
Logging	58,376	14,929
Trucking and additional labor	36,723	12,895
Equipment maintenance	11,530	1,260
Drilling engineering	56,940	13,790
Wellhead and miscellaneous	32,670	42,555
TOTAL	920,325	638,334
Cost per foot (<i>excluding</i> directional costs)	\$153	\$110

There are several points to note in this comparison:

- Even though charges by the drilling contractor were considerably greater for the slimhole than for A-Alt, lower ancillary costs for the slimhole made the total project much cheaper. Part of the greater rig cost was caused by the longer time required for the slimhole, and the remainder is due to the rig day-rates. It is not obvious that the core rig for the slimhole (\$4990/day plus \$5-\$9/foot) should be more expensive than the rotary rig for A-Alt (\$5640/day), but day-rates for drill rigs obey the same principles of supply and demand as other commodities. At the time A-Alt was drilled, rotary rigs were available in abundance and consequently were bid at relatively low prices, while core rigs, mostly employed by the minerals industry, were in short supply when bids for TGC 61-10 were solicited.
- The only aspect of the earlier well which made it inherently more expensive was the directionally drilled interval. Beside the explicit costs of directional tools and services, there may have been additional rig days and bit costs, but even after deducting these items, there are clear savings for the smaller hole.
- The drilling-fluids expense for the slimhole was slightly greater than for A-Alt, but it was inflated by the complete loss of circulation in the lower part of the hole. This meant that we were continually pumping 10 to 15 gpm of mud down the hole for the last 20 days

of drilling. A slimhole which did not lose total returns would have a much smaller mud cost.

- Even though more than half the total footage was rotary-drilled, the smaller bits used in the rotary section and the less expensive core bits in the cored section greatly reduced the cost of bits and tools. In the cored section, the simplified BHA also eliminated the cost of stabilizers and drill collars.
- Smaller sizes of the rig, pad, and sump reduced rig mobilization and site construction costs.
- A mud logging service company was only used for the rotary section of the hole, although we did continue to rent their H₂S monitors for the duration of the project. Once core was being retrieved, cuttings analysis was no longer required. Similarly, contract drilling supervision was only used during rotary drilling. While outside consultation was useful for design of bit hydraulics and BHA programs, these activities are considerably simplified in core drilling and the drillers are accustomed to making these choices independently.
- Smaller casing sizes, with correspondingly smaller cement volumes, were less expensive for the slimhole. Normally, there would be even more of a cost advantage to the smaller hole, but the 6" hole was washed-out over several intervals, requiring more cement for the 4-1/2" casing than originally estimated. Washed-out intervals may have been caused by excessive bit hydraulics, designed in an effort to increase drilling performance. If this was the case, then the trade-off with a \$66,000 cement job was not cost-effective.

Although this hole was geologically informative and the drilling went well, it was, unfortunately, drilled in a location which holds little promise for commercial geothermal development. Still, several useful conclusions can be drawn from this project.

- Drilling this hole to the same depth as a nearby rotary hole provided information of the same quality at substantially lower cost.
 - With some refinement of techniques (hydraulics, etc.) used in the rotary part of the hole, cost savings could have been even greater.
 - Total well cost is sensitive to the ratio of rotary-drilled interval to core-drilled interval. For example, see the table below. If rotary drilling had only gone to 2000', then the extra 1100' feet of coring would have increased the total cost by approximately \$32/foot for that interval. (These costs-per-foot are much lower than shown above because they only count cost during drilling, i.e. no casing, cement, site preparation or other non-
- | Type of drilling | Avg hole advance/day, feet | Avg daily cost, dollars | Avg cost per foot |
|------------------|----------------------------|-------------------------|-------------------|
| Rotary | 289 | 14,408 | \$50 |
| Coring | 129 | 10,573 | \$82 |

drilling costs.) Given the availability of a storage-type logging tool, the method of taking a temperature log with the tool in a core

barrel while tripping pipe has several advantages. It takes almost no extra rig time, it happens when the hole has not seen circulation for a period of several hours, and it is extremely safe (for the logging tool) compared to running the tool in an open hole, which might be fractured, caving, or sloughing.

- If a hole has several intervals which appear (from core examination) to have high permeability, then an inflatable packer is useful in evaluating these intervals individually. If significant lost circulation has been treated by pumping LCM, which may have plugged some of the fractures, then swabbing the hole can relieve this situation and give a better indication of that interval's true permeability. To do this, a specifically designed swabbing tool would have been more effective than the make-shift one used on this hole.

Since this operation supported the validity of slimhole drilling as a lower-cost exploration technique, we should seek other opportunities for cost-shared projects in geothermal reservoirs where subsequent production wells will give comparisons between slimhole tests and production data. This would be part of a general effort to do exploratory drilling and testing in reservoirs with different flow characteristics, and to compare those results with production wells in the new reservoirs.

The pressure-temperature log taken while tripping drill pipe with the memory tool in a core barrel was successful, having as a principal defect the necessity for hand entry of drill pipe length during the trip. A simple drill-pipe-length encoder should be developed to expand the opportunities for this type of logging on core rigs. An encoder would produce time-depth data which could be merged with the logging tool's time-pressure/temperature data to generate a curve of depth versus pressure and temperature.

b.5 Brief Geologic Description

Geologic: The Vale geothermal system is at the west edge of the Western Snake River sedimentary basin, within the western third of the Yellowstone hot spot track. In this area, the volcanic and structural parts of the hot spot track are separated, with the silicic volcanics to the south and west of the area (the Owyhee Lake volcanic center, the Owyhee Plateau volcanics in southwest Idaho, and the McDermott caldera volcanics in northern Nevada) and basalts and sediments to the north. An extensive volcanic episode occurred in this region about 15 million years ago (Ma). Four major calderas formed within 50 miles, roughly in the quadrant from west to south, centered at the town of Vale. Each of these produced voluminous ash flows that probably covered at least part of the Vale area. At about the same time, large Columbia River group/Owyhee basalt flows were entering the area from the north and west. Subsequent volcanic activity was of lesser magnitude on a regional basis, but may have been closer to Vale. Silicic rocks approximately 10-12 million years old and slightly younger basalts (as young as 7.4 Ma) are exposed to the south of Vale, but igneous activity in this area had essentially ended by 5 Ma. The Pliocene rocks (2-6 Ma) are composed of lake-bottom sediments, dominated by siltstone, which are called the Idaho Group. The thickness of these sediments is highly variable. A well 10 miles east of Vale encountered 4600 feet of the sediment and then 2500 feet of

interbedded sediment and basalt, but deeper wells in the Vale area have encountered only 750 to 950 feet of the same sediment.

Geophysical: The well was targeted for the highest probability of encountering commercial production at temperatures in excess of 300°F. The targeting study performed by TGC consisted of a comprehensive suite of geophysical and geological studies including the following:

- Review of existing geologic and geophysical data.
- Detailed gravity survey.
- Detailed ground magnetic survey.
- Controlled-source audio-frequency magneto telluric survey (CSAMT)
- Detailed geologic mapping.
- Detailed self potential (SP) survey.
- Drilling of 17 temperature gradient holes of 300' to 500' in depth.
- Drilling of exploration well A-Alt to a depth of 5757'.

The following is a brief discussion of the study's findings and how these findings were applied to targeting the TGC 61-10 exploration slimhole.

Temperature: The Vale geothermal resource is defined by one of the largest thermal anomalies in the Western United States. Indications of geothermal potential in this area come principally from hot springs, shallow temperature gradient wells and from geophysical (gravity and magnetic) data. A temperature gradient map shows an area of more than 19 square miles with a temperature gradient greater than 7°F/100' and an area of 9 square miles with gradients greater than 9°F/100'. This map is based on a data set of 17 shallow gradient wells drilled by TGC along with more than 40 additional gradient holes drilled by several other exploration entities prior to TGC acquisition of the resource. Gradients in these wells can be used to infer a total heat flow over a large area. In conjunction with measured or assumed thermal conductivity of the rock, this flux can then be extended downward to calculate thermal gradients at greater depths. Because thermal conductivity in the deeper igneous rocks is higher than that in the surface sediments, the thermal gradient decreases with depth, but this kind of gradient extension indicates that temperatures >300°F at depths between 3000 and 4000 feet are a reasonable expectation.

Volume: Based both on volume and electrical generating potential, as calculated by the United States Geological Survey⁴, the Vale geothermal resource is one of the largest geothermal resources in the U.S. As seen from the table below, the Vale resource ranks high among the U.S. geothermal fields which are currently producing power or which contain commercial discoveries.

Surface Geological Manifestations: Massive hydrothermally mineralized fracturing is observed in faults exposed at the surface within the Vale geothermal prospect. These fractures are direct evidence that the faults associated with both Vale and Rhinehart Buttes have in the past been conduits for prolific flows of high-temperature, silica-saturated geothermal fluid. Association of the large thermal anomaly with these faults indicates that the faults are permeable at depth and therefore represent highly attractive exploration drilling targets. These fracture systems are probably fed laterally by regional hot aquifers contained within deep basalt units

including the Owyhee and Columbia River Basalts which extend over an area of several thousand square miles.

Previous Exploration Drilling: Previously, two deep exploration wells have been drilled within the KGRA, one by Unocal (47-10) and one by TGC (A-Alt). Unocal 47-10 had a temperature of 277°F at a depth of 3855' and encountered several zones of significant fracture permeability. Extrapolation of the bottomhole gradient in 47-10 indicated that a temperature of 300°F would be encountered at a depth of 5000'. This well was located approximately 1 mile SE of the center of the central Vale thermal anomaly. The A-Alt well was drilled at the northern end of the thermal anomaly and encountered significant fracture permeability below a depth of 4000'. However, fluid temperatures of 224°F were far below the 300°F target temperature. Fracture permeability in both wells was found primarily in rhyolite flows associated with a local silicic eruptive center.

Resource Area	Volume, cubic km	Energy Content, MWe produced for 30 years	Status
Salton Sea, CA	116	3400	220 MW on-line
Long Valley, CA	135	2100	34 MW on-line
Surprise Valley, CA	210	1490	Discovery well drilled
Roosevelt, UT	47	970	20 MW on-line
Vale, OR	117	870	3 exploration wells drilled
Desert Peak, NV	52	750	9 MW on-line
Newberry, OR	47	740	Discovery well drilled
Coso, CA	46	650	252 MW on-line
Heber, CA	175	650	75 MW on-line
East Mesa, CA	36	360	102 MW on-line

Geophysical Anomalies: The prospect area is characterized by broad positive magnetic and gravity anomalies. Superimposed on these large anomalies are features of much shorter wavelength. The superposition of these shorter wavelength anomalies was used to infer the location of faults and fractures that may contain circulating geothermal fluid. The detailed gravity and magnetic data were modeled using the PC based GMSYS™ modeling program. Modeling showed that certain segments of faults defined by the gravity data are associated with steep magnetic gradients. This correlation was interpreted as zones of intense hydrothermal alteration along steeply dipping fracture zones of high permeability. These zones correlated closely with the central thermal anomaly.

It is possible that the difference in sediment thickness mentioned above could account for the gravity anomaly (sediment density = 2.25 g/cc, basalt density = 2.6-2.7 g/cc), but this is not a unique answer. The western edge of the gravity ridge is parallel to a much stronger gravity anomaly which shows a buried fault, and the overlay of gravity data with high thermal gradient

and high elevation is a strong indicator of upward-flowing hot water along the structure defined by the gravity anomaly. The positive magnetic anomaly centered on the peak of the thermal gradient contours also supports the concept of fluid circulation controlled by permeability distribution in volcanics known to be in this location.

Summary: The Vale thermal anomaly is comparable in size to many U.S. geothermal resources currently sustaining major commercial geothermal production. Close correlation between the central Vale thermal anomaly and gravity and magnetic anomalies indicated that the flow of hot water was fault-controlled at depth. Deep drill holes to the north and southwest of the central anomaly contained fractured, permeable silicic volcanics indicating that the central anomaly also contained this type of permeable lithology.

Although the combination of these factors does not guarantee a geothermal reservoir with potential for commercial development, the geophysical and geologic investigation of this region has been more thorough than in many other developed locales, and is representative of the pre-drilling exploration done by most geothermal operators.

III-c. Newberry Crater, Oregon⁵

c.1 Introduction and Background

Negotiations with California Energy Company, Incorporated (CECI), which owns leases in the Newberry KGRA led to an agreement for a cost-shared exploratory drilling project on CECI's lease. CECI's project management was by CE Exploration (CEE), the CECI subsidiary designated to direct the drilling and construction designed to result in a power plant at this site, and Sandia's management was by the Geothermal Research Department.

The Sandia/CECI agreement was based on the assumption that two slimholes were to be drilled in this area, with at least four production wells to be drilled within the next year. During the slimhole drilling, CECI would pay all the costs of the first hole to an approximate depth of 4500', Sandia and CECI would share equally the costs of the second hole to 4500', and then, if either of the holes had significant probability of reaching a production reservoir, it would be deepened to as much as 7500', with Sandia paying all the costs for the deepening and testing.

In return for the cost-share, Sandia was to receive testing, production, and cost data from the slimholes and from the production wells drilled nearby, giving a direct comparison of productivity predicted from tests on the slimholes and that

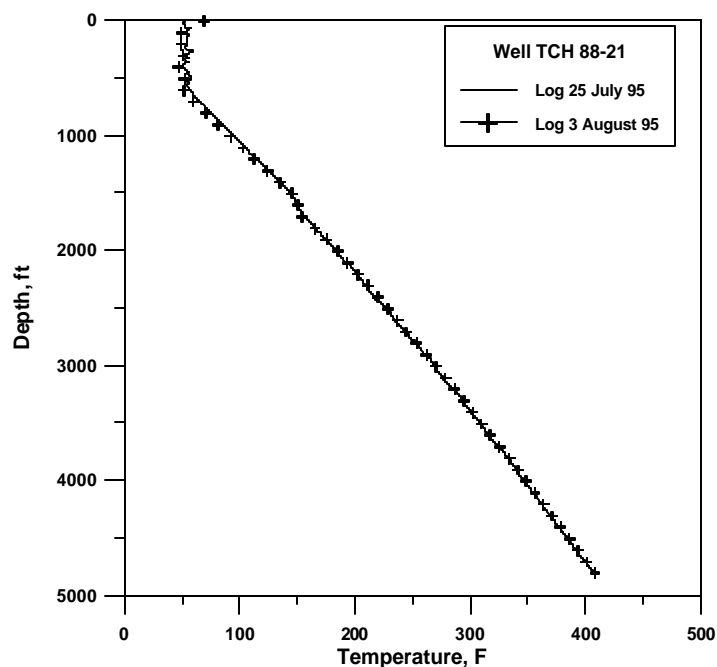


Figure III-7 - Temperatures in slimhole TCH 88-21

achieved by the actual production wells. Since locations, depths and lithology are also similar, there would also be a close comparison of drilling costs.

The first slimhole, TCH 88-21, was drilled to a depth of 4840' and has a stable bottomhole temperature of 410°F. While drilling the lower part of this hole, HQ hole diameter (3.85"), the core rods stuck while drilling at 3709' and could not be freed. The rest of the hole was then drilled with NQ (2.97" diameter) coring tools and 2" tubing was run to approximately 4835'. This tubing serves to keep the hole open for temperature logs and should be removable if the hole is eventually deepened. It is unlikely that, at the present depth, this hole has potential for either production or injection tests because of the low permeability indicated by drilling (almost no lost circulation in the lower hole) and temperature logs (see Figure III-7.)

c.2 Summary of Operations

This cost-shared exploratory slimhole, TCH 76-15, was drilled on the outer northwest flank of Newberry Crater (see Section III-c.8 for geologic description). Its primary objective was to improve evaluation, by measurements of temperature and permeability, of this area's potential for commercial geothermal power production. The plan for data acquisition on this hole was that preliminary temperature measurements would be taken with the Sandia logging tools and truck. If bottomhole temperature and permeability (implied by lost circulation or measured by injection) indicated the possibility of a production flow test, then we would attempt to air-lift, or otherwise stimulate the hole for production. Flow-test data would be taken by a combination of Sandia and service-company instrumentation.

The drilling plan was to set 7" surface casing to approximately 500', then set 4-1/2" casing to a depth dependent on the expected bottomhole temperature at TD, and finally directionally drill/core toward the postulated geothermal resource. Directional drilling was done below the 4.5" casing and was aimed toward the southeast, or toward the center of the caldera. Final well configuration is shown in Figure III-8.

The drilling plan was to set 7" surface casing to approximately 500', then set 4-1/2" casing to a depth dependent on the expected bottomhole temperature at TD, and finally directionally drill/core toward the postulated geothermal resource. Directional drilling was done below the 4.5" casing and was aimed toward the southeast, or toward the center of the caldera. Final well configuration is shown in Figure III-8.

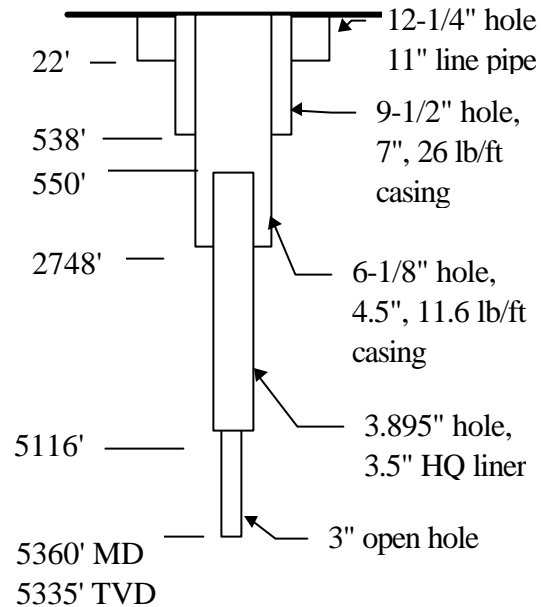


Figure III-8 - TCH 76-15 hole configuration

Drilling operations were lengthy, taking 116 days to TD. This was caused by a number of factors, including, to some degree: extensive lost circulation, stuck pipe, reaming the initial core hole for casing, directional-drilling problems, and forest fires. In spite of the time required for this hole, and the corresponding lessons learned, it still proved to be a cost-effective method of geothermal exploration. Temperature gradients in the lower parts of the two slimholes were similar to each other and were reasonably predictive of gradients in nearby production-size wells.

Although the temperature gradient in the lower part of TCH 76-15 – about 8°F/100' – was almost identical to that in TCH 88-21 (compare Figures III-7 and III-9), the near-isothermal portion of the hole extended much deeper, resulting in a lower bottomhole temperature -- 350°F at 5360'. This temperature, coupled with the reduction to NQ hole size (3") and almost complete lack of permeability (measured by an attempted injection test), indicated that a discharge flow test was extremely unlikely at this depth. Wellbore simulations based on extending this gradient, in NQ-size hole, to the potential TD of 7500' indicated that a discharge test from that depth would be problematic. These factors, coupled with the very slow and difficult drilling at this depth and with the fact that two nearby production wells were already at TD, led to the decision for termination of drilling at this depth. Drilling problems and decisions are described in more detail below.

c.3 Description of Equipment and Methods

The following descriptions cover the major pieces of equipment used during the project and, where applicable, explanations of their use.

Drill rig: The drill rig used for this hole was a Longyear truck-mounted Model HD602, with a 60' mast, capable of pulling 40' stands of pipe, and a hoist rated at 60,000 pounds. The rig was

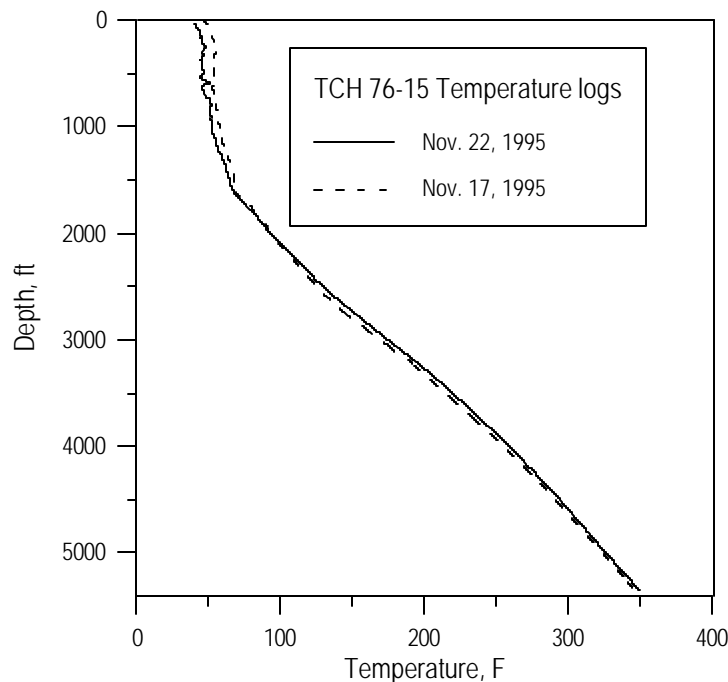


Figure III-9 - Temperatures in TCH 76-15

supported on a hydraulic jack-up substructure which provided approximately 8' clearance between the bottom of the substructure and ground level. Two mud pumps were available; a Gardner-Denver duplex (150 gpm @ 260 psi) for surface drilling and reaming, and an FMC Model M12 triplex (60 gpm @ 1000 psi) for coring. A 40' parts trailer contained tools, bits, spare parts, and a welder.

This particular rig has a depth capability of approximately 8200' with HCQ rods, and below 6750' with CHD101 drill rods (approximately 4" hole diameter); it can reach to 8500' with

CHD76 rods (approximately 3" diameter), and even deeper with hybrid strings, enabling slimhole exploration to be used in most known geothermal areas.

Core recovery in this hole was very good, more than 96% for the cored portion of the well (the interval to the first casing point at 544', and the portion which was directionally-drilled, were not cored).

Surface instrumentation: Several instruments were placed at and near the wellhead, with data collected and recorded continuously in the Sandia mobile office. These measurements comprised the following:

- Drilling fluid inflow -- Flow rate was measured directly by a Doppler flow-meter mounted on the standpipe and indirectly by volume calculated from mud pump speed, obtained by a shaft encoder on the pump's crankshaft. When these readings were compared, the pump-stroke value was usually higher, because inefficiencies in the pump led to less-than-theoretical fluid delivery. The Doppler meter was especially valuable because it included a totalizer, giving an integrated total flow volume after a specified starting time. This enabled very accurate placement of mud, cement, LCM pills, mineral oil, etc.
- Annulus inflow -- When drilling without returns, drilling fluid was pumped down the annulus between the drill rods and the casing. This flow was measured by an encoder on the pump shaft.
- Drilling fluid outflow -- Return flow was measured by a magnetic flow meter (magmeter) on the line from the pitcher nipple back to the mud pits. When outflow becomes significantly less than inflow, this is usually an indication of lost circulation.
- Drilling fluid temperatures -- Temperature transducers were placed in the flow lines into and out of the wellbore.
- Standpipe pressure -- Pressure delivered to the drillpipe is measured. This pressure is not only important as an insight on drilling performance, but sudden drops in this pressure can indicate a hole or washout in the drillpipe.
- Ambient air temperature -- Weather conditions were indicated by the air temperature measured under the rig.
- Rotary speed -- Drill string rotary speed was recorded from the rig's tachometer.
- Chuck height -- During the latter part of the drilling operations, a linear-displacement transducer was connected to the chuck which rotates the drillpipe and travels down as the drill advances. Hole depth at the start of the core run was entered by the driller. Chuck-height versus time gives rate of penetration, which is sometimes useful to identify different lithologies.

All transducers were connected to a signal-processing station at the drill rig and then, via a simple twisted-pair wire to the data-logging computer in the Sandia trailer. Each morning, data from the computer was down-loaded onto diskettes.

Downhole instrumentation: Downhole data collection during this operation was primarily limited to temperature measurements. These temperature logs were taken with Sandia's platinum-resistance-thermometer (PRT) tool which, along with a Sandia logging truck, remained on-site for the entire project. This instrument uses a simple resistance bridge, with changes in

resistance measured from the surface through a four-conductor cable. Since there are no downhole electronics, temperature drift with time is negligible and the PRT temperature measurements are considered a reference standard for this kind of drilling.

The acoustic borehole televiewer (BHTV) was run twice in the wellbore with limited success. There were several problems with the tool's functions, but images were successfully obtained over the interval from 2748' to 3635'.

c.4 Analysis of Data

Temperature: Downhole temperatures were taken during drilling with maximum-reading-thermometers (MRTs) attached to the overshoot which is sent downhole to retrieve the core tube or loaded into the running gear of the single-shot camera which is used to survey the hole trajectory. During reasonably good drilling, these will provide temperature readings

approximately once a day. An MRT is simple and cheap, but does have several drawbacks: It requires some residence time to reach the wellbore temperature; it is subject to pressure effects below 4,000-5,000 feet; it records the highest temperature it has seen, which may not be at the bottom of the hole; and it measures temperature during a short pause in drilling fluid circulation, which tends to cool the wellbore. This latter effect is less important in core drilling, where drilling-fluid flow rates are less than 10% of those in rotary-drilled wells, and the MRT readings for the Newberry

slimholes tended to give good

agreement with post-drilling logs (see Figure III-10).

Logs taken days or weeks after drilling show that temperature gradients in the lower sections of the two slimholes are quite similar, but that the point at which the gradient reaches a relatively constant $\sim 8^{\circ}\text{F}/100'$ is approximately 1000' deeper in TCH 76-15 than in TCH 88-21. It is likely that this effect is related to the relative elevations of the two drill sites; the TCH 76-15 pad is 800' higher than the TCH 88-21 location. Gradients in the slimholes are also reasonably similar to two production-size wells, one very near 88-21 and the other roughly halfway between the slimholes.

Permeability: Even though there was little lost circulation in the last 1000' of the hole, implying little permeability, it was important to quantify the transmissivity of the potential reservoir. After circulating the mud out of the hole and replacing it with clear water, we attempted two injection tests; one into the open hole section (5116' - 5360') below the HQ liner, and one into the

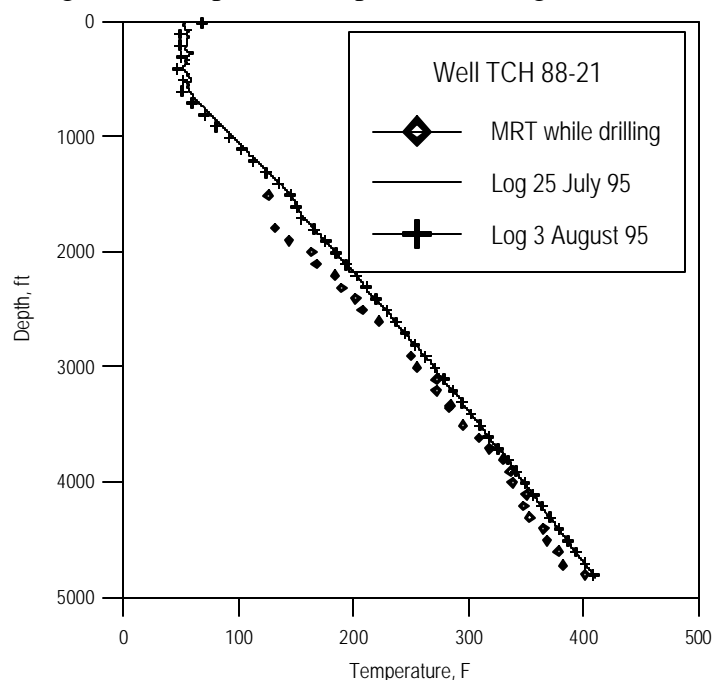


Figure III-10 - Temperature recovery in slimhole

annulus outside the uncemented part (2748' - ~4800') of the liner. The much greater wellbore area exposed outside the liner was offset by the presence of mud which had been sitting there for several weeks, undoubtedly reducing the effective permeability. In both cases, however, surface injection pressures over 300 psi (which was the pressure limit for the instrumentation) could only drive a flow rate of less than 3 gpm. It was not even clear that this small flow rate was into the formation, because a defective joint in the HQ liner may have allowed this amount of leakage into or out of the liner. In either case, the formation was, for all practical purposes, impermeable.

c.5 Discussion

Lost circulation: The upper 800' of this slimhole suffered extensive lost circulation. Even though it is possible to drill blind (without fluid returns), especially while coring, the drilling plan was to repair loss zones as they were penetrated, thus improving the probability of a competent cement job on the casing. This was an important objective, because the test plan included a discharge flow test, which requires good cement around the casing. The cost of this repair, however, was high.

In the interval from surface to 839', seventeen cement plugs were set to combat lost circulation. This led to direct costs for: 376 cubic feet of cement, 114 hours waiting on cement, time to drill out 1033' of cured cement, and trip time for running in and out of the hole with open-ended drill pipe. There were other costs, less well-defined, for: three days and five casing-advance bits consumed by stuck pipe directly attributable to cementing, discarded drilling fluid made unusable by drilling cement, and extra bit wear from drilling cement. Assuming an average daily cost of \$8,000, lost circulation resulted in *at least* \$80,000 in additional expense. Although the costs just mentioned apply solely to TCH 76-15, the experience was similar in TCH 88-21, which required 21 days to set 7" casing at 510'.

These costs would have been much higher if a commercial cementing contractor had been used for the lost circulation plugs, but cement quantities were small enough that the rig crews could mix cement in tanks and pump it with the rig pumps.

Directional drilling: Changing the hole trajectory was also a long process, requiring 12 days to directionally-drill and ream the interval from 2848' to 3388'. A large part of this time was spent in trying to get the proper equipment into the hole. An oil-field directional drilling company was used first, but their motor was inadequate for the job. When a minerals-drilling directional company was later contracted, the mud-motor work went much better, although the deviated section still required considerable reaming. The lesson to be learned from this is to hire companies who are accustomed to doing the job you want done.

Choice of the interval to be directionally-drilled is frequently affected by the casing design. In this hole, the decision was made to turn the hole below the 4.5" casing shoe. The alternative, directional drilling higher in the hole so that the turn would be in the cased section of the hole, would have allowed the use of larger directional-drilling tools and would have put any potential dog-legs behind pipe. Later experience with downhole vibration and difficulty working some of the coring tools through the directional interval indicates that this might have been a better choice.

Value of the trajectory change was also unclear. The directional work turned the hole to an inclination of about 7°, which later built without further deliberate action to about 10°, giving a lateral hole-bottom displacement of about 300 feet. Even considering the hole's previous inclination and azimuth (i.e., where the hole would have gone without correction), the total effect of directional drilling was to change position of the hole-bottom by about 500 lateral feet. It is not clear from geologic data that this could have had much effect on bottom-hole temperatures or permeability.

Reduction in hole size: A major objective of this drilling was to reach a potential reservoir, down to the maximum target of 7500', which could be tested with a discharge test. As depth increases, the penalty of small wellbore-diameter becomes more significant in a slimhole, compared to a production-size well. For that reason, we tried to keep the hole at HQ (3.9") diameter as long as possible, even after drilling problems indicated that we should reduce to NQ (2.98") diameter.

That decision was costly -- the last section of the hole from 4756' to TD required 31 drilling days, an average less than 20 feet per day. Most of the problems in this interval were related to caving, sloughing, squeezing clay, and differentially stuck pipe. If we had set an HQ liner from approximately 2700' (just above the 4.5" casing shoe) to 4800' and reduced to NQ drilling at that point, it is likely that (a) the drilling time in the 4800'-5360' interval would have been reduced by 50-75%, and (b) we would have had the option of continuing the hole to greater depth. Computer modeling, using a wellbore simulator, of discharge tests indicates that this diameter reduction would not have seriously diminished the ability to run a flow test, had the formation been suitable. In short, the decision to maintain HQ diameter after hole problems became severe led to excessive drilling cost which probably could have been avoided with an earlier reduction in hole size.

Cost comparison: During drilling operations at TCH 76-15 detailed daily cost records were kept by on-site Sandia personnel. A summary of total well costs is given below:

<u>ACTIVITY</u>	<u>COST</u>
Rig day rate	\$317,075
Footage charges	199,357
Drilling fluids	87,883
H ₂ S service	12,000
Casing, accessories, and wellhead	92,092
Cement	31,871
Tools (bits, reamers, and directional)	52,570
BOPE rental	40,501
Other rental (sanitary, etc.)	33,712
Site preparation and maintenance	81,694
Supervision	62,250
Water trucks	36,207
Fuel	13,440
Transportation	3,368
Miscellaneous	6,856

TOTAL	1,070,876
Cost per foot	\$199.79

CECI has also released daily reports and total cost figures on the two production wells which were drilled during the same period as the slimhole. That information is summarized below:

Well Number	86-21	23-22
Depth	8869' TVD 9200' TMD	9040' TVD 9602' TMD
Drilling days to TD	75	81
Casing program	20" @ 905' 13-3/8" @ 4199' 9-5/8" liner from 3987-9185'	20" @ 795' 13-3/8" @ 4418' 9-5/8" liner from 4200-9577'
Total cement	9126 cubic feet	8926 cubic feet
TOTAL COST	\$3,333,427	\$2,895,493
Cost per foot	\$362.33	\$301.55

The significant cost difference between these wells is primarily due to two workovers in 88-21, but even averaging the costs of the two wells, for a figure of \$331.29 per foot shows that the slimhole cost per foot was 200/331, or 60.4% of the large hole.

c.6 Conclusions

The principal purpose of drilling a slimhole is prediction of productivity in a large-diameter well; in effect, prediction of temperature and permeability. To examine temperature first, temperature gradients in the two slimholes (TCH 88-21 and TCH 76-15) and in the two production wells (86-21 and 23-22) are given below. These gradients were in the same 1000' interval relative to sea-level elevation; that is, they were not at the same measured depths in the wells. Note that the temperature gradients (derived from temperature logs) are corrected for the inclination of the wells and are defined as °F/100 vertical feet. Note also that 88-21 and 86-21 are within 1000' of each other, 23-22 is approximately 2400' north-east of them, and 76-15 is approximately 4700' north-east of 23-22.

Well Number	Approximate WH elevation, ft. ASL	Gradient in interval 2600-3600' ASL, (°F/100 vertical feet)
88-21 (slimhole)	6240	8.2
76-15 (slimhole)	6820	7.4
86-21	6240	7.1
23-22	6600	6.8

Temperature gradients in the slimholes were consistently higher than in the production wells, which would lead to over-prediction of reservoir temperatures, but there are several possible explanations for this discrepancy. First, it is possible that the production wells actually did have

lower gradients, although 88-21 and 86-21 were only about 1000' apart and 23-22 is spaced between the two slimholes. It does not seem reasonable that the slimholes' formations would have uniformly higher gradients than the production wells. A more likely scenario is related to the way the holes were made. The slimholes were drilled with minerals-type diamond coring tools, which have very low flow rates (15-25 gpm) compared with the production wells drilled with conventional rotary rigs having mud flows of 500-600 gallons per minute. The cooling effect on the wellbore is much greater in the larger-diameter holes and, therefore, so is the temperature recovery once drilling is done. Figure III-10 shows the MRT readings in 88-21 compared with a temperature log taken two weeks after the end of drilling. Temperature recovery is only a few degrees, but regulatory agencies normally assume 50°F recovery in conventional wells. The cooling effect is also aggravated by the short times after drilling at which the logs were done in the production wells; approximately two weeks after end of drilling operations in 86-21, and only four days after circulation and testing in 23-22.

Circulation within the wellbore has a greater effect on the cold-water aquifer ("rain curtain") in the big wells, raising its temperature relative to that in the slimholes. [This zone, at about 6000' ASL, is 90°F in the big wells, but only 50°F in the slimholes, implying that the aquifer is heated by the greater circulation in the production wells.] Wellbore circulation past the warmer aquifer in the big wells, then, causes the top of the well to be warmer and the bottom of the well to be cooler, relative to the slimholes, lowering the temperature gradient.

There is also wellbore circulation after drilling; in Figure III-10a the near-isothermal interval coincides with the "blank" section of an uncemented liner. Spinner logs in that interval show flow downward in the wellbore, which means that there is flow up the outside of the liner. Again, the relationship between this circulation and the marked increase in temperature is not clear.

Since the production wells were approximately 9000' deep and the slimholes were about 5000', predicting permeability is even more chancy. In fact, permeability was low in all the boreholes. It is certainly not the case that corresponding permeabilities would necessarily be similar over this depth range, but the slimholes did reflect the production wells' permeabilities.

In general, the slimholes were informative, particularly in terms of the temperature-gradient data and in the lithologic data inherent in the core samples. They were not, however, especially predictive of reservoir potential because they did not reach the postulated reservoir depth. Even if the temperatures had been accurately extrapolated from the slimhole profiles, little would

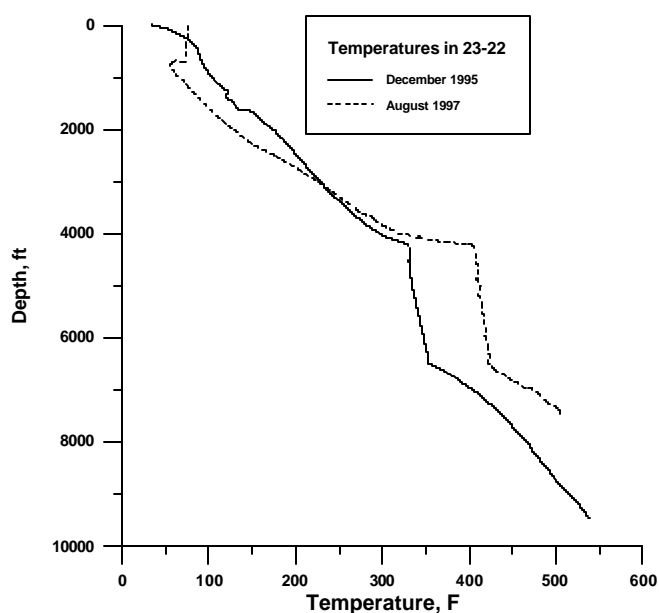


Figure III-10a – Well temperatures over time in 23-22

have been known about the permeability and productivity in a horizon several thousand feet deeper than the slimholes reached. Finally, if the two slimholes had not been drilled, it is highly likely that another production-size well would have been used to confirm reservoir characteristics. This would have entailed an additional cost of approximately \$1 million.

c.7 Recommendations

It would be worthwhile to further evaluate data collected from the slimholes so that we can better understand their benefits and shortcomings. Two major issues to be resolved are the discrepancy between temperature gradients in the slimholes and in the production wells, and the effect of surface elevation on comparison of data among wells. Several activities might clarify these questions:

- Monitoring water level in all the wells could help resolve the effect of wellhead elevation.
- Comparison of lithologic data (especially from core) might enable correlation of strata among the different locations.

c.8 Brief Geologic Description (summarized from Reference 6)

The Newberry Volcano, covering more than 500 square miles, is one of the largest Quaternary volcanoes in the conterminous United States. It lies at the west end of the High Lava Plains province in central Oregon, an extensive volcanic zone measuring approximately 150 miles east-west and 50 miles north-south. There have been many volcanic events in the Newberry area since the first lava flows about 1,200,000 years ago (ya), with major eruptions as recently as 1,250 ya.

grouped around the periods 10,000-12,000 ya, 7,000 ya, and 1250 ya. Ages of most flows at Newberry are described in relation to the eruption of Mt. Mazama, about 7,600 ya, which formed the crater now occupied by Crater Lake. This event, approximately 65 miles south of Newberry, covered this area with two to three feet of ash, so local flows which over- or underlie the Mazama ash can be easily dated with reference to it. The Mazama ashfall also drove away the indigenous Native American population which had previously inhabited this region year-round

During the period 12,000 to 10,000 ya, most eruptive activity was to the south and east of the crater, but about 7,000 ya (shortly after the Mt. Mazama eruption) the Northwest Eruptive Period occurred along the Northwest Rift Zone, which extends nearly 20 miles from the caldera (to the vicinity of the present Lava Lands Visitor Center.) This zone of weakness was the source for at least 13 separate basaltic-andesite flows covering a total area of nearly 40 square miles. Later (about 3,500 ya) the East Lake Eruptive Period produced two small obsidian flows but these flows and the associated tephra were later covered by ashfall from the most recent and well-known event at Newberry, the Big Obsidian Eruptive Period. This was a three-stage eruption which produced, in order, (1) explosively-driven pumice and ash which were carried downwind (ENE) and accumulated almost a foot thick approximately 40 miles away, (2) the Paulina Lake Ashflow extending almost two miles south-east of Paulina Lake, and (3) the Big Obsidian Flow, which covers an area about 0.8 by 1.5 miles, overlying part of the ashflow southeast of Paulina Lake. There is considerable evidence that a magma chamber existed through Holocene time (from 10,000 ya to present), without crystallizing between eruptions or since the last eruption, and may still exist. At present, the east and west flanks of the volcano are mostly covered by ash flows, pumice falls, mudflows, and other pyroclastic deposits; the north and south flanks probably also have these deposits at depth, but they are overlain by basalt and andesite flows.

The Newberry National Volcanic Monument, roughly including Newberry Crater and the Northwest Rift Zone, was created in 1990. The Monument is bounded in places by a Special Management Area, in which surface occupancy is prohibited but directional drilling beneath the SMA is allowed. The boreholes described in this report are just outside the SMA, generally north-west of Paulina Lake.

III-d. Fort Bliss, Texas⁷

d.1 Introduction and Background

Sandia participation, described above, in slimhole drilling projects at Steamboat Hills, Nevada; Vale, Oregon; and Newberry Crater, Oregon, generated an experience base in slimhole drilling and testing technology. When the U. S. Army was in the planning stages for a geothermal exploration program at Ft. Bliss, they approached the Geothermal Research Department for input on the structure of this program; this consultation led to a Work-for-Others (WFO) contract from the Army to Sandia for assistance on the exploratory holes. That assistance included consultation and direction of drilling operations, numerous temperature logs during and after drilling, and project documentation. This report comprises a summary of operations, a

detailed narrative of the project, daily drilling reports completed by Sandia personnel, representative temperature logs from the holes, and cost information on the drilling operations.

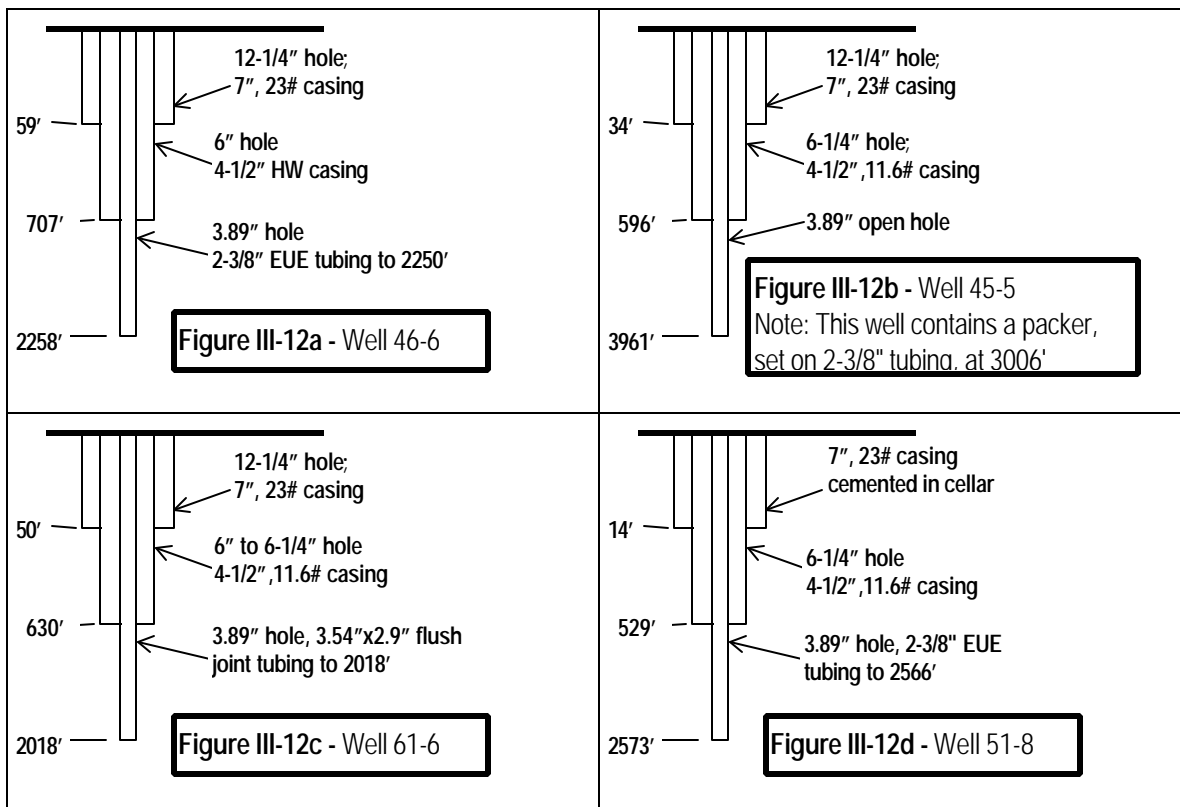
d.2 Summary of Operations

Principal goals for this program were to evaluate the temperatures, temperature gradients, and permeabilities for a series of holes situated along thermal anomalies near a prominent geologic feature called Davis Dome. Hole locations were chosen by consultation among representatives from Ft. Bliss, New Mexico State University, University of Texas - El Paso, and the Navy's Geothermal Program Office at China Lake, California. In all cases, the drilling objective was to reach the target depth as cheaply as possible while assuring hole integrity for the necessary measurements.

Designs of the four holes are shown in Figures III-12a-12d, and summary wellbore descriptions, including cost comparison, are given below.

Drilling for the four holes followed the same general pattern: 1) set a conductor casing to a depth of 30-50', 2) drill ~ 6" hole through mostly sand/clay sedimentary formations to 500-600', 3) set 4-1/2" surface casing at that depth, 4) core HQ (3.89" dia.) mostly through limestone/dolomite or intrusive bedrock to TD.

Although all the drilling was plagued by lost circulation, this is not a critical problem when core drilling, so little effort was made to correct it below the surface casing. Below 1000' none of the holes had more than 30% fluid returns, and usually there were none at all. In most of these cases, drilling fluid was pumped into the drill rod annulus to improve lubricity and to help control downhole vibrations. In contrast, it is difficult or impossible to get a good cement job on



Hole number	46-6	45-5	61-6	51-8
Total Depth, ft	2258	3961	2018	2573
Drilling days	30	37	19	23
Completion	2-3/8 EUE tubing to 2250'	3.89" open hole 596-3961'	2.9" ID tubing to 2018'	2-3/8 EUE tubing to 2566'
Maximum temp. @ depth	192.4°F @ 2244 ft.	182.4°F @ 495 ft.	173.2°F @ 728 ft.	180.8°F @ 2533 ft.
Bottom-hole temperature	192.4°F	181.9°F	169.3°F	180.8°F

the surface casing if there are un-healed loss zones behind it, so most of the loss zones in the upper parts of the holes were plugged with cement. This procedure varied in difficulty; loss zones in the surface holes required a total of 23 cement plugs, but 18 of these were on the first two holes. When loss zones could not be plugged while drilling, staged cement jobs were used on the surface casing.

Cost Category	Hole Number			
	46-6	45-5	61-6	51-8
Rig, Mobilization	9375	9375	9375	9375
Rig, Time charges	39,560	31,810	28,493	28,988
Rig, Footage charges	88,186	190,218	78,511	106,775
Drilling fluids	22,938	19,791	10,716	20,789
Casing/Liner	10,530	4,995	13,662	2,300
Cement (casing)	5,000	5,227	3,528	3,782
BOP rental	3,500	5,500	1,200	1,500
Core boxes	716	2,067	675	1,017
Miscellaneous	1,400	3,290	2,960	5,000
Total Well Cost	\$184,339	\$272,273	\$149,120	\$179,526
Well depth	2258	3961	2018	2568
Cost per foot	\$81.64	\$68.74	\$73.89	\$69.91

d.3 Description of Test Equipment and Methods

The following descriptions cover the major pieces of equipment used during the project and, where applicable, explanations of their use.

Drill rig: The drill rig used for this hole was a Boart-Longyear truck-mounted Model HD602, with a 60' mast, capable of pulling 40' stands of pipe, and a hoist rated at 60,000 pounds. The rig was supported on a hydraulic jack-up substructure which provided approximately 8' clearance between the bottom of the substructure and ground level. Two mud pumps were available; a Gardner-Denver duplex (150 gpm @ 260 psi) for surface drilling and reaming, and

an FMC Model M12 triplex (100 gpm @ 1000 psi) for coring. A 40' parts trailer contained tools, bits, spare parts, and a welder. A water truck was also supplied with the rig.

This particular rig has a depth capability of approximately 8200' with HQ rods, and below 10,000' with a composite string of CHD101 (approximately 4" diameter) and HQ drill rods. It can reach to 14,000' with a composite string of CHD76 and NQ rods (approximately 3" diameter), enabling slimhole exploration to be used in most known geothermal areas.

Core recovery in this hole was very good, more than 99% for the H-size core and more than 90% for the larger BSF (6-1/4" diameter hole, 4" diameter core) string. The lower percentage for the BSF string was primarily a function of large voids encountered in the upper part of the hole, where the rock was more broken.

Surface instrumentation: Several instruments were placed at and near the wellhead, with data collected and recorded continuously in the Sandia mobile office and displayed in real time on the rig floor and at other on-site locations. These measurements comprised the following:

- Drilling fluid inflow -- Flow rate was measured directly by a magnetic flow meter mounted on the suction side of the mud pump, a Doppler flow-meter mounted on the standpipe and indirectly by volume calculated from mud pump speed, obtained by a shaft encoder on the pump's crankshaft. The Doppler meter was especially valuable because it included a totalizer, giving an integrated total flow volume after a specified starting time. This enabled very accurate placement of mud, cement, LCM pills, mineral oil, etc.
- Drilling fluid outflow -- Return flow was measured by a SNL rolling float meter during surface hole drilling and magnetic flow meter (magmeter) during HQ core drilling; both of these instruments were mounted on the line from the pitcher nipple back to the mud pits. When outflow becomes significantly less than inflow, this is usually an indication of lost circulation.
- Drilling fluid temperatures -- Temperature transducers were placed in the flow lines into and out of the wellbore.
- Standpipe pressure -- Pressure delivered to the drillpipe is measured. This pressure is not only important as an insight on drilling performance, but sudden drops in this pressure can indicate a hole or washout in the drillpipe.
- Ambient air temperature -- Weather conditions were indicated by the air temperature measured under the rig.
- Rotary speed -- Drill string rotary speed was measured by an encoder just above the drill chuck.
- Chuck height and hole depth -- During most of the later drilling operations, a linear-displacement transducer was connected to the chuck which rotates the drillpipe and travels down as the drill advances. This gives instantaneous depth in real time, because the driller also increments the drill string length each time a connection is made. Chuck-height versus time gives rate of penetration, which is sometimes useful to identify different lithologies.

All transducers were connected to a signal-processing station at the drill rig and then, via a simple twisted-pair wire to the data-logging computer in the Sandia trailer. Each morning, data from the computer was downloaded onto diskettes.

Downhole instrumentation: Downhole data collection during this operation was primarily limited to temperature measurements. These temperature logs were taken with Sandia's platinum-resistance-thermometer (PRT) tool which, along with a Sandia logging truck, remained on-site for the entire project. This instrument uses a simple resistance bridge, with changes in resistance measured from the surface through a four-conductor cable. Since there are no downhole electronics, temperature drift with time is negligible and the PRT temperature measurements are considered a reference standard for this kind of drilling.

An additional temperature/inclination tool was also run as part of its development program. This tool rode in the inner core tube, measured temperatures (within a few feet of the bit) and hole inclination as a function of time while drilling, and stored this data in an on-board memory. When the core tube was pulled out of the hole to retrieve core, data from the "core tube logger" (CTL) was downloaded into a computer for plotting and analysis. Letting the CTL ride in the core tube while drilling gave temperatures in that drilled interval, but the tool was also used to temperature log the entire borehole when the pipe was tripped for bit changes. Using the CTL as part of the normal drilling operation also meant that no additional rig time was consumed in satisfying regulatory requirements for temperature and inclination measurements at regular depth increments.

Inflatable packer: Approximately six weeks after completion of drilling on well 45-5 an inflatable packer was run into the hole and set at 3000 feet. Principal motivation for this was the possibility (based on temperature logs) that higher temperatures at the bottom of the hole were being reduced by cooler waters from above. The packer isolated the intervals above and below it, while providing passage for a logging tool through the tubing which suspended the packer, through the packer inside diameter, and on to final hole depth. By observing temperature and water level changes before and after installing the packer, a way of assessing possible flow between upper and lower zones was available. Temperature changes were not significant (see Figure III-18) but water level inside the tubing dropped very slowly and was different from water level outside the tubing. This implies that the packer seal remained intact and that permeability in the interval below the packer is low. If it would be useful to define permeability more accurately, injection tests into the intervals above and below the packer can be done later.

d.4 Description of Data

Three principal types of data were obtained from this drilling project: core samples of the lithology penetrated by the holes, records of drilling behavior (such as water level in the hole, changes in rate of penetration, etc.), and multiple temperature logs (both during and after drilling) in each well. A suite of geophysical logs (gamma ray, neutron, sonic, and resistivity) was also run after completion of drilling.

Core-sample logs are combined to construct lithologic columns of the formations penetrated by each well, and these columns can then be used to validate or compare with conceptual

models of the reservoir's structure. Cores can also give a reasonably clear picture of fractures in the formation, with indications of their density, dip, and aperture.

Temperature logs are generally used to show either a comparison among several wells (as in Figure III-13) or the changes in a given well over time (Figures III-14 to III-17). Correlation of temperature logs with lithologic logs and drilling records is also useful in identifying reservoir features such as the lost circulation zone between 950 and 1000 feet in well 45-5 (Figure III-14).

From this data, the objectives are to evaluate the geothermal potential and to develop a conceptual model of this reservoir. This analysis, however, is beyond Sandia's purview and is the responsibility of New Mexico State University and the U. S. Army.

d.5 Discussion, Conclusions, and Recommendations

Sandia's goals in this project were to (1) consult with and advise the U. S. Army on drilling techniques which would provide an informative, cost-effective exploratory program, (2) expand our database on slimhole drilling costs and performance, and (3) test developmental flow measurement and core-tube logging tools. All these goals were met.

In planning the exploratory program, the principal decision to be made was whether to use slimhole or conventional rotary drilling. Rotary drilling is well understood and has reasonable cost, if drilling conditions are good. In geothermal wells, however, there is almost always lost circulation (which is usually necessary for production of geothermal fluids) and these losses must be plugged or repaired before drilling very far ahead with conventional rotary tools. Wireline (slimhole) core drilling, in contrast, can drill without fluid returns for intervals of several thousand feet. A slimhole also gives significant cost reduction because of its smaller casing sizes and the smaller cement volumes required for the casing. All four slimholes in this program experienced severe-to-total lost circulation, so conventional drilling with cement (or LCM, although it is unlikely that would have been sufficient) in the loss zones would have been extremely expensive.

From the summary on page III-29, the average cost per foot was just under \$73 for the four holes. This compares very favorably with other slimholes in Sandia's program. Costs at Steamboat NV, Vale OR, and Newberry OR were \$151, \$110, and \$199 per foot, respectively, and in each of those cases the slimhole costs were 45 to 65% of rotary drilling costs at these same locations. Although there are no large-diameter, rotary-drilled holes at McGregor Range for direct comparison, we believe that cost savings in these slimholes would have been at least as favorable.

Another comparison can be made with rotary-drilled "slim holes", although the conventional-drilling definition of slimhole is rather vague. For example, the rotary-drilled hole at Vale, OR, was considered a "slim hole", with 7" casing and 5" slotted liner, but it still cost approximately \$160/foot, compared with \$110/foot for a slimhole drilled to the same depth approximately two miles away (see Reference 3 for a detailed cost comparison of the two holes at Vale.) To repeat a point made above, the extreme lost circulation in these holes would have made any conventional-rotary drilling difficult and expensive. Indications of this are seen with the rotary-drilled intervals in well 46-6, which had many cement plugs and unsuccessful use of lost circulation material. Even without lost circulation problems, however, the method used here, compared to "slimhole" rotary, gives cost savings in downhole tools (bits, stabilizers, etc.),

casing, and cement, and is far more informative about the reservoir's geologic structure because of the recovered core.

In assessing a reservoir's geothermal potential, the two most important properties are temperature and permeability. Temperature was thoroughly measured in all these holes, but, aside from the obvious loss zones, permeability distribution is not well known. This could be clarified with either discharge or injection tests in the wells. We believe, from Sandia's experience and analysis, and based on extensive study of data from Japanese slimholes and production wells^{1,8,9}, that discharge tests in slimholes can accurately predict productivity of a large hole. This question did not arise at McGregor Range, however, for the temperatures were not high enough to consider a self-supporting flow test. If this potential resource is investigated further, it is still possible that a pumped production-flow test or an injection test could be useful for better permeability definition.

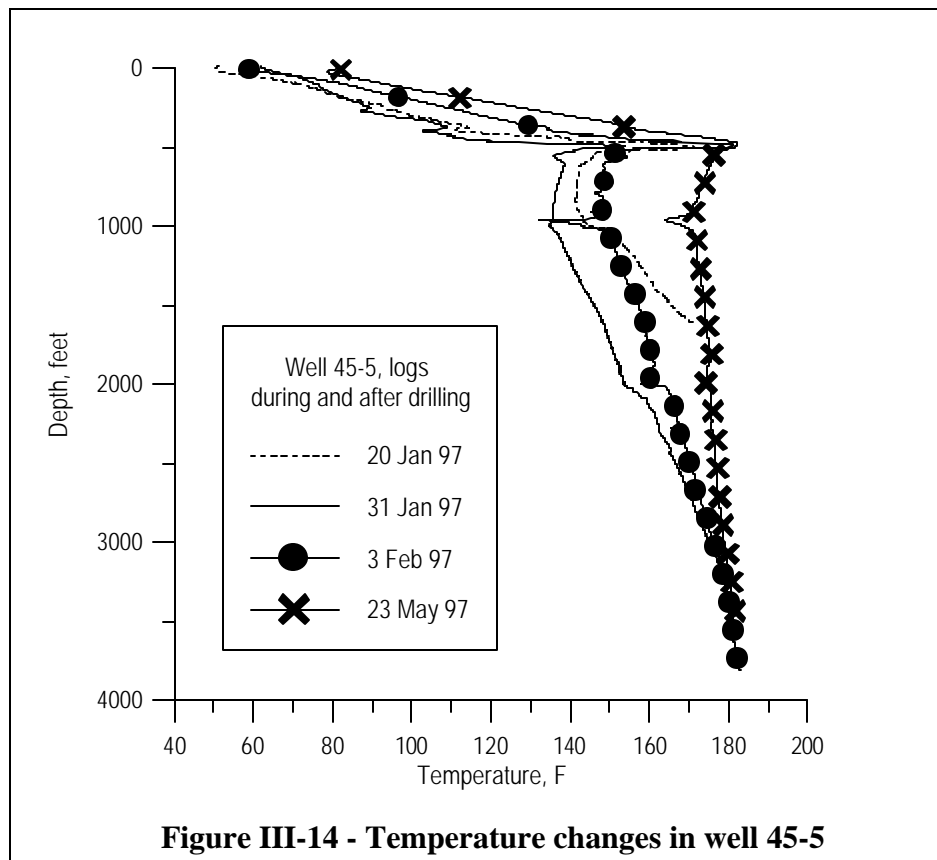
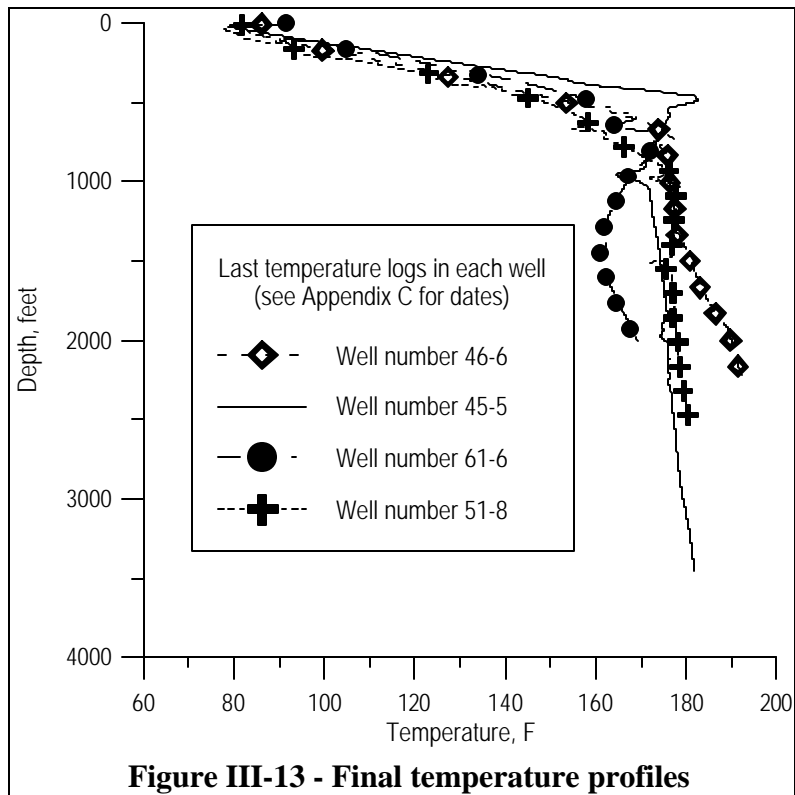
This was a successful drilling operation in terms of the information acquired within the project budget. This rig's drilling performance through extensive lost circulation zones re-confirmed the concept that wireline coring is an excellent exploration technique in terrain which is likely to have this kind of geologic structure. We have made the case above as to why these holes were cost-effective and, although interpretation will be left to others, the data collected from the slimholes was in no way incomplete compared to information from a larger-diameter well.

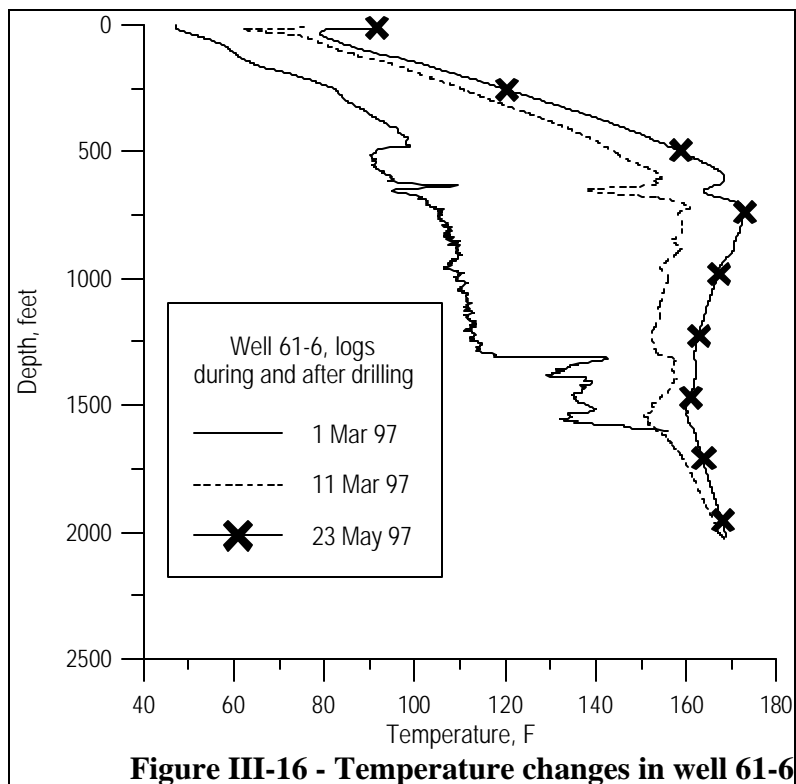
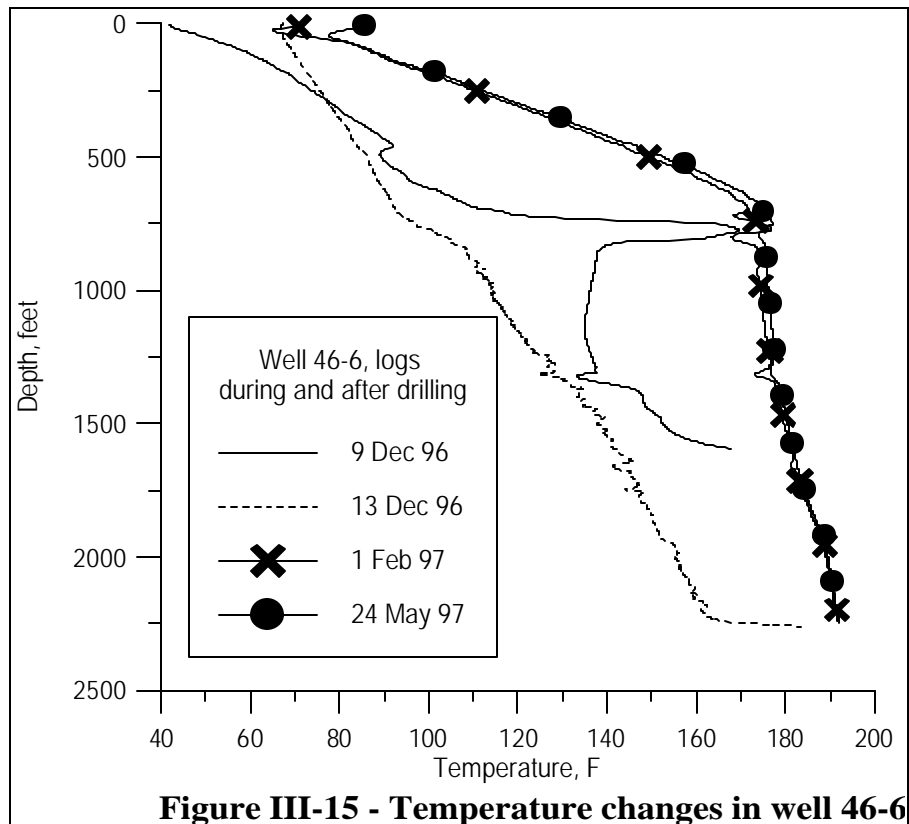
The drilling operations also provided an opportunity to test, calibrate, and validate the performance of Sandia-developed flow instrumentation and downhole logging tools (the CTL memory tool). These instruments were not only useful for this drilling project, but additional testing helps to verify their performance as a step toward commercialization.

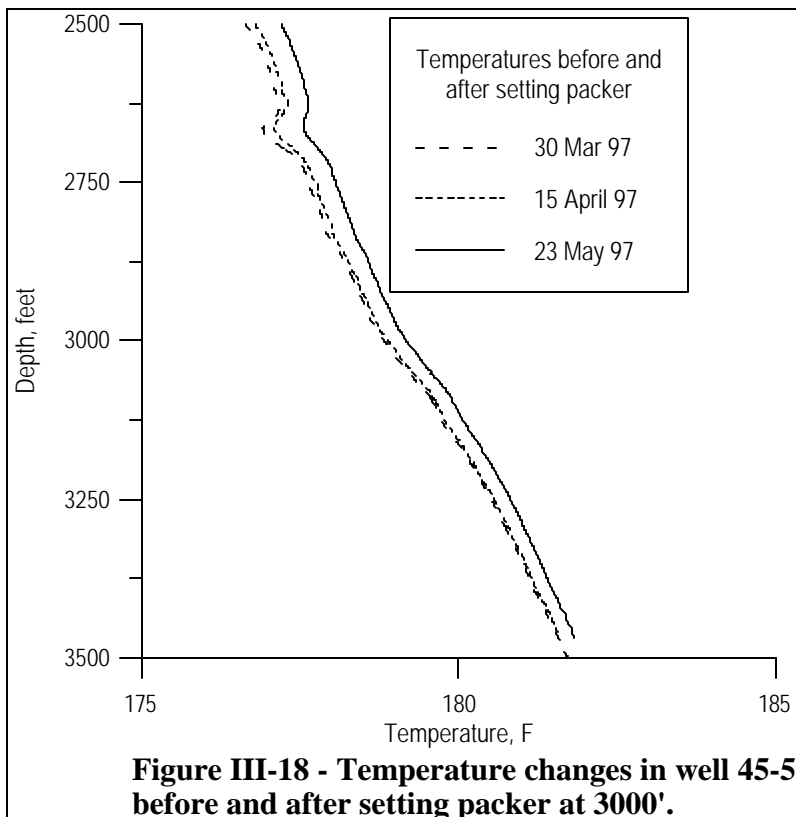
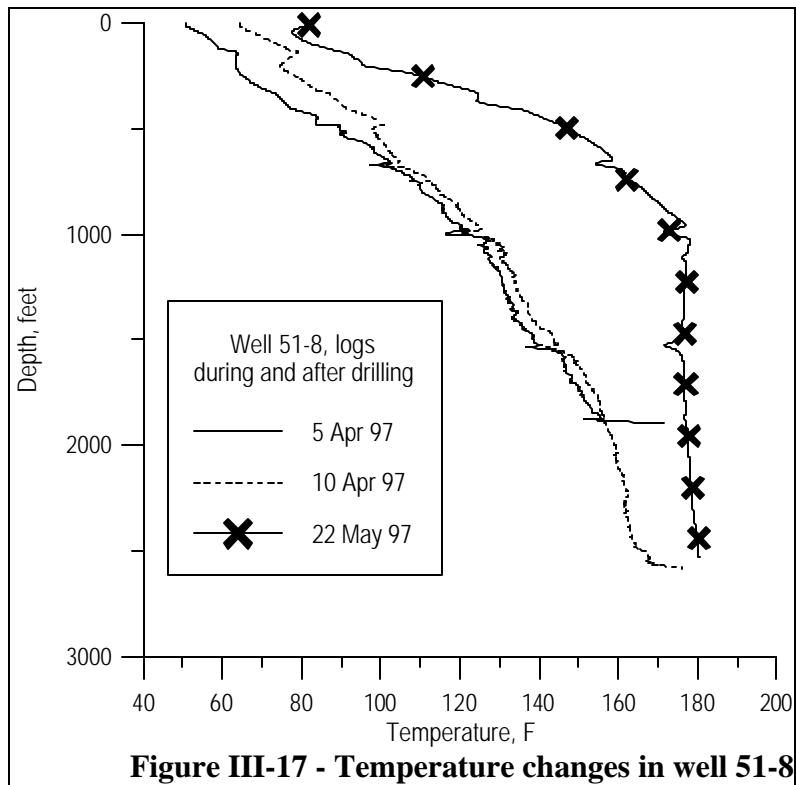
Although the data collected from these holes is typical of exploration drilling, there is still considerable uncertainty in modeling the geothermal reservoir here. Two methods appear to be important in further resolution of this structure: surface geophysics, specifically a CSAMT (controlled-source audio-frequency magnetotelluric) survey, and downhole fluid sampling.

CSAMT is a survey method¹⁰ which uses either a grounded electric dipole or a current loop as a source on the surface of the area to be investigated. When the source is excited at some frequency, then measurements of orthogonal components of the electric and magnetic fields are made over the survey area. The ratio of these orthogonal components can be used to calculate an apparent resistivity of the formation below the survey area. Since an aquifer, particularly one with hot, mineralized water, will show lower resistivity, the CSAMT survey is a means of identifying these low-resistivity zones.

As an adjunct to estimating resistivity from surface measurements, downhole sampling of formation fluids can be used to compare the water chemistry from different wells and to determine if the waters derive from the same source. Given the configuration of the wells, however, fluid sampling is not straightforward. All the wells except 45-5 are completed with tubing or liners to near TD, and 45-5 has an inflatable packer set at about 3000 feet. Bailing the packer tubing could draw formation waters into the interval below the packer, and the packer could probably be removed to sample the interval above it. The tubing in the other wells could be perforated for attempted water samples, but the heavy mud on the outside of the liners would make the source of any fluids collected uncertain.







A final option would be additional drilling, if analysis of data from the existing wells gives clear indication of where the next target should be, but that decision must await interpretation of information compiled to date.

d.6 Brief Geologic Description (summarized from Reference 11)

The McGregor Range geothermal system is one of twenty-seven known convective hydrothermal systems within the southern Rio Grande rift. Its co-location with the U. S. Army's Fort Bliss McGregor Range Base Camp provides a potential user for this geothermal resource, which is located in New Mexico about 30 km northeast of El Paso. The system is within a major Rio Grande rift structure, the Tularosa-Hueco basin, which has a major east-dipping boundary fault, the East Franklin Mountain fault, as its western margin. The geothermal system occurs along the eastern margin of the basin, within a small intra-basin uplift which is partially buried by basin fill and has bedrock outcrops at Davis Dome and in the vicinity of Meyer Range near the New Mexico border.

The geothermal system is described by a variety of geophysical and geochemical surveys which provided a framework to select the sites for the exploratory drilling. Three shallow seismic reflection profiles by the University of Texas at El Paso (UTEP) assisted in determining the depth to bedrock. The UTEP gravity and aero-magnetic data bases provided supplemental subsurface structural information. Reconnaissance geologic mapping, a radon soil gas survey, a soil mercury survey, and a shallow temperature gradient survey by New Mexico State University (NMSU) delineated the thermal regime and probable upflow zones and identified a previously unmapped Pleistocene fault. Also, a detailed self-potential geophysical survey by NMSU and the University of Utah provided additional information to assess the dynamics of the geothermal system. Published ground water and geothermal surveys provided important, but poorly constrained, information on water levels, temperature gradients, fluid chemistry, and reservoir geothermometry.

Depth to bedrock is highly variable among the drill sites. Basin fill thickness ranges from 710 feet in well 46-6 to about 30 feet in well 45-5. Basin fill consists of variably indurated pebbly-sand, sand, silt, and clay. Highly-indurated caliche (about 10 feet maximum thickness) caps the basin-fill sequence. Wind-blown sand forms a thin surficial veneer over the caliche cap.

Paleozoic limestone and dolomite and Tertiary felsite intrusives are the major bedrock units cored. Paleozoic rocks cored include: 1) Ordovician and Silurian dolomite, cherty dolomite, and chert of the Montoya Group and Fusselman formations; 2) Devonian (?) and Mississippian black argillaceous limestone and calcareous shale and dark fossiliferous and sometimes cherty limestones of the Las Cruces, Rancheria, and Helms Formations; and 3) Pennsylvanian gray to dark gray cherty, fossiliferous limestones of the Magdalena Group. Nearly all Paleozoic units have fracture permeability, but it is less in the black Mississippian limestone and shale units. Important vuggy solution porosity and permeability is prominent in the Ordovician and Silurian dolomitic units and in Pennsylvanian limestones. Also, stylolites, when present, frequently have important solution permeability. Tertiary felsite intrusives show concordant contacts and are generally interpreted as sills. Fracture permeability also occurs in the intrusive bodies.

Formation tops and thickness drilled in each well are shown below. Coring allowed and enhanced the identification and detailed characterization of several features which have important bearing on the configuration and dynamics of this geothermal system. A "blind" major thrust fault is characterized in well 51-8. The thrust fault juxtaposes gently dipping Silurian dolomite over steeply-dipping and overturned Mississippian black limestone and shale. Units on the hanging and footwall of the fault are pervasively fractured and deformed. This hidden structure may have important regional tectonic significance. In any case, the fault enhances the potential for deeply-circulating regional ground water flows through basement rocks and may help explain the McGregor geothermal system.

Well 45-5 cored a small laccolith (an intrusion of igneous rock or magma which pushes up layered rock above it). Limestone above the felsite intrusion shows moderate dips; however, the intrusion is floored by flat-lying limestone. Important fracture permeability is associated with the interior of the intrusion.

Major solution permeability is found in wells 45-5 and 46-6 and is especially dramatic in Pennsylvanian limestones near the static water level, above and below intrusive contacts, and near the bedrock-basin fill unconformity.

Well 45-5 (formation water level 466 feet)

Depth (below KB)	Unit
0-32	Tertiary/Quaternary basin fill
32-433	Pennsylvanian cherty limestone
433-464	Tertiary felsite porphyry sill
464-550	Pennsylvanian cherty limestone
550-864	Tertiary felsite porphyry sill
864-1195	Pennsylvanian cherty limestone
1195-1857	Devonian/Mississippian limestone and shale
1857-3099	Tertiary felsite porphyry sill
3099-3129	Devonian/Mississippian limestone and shale
3129-3649	Silurian Dolomite
3649-3961	Ordovician Dolomite

Well 46-6 (formation water level 451 feet)

Depth (below KB)	Unit
0-684	Tertiary/Quaternary basin fill
684-1145	Pennsylvanian cherty limestone
1145-1284	Tertiary felsite porphyry sill
1284-1741	Pennsylvanian cherty limestone
1741-2258	Devonian/Mississippian limestone and shale

Well 51-8 (formation water level 473 feet)

Depth (below KB)	Unit
0-460	Tertiary/Quaternary basin fill
460-655	Tertiary felsite porphyry sill

655-770	Pennsylvanian cherty limestone
770-1503	Devonian/Mississippian limestone and shale
1503-2239	Silurian Dolomite
2239-2240	thrust fault (gouge)
2240-2479	Mississippian limestone and shale (steeply overturned)
2479-2573	Pennsylvanian cherty limestone (steeply overturned)

Well 51-8 (formation water level 463 feet)

Depth (below KB)	Unit
0-605	Tertiary/Quaternary basin fill
605-1430	Tertiary felsite porphyry sill
1430-1760	Pennsylvanian cherty limestone
1760-2018	Devonian/Mississippian limestone and shale

III-e. Other Slimhole Experience

e.1 Oregon/Nevada¹²: Anadarko Petroleum Corporation drilled two slimhole discoveries in the 1980s, one at Salt Wells, NV, and the other at Pueblo Valley, OR. Both of these slimholes were hot enough to discharge unassisted and were successfully flow tested.

The Salt Wells hole, in west-central Nevada, was originally rotary-drilled to 530' for temperature-gradient measurements and completed with 6-5/8" casing and 2" line pipe, but later the line pipe was withdrawn and an inflatable packer on 4-1/2" tubing was set at 401 feet. One-inch line pipe was run to 105' and, after using this for an air-lift, flow through the packer (2" ID) and tubing stabilized at a rate of about 49 gpm; temperature logs after the flow gave a maximum reading of 271°F.

A confirmation well, approximately 100' from the slimhole, was drilled to a depth of 700' with 13-3/8" casing set to 385 feet. This hole flowed unassisted at approximately 347 gpm and was later pumped for 100 hours at rates up to 1750 gpm. Pressure data from this well indicated reservoir transmissivity of 800-900 darcy-feet.

A slimhole at Pueblo Valley, in south-east Oregon, was planned and permitted as a test well to evaluate an interval of fractured basalt which had been discovered while drilling an earlier thermal-gradient hole. Using a UDR1500 rig, the hole was rotary-drilled to 1087' and then core-drilled (HQ) to TD of 1479 feet. Artesian wellbore pressures during the core-drilling were controlled with weighted mud. The discharge test did not require air-lift to start and the slimhole flowed at 400 gpm through a 4" line and 3" orifice plate. Wellhead pressures and temperatures during discharge were 69-75 psig and 300-305°F, so flow was almost completely liquid, which accounts for the relatively high flow rate from this size hole. Transmissivity, estimated at 1000 darcy-feet, was also very high. Shut-in wellhead pressure was 64 psi. After a long delay from injunctions sought by environmental groups, two additional slimholes were drilled at this location in 1993 with results similar to the original well in 1989.

Using typical exploratory success rates and well costs for the Basin and Range province, the reference author estimates that slimholes could reduce exploratory drilling costs by 50% and total exploration costs by 28%.

e.2 Other Basin and Range^{13,14}: Exploratory geothermal drilling in the United States essentially began in the early to mid-1970s, and almost all of it was large-diameter. Small-diameter holes were used for temperature-gradient measurements but, for reasons which are now unclear, they were limited by regulation to an uncased depth of 500 feet. This was thought by the industry to be sufficient for prediction of temperature at depth, but the Desert Peak 29-1 well in 1974 had a major temperature-gradient reversal at 700', and subsequent wells in the next two years showed that temperature reversals below 500' were common in the Basin and Range province.

Over the next few years, a number of deeper observation boreholes (also called "strat tests") were drilled with casing to about 300' and then ~6" open hole to about 2000 feet. This depth was adequate to give linear temperature gradients below any reversals, but these wells were generally completed with hanging tubing or pipe for repeated temperature measurements and Benoit¹³ states that none were successfully flow tested. Although Desert Peak has 11 strat test holes, this technique never achieved widespread acceptance in the industry.

The first thermal gradient core-hole¹³ in the Basin and Range was PLV-1 in Long Valley caldera, drilled by Phillips Petroleum in 1982. The hole was rotary-drilled to 458', where continuous and severe lost circulation in the moat rhyolite domes prevented any further advance; a core rig was then brought on location and the hole was completed to 2345 feet. Immediately after completion of PLV-1, PLV-2 was completely and successfully core-drilled to 2085 feet. Both of these holes used core drilling strictly to solve the lost circulation problem (little analysis was done on the core) and this continued to be the principal reason for core drilling in young, highly permeable, volcanic rocks.

From 1977 to 1987 all geothermal exploration (by Unocal and Mother Earth Industries) in the vicinity of Cove Fort and Sulphurdale, Utah was done with production-size wells, but several consecutive unsuccessful holes persuaded MEI to try a slimhole exploration program. This exploratory strategy was fairly conservative, with minimum step-outs from proven producers, but had a 71% success rate in the exploratory holes. The successful slimholes were later twinned with production wells approximately 10-20 feet away, and the slimholes were used as sources of supplementary steam.

The 6-1/4" slimholes, which ranged from 628 to 2338' in depth, were drilled with a truck-mounted rig at costs between \$45,000 and \$70,000, compared to full-scale well costs of \$250,000 to \$400,000. Even these production-well costs were probably lower than usual because of the "forecast" of drilling conditions, lithology, and casing points gained from the slimholes.

e.3 Geysers Coring Project^{15,16}: As discussed above, most core-drilled slimholes have used that technology to reduce lost circulation problems, not to gain access to core for any significant amount of analysis. In contrast, the Geysers Coring Project (GCP) in 1994 was specifically directed toward retrieving enough core to study several important parameters of the world's largest developed geothermal resource.

The original drilling plan for this hole was to deepen an existing well (Unocal SB-15) by wireline coring, but the extreme difficulty of cleaning out this hole in preparation for coring led to

a sidetrack somewhat shallower than intended. In spite of this problem, the core from 251 m to 488 m depth was retrieved with almost 100% recovery and was then analyzed in several ways.

For maximum protection of the core -- preserving delicate features such as fault gouges, fracture networks, and intensely clay-altered rocks -- this project used a triple-tube coring system, which encases the core in an additional tube (inside the normal inner barrel) which allows it to be withdrawn from the core barrel but still protected by the inside tube. In this way, the project's paramount objective -- to characterize and quantify porosity, permeability, and remaining indigenous fluid saturation -- could be met with core in as nearly an *in situ* condition as possible. Several items of new information were derived from the core examination:

- Reservoir rocks in this long-produced (30 years) section of The Geysers have been mostly depleted of their indigenous water.
- Permeability in the unfractured reservoir rock are extremely low -- a few tens of nanodarcies in some cases.
- Electrical conductivity of the reservoir rocks is dependent on pore microstructure as well as pore-fluid properties.
- Open fractures and vuggy veins, which are the likely fluid-storage and fluid-transmission elements of the reservoir, are mostly high-angle, rather than low- to moderate-angle as previously thought.

This information will help steam-field operators refine reservoir models and production forecasts, but perhaps most importantly it validates the concept of wireline coring in a high-temperature, vapor-dominated geothermal regime.

e.4 Central America^{17,18,19}: From 1986 to 1990, Los Alamos National Laboratory drilled four intermediate-depth (428-808 m) exploratory slimholes in Central America to aid the national utility companies of Honduras and Guatemala in evaluation of the indigenous geothermal resources. Because of the expected lost circulation and hard, abrasive rock, minerals-type diamond core drilling was used for all these holes.

Three mostly-HQ holes were drilled near Platanares, Honduras, and two of them were successfully flow tested. Both of these slimholes had artesian flow (each of them experienced a blowout during drilling) at relatively high rates -- 400 l/min from one, 550 l/min from the other -- and temperatures approximately 160°C. These high flow rates supported estimates of permeability up to 1400 millidarcies. Flow test durations were 8-10 days; the first well experienced a sharp decrease in production due to scaling, but the second well flowed undiminished for ten days without scale problems, probably because of its higher wellhead pressure (70 psia versus 30 psia). No production wells are available for cost comparison with the slimholes, but progress up the learning curve dropped drilling costs from \$533/m for the first well to \$284/m for the third.

Another slimhole, designed to gather information on temperature gradients, stratigraphy, fracturing, hydrothermal alteration, and hydrothermal fluids, was drilled near Tecuamburro Volcano, Guatemala. This hole reached 808 m and a bottomhole temperature of 238°C, but either the formation was not permeable enough or there was not enough fluid to support a flow test (flow was started by swabbing the well, but subsided after the wellbore was purged of drilling fluids.) Integration of temperature gradients and other data indicates that this hole

probably overlies a 300°C resource at a depth of about 1100 m, but no further exploration has been done there since this drilling in 1990.

This exploratory drilling yielded a vast amount of data on lithology, structure, alterations, paragenesis, fluid inclusion history, temperature, thermal conductivity and other physical properties, surface and in-situ fluid samples, and flow tests. It is an effective, efficient, and economic exploration tool for abrasive, high-temperature rocks, with both the core and the hole providing unambiguous, reliable subsurface information.

III-f. Summary of Japanese Case Histories

f.1 Introduction and Background

As noted earlier, since a major barrier to the exploration for and assessment of new geothermal areas worldwide is the high cost of conventional rotary drilling, it would be desirable to use low-cost slim holes (≤ 150 mm diameter) for geothermal exploration and definitive reservoir assessment. Garg and Combs²⁰ presented a review, based on publicly available Japanese slimhole data, which noted that slim holes have been successfully used in Japan to (1) obtain core for geological and stratigraphic studies, (2) characterize the geothermal reservoir fluid state, and (3) provide observation boreholes in pressure interference tests. To establish the utility of slim holes for definitive reservoir assessment, however, it is also necessary to be able to predict the discharge characteristics of large-diameter wells based on injection/discharge tests of slim holes. A major goal in the slimhole program was to establish a statistically meaningful relationship between the injectivity and productivity indices of slim holes and large-diameter production and/or injection wells. Sufficient published data to establish such a relationship, however, existed neither in Japan nor elsewhere.

The U.S. Department of Energy (DOE), through Sandia National Laboratories (Sandia), initiated a research effort to demonstrate that slim holes can be used to provide reliable geothermal reservoir parameter estimates, comparable to those obtained from large-diameter wells, and to predict the discharge behavior of large-diameter wells²¹. As part of its research program, DOE/Sandia planned to drill and test slim holes paired with existing large-diameter production wells in several geothermal fields in the western United States; the first of these tests was completed at the Steamboat Hills Geothermal Field, Nevada (Section III-a). Because of fiscal constraints on the slimhole R&D program during the last few years, however, it became unlikely that sufficient U.S. data would be developed. Fortunately, the Japanese geothermal industry has had extensive experience in the use of slim holes for geothermal exploration and reservoir assessment, although most of the Japanese slim hole data are proprietary with the individual geothermal developers.

Based on personal relationships between Maxwell scientists and Japanese geothermal developers, production and injection data from 64 slim holes and 79 large-diameter wells (see table below) at four Japanese geothermal fields (Oguni, Sumikawa, Takigami, and Kirishima) have been obtained. In general, these data sets included:

- Wellbore depths, diameters, and casing programs,

- Downhole pressure, temperature, and spinner surveys from which feedzone depths can be inferred,
- Repeated temperature logs during and after drilling,
- Mass flow rates and downhole pressures during injection/discharge tests (downhole pressures were often measured at a depth much shallower than the feedzone), and
- Date and duration of injection/discharge tests.

The boreholes described in this section penetrated a number of different formations (see the stratigraphic sequences later in this section) but both time and cost data for drilling are still considered proprietary, so it is not possible to make the same kinds of comparisons given in earlier sections. The rotary large-hole drilling and wireline coring for slimholes were similar to cases already described, however, and it is reasonable to assume that the same sort of cost relationship existed.

Geothermal Field	Slim Holes	Large-Diameter Wells	Total Boreholes
Oguni, Kyushu	15	10	25
Sumikawa, Honshu	15	11	26
Takagami, Kyushu	11	27	38
Kirishima, Kyushu	23	31	54
Totals	64	79	143

The data described above were analyzed to establish and examine the following relationships:

- (1) between injectivity and productivity indices,
- (2) between productivity/injectivity index and borehole diameter, and
- (3) between discharge capacity of slim holes and large-diameter wells²²⁻²⁷.

In addition, repetitive surveys of downhole temperature and standing water level were performed in most of the boreholes for at least several days after cold-water injection was terminated. These heat-up surveys permit the estimation of reservoir pressure and temperature.

Summary conclusions on wellbore relationships:

For boreholes with liquid feedzones, the productivity and injectivity indices are more or less equal. Except for Oguni boreholes, the productivity and injectivity indices display no correlation with borehole diameter. Thus, the productivity index (or, more importantly, the injectivity index when there is no discharge data) from a slim hole with a liquid feed can provide a first estimate of the probable discharge capacity of a large-diameter geothermal production well in the same reservoir. The large-diameter wells at the Oguni, Sumikawa and Kirishima Geothermal Fields have a more or less uniform inside diameter and the discharge capacity of these wells (with liquid feedzones) can be predicted using the “scaled maximum discharge rate” of Pritchett²⁸ in conjunction with discharge data from slim holes.

Because the large-diameter Takigami wells had a non-uniform internal diameter, it was not possible to use a simple scaling rule to relate the discharge capacities of slim holes and large-diameter wells. A numerical simulator was used to model the available discharge data from Takigami boreholes and those results indicate that the flow rate of large-diameter production

with Sandia National Laboratories -- approached several Japanese geothermal developers for release of their proprietary data for use in the DOE/Sandia slimhole program. As a result of these negotiations, Maxwell was fortunate to obtain permission from Electric Power Development Company (EPDC) for use of pertinent data from the Oguni Geothermal Field. The Oguni Geothermal Field, Kumamoto Prefecture, northern Kyushu, Japan, is a particularly good candidate for a case history on the use of slim holes in geothermal exploration and reservoir assessment. The detailed analysis of the borehole data from the Oguni Geothermal Field, from which the information presented in this handbook was derived, is presented in Refs 22, 23, and 29. Since 1983, EPDC had carried out an extensive exploration and reservoir assessment program in the area. As of mid-1993, EPDC had drilled and tested more than twenty boreholes ranging in depth from 500 to 2000 meters. EPDC had utilized slim holes not only for selecting large-diameter well locations, but also for predicting the production capacity of the large-diameter wells being drilled. An article by M. Abe of EPDC, reproduced in Appendix A of Ref. 29, explains in some detail EPDC's approach to the use of slim holes in geothermal exploration and reservoir assessment.

The Oguni and the Sugawara Geothermal Fields together comprise the northwestern Hohi geothermal region, Kumamoto and Oita Prefectures, northern Kyushu, Japan (see Figure III-19). The Hohi geothermal region is an area of numerous hot springs, approximately 40 km southwest of the coastal resort of Beppu, and some 20 km north of Mt. Aso, an active caldera. The New Energy and Industrial Technology Development Organization (NEDO) carried out a regional (200 km² area) exploration program in the Hohi area during the years 1979–1985. This work resulted in the identification of a high permeability geothermal area in the northwestern Hohi area.

EPDC initiated a geothermal exploration program in the Oguni area in 1983. The Oguni field is located at the northeast end of Kumamoto Prefecture. Oita Prefecture is to the north and northeast of the Oguni area. The Sugawara field, to the north of the Oguni area, is being surveyed by NEDO as a possible site for the demonstration of a binary power plant. Although the northern Hohi area has been subdivided into two separate geothermal fields (Oguni and Sugawara), the area constitutes a single hydrological unit.

The topography of the Oguni field is dominated by Mt. Waita, which rises to an elevation of about 1500 m ASL (meters above sea level) to the southeast of the field. Many of the boreholes are located on the flanks of Mt. Waita. The Oguni boreholes are in Kumamoto Prefecture. Striking WNW-ESE is the valley containing the hot spring areas (and towns) of Takenoyu and Hagenoyu. To the north of the valley is the Sugawara plateau (in Oita Prefecture) where NEDO has drilled a number of boreholes (BS series, Figure III-19) for a binary power plant. The Takenoyu/Hagenoyu valley forms a natural division of the field into two parts, north and south of the valley.

The subsurface stratigraphy and structure in the northern Hohi area is shown in Figures III-20. The granitic basement (not shown in Figure III-20) was encountered in only two boreholes (DW-7 and DY-2) at about –960 m ASL in the Oguni area, and drops off steeply to the northeast in the Sugawara area. In order of increasing depth, the stratigraphic sequence above the granitic basement consists of the following:

- Kuju formation:** Upper Pleistocene volcanics, apparently functioning as a caprock for the geothermal system, consisting of Waita and Itchimoku lavas, Yamakawa tuff breccia.
- Kusu formation:** Lower to middle Pleistocene, Nogami mudstones and Machida lava, the Nogami mudstones appears to function as a caprock for the geothermal system.
- Hohi formation:** Lower to middle Pleistocene, consisting of the Kotobakiyama, Nambira, and Hatchobaru lavas, pyroxene andesitic rocks.
- Shishimuta formation:** Late Pliocene to early Pleistocene, dacitic pyroclastics.
- Taio formation:** Pliocene, altered andesitic pyroclastics.

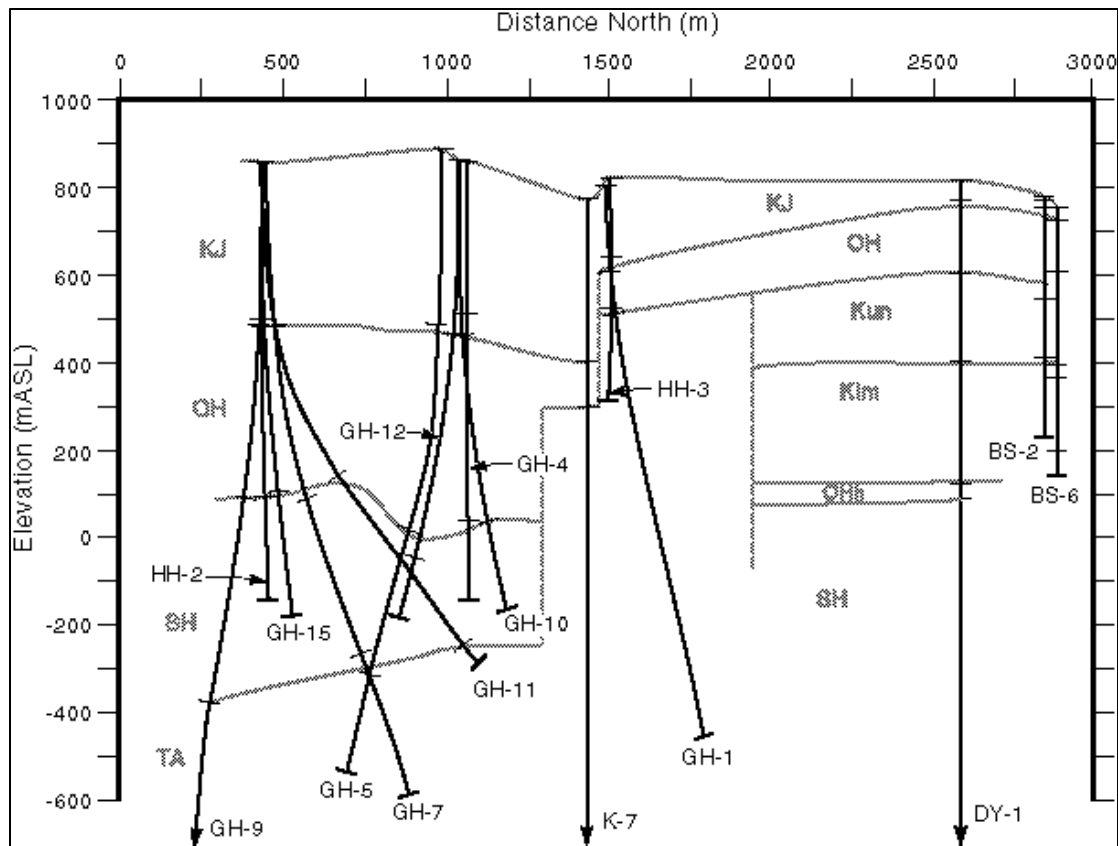


Figure III-20 Oguni Stratigraphic Cross-section

Garg, *et al.* have analyzed^{22, 23, 29} drilling information, and downhole pressure, temperature, and spinner surveys for 45 boreholes in the northern Hohi area in an effort to deduce feedzone depths and pressures. The feedzone pressures imply that the northern Hohi region consists of two pressure zones (a high pressure zone in the area of boreholes GH-15, GH-19, GH-6, HH-2, N2-KW-3 and DY-2 in the southern part of the Oguni field; a low pressure zone in the central and northern parts of the area shown in Figure III-19). At present, the reasons for the

existence of two pressure regions in close proximity to each other (within at most a few hundred meters) are poorly understood.

The feedzone pressures (at feedzone elevation, Z) for the “low-pressure zone” boreholes can be fit by the following correlation:

$$P = 56.0888 - 0.08531Z^*$$

$$Z^* = Z + 7.619(x_N - 15)$$

where P is in bars (absolute), Z^* and Z are in m ASL, and x_N is the distance in kilometers from the origin of the Central Kyushu Co-ordinate System. As can be seen from Figure III-21, the pressure correlation agrees closely with all the pressure measurements for low-pressure zone boreholes. The pressures for “high-pressure zone” boreholes (GH-6, GH-15, GH-19, HH-2,

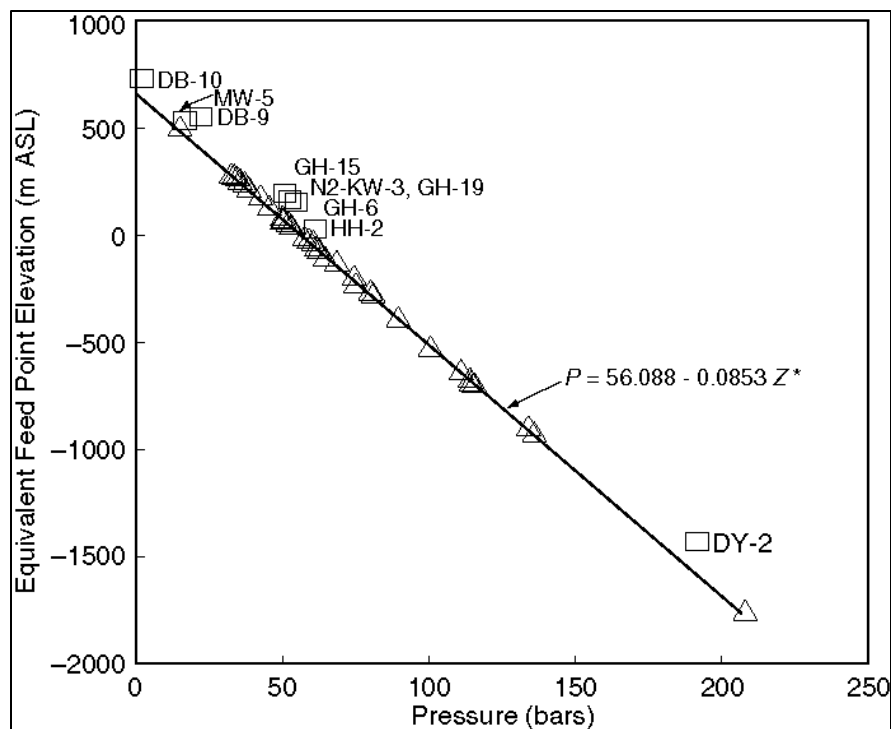


Figure III-21 Oguni Pressure vs. Elevation

DY-2, N2-KW-3) do, however, lie considerably above the straight line in Figure III-21, as do those from the shallow boreholes (MW-5, DB-9, DB-10) which do not penetrate the deep reservoir.

The vertical pressure gradient in the Oguni/Sugawara area is 8.531 kPa/m and corresponds to a hydrostatic gradient at $\sim 195^\circ\text{C}$. This implies fluid upflow in regions of the reservoir where temperature exceeds 195°C . The pressure correlation also implies that pressures decrease to the north; the pressure gradient is ~ 0.65 bars/km. Thus, in the natural state there exists a regional flow (to the north) in the northern Hohi area.

The Oguni reservoir fluid is single-phase liquid. The geothermal boreholes do not provide any direct evidence of a two-phase zone at depths greater than 300 meters in the Oguni area. (The feedzones for all of the Oguni boreholes are deeper than 400 meters.) The presence of boiling at shallow depths (*i.e.*, depths less than 300 meters) is, however, suggested by the occurrence of warm and boiling steam-heated sulfate and bicarbonate spring waters in the Takenoyu and Hagenoyu areas.

EPDC has performed numerous pressure transient tests to define the detailed permeability structure in the Oguni/Sugawara area. The available data set includes (1) cold fluid injection and fall-off tests in single boreholes, (2) pressure drawdown (*i.e.*, production tests) and buildup tests in single boreholes, and (3) pressure interference tests involving multiple boreholes. A detailed consideration of pressure interference data is, however, outside the scope of this handbook. Analyses of pressure interference data from the low-pressure zone boreholes imply that the northern Hoho reservoir has a transmissivity of about 100–250 darcy-meters²⁰. In contrast to the high transmissivity obtained in the low-pressure zone, the high-pressure zone has only a modest transmissivity (~ 15 darcy-meters).

f.3 Sumikawa Geothermal Field, northern Honshu, Japan

The Sumikawa Geothermal Field (Figure III-22) is located in the Hachimantai volcanic area in northern Honshu, Japan, about 1.5 kilometers to the west of Ohnuma geothermal power station operated by Mitsubishi Materials Corporation (MMC). The Hachimantai area also includes the

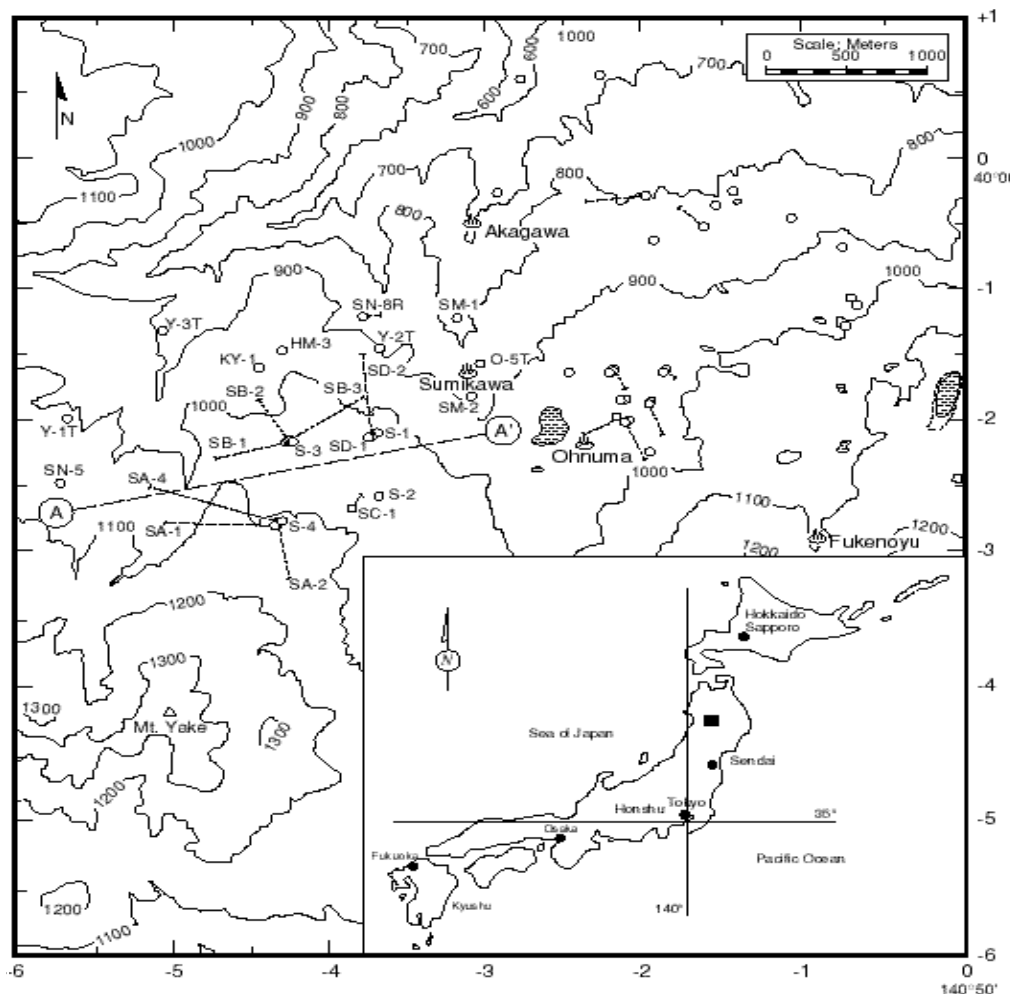


Figure III-22 Sumikawa Location Map

Matsukawa and Kakkonda Geothermal Fields. After the completion of the Ohnuma power station (~ 10 MWe) in 1973, MMC began to conduct exploratory investigations of the Sumikawa geothermal prospect. An extensive well drilling and testing program was initiated in October 1981 with the spudding of boreholes S-1 and S-2 by MMC and the Mitsubishi Gas Chemical Corporation (MGC). NEDO became involved in the field characterization effort with the drilling of borehole N59-SN-5 (~ 2 km west of S-1 and S-2) in 1984–1985.

During the years 1986–1990, under NEDO sponsorship, S-Cubed carried out geothermal reservoir engineering studies of the Sumikawa Geothermal Field. All aspects of the five-year study of the Sumikawa Geothermal Field performed by S-Cubed have been summarized³⁰ by Pritchett, *et al.* The detailed analysis of the borehole data from the Sumikawa Geothermal Field, from which the information presented in this handbook was derived, is presented in Ref. 24. The field exploration and characterization program at Sumikawa was successfully concluded in 1990 with a decision to build a power plant. The Sumikawa Geothermal Power Plant (50 MW) of Electric Power, Co., Inc., fueled by MMC from the Sumikawa Geothermal Field, was placed in commercial operation in 1995.

The Sumikawa/Ohnuma geothermal area is shown in Figure III-22. The area depicted is about 42 km²; the Sumikawa Geothermal Field lies in the western part of the area. The terrain is extremely irregular. Mt. Yake lies to the southwest of the Sumikawa area, and Mt. Hachimantai is just to the southeast (outside the area illustrated in Figure III-22). To the north of these volcanic peaks, the terrain drops away rapidly. Between the Sumikawa prospect (which may be regarded as centered in the neighborhood of the S-series boreholes, S-1, S-2, S-3, and S-4) and the Ohnuma borefield is a north-south region of relatively low ground surface elevation where natural hot springs and fumaroles are found.

The Sumikawa/Ohnuma area lies within a north-south oriented regional graben structure which extends many kilometers both north and south of the Sumikawa area. Indeed, the Sumikawa Geothermal Field itself appears to be located along the western edge of the graben.

The Sumikawa/Ohnuma area lies within a north-south oriented regional graben structure which extends many kilometers both north and south of the Sumikawa area. Indeed, the Sumikawa Geothermal Field itself appears to be located along the western edge of the graben.

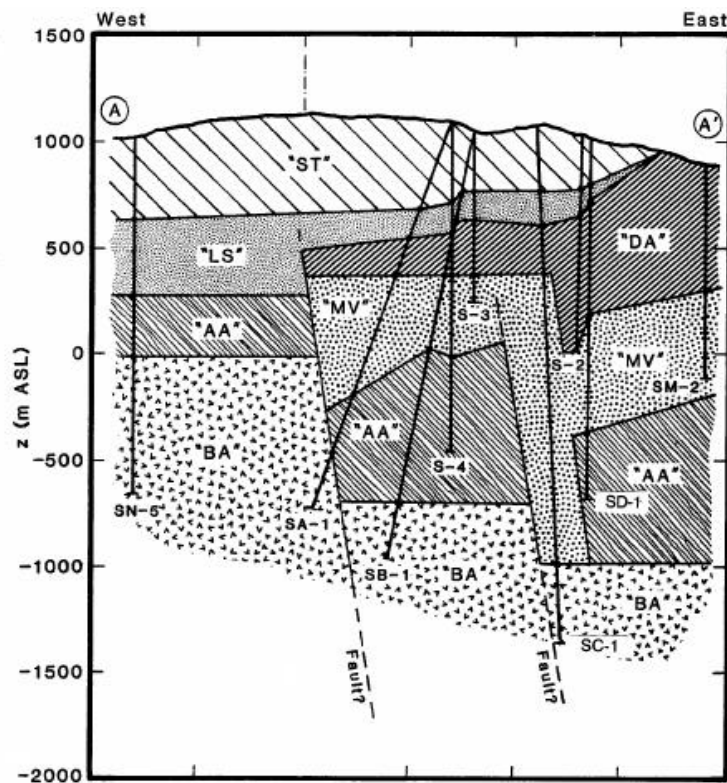


Figure III-23 Sumikawa EW Cross-section

An east-west cross section corresponding to line A-A' is depicted in Figure III-23. These structural interpretations are based almost exclusively upon drilling experience—the only available seismic survey was far too regional in scope to be useful for local structure interpretation, and the results of a gravity survey are difficult to interpret because of a lack of density contrast among the various subsurface formations in the area.

Extensive faulting has rendered the detailed geological structure at Sumikawa somewhat obscure, but the abundance of drilling logs from the various boreholes in the area has revealed an underlying geological sequence which applies to most of the area illustrated in Figure III-22. In order of increasing depth, these formations are:

- ST formation:** Surficial andesitic tuffs, lavas, and pyroclastics of recent origin (from Mt. Yake).
- LS formation:** Lake sediments; Pleistocene tuffs, sandstones, siltstones, and mudstones.
- DA formation:** Pliocene dacites, dacitic tuffs, and breccias.
- MV formation:** “Marine/volcanic complex”; interbedded Miocene dacitic volcanic rocks and “black-shale” oxygen-poor marine shales and sediments.
- AA formation:** Altered andesitic rocks that apparently are extensively fractured.
- BA formation:** Crystalline intrusive (?) rocks (mainly granodiorite and diorite).

The BA formation is the deepest so far encountered by drilling (well SC-1 bottomed in the BA formation at 2486 m depth), but the pre-Tertiary basement, which presumably underlies the above sequence, has not yet been reached. Little evidence exists that there is significant permeability deep within the BA formation, however, it may be permissible to regard this formation as the “basement” from a hydrological standpoint.

The highest temperature so far measured in the field is at the bottom of well SA-2 (320°C at 840 m below sea level). SA-2 is also the southernmost deep borehole at Sumikawa. Temperatures are significantly higher at Sumikawa (near the S-series boreholes) than at the nearby operating Ohnuma borefield. On the whole, temperatures appear to increase monotonically with depth and large-scale temperature inversions (with the exception of well SC-1) are not observed.

Pritchett, *et al.*, have examined³⁰ the various downhole feedpoint pressure determinations available from boreholes in the Sumikawa/Ohnuma area in detail. Evidence from a series of thirty-two shallow (80 m) heat-flow holes drilled throughout the area (but not shown in Figure III-22) indicates that near-surface pressures are cold-water hydrostatic relative to a water table depth that follows the local surface very closely. The water table is approximately 45 (± 21) m below ground. At great depth, however, pressures are surprisingly uniform throughout the area; apart from a small region immediately adjacent to the Ohnuma Geothermal Power Plant, deep shut-in pressures may be determined from the empirical correlation

$$P = 61.170 - 79.985Z - 6.492Z^2$$

where P is the feedzone pressure in bars, Z is elevation, measured in kilometers with respect to sea level (km ASL). The standard deviation of this correlation from the measurements is only 0.88 bars (comparable to the reliability of the pressure determinations themselves).

This “deep pressure correlation” is in excellent agreement with measurements (Figure III-24). This dependence of deep pressures on elevation and not on depth is in sharp contrast to the situation at shallow depths, where the reverse is true (see above). The pressure data from several boreholes in the Ohnuma borefield, obtained prior to the startup of Ohnuma Geothermal Power Plant, are also in good agreement with the deep correlation obtained above.

The Ohnuma Geothermal Power Plant started producing electric power in 1973. The sparse pressure data available for the Ohnuma boreholes suggest that the pressures at Ohnuma have fallen by several bars during the last 17 years. Since the pressure measurements upon which the deep

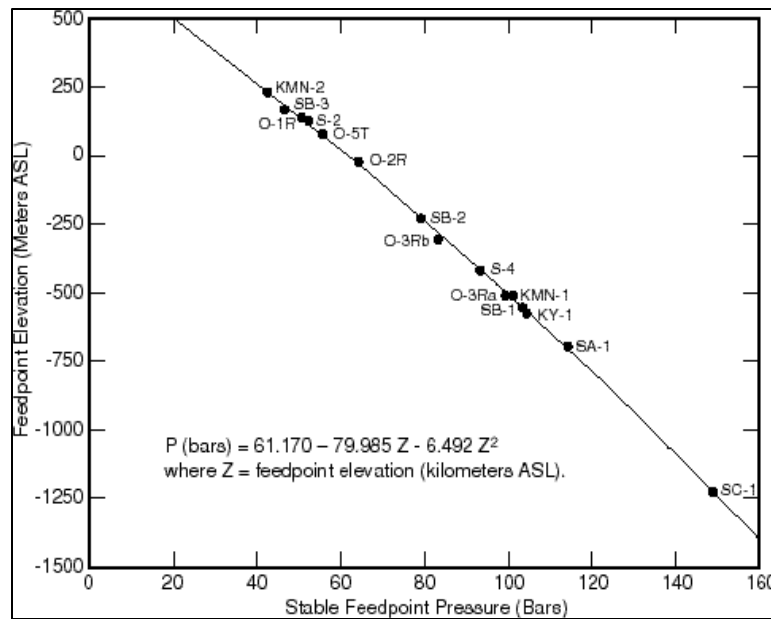


Figure III-24 Sumikawa Pressure vs. Elevation

based were made between 1968 and 1988 (average date = 1980), it is apparent that any pressure disturbance induced by operations associated with the Ohnuma power station must be of limited areal extent. According to Pritchett *et al.*³⁰, the influence of Ohnuma operations is confined to a north-south channel which extends 1.5-km north of the power station and an undetermined distance south of Ohnuma, but which appears to be only about one kilometer wide in the east-west direction.

It is virtually certain that a two-phase (water and steam) flow region is present in the southern part of the reservoir system at depth, extending from the lower part of the lake sediment layer (600 m ASL to 800 m ASL) down to a considerable depth. Slim hole S-1 (feedpoint elevation ~ 580 m ASL) discharged nothing but dry steam. Furthermore, it appears that the two-phase region in the neighborhood of borehole S-3 reaches at least as deep as +400 m ASL. Since temperatures generally increase to the south in the Sumikawa area, it would appear that the depth of the bottom of the two-phase zone will likewise increase to the south.

The deep pressure correlation yields one atmosphere pressure at $Z = +711$ m ASL; it follows that in regions with lower ground surface elevation, underground pressures must be lower than the above. Indeed, measured pressures in boreholes in the extreme northern part of

the area are less than the above correlation. The clear implication is that a deep reservoir boundary must be present, oriented roughly east-west, at about the location of the 750 m ASL ground surface elevation contour.

The vertical permeabilities at Sumikawa are small in comparison with horizontal permeabilities. Permeability in the field is due primarily to the pervasive network of fractures. Both the volcanic and sedimentary country rocks between the fractures appear to be essentially impermeable.

The lake sediments are nearly impermeable and act as a caprock for the underlying geothermal reservoirs. Pressure transient tests have been interpreted^{26, 30} to imply the presence of two high-transmissivity geothermal aquifers within the “altered andesite” and the deeper “granodiorite” formations. The shallower of these two reservoirs (in the andesite formation) is usually encountered between 1000 and 1800 meters depth, and has been penetrated by several wells. At present, only well SC-1 produces a substantial quantity of hot fluid from a permeable horizon in the “granodiorite” formation. Pressure interference data have also been used to confirm the presence of a moderately transmissive layer in the “marine-volcanic complex” formation. Because of its low vertical permeability, the “marine-volcanic complex” formation will be used for injecting waste brine.

Discharge tests have shown that production wells SA-2 and SA-4 produce essentially dry steam from entries in the “altered andesite” formation. This is somewhat puzzling in that pressure interference data indicate (see above) that the “altered andesite” formation is characterized by high transmissivity. Perhaps, the production of dry steam is associated with the nature of permeability (*i.e.*, high permeability fractures separated by low permeability matrix blocks) encountered in the “altered andesite” layer.

f.4 Takigami Geothermal Field, northern Kyushu, Japan

The Takigami Geothermal field is located in northeastern Hohi geothermal region, Oita Prefecture, northern Kyushu, Japan. The Otake and Hatchobaru geothermal power stations are situated about 15 km to the southeast of the Takigami area. The Hohi geothermal region also includes the Oguni and Sugawara Geothermal Fields. Although the Hohi region contains numerous hot springs, fumaroles and hydrothermal alteration halos, no surface geothermal manifestations are present in the Takigami area.

Since 1979, Idemitsu Geothermal Company, Ltd. (Idemitsu) has carried out extensive geological, geochemical, and geophysical surveys, as well as a comprehensive well drilling program in the area. Because of the lack of surface manifestations, the boreholes were sited on the basis of magnetotelluric, remote sensing, and other geophysical surveys³¹. As of early 1995, Idemitsu had drilled more than thirty-five boreholes (including re-drills and side-tracks) in the area. The detailed analysis of the borehole data from the Takigami Geothermal Field, from which the information presented in this handbook was derived, is presented in Ref. 25. Idemitsu and Kyushu Electric Power Company (KEPCO) commissioned the 25-MWe Takigami Geothermal Power Plant, fueled by the Takigami Geothermal Field, in 1996.

The Takigami borefield is shown in Figure III-25; the area depicted is about 24 km². The terrain is highest in the southwest, and drops off to the north and to the east. Idemitsu has used

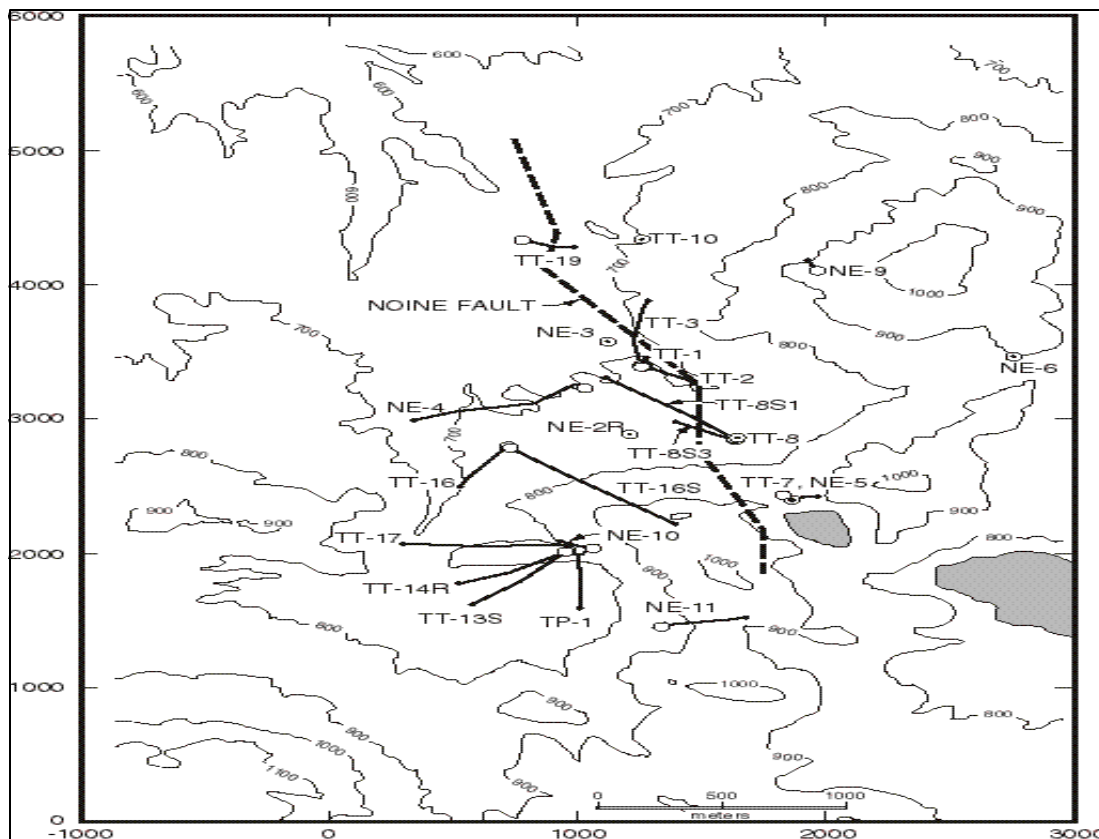


Figure III-25 Takigami Location Map

numerous drilling logs to delineate the geological sequence which underlies the Takigami area. In order of increasing depth, these formations³² are (Figure III-26):

Noinedake volcanics: Late Pleistocene (0.4–0.7 Ma) volcanics from Mt. Noine (mainly andesite).

Kusu formation: Late Pleistocene volcanics.

Ajibaru formation: Late Pleistocene (0.7 Ma) volcanics (mainly andesite).

Takigami formation: Early Pleistocene volcanic rocks. Takigami formation is subdivided into upper (dacites), middle (andesites) and lower (dacites) parts.

Usa group: Tertiary rocks comprised of altered andesite lava flows and pyroclastics.

The Usa group is the deepest so far reached by drilling; the deepest borehole at Takigami (TT-1) bottomed in this formation at –2293 m ASL. The pre-Tertiary granitic basement has yet to be encountered at Takigami.

At Takigami, subsurface temperatures are highest in the south and southwest, and decline to the north and to the east. The highest temperature (250°C) so far measured at Takigami is in borehole NE-10 at –1330 m ASL in the southern part of the field. Temperatures in excess of 240°C have been recorded in southern boreholes NE-4, TT-13S, TT-14R and TT-16S. A

detailed examination of feedpoint pressures for Takigami boreholes indicates that the stable

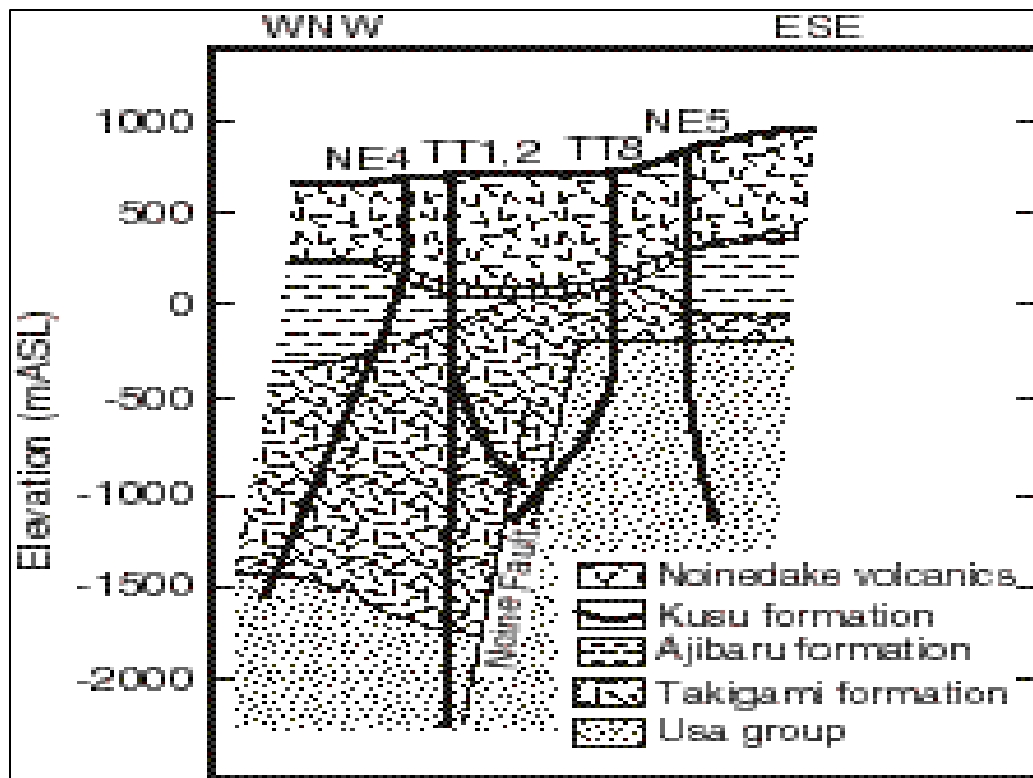


Figure III-26 Takigami EW Cross-section

shut-in pressures (Figure III-27) are closely fit by the following empirical correlation:

$$P = 51.144 - 0.08651 (Z + 25.52 X_E),$$

where P is the feedzone pressure in bars, Z is the feedzone elevation in meters above sea level (m ASL), and X_E is the distance to the east in kilometers from the origin ($33^{\circ}11'$ latitude, and $131^{\circ}16'$ longitude).

The vertical pressure gradient in the Takigami Geothermal Field is 8.651 kPa/m and corresponds to a hydrostatic gradient at about 185°C. This implies fluid upflow in regions of the subsurface where temperatures exceed 185°C. The pressure correlation indicates a regional pressure gradient (and hence fluid outflow) to the east. The Takigami temperatures and pressures are such that the reservoir fluid is single-phase liquid in the natural state. Furthermore, production from all the existing Takigami boreholes is not accompanied by *in situ* boiling.

As discussed above, most of the feedzones for Takigami boreholes are located in the lower Takigami formation and Usa group. Permeability in the Takigami Geothermal Field, like other volcanic geothermal areas, is due primarily to the pervasive network of fractures. Idemitsu has performed several long-term pressure interference tests; data from

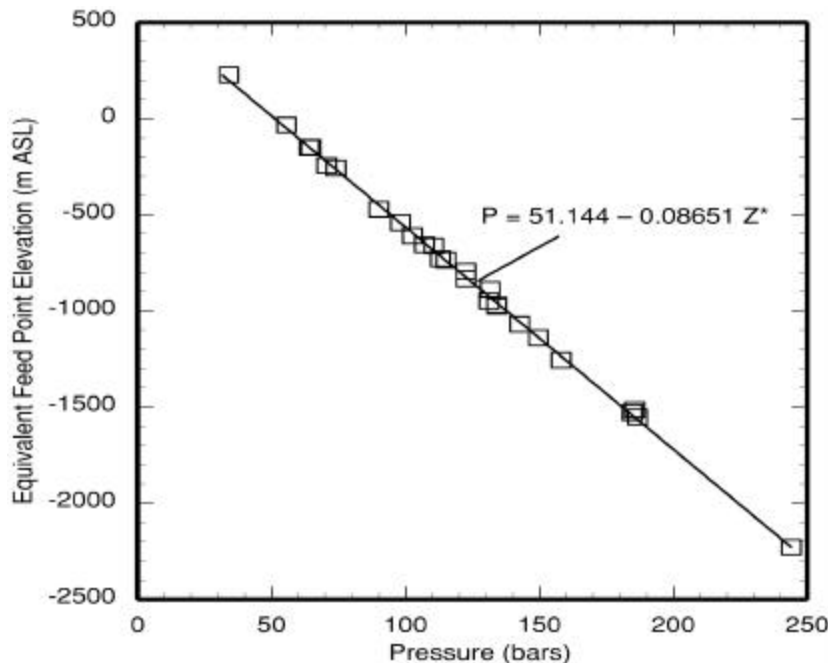


Figure III-27 Takigami Pressure vs. Elevation

these tests have been analyzed in Refs. 33, 34, and 35. The transmissivity (*i.e.*, permeability-thickness product) for the southwestern part of the field (*i.e.*, production area) is estimated³³ to be ~50 darcy-meters. Analyses of pressure interference data also indicate³⁴ that the transmissivity in the northern sector of the field (injection area) is much higher (200 to 300 darcy-meters).

f.5 Kirishima Geothermal Field, southern Kyushu, Japan

The Kirishima Geothermal Area is located in the Kagoshima Prefecture of southern Kyushu, Japan, in the Kagoshima graben (a volcano-tectonic depression) which trends from NNE to SSW. The Kirishima Geothermal Field is situated about 40 km north of the presently active Sakurajima volcano in a belt of recently active volcanoes, fumaroles, numerous hot springs, and hydrothermal alteration halos. The Kirishima volcano is located about five kilometers to the east of the explored geothermal area which is located on the southwestern flank of the volcano (see Figure III-28). The field is underlain almost entirely by young volcanic rocks of early to late Pleistocene age. These volcanic rocks overlie the pre-Neogene basement rocks of the Shimanto supergroup.

Geothermal exploration of the Kirishima area was commenced in 1972 by Nittetsu Mining Co., Ltd. (NMC) with conducting of surficial geological surveys, electrical soundings, heat measurement surveys and 30 m-deep heat flow holes. Based on the results of these exploratory surveys, NMC and Nippon Steel Co., Ltd (NSC) drilled 23 exploratory boreholes, of which eight were slim holes. Of the other fifteen large-diameter wells, three were eventually converted to production wells and two were converted to injection wells. During the period from 1975 to 1985, NEDO drilled an additional fifteen exploratory slim holes in and around the immediate vicinity of the Kirishima Geothermal Field. After 1985, the geothermal exploration has been

focused on the Ginyu fault area which occupies a northern section of the Kirishima area, covering an area about 1km by 2 km in areal extent. Based on the discharge and injection data obtained from these 38 exploratory boreholes, NKGK drilled sixteen large-diameter production and injection wells in the Ginyu area during 1990 and 1991. Subsequently, NKGK confirmed that the Kirishima reservoir is sufficient for supplying a geothermal power plant of 30 MW capacity. The detailed analysis of borehole data from the Kirishima Geothermal Field, from

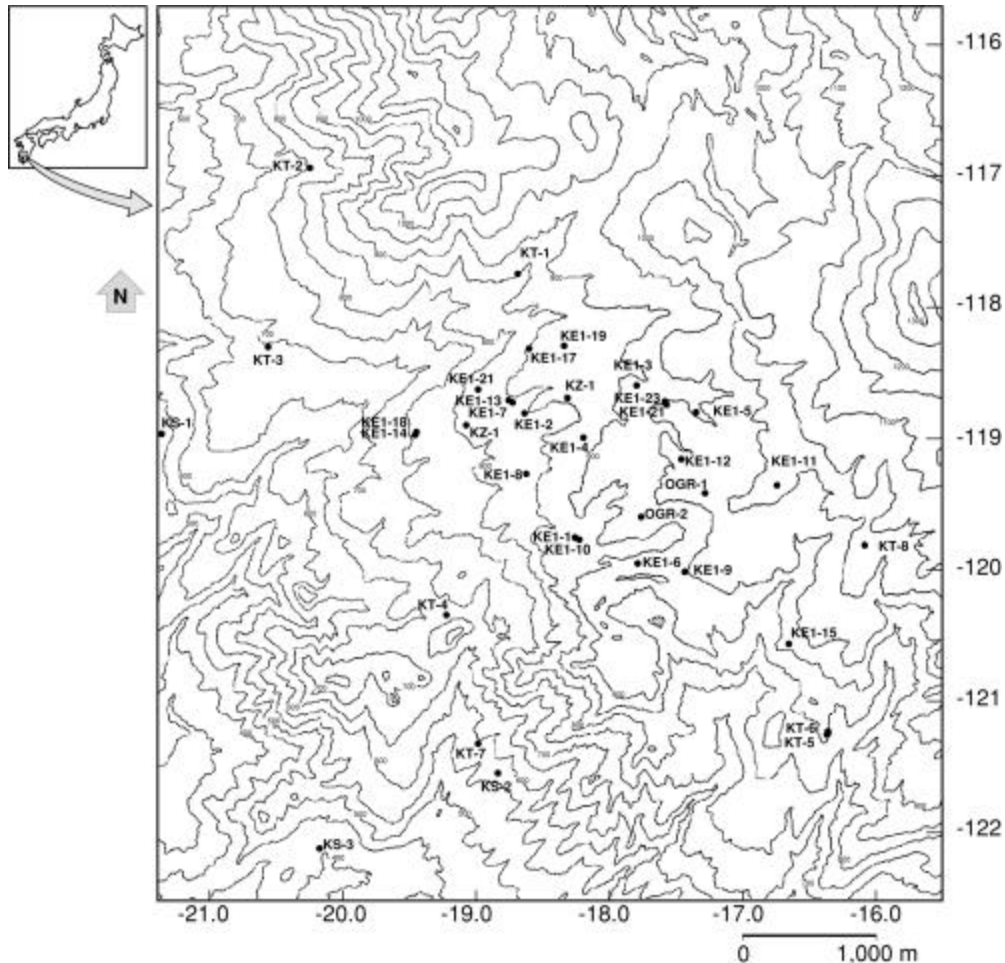


Figure III-28 Kirishima Location Map

which the information presented in this handbook was derived, is presented in Ref. 27.

Of the 54 boreholes, including re-drills, the total depths range from about 1000 to 2000 meters. The deepest borehole in the Kirishima field (slim hole KE1-4) was drilled to a total depth of about 2000 meters. The production wells in the Ginyu fault zone, supplying the Ogiri Geothermal Power Plant, have a base temperature of about 230°C and the feedzones are situated between about 1100 and 1350 meters true vertical depth. The reservoir fluid in the Kirishima Geothermal Field is single-phase liquid at feedzone depth for most of the boreholes; thus, discharge from both the slim holes and large-diameter wells does not lead to *in situ* boiling. However, two-phase conditions seem to exist at shallow depths in the Ginyu fault zone and the discharge from two slim holes and one large-diameter well is accompanied by *in situ*

boiling. Outside the Ginyu fault zone, the formation permeability is low, and well discharge often leads to *in situ* boiling.

In the vicinity of the Kirishima volcano, especially on the western flank where the Kirishima Geothermal Area is located, surface thermal manifestations such as fumaroles, hot springs, and altered zones are widely developed.

Vigorous volcanic activity took place in the Pleistocene epoch and has continued until the present. The Sakurajima volcano is presently erupting, depositing a thick pile of volcanic rocks, such as andesitic lava flows and pyroclastics with minor lake deposits. These young volcanic rocks reach 2000 meters and more in thickness in the area. These volcanic rocks overlie the Pre-Neogene basement rock of the Shimanto supergroup. The Shimanto supergroup, basement in the Kirishima area, outcrops at the southeastern end of the Kirishima volcano and throughout southern Kyushu. The Shimanto was first encountered³⁶ in slim hole N56-KT-7 at a depth of -1070 meters, drilled by NEDO. A correlation between the outcropping of the Shimanto supergroup (300-400m above sea level) and exploratory slim hole N56-KT-7 (-1070m below sea level) indicated that the basement of the Kirishima Geothermal Field is depressed to a depth of more than 1300 meters.

The Kirishima Geothermal Field, the so-called Ginyu/Ogiri borefield, covers an areal extent of about 1 km by 2 km. The terrain is highest in the northeast, and drops off to the southwest. NKGK has used numerous drilling logs to delineate the geological sequence and hydrothermal alteration which underlies the Kirishima area. The chlorite-sericite zone occurs in the deeper part of the boreholes with increasing temperature. The upper level of the crystallization of quartz and wairakite coincides with the present isotherms of 100°C-180°C and 190°C-240°C, respectively, which suggests³⁶ that the hydrothermal system in the Kirishima area is now active. In order of increasing depth (see Figure III-29), these formations in the Kirishima area are^{36,37} the following:

Older Kirishima Volc. Rock:	Late Pleistocene to Recent (0.13 - 0.60 Ma), consists of the following two units that have been identified and age dated.
Old Shiratori Lava:	Late Pleistocene, andesitic lava flows and pyroclastics.
Takahara Conglomerate:	Late Pleistocene (0.028 Ma), pyroclastics and minor lake deposits.
Kakkuto Andesites:	Pleistocene (0.23 - 1.21 Ma), consists of the following three separate lavas that have been identified and age dated.
Kurino Lava:	Late Pleistocene (0.12 - 0.60 Ma), mostly andesitic lava flows, locally hydrothermally altered and acts as impermeable zone.
Sagari Lava:	Middle Pleistocene (0.96 Ma), mostly andesitic lava flows, locally hydrothermally altered and acts as impermeable zone.
Makizono Lava:	Middle to Early Pleistocene (0.70 - 1.21 Ma), upper and middle lavas have undergone extensive hydrothermal alteration and act as caprock, faulted materials and feedzones in many boreholes occur in lower lavas.

- Ebino Formation/Iino Lava:** Early Pleistocene (1.37 Ma), most borehole feedzones occur in these units.
- Kirishima Welded Tuff:** Early Pleistocene (1.50 - 2.3 Ma), pyroclastics and welded tuffs.
- Shimanto Supergroup:** Tertiary (>25.0 Ma), basement in the Kirishima area, highly decomposed, mainly consisting of sandstones and shales.

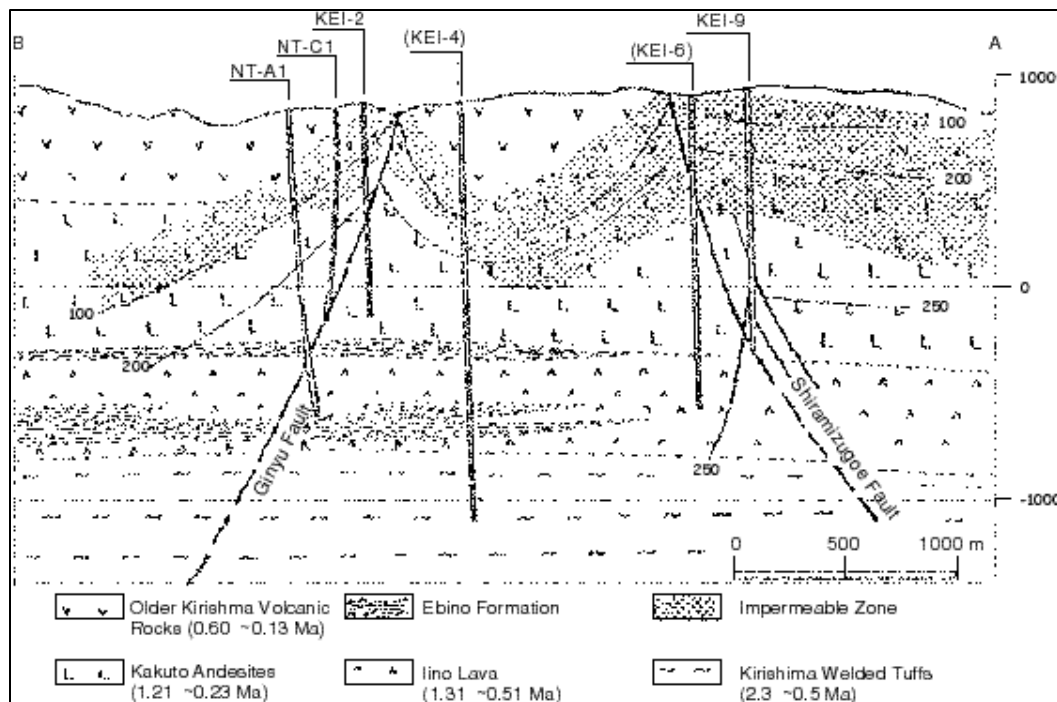


Figure III-29 Kirishima Geological Cross-section

Most of the feedzones for the Kirishima boreholes tend to align along the faults and are located in the Makizono lavas, Ebino formation and Iino lavas. Most of the boreholes have no feedzones in the upper and middle Makizono lavas which have undergone extensive hydrothermal alteration; and therefore, this relatively impermeable region of the Makizono lavas acts as a caprock for the Ginyu/Ogiri reservoir.

The Kirishima Geothermal Area, generally ranging in altitude from 600 meters to 1000 meter, is located on the southwestern slope of the Kirishima volcano. The geothermal manifestations of the Kirishima Geothermal Field have been thought to be controlled in their distribution by both the NW trending tectonic lines and the NE trending faults. The NW-SE direction is the same as that of the longer axis of the Kirishima volcano. However, thermal manifestations such as fumaroles, hot springs, and altered zones are aligned along an ENE-WSW direction. In other words, most of the fractures in the Kirishima Geothermal Field strike NW-SE and ENE-WSW, although there are faults and surface lineaments^{36,38,39} which strike NNE-SSW, NE-SW and E-W.

In most of the Kirishima boreholes, repetitive surveys of downhole temperature and standing water level were carried out for at least several days after cold-water injection was

terminated. These heatup surveys permit the estimation of reservoir pressure and temperature. Feedzone pressures for the Kirishima boreholes were determined and plotted versus elevation in Figure III-30. In order to determine the pre-production pressure distribution in the Kirishima

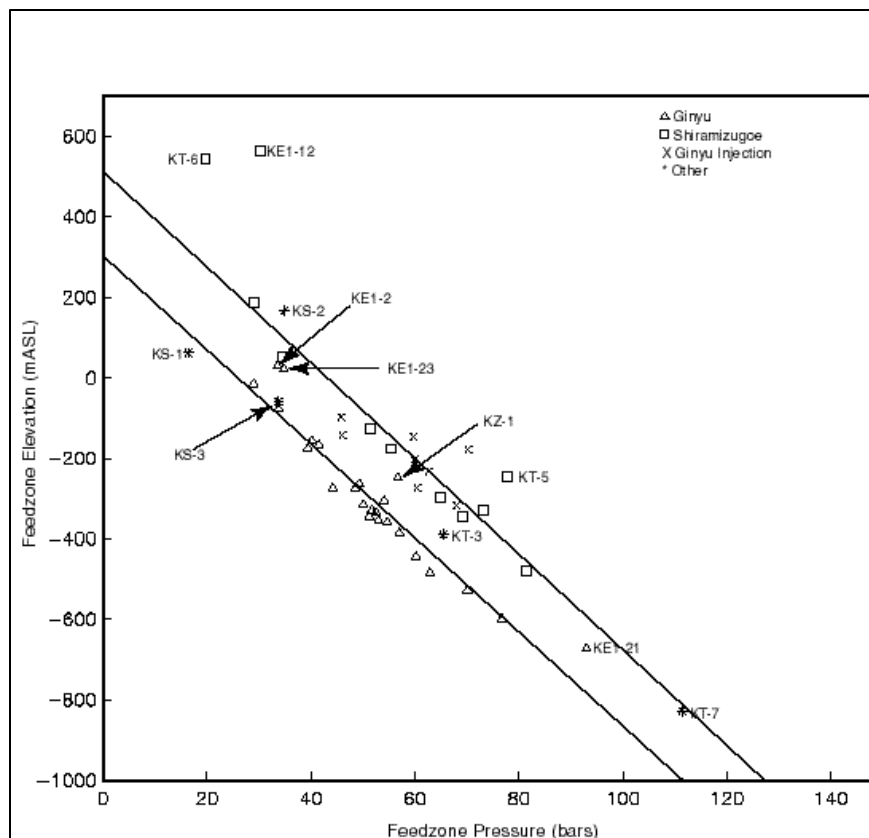


Figure III-30 Kirishima Pressure vs. Elevation

Geothermal Area, it was useful to divide Kirishima boreholes into four groups. The feedzone pressures for most of the Ginyu/Ogiri and Shiramizugoe boreholes lie along two trendlines. The vertical pressure gradient for the Ginyu/Ogiri area is 7.792 kPa/m and corresponds to a hydrostatic gradient at 253°C. Since the reservoir temperatures in the area are only about 230°C, it is likely that the Ginyu fault zone is a downflow zone of the Kirishima Geothermal Field.

The reservoir pressure in the Shiramizugoe area is about 15 bars higher than that in the Ginyu/Ogiri area, indicating that these reservoirs are separated by an impermeable barrier. For the Shiramizugoe fault zone, the least-square vertical pressure gradient is 8.298 kPa/m and corresponds to a hydrostatic gradient at about 215°C. Since the reservoir temperatures in the Shiramizugoe area are considerably higher than 215°C, it is reasonable to conclude that fluid upwelling is taking place in the Shiramizugoe area.

Reservoir temperatures were estimated from temperature recovery tests, shut-in temperature-depth profiles, and production logs⁴⁰; from geochemical fluid geothermometers⁴¹, and from the homogenization temperature of the fluid inclusions in hydrothermal minerals⁴²⁻⁴⁴.

The stable pre-production temperature measurements in the Kirishima boreholes were used to estimate the natural-state temperature distribution (in °C) at 300 meters below sea level, about 1100 meters depth. When these isotherms were plotted, two major features were evident, i.e., first, there is a general tendency for temperatures to decrease from east to west implying that the thermal anomaly is associated with the volcanoes located northeast of the field, and second, a local high-temperature (over 220°C) feature is evident at this depth in the center of the Kirishima Geothermal Area.

The temperature of the Ginyu/Ogiri Fault geothermal reservoir was estimated⁴¹ using standard chemical geothermometers. The SiO₂ geothermometer indicates temperatures of 236°C to 242°C while the Na-K geothermometer indicates temperatures of 234°C to 238°C. These temperatures are in good agreement with the temperature logging data.

The homogenization temperature of fluid inclusions in hydrothermal quartz, anhydrite and calcite from the Kirishima Geothermal Field have a wide range of homogenization temperature (216°C to 320°C) and the minimum values are quite close to the presently measured^{42,43} downhole temperatures. This suggests that the geothermal field has cooled down to some extent and also that the fluid inclusions have been formed at various stages of the cooling process. Additionally, a series of the highest homogenization temperature at each depth parallels the boiling curve of water when the ground water level is set to the present depth.

Downhole temperature surveys were analyzed to determine feedzone locations and temperatures. Several measured and calculated temperatures for six of the Kirishima reservoir boreholes are presented in the table below. The column marked (K&N, 88) is

Borehole Name	Temp.(°C) (K&N, 88)	Temp. (°C) (Garg, <i>et al.</i> , 1998)	Temp. (°C) (T-quartz)	Temp. (°C) (T-Na/K)
KE1-3	242	231	236	242
KE1-5	241	240	246	241
KE1-7	238	232	242	238
KE1-17	237	232	242	237
KE1-19S	234	230	236	234
KE1-22	238	231	240	238

original data from the paper by Kodama and Nakajima⁴⁵. The column marked (Garg, *et al.*, 1998) are the temperatures derived from the analysis of the borehole data by Garg and co-workers²⁷. The T-quartz and T-Na/K columns are the temperatures calculated from chemical species measured in the liquid phase using the quartz geothermometer assuming maximum steam loss and the sodium/potassium geothermometer, respectively⁴⁶. Based on these data, which are all fairly consistent with little variation, it appears that the base temperature of the Ginyu fault zone reservoir is approximately 230°C.

The temperature distribution along a northwest-southeast plane in the Kirishima Geothermal Area on a geological cross-section is shown in Figure III-29. Temperatures in the Ginyu fault zone large-diameter production wells (NT-A1 and NT-C1) are about 230°C. The temperature

increases toward the southeast near the Shiramizugoe fault zone, with the maximum temperature (~250°C) occurring near exploratory well KE1-9.

The highest temperature (~298°C) at Kirishima was recorded in slim hole N56-KT-8 (see Figure III-28) located to the east of the Shiramizugoe fault zone. A temperature of ~282°C was recorded in slim hole N55-KT-5 which is located about 2 km south of N56-KT-8. Several of the boreholes (KE1-9, KE1-11, and KE1-15) in the Shiramizugoe fault zone have temperatures in excess of 240°C.

The temperature data imply that the hot fluid source for the Kirishima Geothermal Field is located in the eastern and southeastern parts of the field and the hot fluid appears to flow laterally to the west and to the north. Convective heat flow was measured at three of the major fumarole areas. The Ginyu, Shiramizugoe and Yunoike areas are discharging 13, 2 and 32 MW_{thermal}, respectively⁴⁵. The Yunoike fumarole area is located about 1km southwest of the Shiramizugoe fumarole area.

In Kirishima, the basement rock, Shimanto Supergroup, is rich in fractures allowing fluid-rock interaction during ascent, though the main geothermal reservoir is andesitic rocks at shallower depth⁴⁵. Carbon dioxide constitutes the bulk of the non-condensable gases in the reservoir fluid.

Gaseous compositions (i.e., CO₂, CH₄ and H₂) are very good indicators to identify processes in the geothermal reservoir, such as boiling and dilution. All gas data from the Kirishima boreholes⁴⁶ indicate steam loss in the reservoir, with boiling beginning at about 245°C. In fact, among the seven Japanese geothermal systems (i.e., Nigorikawa, Kakkonda, Sumikawa, Okuaizu, Hatchobaru, Takigami, and Kirishima) studied by Chiba⁴⁶, Kirishima appears to be representative of a system influenced by steam loss based on the carbon-bearing gases, in fact, the amount of steam lost from the reservoir is as high as ten percent. Fluids from Kirishima boreholes which show a strong boiling trend are also best explained by CO₂ loss accompanying steam loss.

In order to characterize and understand the features and properties of the reservoir, NEDO sponsored studies, including the drilling of two deep (1500m - 1700m) observation boreholes. Single-well pressure transient tests, buildup tests, drawdown tests, multiple-rate tests, injection tests, long-term discharge tests, pressure interference tests and tracer tests were carried out, using both existing boreholes drilled by the NSC, NMC and NKGK and the new NEDO boreholes, to obtain data concerning the reservoir permeability distribution, the locations and types of reservoir boundaries and to estimate the extent of the reservoir and the long-term behavior of the reservoir^{40,47,48}. In the Kirishima Geothermal Area, transmissivity (i.e., permeability-thickness product) values ranged from 0.003 to 300 darcy-meters⁴⁰. Based on discharge and injection testing, the transmissivity in the Shiramizugoe reservoir appears to be less than for the Ginyu/Ogiri reservoir.

As discussed above, most of the feedzones for the Kirishima boreholes tend to align along the faults and are located in the Makizono lavas, Ebino formation and Iino lavas. Like most volcanic geothermal areas, permeability in the Kirishima Geothermal Field is due primarily to the pervasive network of fractures. Most of the boreholes have no feedzones in the upper and middle Makizono lavas which have undergone extensive hydrothermal alteration; and therefore, this relatively impermeable region of the Makizono lavas acts as a caprock for the Ginyu/Ogiri

reservoir. Pressure transient tests, pressure interference tests, and the analysis of them^{40,47-49}, including monitoring of shut-in observation boreholes using capillary-tube type downhole pressure gages, have been carried out for the Ginyu/Ogiri reservoir. Transmissivity values ranging from 11 to 185 darcy-meters were obtained with the average value about 65 darcy-meters⁴⁷. The transmissivity for the Ginyu/Ogiri reservoir is estimated to be 40 darcy-meters from analyses of the long-term pressure transient tests.

The Ginyu fault is the major reservoir in the Kirishima Geothermal Area. The fault zone is characterized by the following features, i.e., (1) the fault strikes to the ENE-WSW and is dipping to the NW, (2) the fault system is an en echelon arrangement, (3) it has a width of about 100 to 200 meters and has several smaller fractures, (4) complete losses of circulation always occurs while drilling through the zone and plugging material has no effect⁵⁰, and (5) drilling through the fault zone is accomplished by using hot water from discharging boreholes for drilling fluid and penetrating the zone as rapidly as possible. Therefore, the Ginyu fault is a highly permeable zone with massive loss of circulation encountered while drilling through it to set a production liner. For example, before reaching total depth after crossing the Ginyu fault, the exploratory well KE1-17 was drilled for 343m and KE1-22 was drilled for 439m with total loss of circulation. All of above suggests that the Ginyu/Ogiri reservoir is highly permeable and susceptible to future problems associated with communication among production and injection wells drilled which have been completed in such a limited volume of the subsurface.

III-g References

1. J. T. Finger, R. D. Jacobson, Charles E. Hickox, and R. R. Eaton, "Steamboat Hills Exploratory Slimhole: Drilling and Testing", Sandia Report SAND94-0551, Sandia National Laboratories, October 1994
2. T. Flynn, P. K. Buchanan, J. D. Miller, "Core Lithology and Photographs, Slimhole SNLG 87-29, Steamboat Hills, NV"; Division of Earth Sciences, University of Nevada, Las Vegas; Las Vegas, NV 89154; Sandia National Laboratories Contractor Report
3. J. T. Finger, R. D. Jacobson, Charles E. Hickox, "Vale Exploratory Slimhole: Drilling and Testing", Sandia Report SAND96-1396, Sandia National Laboratories, June 1996
4. L. J. P. Muffler (editor); "Assessment of Geothermal Resources of the United States - 1978", U. S. Geological Survey Circular 790, 1979
5. J. T. Finger, R. D. Jacobson, Charles E. Hickox, "Newberry Exploratory Slimhole: Drilling and Testing", Sandia Report SAND97-2790, Sandia National Laboratories, November 1997
6. R. A. Jensen, "Roadside Guide to the Geology of Newberry Volcano", second edition; CenOreGeoPub 1995
7. J. T. Finger, R. D. Jacobson, "Fort Bliss Exploratory Slimholes: Drilling and Testing", Sandia Report SAND97-3075, Sandia National Laboratories, December 1997
8. S. K. Garg, J. Combs, M. Abe, "A Study of Production/Injection Data from Slim Holes and Production Wells at the Oguni Geothermal Field, Japan", Contractor Report SAND94-2870/1, Sandia National Laboratories, Albuquerque, NM, 87185-1033

9. S. K. Garg, J. Combs, F. Azawa, H. Gotoh, "A Study of Production/Injection Data from Slim Holes and Large-Diameter Wells at the Takagami Geothermal Field, Kyushu, Japan", Contractor Report SAND95-2555, Sandia National Laboratories, Albuquerque, NM, 87185-1033
10. L. C. Bartel, "Results from a controlled-source audio-frequency magnetotelluric survey to characterize an aquifer" in *Geotechnical and Environmental Geophysics, Vol. II*, 1990, S. H. Ward editor, Soc. of Exploration Geophysicists, 219-233.
11. J. C. Witcher, "*Summary of geothermal exploration activities on McGregor Range, Fort Bliss, New Mexico*", Southwest Technology Development Institute, New Mexico State University, Las Cruces, NM SWTDI Report GEO-4-97 (in preparation)
12. R. C. Edmiston, "Using Flow Tests in Slimholes to Reduce Geothermal Exploration Costs in The Basin and Range Geologic Province of the USA", Geothermal Resources Council TRANSACTIONS, Vol. 17, October 1993
13. W. R. Benoit, "The Evolution of Small Diameter Geothermal Drill Holes and Wells in the Basin and Range Province", PROCEEDINGS Sandia National Laboratories and Geothermal Resources Council *Geothermal Slimhole Technology Workshop*, Reno NV, July 1996
14. G. W. Hutter, "Slimhole Drilling of the Cove Fort-Sulphurdale, Utah Geothermal Resource, PROCEEDINGS Sandia National Laboratories and Geothermal Resources Council *Geothermal Slimhole Technology Workshop*, Reno NV, July 1996
15. J. B. Hulen and D. L. Nielson, "Slim Hole Drilling for Scientific Investigations -- An Example from the Geysers Coring Project", PROCEEDINGS Sandia National Laboratories and Geothermal Resources Council *Geothermal Slimhole Technology Workshop*, Reno NV, July 1996
16. J. B. Hulen, B. A. Koenig, and D. L. Nielson, "The Geysers Coring Project, Sonoma County, California -- Summary and Initial Results", PROCEEDINGS World Geothermal Congress, Florence, Italy, May 1995
17. S. J. Goff, F. Goff, J. N. Gardner, "Slimhole Exploration in Central America", PROCEEDINGS Sandia National Laboratories and Geothermal Resources Council *Geothermal Slimhole Technology Workshop*, Reno NV, July 1996
18. S. Goff (editor), "Results of geothermal gradient hole TCB-1, Tecuamburro Volcano geothermal site, Guatemala, Central America", Los Alamos National Laboratory Report LA-12185-MS, 1992
19. S. Goff, et. al., "Exploration geothermal gradient drilling, Platanares, Honduras, Central America", Los Alamos National Laboratory Report LA-11349-MS, 1988
20. Garg, S. K. and J. Combs (1993), "Use of Slim Holes for Geothermal Exploration and Reservoir Assessment: A Preliminary Report on Japanese Experience", *Proceedings, Eighteenth Workshop on Geothermal Reservoir Engineering*, Stanford University, Stanford, California, January 26-28, pp. 173-179.
21. Combs, J. and J. C. Dunn (1992), "Geothermal Exploration and Reservoir Assessment: The Need for a U.S. Department of Energy Slim-Hole Drilling R&D Program in the 1990s", *Geothermal Resources Council Bulletin, Vol. 21, No. 10*, pp. 329-337.

22. Garg, S. K., J. Combs and M. Abe (1994a), "A Study of Production/Injection Data from Slim Holes and Production Wells at the Oguni Geothermal Field, Japan", *Proceedings Nineteenth Workshop on Geothermal Reservoir Engineering*, Stanford University, Stanford, California, January 18–20, pp. 75–82.
23. Garg, S. K., J. Combs and M. Abe (1995), "A Study of Production/Injection Data from Slim Holes and Large-Diameter Production Wells at the Oguni Geothermal Field, Japan", *Proceedings World Geothermal Congress*, Florence, Italy, May 18–31, pp. 1861–1868.
24. Garg, S. K., and J. Combs (1995), "Production/Injection Characteristics of Slim Holes and Large-Diameter Wells at the Sumikawa Geothermal Field, Japan", *Proceedings, Twentieth Workshop on Geothermal Reservoir Engineering*, Stanford University, Stanford, California, January 24–26, pp. 31–39.
25. Garg, S. K., J. Combs, F. Ozawa and H. Gotoh (1996), "A Study of the Production/Injection Data from Slim Holes and Large-Diameter Wells at the Takigami Geothermal Field, Kyushu, Japan", *Geothermal Resources Council Transactions*, Vol. 20, pp. 491–502.
26. Garg, S. K., J. W. Pritchett, K. Ariki, and Y. Kawano (1991), "Pressure-Interference Testing of the Sumikawa Geothermal Field," *Proceedings Sixteenth Workshop on Geothermal Reservoir Engineering*, Stanford University, Stanford, California, January 23–25, pp. 221–229.
27. Garg, S.K., J. Combs, M. Kodama and K. Gokou (1998), "Analysis of Production/Injection Data from Slim Holes and Large-Diameter Wells at the Kirishima Geothermal Field, Japan", *Proceedings, Twenty-Third Workshop on Geothermal Reservoir Engineering*, Stanford University, Stanford, California, January 26–28, in press.
28. Pritchett, J. W. (1993), "Preliminary Study of Discharge Characteristics of Slim Holes Compared to Production Wells in Liquid-Dominated Geothermal Reservoirs," *Proceedings Eighteenth Workshop on Geothermal Reservoir Engineering*, Stanford University, Stanford, California, January 26–28, pp. 181–187.
29. Garg, S. K., J. Combs and M. Abe (1994b), "A Study of Production/Injection Data from Slim Holes and Production Wells at the Oguni Geothermal Field, Japan", Report No. SSS-TR-94-14464, S-Cubed, La Jolla, California, June.
30. Pritchett, J. W., S. K. Garg, T. G. Barker and A. H. Truesdell (1990), Case Study of a Two-Phase Reservoir, Sumikawa Geothermal Field (Phase 5)," Report Number SSS-FR-90-11401, S-Cubed, La Jolla, California.
31. Takenaka, T. and S. Furuya (1991), "Geochemical Model of the Takigami Geothermal System, Northeast Kyushu, Japan," *Geochemical Journal*, Vol. 25, pp. 267–281.
32. Furuya, S. (1988), "Geothermal Resources of Takigami Field in Oita Prefecture, Japan", *Proceedings International Symposium on Geothermal Energy, 1988: Exploration and Development of Geothermal Resources*, Kumamoto and Beppu, Japan, November 10–14, pp. 119–120.
33. Shimada, T. (1988), "Application of Reservoir Engineering to Takigami Geothermal Field, Oita Prefecture, Japan," *Proceedings International Symposium on Geothermal Energy, 1988: Exploration and Development of Geothermal Resources*, Kumamoto and Beppu, Japan, November 10–14, pp. 121–123.

34. Gotoh, H. (1990) "Reinjection Plan for the Takigami Geothermal Field, Oita Prefecture, Japan," *1990 International Symposium on Geothermal Energy, Transactions Geothermal Resources Council, Vol. 14, Part II*, pp. 897–899.
35. Itoi, R., M. Fukuda, K. Jinno and H. Gotoh (1992), "Interference Test Analysis Method Using the Kalman Filtering and Its Application to the Takigami Geothermal Field, Japan", *Geothermal Resources Council Transactions, Vol. 16*, pp. 657–662.
36. Gokou, K., A. Hiyashita and I. Abe (1988), "Geologic Model of the Ginyu Reservoir in the Kirishima Geothermal Field, Southern Kyushu, Japan," *Proceedings, International Symposium on Geothermal Energy, Exploration and Development of Geothermal Resources*, Kumamoto and Beppu, Japan, Nov. 10-14, pp. 132-135.
37. Saga, Y. and R. Nobumoto (1988), "Kirishima Geothermal Area," *Proceedings, International Symposium on Geothermal Energy, Exploration and Development of Geothermal Resources*, Kumamoto and Beppu, Japan, Nov. 10-14, pp. 125-132.
38. Hayashi, M. and H. Takagi (1983), "Fracture Analysis at the Kirishima Geothermal Field, Southern Kyushu, Japan," *Geothermal Resources Council Transactions, Vol. 7*, pp. 153-156.
39. Ishido, T., T. Kikuchi, Y. Yano, M. Sugihara and S. Nakao (1990), "Hydrogeology Inferred from the Self-Potential Distribution, Kirishima Geothermal Field, Japan," *Geothermal Resources Council Transactions, Vol. 14, Part II*, pp. 919-926.
40. Yokoi, K., I. Kasagi, Y. Hazama and S. Nagao (1988), "Temperature, Pressure and kh Distribution in the Kirishima Geothermal Field," *Proceedings, International Symposium on Geothermal Energy, Exploration and Development of Geothermal Resources*, Kumamoto and Beppu, Japan, Nov. 10-14, pp. 594-597.
41. Shimizu, A., S. Miss, and K. Gokou (1988), "Geochemical Studies of the Ginyu Reservoir in the Kirishima Geothermal Field," *Proceedings, International Symposium on Geothermal Energy, Exploration and Development of Geothermal Resources*, Kumamoto and Beppu, Japan, Nov. 10-14, pp. 136-139.
42. Hayashi, M., S. Taguchi and T. Yamasaki (1981), "Activity Index and Thermal History of Geothermal Systems", *Geothermal Resources Council Transactions, Vol. 5*, pp. 177-180.
43. Taguchi, S., and M. Hayashi (1982), "Application of the Fluid Inclusion Thermometer to Some Geothermal Fields in Japan," *Geothermal Resources Council Transactions, Vol. 6*, pp. 59-62.
44. Taguchi, S., and M. Hayashi (1983), "Past and Present Subsurface Thermal Structures of the Kirishima Geothermal Area, Japan," *Geothermal Resources Council Transactions, Vol. 7*, pp. 199-203.
45. Kodama, M., and T. Nakajima (1988), "Exploration and Exploitation of the Kirishima Geothermal Field," *Chinetsu, Vol. 25*, pp. 201-233 (in Japanese).
46. Chiba, H. (1991), "Attainment of Solution and Gas Equilibrium in Japanese Geothermal Systems", *Geochemical Journal, Vol. 25*, pp. 335-355.
47. Kitamura, H., T. Ishido, S. Miyazaki, I. Abe and R. Nobumoto (1988), "NEDO's Project on Geothermal Reservoir Engineering - A Reservoir Engineering Study of the Kirishima

- Field, Japan,” *Proceedings Thirteenth Workshop on Geothermal Reservoir Engineering*, Stanford University, Stanford, CA, January 19-21, pp. 47-51.
48. Maki, H., T. Ishido, I. Abe, R. Nobumoto and Y. Oikawa (1988), “A Modeling Study of the Natural State of the Kirishima Field,” *Proceedings, International Symposium on Geothermal Energy, Exploration and Development of Geothermal Resources*, Kumamoto and Beppu, Japan, Nov. 10-14, pp. 144-147.
49. Hazama, Y., S. Nagao, I. Abe, Y. Monden, and R. Nobumoto (1988), “Reservoir Simulation on the Kirishima Geothermal Field”, *Proceedings, International Symposium on Geothermal Energy, Exploration and Development of Geothermal Resources*, Kumamoto and Beppu, Japan, Nov. 10-14, pp. 140-143.
50. Haruta, S., N. Hagino, K. Nakao, A. Iijima, and N. Satoh (1988), “Geothermal Well Drilling at Productive Zones in the Kirishima Geothermal Fields, *Proceedings, International Symposium on Geothermal Energy, Exploration and Development of Geothermal Resources*, Kumamoto and Beppu, Japan, Nov. 10-14, pp. 473-476.

IV. ANALYSIS

Introduction: After drilling an exploratory geothermal slimhole, it is clearly essential to evaluate the reservoir's potential for commercially viable production from large-diameter wells. The two most important reservoir qualities are its temperature and its resistance to fluid flow. Flow resistance is quantified as permeability, in units of Darcies (see Equation 1), but that is a local measurement and, for purposes of fluid production, it is more useful to evaluate permeability integrated over some wellbore length. This is called transmissivity, and has units of Darcies times length.

Reservoir temperature can usually be known fairly easily, either through logs after drilling and completion, or even from logs or maximum-reading thermometers during drilling (most geothermal drilling permits require periodic downhole temperature measurements as a criterion for when it is necessary to set casing.) Because of the low circulation rates used for slimhole drilling (typically 12-20 gpm), the formation temperature recovers from the cooling effect of drilling much more quickly than in conventional rotary drilling (where mud circulation is usually several hundred gpm.)

Estimating or measuring transmissivity is more complicated, although lost circulation during drilling is usually a good indication of the formation's transmissivity. To get better definition of the actual transmissivity, there are two principal methods, listed here in order of desirability.

- If the combination of temperature, depth, and fluid level allows the slimhole to be discharged, this is the optimum case. Both analysis and field data support the conclusion that slimhole flow data can be used to calculate not only the reservoir permeability but also the potential productivity of a large-diameter well. Calculation of permeability is usually based on pressure-transient testing (pressure build-up or draw-down at the production zone), productivity index is calculated from pressure change at the production zone as a function of mass-flow rate, and total mass flow from a production-size well is modeled from the slimhole flow with a flow simulator. Correlation of field data with wellbore simulators is discussed in Sections IV-b through IV-d, while a comparison of production flow rates predicted from slimhole data with actual production flow rates from field data is given in Section IV-e.
- In many cases, however, either the temperature or depth do not allow self-supporting flow from the well. The most common method of evaluating transmissivity in this situation is to inject fluid into the well while measuring downhole pressure at or near the production zone. Two possible parameters can be measured by this procedure: injectivity index, which has the form $\frac{\Delta \dot{M}}{\Delta p_{fz}}$, or change in mass flow rate per change in feed-zone pressure (and is the same form as productivity index – see Section IV-e.3), and transmissivity, as described above, which is calculated as described below. Transmissivity calculated from slimhole measurements is directly comparable for a large-diameter well, because it is a property of the reservoir. Predicting large-well production from slimhole data, however, will require some sort of wellbore simulator, because the relative importance of flow resistance in the

wellbore and in the formation will affect total mass-flow rate. A further caveat is in assuming the general equality of injectivity index with productivity index, especially if there is two-phase flow at the feed zone. It is almost always true that injection data provides a bound on transmissivity or productivity; that is, for a given pressure change at the feed zone, more fluid can be injected than produced.

Comparison of injectivity and productivity indices, based on extensive data from five Japanese geothermal fields, is discussed in Section IV-e, and the elements of pressure-transient analysis are presented below.

a. Transmissivity estimates by pressure-transient analysis

Governing Equations: Although most geothermal reservoirs are dominated by fracture permeability, porous media permeability can be used as first approximation. When a rigid porous medium is saturated with a "slightly" compressible, low-velocity liquid, the transient pressure distribution based on Darcy's Law is described¹ by

$$(1) \nabla^2 p = \frac{1}{\alpha} \frac{\partial p}{\partial t}$$

where p is the pressure, t is the time, and $\alpha = k / \Phi \mu c$ is the apparent diffusivity for the saturated medium. In the definition of α , k is the intrinsic permeability, Φ is the porosity, and μ is the fluid viscosity. The fluid compressibility c is defined by

$$(2) c = \frac{1}{\rho} \frac{\partial \rho}{\partial p},$$

where ρ is the fluid density. In practice, the compressibility of the formation can be accommodated by combining the formation and fluid compressibilities into a single, effective, compressibility. The form of the governing equation is unchanged. In typical applications, the effective geometry of the formation is not known. Hence, it is generally possible to estimate only the products kh (transmissivity) and Φch (storativity) from field measurements, where h is the effective thickness of the reservoir, which is assumed to consist of a single, uniform, porous, layer.

Mathematical Models: Eq. (1) is of the same form as the parabolic transient heat conduction equation, provided p is replaced by the temperature and the apparent diffusivity α is identified with the thermal diffusivity. Hence, solutions for transient thermal conduction can be interpreted in terms of transient flows in porous media. Based on results for heat conduction given by Carslaw and Jaeger², several flow problems of interest can be analyzed. Since the book of Carslaw and Jaeger will be cited several times, we will henceforth denote this reference by C&J.

Constant flux: If a constant flux q , from a borehole to the surrounding formation, is established at the wall of the hole, then the nondimensional pressure distribution at large time is given by (C&J, pg. 338)

$$(3) \quad p'(\eta, \tau) = \frac{kp}{a\mu q} \approx \frac{1}{2} \ln \left(\frac{4\tau}{C\eta^2} \right) + \frac{1}{2\tau} \ln \left(\frac{4\tau}{C\eta^2} \right) + \frac{1}{4\tau} + \eta^2 - 2 \ln \left(\frac{1}{\eta} \right) + \dots$$

where $\eta = r/a$, $\tau = \alpha t/a^2$, a = borehole radius, $C = \exp(\gamma)$, γ is Euler's constant (0.57721...), and Eq. (3) is restricted to values of η for which $4\tau/C\eta^2 > 1$. The leading term in Eq. (3) corresponds to the solution for the pressure distribution established by a continuous line source (C&J, pg. 261), a result which can be used to advantage in the subsequent shut-in analysis.

Shut-in analysis: Based on the result given in Eq. (3), the borehole is represented by a continuous line source. If flow is established from the hole at a constant flow rate Q over the thickness h , then the pressure response is given by (C&J, pg. 261)

$$(4) \quad p(\eta, \tau) = \frac{\mu Q}{4\pi kh} \int_{\eta^2/4\tau}^{\infty} \exp(-u) \frac{du}{u} = \frac{\mu Q}{4\pi kh} E_1 \left(\frac{\eta^2}{4\tau} \right)$$

where E_1 denotes the exponential integral and it is assumed that the initial formation pressure is zero. Equation (4) is generally referred to as the Theis solution³. For large time, the solution can be approximated by

$$(5) \quad p(\eta, \tau) = \frac{\mu Q}{4\pi kh} \ln \left(\frac{\eta^2}{4\tau} \right) + \gamma.$$

The borehole radius cancels in the nondimensional term $\eta^2/4\tau$, as it should, since there is no physical length scale in the solution for a line source. However, as pointed out by Collins¹, reasonable results can be obtained upon evaluation of Eq. (4) at $r=a$, corresponding to conditions which exist at the physical borehole radius. If the volumetric flow rate from the hole is constant at a value Q over the period $0 \leq \tau \leq \tau_s$ and is then zero for subsequent time, the hole is said to be shut-in. Using superposition, the subsequent pressure response is

$$(6) \quad p(\eta, \tau) = \frac{\mu Q}{4\pi kh} \left[E_1 \left(\frac{\eta^2}{4\tau} \right) - E_1 \left(\frac{\eta^2}{4(\tau - \tau_s)} \right) \right],$$

or for large time

$$(7) \quad p(\eta, \tau) = \frac{\mu Q}{4\pi kh} \ln \left[\frac{\tau}{\tau - \tau_s} \right]$$

where Eqs. (6) and (7) are valid for $\tau > \tau_s$.

A useful interpretation of Eq. (5) is obtained by rewriting the equation in dimensional form as

$$(8) \quad p(\eta, \tau) = \frac{\mu Q}{4\pi kh} \ln \left[\frac{4kht}{Ca^2 \mu \phi ch} \right]$$

The coefficient $\frac{\mu Q}{4\pi kh}$ can be estimated from the slope of a plot of pressure versus $\ln(t)$, thus providing an estimate of the transmissivity kh , since Q and μ are known. Extrapolation to obtain the intercept t_0 with the time axis for zero pressure change from a plot of pressure versus $\ln(t)$ allows for the estimation of Φch from

$$(9) \quad \frac{4kht_0}{Ca^2 \mu \phi ch} = 1.$$

The shut-in analysis is interpreted in a similar manner. If τ_p is the total, constant-rate, injection time prior to shut-in and $\Delta\tau$ is the elapsed time since shut-in, Eq. (7) can be written in the equivalent form

$$(10) \quad p(\eta, \tau) = \frac{\mu Q}{4\pi kh} \ln \left[\frac{\tau_p + \Delta\tau}{\Delta\tau} \right],$$

where the term in parentheses is referred to as the Horner time.

In the practical application of results based on these approximate models, numerous restrictions must be observed. Specifically, the porous layer must be uniform and of infinite extent and the saturating fluid must be a slightly compressible liquid. For the shut-in analysis, the injection must have been at a constant rate prior to shut-in. The shut-in process is assumed to occur within the borehole, rather than at the surface, which is typically several thousand feet above the formation investigated. For large shut-in times, the reservoir boundary can affect the results. Simple modifications to this basic result can be used to help explain deviations from the ideal case which are frequently observed in the field.

Example injection tests: The tests described below were done at the end of drilling in the Vale Exploratory Slimhole (Section III-b). Two injection tests were performed during the two-day period, May 11-12, 1995. The test procedure involved establishing a constant injection-flow rate which was maintained for a sufficient period to eliminate the effects of initial variations in the flow. The well was then shut in and the pressure decay monitored with downhole instrumentation positioned near the postulated feed zone. The location of the feed zone was

inferred from prior temperature logs of the well. Details of the instrumentation used are provided in Section II-c. This discussion is concerned with interpretation of the test results and the resulting estimates of the permeability-depth product (transmissivity) for the well. Important details of the two injection tests are summarized in the table below. The terms P_{wh} , P_{dh} , Q , T_{dh} denote the wellhead pressure, downhole pressure, volumetric flow rate, and downhole temperature, respectively. The pressures in the table are the values immediately preceding shut-in.

Test No.	Injection start time	Shut-in time	Elapsed time, hr	P_{wh} psi	P_{dh} psia	Q gpm	T_{dh} °F	Depth ft
1	18:32:57	20:51:38	2.311	145	1748	26	69	3700
2	08:39:56	10:05:49	1.431	240	1584	42	57	3109

Pressure Fall Off Analysis: The pressure fall off ΔP for the first injection test is plotted in Fig. IV-1 as a function of the log of the Horner time, $(t_p + \Delta t)/\Delta t$, where ΔP is the pressure drop, t_p is the total injection time prior to shut-in, and Δt is the elapsed time after shut-in. [Note that,

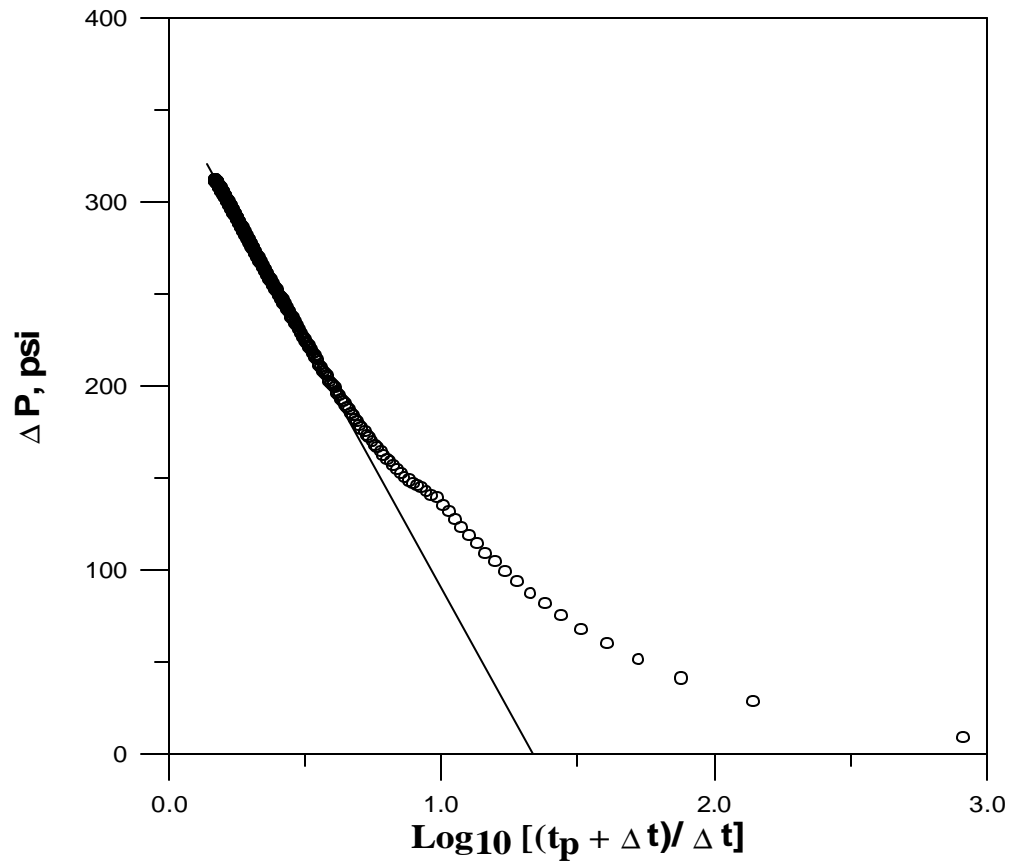


Figure IV-1 – Downhole pressure fall-off after first injection test (5/11/95) at Vale Exploratory Slimhole

in the horizontal axes of Figures IV-1 and IV-2, increasing time runs from right to left.] A curve fit to the late-time, straight line, segment of the response yields

$$(11) \quad \Delta P = 358.74 - 267.26 \log \left[\frac{t_p + \Delta t}{\Delta t} \right]$$

The slope m of this line can be used to determine the effective value of the transmissivity kh from the relation

$$(12) \quad kh = \frac{2.303Q\mu}{4\pi m}$$

where Q is the volumetric flow rate and μ is the viscosity. For the first injection test, the numerical values of the various parameters are: $Q = 26 \text{ gpm} = 1.64 \times 10^{-3} \text{ m}^3/\text{s}$, $\mu = 4.71 \times 10^{-4} \text{ kg/m s}$, $m = 267.26 \text{ psi/cycle} = 1.843 \times 10^6 \text{ N/m}^2/\text{cycle}$. The estimated value for kh is then

$$(13) \quad kh = 7.68 \times 10^{-14} \text{ m}^3 = 0.077 \text{ Da-m} = 0.253 \text{ Da-ft}$$

For the second injection test, a straight line fit to the late time portion of the response curve in Fig. IV-2 yields

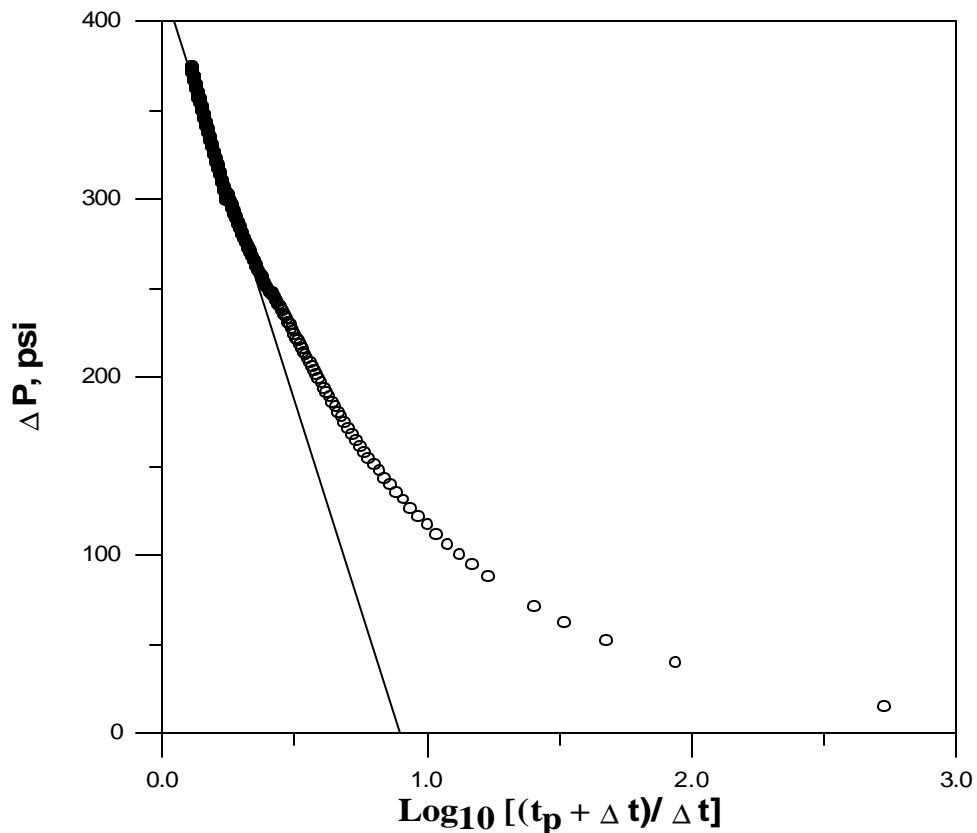


Figure IV-2 – Downhole pressure fall-off after second injection test (5/12/95) at Vale Exploratory Slimhole

$$(14) \quad \Delta P = 422.17 - 468.94 \log \left(\frac{t_p + \Delta t}{\Delta t} \right)$$

Performing the same analysis as that applied to the first injection test results in the following estimate for the transmissivity

$$(15) \quad kh = 7.07 \times 10^{-14} \text{ m}^3 = 0.071 \text{ Da-m} = 0.232 \text{ Da-ft}$$

Pressure Buildup Analysis: An additional measure of the effective transmissivity can be obtained from the initial pressure response obtained when the injection flow is established. The downhole pressure buildup is available only for the second injection test. In Fig. IV-3, the

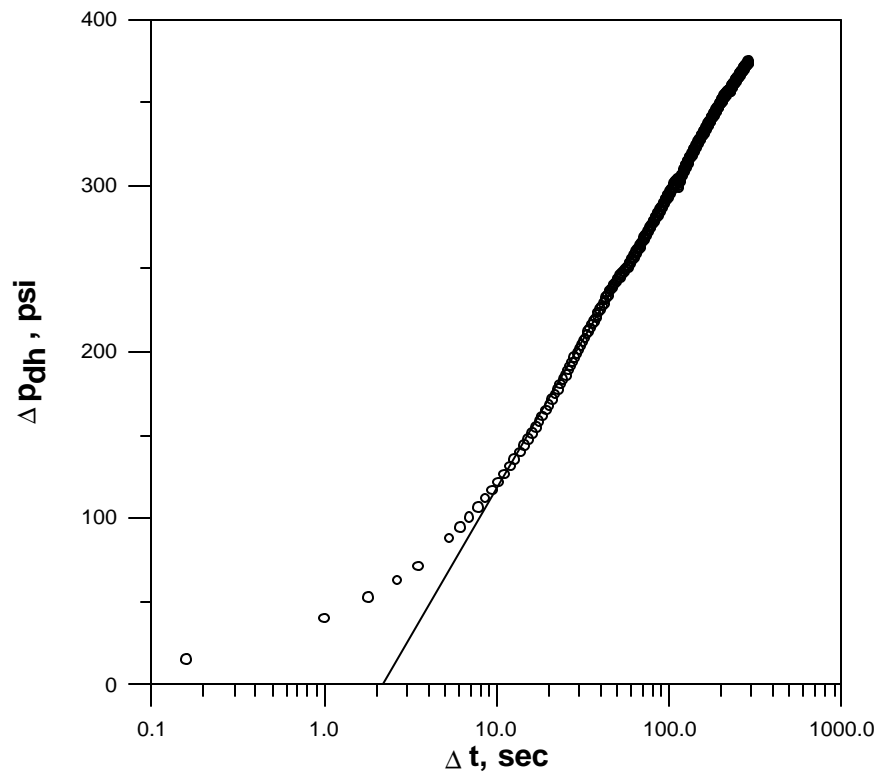


Figure IV-3 – Downhole pressure build-up during second injection test (5/12/95) at Vale Exploratory Slimhole

pressure rise is plotted as a function of the log of the elapsed time since the start of injection. A curve fit to the late-time response yields

$$(16) \quad \Delta P = -62.84 + 77.48 \ln(\Delta t)$$

The effective transmissivity can be obtained by using the slope m in the relation

$$(17) \quad kh = \frac{Q\mu}{4\pi m}$$

which is essentially identical to Eq. (12) except for the factor 2.303 which is the conversion between the natural log and the log to base ten. Eq. (17) yields the following estimate for the transmissivity

$$(18) \quad kh = 1.858 \times 10^{-13} \text{m}^3 = 0.186 \text{ Da-m} = 0.610 \text{ Da-ft}$$

which is approximately a factor of 2.5 larger than the estimate based on the pressure fall off analysis. Variations of this magnitude are not uncommon when analyzing field data.

Productivity Index: The productivity index is defined by

$$(19) \quad \text{PI} = M/(P_{ns} - P_{fp})$$

where M is the discharge (*i.e.*, mass production) rate, P_{ns} is the stable (static) feedzone (or gauge depth) pressure, and P_{fp} is the flowing feedzone (or gauge depth) pressure. Based on the information in Table 1 and an estimated ambient pressure of 1475 psi, the productivity index is 0.09 kg/s/bar for test 1 and 0.35 kg/s/bar for test 2. These results are only approximate since the position of the downhole tool was not exactly the same for each test and the estimate for the downhole pressure is based on an average density rather than on an actual static measurement. These estimates are substantially lower than prior estimates for the nearby A-Alt well which were on the order of unity. Based on the theoretical study of Pritchett⁴, it is assumed that the productivity index can be determined from an injection test and the productivity index for a large-diameter production well can be scaled geometrically, based on the ratio of borehole diameters, from the result for a slimhole.

b. Comparison of field data with wellbore simulators

The results discussed below are based on data from the first series of tests at Steamboat Hills (Section III-a), conducted during August 5-6, 1993, at a total depth of 968 feet in the slimhole. A large fracture system identified at 815' was verified by spinner measurements to be the primary feedzone for this series of tests and was later observed to be the major feed zone for the 4001' completed well. Hence, the flow and injection tests conducted during this first series are representative of the performance observed in subsequent tests when the well was deeper.

Flow testing: In Figures IV-4, IV-5, and IV-6 the temperature, pressure, and spinner response are plotted versus depth. These measurements were made at a total (liquid plus vapor) production rate of 7.1 kg/s (56,350 lb/hr). The liquid water flow rate through the magnetic flow meter and weir box was 6.1 kg/s at 192°F (100 gpm, 48,425 lb/hr). Numerical flow simulations are included in Figures IV-4 and IV-5 for comparison and are discussed later. The spinner response, which clearly shows a feed zone at 815', is proportional to the rotational speed of the impeller, but it was not calibrated as a quantitative measure of relative flow

velocity. Based on *in situ* measurements, we have deduced a relation between spinner output and flow velocity which is consistent with observations in the flowing well.

A secondary objective of flow testing was evaluation of the James tube for slimhole application. The advantage of this method is that only simple equipment is needed to measure the total flow rate and heat rate of the well. Calculations using the James tube flow area, the water flow rate (measured with a weir box), and the lip pressure in the James tube (see Section II-d) will yield total mass flow rate and flow enthalpy, thus simplifying the necessary measurements for those performance criteria. Although there was considerable scatter in the James tube pressure data for these tests, flow rate calculations were in agreement with the measured flow rates.

Wellhead pressures, measured during discharge for all test series, are plotted versus total mass flow rate in Figure IV-7. Mass flow rate and total enthalpy were calculated from measurements made with James tubes of various diameters, according to the procedure described by Grant, et al.⁵ For those cases when critical flow in the James tube could not be attained, total fluid enthalpy was estimated from downhole temperature measurements. Knowing total enthalpy, the steam-flash fraction could then be calculated from the enthalpy of the flashed water in the weir box and the latent heat of vaporization at the local atmospheric pressure, total mass flow rate following from these data. Unsteadiness of the two-phase flow in the James tube and flash tank created significant scatter in the measurements of James tube lip pressure, flow rate, and wellhead pressure. Nevertheless, the data in Figure IV-7 are typical of two-phase flow from a liquid-dominated geothermal well. For example, a weak wellhead-pressure maximum apparent in the data at a mass flow rate of approximately 1 to 4.5 kg/s is reflected in the superposed curves obtained from numerical simulations of flow in the well.

Reservoir transmissivity: The fracture system at 815' has such large apparent permeability that only very small pressure increases were observed when relatively large volumes of water were injected. Difficulties with downhole instrumentation and with the injection equipment precluded an accurate estimate of reservoir transmissivity based on these injection tests, but some reservoir properties can be estimated by considering the downhole pressure response during flow rate changes in production tests⁶. During the first series of flow tests, very small, abrupt, changes in downhole pressure were observed when the flow rate was varied in relatively small increments. For flow rate changes between 6 and 16 gpm, pressure changes ranged from 0.05 to 0.07 psi. If steady-state conditions are assumed, the apparent effective transmissivity, or permeability-depth product, kh , can be estimated from the Dupuit, or Theim, formula⁷

$$(20) \quad \Delta p = \frac{\mu \Delta Q}{2\pi kh} \ln \frac{r_o}{r_w},$$

where Δp is the pressure change, μ is the fluid viscosity, ΔQ is the change in volumetric flow rate, r_w is the borehole radius, and r_o is the outer radius of the reservoir. An arbitrary value of 100 m is selected for the outer radius, recognizing that the logarithmic term makes the Dupuit formula relatively insensitive to this parameter. Using the fluid viscosity evaluated at downhole conditions, the transmissivity is then estimated to lie in the range 160-600 Da-m, with an

average value of approximately 400 Da-m. This estimated average value of transmissivity indicates a pressure increase of only 0.5 psi for an increment of 100 gpm in the injection rate of liquid water.

A shut-in test was also performed immediately following a 100 gpm discharge test, and this produced a pressure change of 0.2 psi. Based on the Dupuit formula, this latter pressure rise indicates a transmissivity in the range of 900 Da-m. Using Equation 10, the Theis equation, a plot of pressure versus the log-term can provide an estimate for the transmissivity kh . Application of this analysis to the shut-in data above indicated a transmissivity on the order of only 25 Da-m, however, the apparent temperature-induced drift in the pressure-measurement electronics and the very small overall pressure increase detract from the validity of this approach for this particular test. In reservoirs with much lower apparent transmissivity, such as the examples in IV-a, application of the Theis equation is the preferred method to estimate reservoir properties.

It is informative to note that laminar, axisymmetric, creeping flow in a horizontal fracture is described by an equation similar to the Dupuit formula if the transmissivity is replaced with the quantity $b^3/12$, where b is the fracture aperture. Assuming flow occurs in a single fracture, and using the same numerical values used to estimate the transmissivity, the predicted fracture aperture lies in the range 1-4 mm, which is consistent with fractures observed in the core samples, but much less than the apparent size of the feed zone based on drilling data (drillstring dropped approximately 2', without rotation, when it reached this interval.) This indicates that, although a large void may have been penetrated, a much smaller fracture can carry the amount of fluid produced. The ability of the large fracture to carry much more fluid than was actually produced, along with the simulations described below, indicate that the wellbore diameter, not the reservoir, was the parameter limiting flow rate.

Analysis of spinner data: Spinner data, in some cases, can be the most informative measurement taken in a flowing well. In holes which penetrate several potential production or injection zones, it is frequently difficult to analyze internal flow in the wellbore, and good spinner data can be extremely useful in this aspect of interpretation. Obtaining fine resolution is difficult, however, because spinners are not usually calibrated to give absolute flow velocity, or even velocity relative to the tool, but instead to give a number of counts that measures how fast the impeller on the tool is rotating. In some instruments, such as those used in these tests, it is not even possible to determine flow direction relative to the tool.

There are, however, two features of the test configuration which make it possible to, in effect, calibrate the spinner after the fact: (1) the logging line speed, or tool velocity, is known in all cases, and (2) total mass flow rate is known and, in the casing where flow is single-phase, fluid velocity can be accurately calculated. Combination of the logging tool speed and absolute fluid velocity gives the fluid velocity relative to the logging tool, and repetition of this procedure at several flow rates produces a "calibration curve" for the spinner tool. In deriving these calibration curves, only the cases in which the relative fluid velocity was toward the bow of the spinner tool were considered; generally, the tool body appeared to shadow the impeller when relative flow was from the stern of the tool. Use of these calibration curves to analyze flow test data revealed that flow from the major feed zone at 815' is divided, with the majority of the fluid

going up the well and the remainder going down. The down-going flow rate, which varies from approximately 20 to 50 gpm, is a very weak function of the wellhead flow rate.

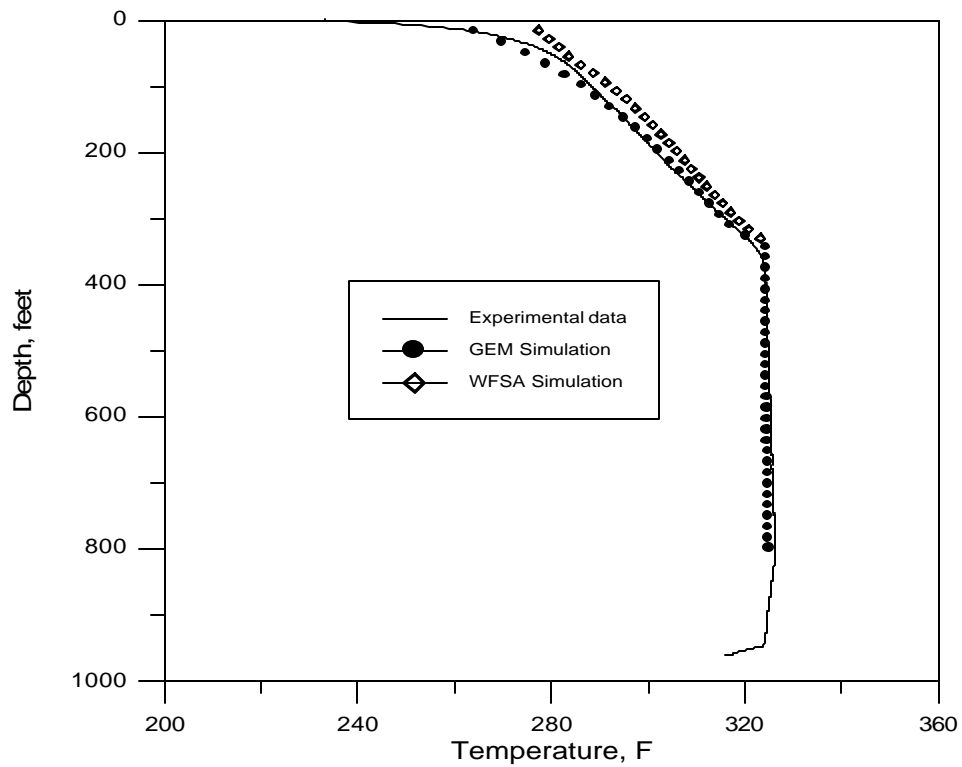


Figure IV-4. Downhole temperature versus depth in slimhole SNLG 87-29; field data and numerical simulation.

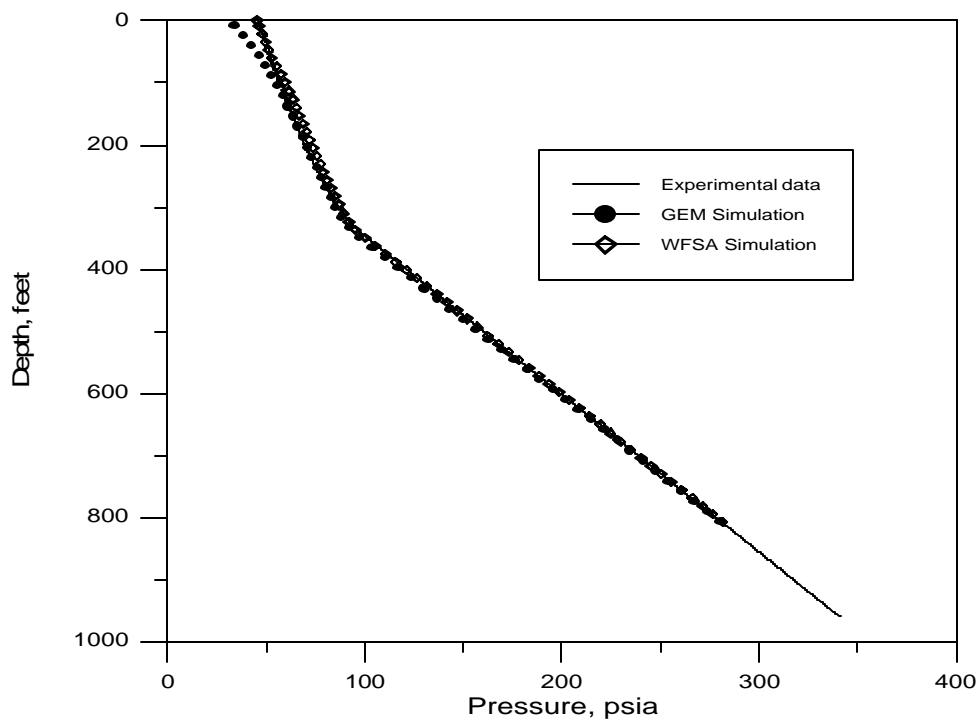


Figure IV-5. Downhole pressure versus depth in slimhole SNLG 87-29; field data and numerical simulation.

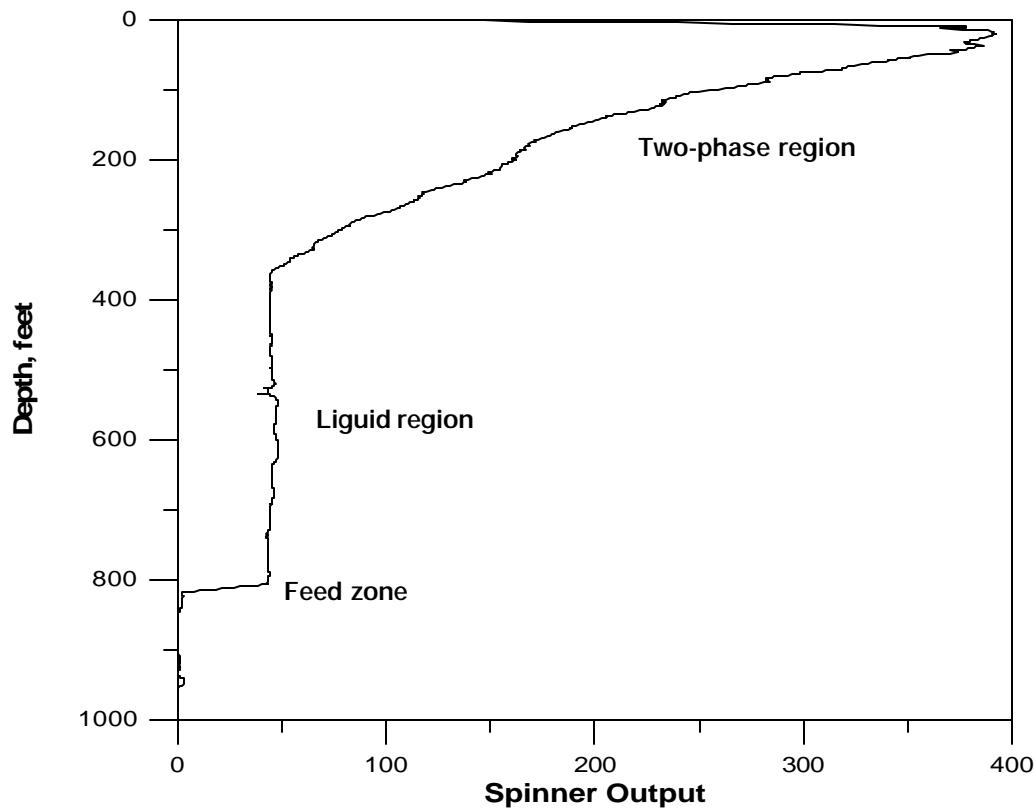


Figure IV-6. Spinner response versus depth while flowing 56,000 lb/hr in SNLG 87-29

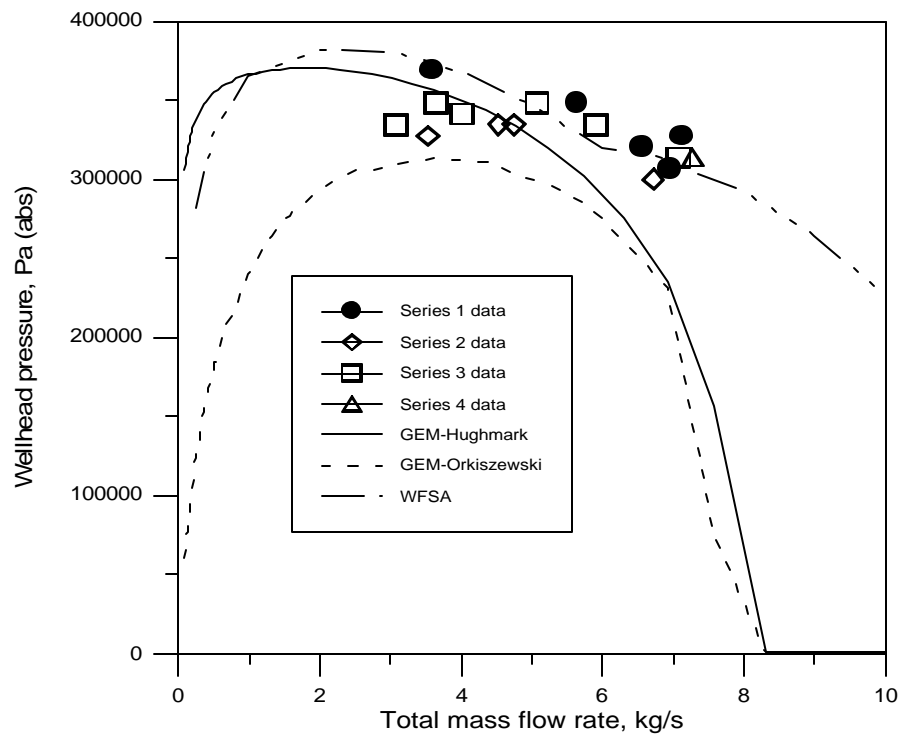


Figure IV-7. Wellhead pressure versus mass flow rate in SNLG 87-29; field data and numerical simulation.

c. Description of various wellbore simulators

Numerical simulation of flow in a wellbore is critically dependent on the correlation or mathematical model used to describe the two-phase flow regime. Depending on well depth and temperature of the surrounding formation, representation of heat transfer between the formation and the wellbore may be equally important. Three computational packages are currently publicly available for numerical simulation of flow in slimholes.

- GEM requires input of downhole pressure, formation-temperature profile, and wellhead pressure, and then calculates flow rate. It allows simulations⁸ with no slip in the two-phase region or with either of the slip models proposed by Orkiszewski⁹ and Hughmark¹⁰. In GEM, heat conduction in the surrounding formation is simulated using finite differences.
- WFSA requires input of downhole pressure, formation temperature, and flow rate, and then predicts wellhead pressure. It allows for multiple feed zones and the effects of dissolved solids, is based on the work of Hadgu¹¹, and uses a specially developed two-phase flow model. Heat transfer between the formation and the wellbore is described with an analytical model.
- GEOTEMP2 simulates drilling processes¹², with some capability for simulating injection and two-phase production. For production, the program requires input of downhole pressure (or temperature and quality, if feed is two-phase), formation temperature, and flow rate, then calculates wellhead pressure. This program uses the Orkiszewski two-phase slip model and treats heat transfer between the wellbore and the surroundings with a finite difference numerical model.

The codes agree reasonably well with each other and with the measured field data, except that the surface temperature calculated by GEOTEMP2 is noticeably lower than the other codes. All codes predicted transition to two-phase flow at approximately the same point. Effort required to set up the input files, and computer run time (cpu), are similar for all three codes.

Each of these codes can be used to iterate a series of solutions with varying initial conditions to produce a curve of flow rate versus wellhead pressure, along with the associated predictions of downhole pressure and temperature. This predictive capability can be scaled up to a larger-diameter well in the same reservoir, if the downhole pressure is assumed to remain the same. In this highly permeable situation, that assumption was valid, but in other reservoir types the pressure drawdown during production might seriously distort the predicted output. This phenomenon emphasizes the need for a coupled wellbore-reservoir simulator.

Both GEM and WFSA were used for initial simulations of flow in SNLG 87-29. In Figures IV-4 and IV-5, the pressure and temperature distributions with depth, assuming adiabatic flow, are compared with downhole measurements for the first test series (well depth is 968'). The GEM simulations used the Orkiszewski two-phase flow option. Most of the calculations are in good agreement with the measurements, but near the surface unmodeled heat transfer mechanisms are suspected to be responsible for the difference between predictions by WFSA and observed temperature distributions. The two-phase flow correlation used in GEM apparently causes it to under-predict wellhead pressure, as shown in Figures IV-5 and IV-7,

and there is a slight variation of temperature with depth in the single-phase region, shown in Figure IV-4, as contrasted with the constant-temperature assumption in WFSa; otherwise, temperature and pressure distributions predicted with GEM differ little from those predicted with WFSa.

Predictions made with GEM and WFSa of wellhead pressure as a function of mass flow are shown in Figure IV-7, and those predictions are compared with the experimental measurements from all flow tests. The WFSa prediction compares best with the experimental data, although the simulation has a local minimum, most likely attributable to a change in flow correlation, near a flow rate of 6 kg/s. The GEM prediction, using the Orkiszewski correlation, consistently under-predicts the pressure, but if the downhole pressure at the feed zone is increased by 5%, the GEM prediction then passes through the experimental data. The prediction from GEM using the Hughmark correlation tends to agree with the WFSa prediction for mass flow rates less than 6 kg/s, but predicts significantly lower wellhead pressures for larger flow rates. The agreement among the computational approaches and experimental data is reasonable, considering the variability of the measurements involved and the sensitivity of the simulations to the two-phase flow correlations employed. These comparisons should be viewed as preliminary.

Keeping all parameters except wellbore diameter fixed, GEM and WFSa predictions were applied to a full size production wellbore with diameter of 12.25 inches. For a mass flow rate of 62 kg/s, wellhead pressures of 56, 66, and 55 psia were predicted, respectively, with WFSa, GEM(Orkiszewski), and GEM(Hughmark). The flow rate of 62 kg/s corresponds to a 1990 test of the nearby 12.25" production well Hot Air-4 (HA-4), which produced 900 gpm of liquid water at a wellhead pressure of 72.5 psia. When corrected for flashing, that measured flow rate corresponds to a total mass flow rate of approximately 62 kg/s. The production from well HA-4 is associated with a feed zone at 729', which is somewhat shallower than the slimhole production zone at 815'. However, tracer tests in the Steamboat Hills geothermal field indicate pervasive interconnections between fracture zones, so it does not seem unreasonable to expect similar production rates among nearby fracture zones. Based on a single test, simulation of a production well extrapolated from a slimhole tends to indicate a lower wellhead pressure at a specified mass flow rate than that observed experimentally. The results, however, appear to be within a normal range of variation for the experimental measurements and the models used in the simulations.

d. Flow test planning

To demonstrate the effect of wellbore geometry on flow rates, the exercise below was done using parameters from the slimhole at Newberry (Section III-c).

The wellbore simulator GEM⁸ was used to compare three possible configurations for a 6000' well in formations with temperatures like Newberry well TCH76-15. Each scenario assumed the existing 4.5" casing to 2748'; case 1 assumes an HQ-size (3.85") hole from the casing shoe to 6000', case 2 assumes an HQ core-rod liner (ID 3.06") from the casing shoe to 4800' and an NQ-size (3.03") hole from 4800' to 6000', case 3 assumes HQ core-rod from

surface to 4800', then NQ hole to 6000 feet. Each of these cases was modeled as adiabatic (no heat loss to the formation) and the first two cases were also modeled as transient problems. A number of other assumptions are built into the calculations:

1. The feed zone is at the bottom of the well,
2. Formation temperature at 6000' is 401°F (based on extending the measured temperature profile),
3. Bottomhole pressure is approximately 2132 psia (based on the static head from the measured water level of 815' and integrating water density with temperature from there to TD),
4. The Hughmark slip correlation is used for two-phase flow, and
5. Permeability is high enough that pressure drawdown with flow is negligible at the feed zone. (This is clearly **not** true for TCH 76-15, since injection testing after drilling showed the permeability to be unmeasurably small.)

These assumptions may not be sufficiently realistic for flow-rate predictions, but by being

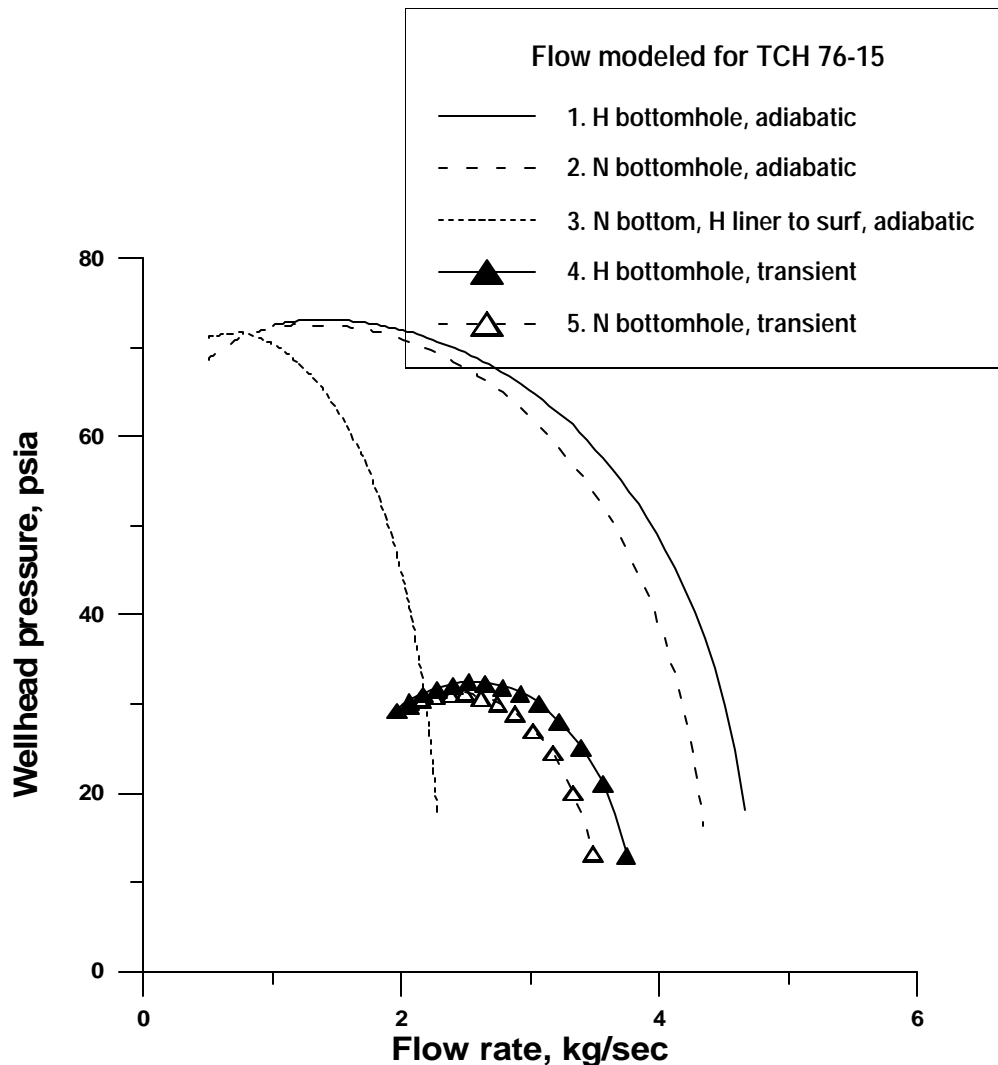


Figure IV-8 Modeled flow rates in TCH 76-15

consistent among scenarios they allow comparison of the potential performance in the different wellbore geometries.

Adiabatic: This is a highly idealized situation in which there is no heat transfer to or from the formation. It is possible that a real, high-volume flow might asymptotically approach this condition after very long time but, again, it is useful as a method of comparing borehole geometries. Curves 1 and 2 in Figure IV-8 show a relatively small difference between the performance of the two borehole geometries in this flow condition, but Curve 3 shows significant decrease in performance. This decrease is apparently related to the greatly increased frictional effects of two-phase flow, which begins at approximately 1000' depth. This result indicates that having the two-phase flow occur in the larger ID of the casing (4") instead of the HQ rods (3.06") is important for optimizing well performance. Another benefit is that reducing the amount of HQ rod left in the hole lowers the cost of well completion.

Transient: A more interesting, and realistic, simulation is one which models heat transfer to the wellbore at temperatures representative of the actual formation. When the static wellbore temperatures are taken to be those shown by actual temperature logs, the transient solutions for cases 1 and 2 indicate that the well will not spontaneously flow with the feedzone conditions specified above. There are two possible ways to overcome this; assume that the well has been forced to flow long enough to significantly heat the formation, or assume that the fluid enters the wellbore at a higher temperature than that in the original cases. In the forced-flow situation, iteration of time for a transient solution showed that both wells would sustain flow after being pumped or air-lifted for a period of 20 to 50 hours. Their performances in this condition, shown in Curves 4 and 5, are much lower than in the adiabatic case, which is to be expected, but are little different from each other.

When feedzone temperatures are incremented (formation temperatures are held constant) until spontaneous flow begins, it is found that the case 1 requires a fluid temperature of 592°F and case 2 requires 608°F. Once again, the difference between these two well configurations is relatively small. To summarize, the general statement that keeping wellbore diameter as large as possible to improve production is true, but it is more important in any wellbore region where there is two-phase flow.

e. Summary of Japanese data; correlation of productivity/injectivity

e.1 Introduction and Background In general, two kinds of measurements were taken in the Japanese geothermal fields: those to help define a large-scale model of the reservoir structure, and those to analyze or predict the productivity of wells in a specific area. Examples of the first type are the repetitive surveys of downhole temperature and standing water level that were carried out in most of the boreholes for at least several days after cold-water injection was terminated. These heat-up surveys permit the estimation of reservoir pressure and temperature, allowing feedzone pressures to then be determined and plotted versus elevation. The resulting vertical pressure gradient and the corresponding hydrostatic gradient can be used to analyze the temperature distribution and flow patterns in the geothermal reservoir.

This section, however, will focus primarily on analysis of discharge data and the wellbore parameters which affect discharge rate. Discharge and injection capacity of a geothermal borehole is principally determined by pressure losses associated with flow (1) in the reservoir rocks, and (2) in the wellbore. Given mass flow rate and feedzone pressure and flowing enthalpy, equations governing mass and energy transport in the wellbore may be solved to obtain the wellhead conditions (pressure and flowing enthalpy). At present, two-phase fluid flow in the wellbore (a common condition in geothermal boreholes) is not amenable to rigorous analytical treatment; instead, various empirical correlations for flowing steam quality, friction factor and heat loss must be used. Unfortunately, using different empirical correlations does not always lead to comparable results but, despite the uncertainties, the available correlations are adequate for computing a first approximation to the pressure losses in the wellbore.

A borehole must be discharged to ascertain its productive capacity. As part of the discharge tests of most of the Japanese boreholes, the characteristic output curves (*i.e.*, mass flow and enthalpy versus wellhead pressure) were also obtained. An oddity of the “Well Characteristic” data set from some boreholes is that the measured wellhead enthalpies often exceed downhole enthalpies computed from feedzone temperatures. Because there was no evidence for a two-phase or a steam feed in most of these boreholes, it would appear that the measured enthalpies may be in error. These are computed from measured water and steam flow rates at the surface, so it is likely that there is a systematic error in water-flow (underestimate) or steam-flow (overestimate). For total discharge rate, the errors in water and steam flow rates would tend to cancel each other out. The mass output curves for the various boreholes are plotted as a function of wellhead pressure, but the wellhead pressure corresponding to the maximum discharge rate varies from borehole-to-borehole.

During almost all of the discharge tests, pressure and temperature (or pressure, temperature and spinner) surveys were run. The pressure and temperature data from these surveys are used to calculate the productivity indices for the boreholes. Following the discharge tests (varying in duration from a few days to several months) pressure buildup was recorded by lowering a gauge (usually Kuster) into the borehole. The pressure buildup data can be analyzed to obtain estimates of reservoir formation properties.

e.2 Formation Transmissivity After start of injection in a borehole, the pressure at first rapidly rises and then slowly falls. As soon as injection is terminated, the pressure begins to decline very rapidly. The rapid fall-off at shut-in is not unusual. The fall-off data from injection tests may be analyzed to obtain formation transmissivity (the product of permeability and effective formation thickness). Conversely, after a production test is ended, feedzone pressure begins to build up and analysis of that data can also yield transmissivity.

Pressure buildup data are available for most of the Japanese boreholes that have been discharged. In all cases, the pressure buildup responses were recorded by lowering a mechanical pressure gauge (usually a Kuster tool) into the borehole, either just before or immediately after completion of the discharge test. Because of instrument time limitations, it was necessary in several cases to pull the gauge from the hole after a few hours (and later reinsert it). This caused a gap in the pressure buildup record which should be avoided if possible.

Multi-rate Horner plots of pressure buildup data can be used for inferring formation properties. Pressure buildup data for boreholes can be approximated by straight lines on the multi-rate Horner plots. The slope m of the straight line can be used to estimate the formation transmissivity, kh , from the following relationship (compare with Eq. 12, Section IV-a):

$$kh = 1.15 Mv/2\pi m$$

where M is the last flow rate prior to shut-in and v is the kinematic viscosity of the reservoir liquid.

Transmissivity values for the four Japanese geothermal fields (Oguni, Sumikawa, Takigami and Kirishima) were determined by the separate Japanese developers primarily from pressure interference tests. Since kh values for the geothermal fields have been presented above in Section III-f, we will not dwell on them, except for the anomalous kh values obtained at the Oguni Geothermal Field. Because of funding limitations, Maxwell scientists did not attempt to analyze pressure transient data available from the Sumikawa, Takigami and Kirishima Geothermal Fields.

The Oguni Geothermal Field is apparently divided into a high-pressure reservoir and a low-pressure reservoir. Analyses of pressure interference data from the low-pressure reservoir indicate good transmissivity ($kh = 100$ to 250 darcy-meters); while the value for the high-pressure reservoir is about 10 darcy-meters¹³. Permeability-thickness values inferred from pressure fall-off and pressure buildup data from individual Oguni boreholes are not in agreement with those from the pressure interference tests^{14, 15}.

In fractured geothermal reservoirs, interference tests commonly yield higher kh values than those given by pressure buildup (and pressure fall-off) tests. An individual borehole intersects at most a few major fractures, which join the fracture network at some distance from the borehole, so a pressure buildup test generally samples a smaller region of the reservoir than that investigated by an interference test.

Analyses of pressure transient data from the boreholes in the Oguni Geothermal Field indicate that (1) the kh values inferred from pressure interference and pressure buildup tests are significantly greater than those derived from pressure fall-off tests, and (2) the slim holes yield kh values which are smaller than those obtained from large-diameter wells.

The reservoir radius investigated during a borehole test is roughly proportional to the square root of time. In contrast with longer term discharge tests (days to months in duration), short term injection tests (a few hours) sample only the near wellbore region. The pressure fall-off data yield kh values (5 to 25 darcy-meters for large-diameter wells) which are much smaller than those obtained from pressure buildup and pressure interference tests. These results suggest that short term injection tests are likely to yield a lower bound on reservoir transmissivity.

Garg, et al.¹⁴⁻¹⁶ speculated that the differences in kh values inferred for slim holes and large-diameter wells may be caused by the differences in drilling techniques (*i.e.*, core drilling versus rotary drilling). Many of the slim holes at the Oguni Geothermal Field were drilled with a complete loss of circulation fluid (see Appendix B¹⁵). The circulation fluid, in most cases, consisted of a dilute (mud density ~ 1.00 to 1.05 gm/cm³) bentonite based mud. In contrast with slim holes, blind drilling was rarely used for rotary drilled large-diameter wells. It is thus possible that core drilling without returns (at least in the case of Oguni Geothermal Field)

deposits rock flour and mud in the formation and causes greater formation plugging than that resulting from rotary drilling, but this difference in kh values as a function of borehole diameter was not observed in the borehole data from the Sumikawa, Takigami and Kirishima Geothermal Fields¹⁷⁻¹⁹.

e.3 Productivity and Injectivity Indices – Boreholes with Liquid Feedzones Productivity and injectivity indices are measures of the formation's resistance to flow. The injectivity index (II) is defined as follows:

$$II = M / (P_f - P_i)$$

where M is the mass rate of injection (single rate test), P_f is the flowing pressure at the gauge depth and P_i is the initial shut-in or static pressure at the gauge depth. During injection testing of a borehole, the pressure gauge is located as near as possible to the principal feedzone. A static pressure is recorded at the gauge depth prior to the start of cold water injection. The pressure measurements taken at the end of each injection interval can then be used to compute the injectivity index.

For multi-rate injection tests, the equation above can be rewritten as follows:

$$II = \Delta M / \Delta P$$

where $\Delta M / \Delta P$ is the slope of the straight-line fit to the multi-step injection rate versus injection pressure (at gauge depth) data.

Productivity index, PI, is defined as follows:

$$PI = M / (P_{ns} - P_{fp})$$

where M is the discharge (*i.e.*, mass production) rate, P_{ns} is the stable (static) feedzone (or gauge depth) pressure, and P_{fp} is the flowing feedzone (or gauge depth) pressure.

The productivity and injectivity indices for the various Japanese boreholes with liquid feedzones appear to be approximately equal. The latter observation is at variance with the results of the classical porous-medium flow analyses²⁰ which suggest that the injectivity index should be a strong function of the sand face injection temperature.

Grant *et al*²¹, however, maintain that the classical analyses do not apply to geothermal systems which are mostly associated with fractured formations; and that injectivity is at least as great as productivity in discharge tests. The Japanese borehole data are consistent with this viewpoint and imply that in the absence of discharge or productivity data, the injectivity index may be used to characterize the flow resistance of the reservoir rocks with liquid feedzones.

In many cases, the downhole pressure tool (Kuster gauges) was placed substantially above the feedzone depth during the injection (or discharge) tests. Because of temperature changes caused by injection of cold fluid or discharge of hot fluids, the measured change in pressure at the gauge depth (gauge depth \ll feedzone depth) will be different from the change in pressure at the feedzone depth. This discrepancy in rates of pressure change at the gauge and feedzone

depths will decline with continued injection or discharge. After the flow of a few wellbore volumes (say 2 or 3), the temperature in the depth interval between the gauge and feedzone depths should approach a stable value and the rates of pressure change at the two depths will be similar.

When measured pressure and temperature values in the two-phase zone are compared with the corresponding steam table values, there were often significant discrepancies. It has been our experience that the pressure gauges are often out of calibration, so measured pressure values were corrected to the corresponding saturation pressures using the measured temperatures (in the two-phase zone) and that correction value was added to (or subtracted from) the measured pressure values in the single-phase liquid zone.

Oguni -- The injectivity index was obtained for six slim holes and eight large-diameter wells at the Oguni Geothermal Field^{14, 15}. The productivity index was determined for nine slim holes and five large-diameter wells. Both the productivity and injectivity indices were available for seven of the Oguni boreholes. The values are in the table below. Except for borehole GH-15 which was characterized by *in situ* boiling during discharge, all of the boreholes had liquid feedzones. It appears from the values displayed in the table that, to first order, the productivity and injectivity indices are equal for the Oguni boreholes with liquid feedzones. GH-15 is discussed in Section IV-e.9.

Oguni Borehole Name	Final Diameter (mm)	Productivity Index (kg/s-bar)	Injectivity Index (kg/s-bar)
GH-10	159	3.88	3.39
GH-11	216	5.65	1.53
GH-12	216	5.77	5.12
GH-15	216	0.25	1.75
GH-20	216	15.2	7.82
IH-2	216	11.9	33.0
N2-KW-3	76	3.85	5.85

Sumikawa -- The injectivity indices for ten of the twelve Sumikawa boreholes (the two exceptions are S-1 and SC-1) are all of the order of unity¹⁷. The injectivity index for SC-1 (~ 5 kg/s-bar) is significantly larger than that for other Sumikawa boreholes, but it is an exceptionally productive well and it is reasonable that it would have high injectivity as well. In S-1, it appears that injected fluid enters the formation through a casing break at 70–100 meters, so the injectivity index for S-1 is not realistic.

The injectivity indices for Sumikawa boreholes are significantly smaller than productivity/injectivity indices for Oguni production wells. Two Sumikawa boreholes have liquid conditions at the feedzone and productivity indices (1.3 kg/s-bar and 5.7 kg/s-bar) for these boreholes are more or less the same as the corresponding injectivity indices (1.7 kg/s-bar and 5.2 kg/s-bar). The latter conclusions agree with results from the Oguni boreholes²².

Production from Sumikawa boreholes other than the above two is accompanied by *in situ* boiling caused by low formation permeability and high formation temperatures ($250^{\circ}\text{C} < T <$

320°C). The formation transmissivity for two-phase flow is always smaller than that for liquid flow and for these wells the productivity index is, as expected, smaller than the corresponding injectivity index¹⁷.

Takigami -- Injection tests were performed on seven slim holes and sixteen large-diameter wells at the Takigami Geothermal Field¹⁸. It was a standard practice at Takigami to perform a short (a few minutes to a few hours) injection test either just before or soon after completion of a well. A typical injection test at Takigami consists of injecting cold water into a borehole at a fixed rate and simultaneously monitoring pressure downhole. In several cases, injection was performed using two or more different rates.

For several Takigami boreholes, the computed injectivity indices are very large, which implies that measured downhole pressure change is rather small (less than 1 bar). The Kuster gauges used in the Takigami tests have a resolution of 0.1 bars and the two tools used in most of the tests gave pressures that differed from each other by as much as 0.5 bar. Because of these limitations, the computed injectivity indices for high-permeability boreholes may be in substantial error.

At the Takigami Geothermal Field, seven slim holes and nine large-diameter wells have been discharged. All of the Takigami boreholes produce from liquid feedzones. As part of the discharge tests, the characteristic output curves, *i.e.*, mass and enthalpy versus wellhead pressure, were also obtained. With the exception of one slim hole and one large-diameter well, downhole pressure and temperature surveys were run during the discharge tests of the Takigami boreholes. These pressure and temperature surveys were used to calculate the productivity indices.

Both productivity and injectivity indices are available for five slim holes and eight large-diameter wells at Takigami (see table below). The injectivity indices for the Takigami boreholes range from 0.22 kg/s-bar to 28.0 kg/s-bar; while the productivity indices range from 0.08 kg/s-bar to 28.0 kg/s-bar. Like the Sumikawa and Oguni boreholes with liquid feedzones, the productivity and injectivity indices for Takigami boreholes are essentially equal to first order.

Takigami Borehole Name	Final Diameter (mm)	Productivity Index (kg/s-bar)	Injectivity Index (kg/s-bar)
NE-4	79	0.07	0.22
NE-5(i2)	98	28.0	28.0
NE-6(i2)	100	18.0	6.9
NE-11	100	0.73	0.55
NE-11R	100	3.8	2.7
TT-2	216	11.0	25.0
TT-7	216	26.0	24.0
TT-8(i)	311	7.9	12.0
TT-8S1(i)	311	11.0	7.5
TT-8S3	216	2.6	2.3
TT-13S	216	0.94	3.2
TT-14R	216	1.5	2.0
TT-16S	216	0.82	1.4

Kirishima -- Injection tests were performed on eighteen slim holes and eleven large-diameter wells at Kirishima^{19,23}. Injection tests were usually carried out either just before or soon after drilling and completion of a borehole. A typical injection test at Kirishima consists of injecting cold water into a borehole at a fixed rate and simultaneously monitoring pressure downhole. In most cases, injection was performed using two or more different rates. The injectivity indices for the eighteen slim holes ranged from 0.04 kg/s-bar to 3.63 kg/s-bar; while the eleven large-diameter wells ranged from 1.00 kg/s-bar to 8.81 kg/s-bar.

Kirishima Borehole Name	Final Diameter (mm)	Productivity Index (kg/s-bar)	Injectivity Index (kg/s-bar)
N56-KT-8	100	3.94	1.11
N60-KZ-2	101	0.04	0.07
KE1-3	79	0.36	0.72
KE1-4	98	4.14	3.63
KE1-5	102	0.56	1.64
KE1-7	216	4.39	8.81

During the injectivity testing at Kirishima, multi-rate injection tests were conducted using essentially different injectate temperatures. Injection tests for three boreholes were performed with both cold water (~ 0°C) and hot water (~85°C). Although the viscosity of water at 85°C is much less than that at 0°C, the injectivity indices display no significant correlation with the temperature of the injected water. This result is consistent with the observation that injectivity and productivity indices for boreholes with liquid feedzones are more or less equal²⁴. Apparently, the resistance of the reservoir rocks to fluid flow is determined by the *in situ* fluid temperature.

Downhole pressure surveys were run during the discharge tests of various Kirishima boreholes. For about half the boreholes, multi-rate discharge tests were performed, and pressures were recorded downhole with capillary tube type gauges. The productivity indices for boreholes outside the Ginyu fault zone range from 0.04 kg/s-bar to 4.14 kg/s-bar; while those completed in the fault zone ranged from 4.39 kg/s-bar to 550.00 kg/s-bar to very large or essentially infinite. Only one Ginyu/Ogiri production well has a productivity index less than 10 kg/s-bar. Boreholes completed in the Ginyu fault zone have large productivity indices, and production from these boreholes was accompanied by little or no pressure drop. As discussed above, measurement of small pressure changes downhole makes productivity indices for high-permeability Ginyu/Ogiri boreholes problematical.

Both productivity and injectivity indices were available for seven slim holes and one large-diameter well at the Kirishima Geothermal Field (see table above). Five slim holes and the single large-diameter well discharge from liquid feedzones¹⁹. Discharge from two Kirishima slim holes was accompanied by *in situ* boiling. Injectivity and productivity indices for Oguni, Sumikawa, Takigami, and Kirishima boreholes with liquid feedzones are displayed in Figure IV-9 below. Similar to the Oguni, Sumikawa, and Takigami geothermal boreholes with liquid feedzones, the productivity and injectivity indices for Kirishima boreholes are equal to first order.

Summary -- Based on the rather large volume of data presented in Figure IV-9 (above),

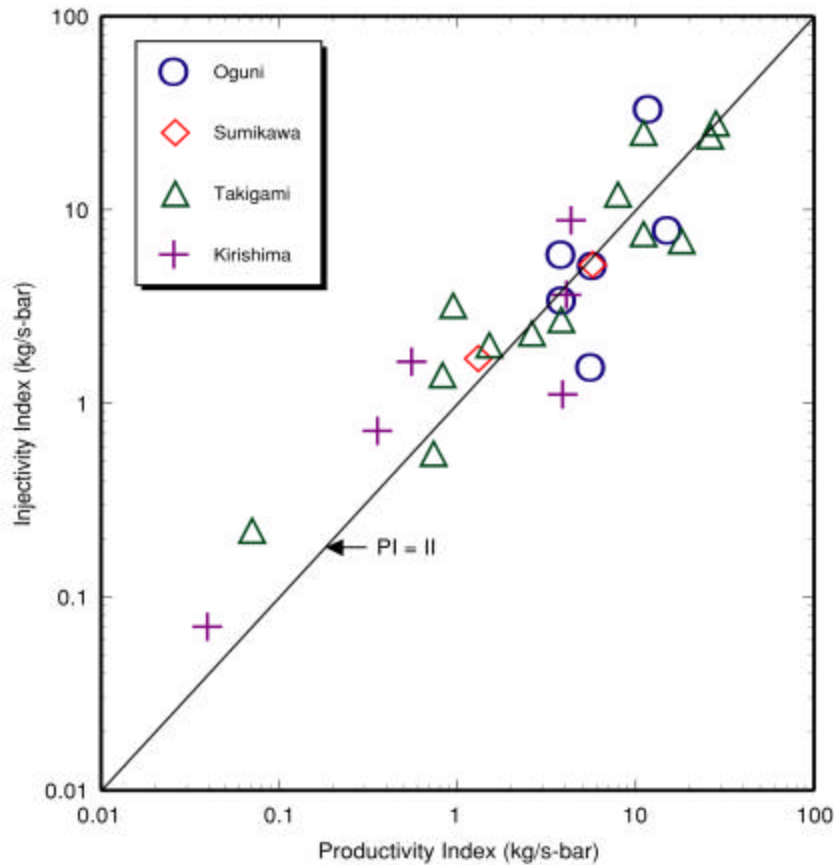


Figure IV-9 – PI vs II in Liquid Feedzones

indicating that the productivity and injectivity indices are equal to first order, it is reasonable to conclude that the injectivity index may be used to compute the flow resistance of naturally fractured geothermal formations to liquid production. Thus, in the absence of discharge testing and the resulting productivity index, the injectivity index may be used with a flow simulator to compute the probable discharge characteristics of large-diameter geothermal wells. Furthermore, the productivity and/or injectivity indices for slim holes provide a lower bound on the corresponding indices for large-diameter geothermal wells.

e.4 Productivity and Injectivity Indices – Boreholes with Two-Phase Feedzones

Borehole data included that from seven wells at Oguni, Sumikawa, and Kirishima which were characterized by *in situ* boiling^{19,23}. It is apparent from the table below that the productivity index for a borehole with *in situ* boiling is much smaller than the injectivity index.

Geothermal Field	Borehole Name	Final Diameter (mm)	Productivity Index (PI) (kg/s-bar)	Injectivity Index (II) (kg/s-bar)	II/PI
Oguni	GH-15	216	0.25	1.75	7

Sumikawa	S2(i)	101	0.03	0.76	25
Sumikawa	S-4	159	0.94	1.4	15
Sumikawa	SA-1	216	0.16	1.5	9
Sumikawa	SA-4	216	0.11	0.94	9
Kirishima	KE1-1	78	0.05	0.16	3
Kirishima	KE1-6	98	0.05	1.15	23

Because of the relative permeability effects, the flow resistance of reservoir rocks is much greater for two-phase flow than for single-phase liquid transport. The two-phase injectivity and productivity index data for Oguni, Sumikawa, and Kirishima boreholes, presented in Figure IV-10, suggest that the productivity index for two-phase transport is approximately one-tenth of the corresponding injectivity index. Because of the sparseness of the data set, the latter conclusion must be regarded as tentative. Additional studies are required to draw firm conclusions regarding the relationship between injectivity index and two-phase productivity index. Data from high-temperature geothermal fields spanning a wide range of transmissivities are needed for these studies.

e.5 Productivity and Injectivity Indices Versus Borehole Diameter Prediction of the mass output of a large-diameter well based on discharge data from a slim hole requires, among other things, a relationship between productivity index and borehole diameter. Theoretical

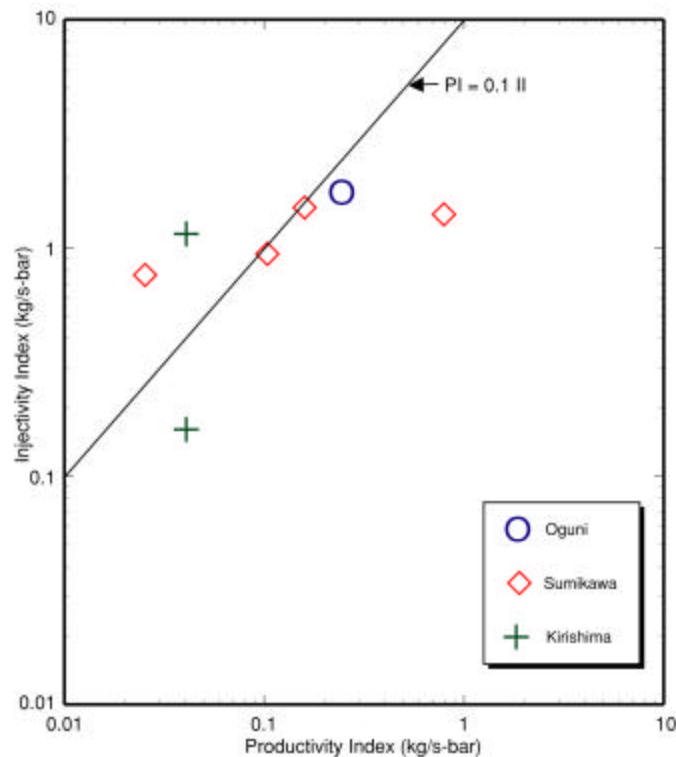


Figure IV-10 - PI vs II for Two-Phase Feedzones

considerations^{25, 26} suggest that apart from any differences associated with differences in

wellbore skin (*i.e.*, near-borehole formation damage or stimulation), the productivity (or injectivity) index should exhibit only a weak dependence on borehole diameter. As noted above, both these indices (and hence wellbore skin) display a strong dependence on borehole diameter for Oguni, but not for the other three Japanese fields.

The difference between the Oguni and Sumikawa results appears to be due to the differences in drilling practice at the two fields. At Oguni, most of the slim holes were drilled with a complete loss of circulation; the drilling mud and/or rock flour apparently plugged some of the permeable fractures. In the case of Sumikawa slim holes, no blind drilling was necessary. Rotary drilling -- employed to drill large-diameter holes in both the Sumikawa and Oguni Geothermal Fields -- is rarely carried out with complete loss of circulation. Thus, it is likely that formation plugging is responsible for the apparent variation of productivity and injectivity indices with diameter at Oguni.

The productivity and injectivity indices for Takigami boreholes¹⁸ do not exhibit any systematic dependence on borehole diameter. Like the Oguni slim holes, most of the slim holes at Takigami were also drilled with a complete loss of circulation, but this apparently did not result in any impairment of borehole injectivity/productivity.

Unfortunately, the borehole data from the Kirishima Geothermal Field^{19, 23} were not well-suited for evaluating the effect of borehole diameter on the injectivity/productivity index. Most of the slim holes -- drilled early in the exploration phase -- are located in the less permeable parts of the reservoir, whereas a large fraction of the large-diameter production/injection wells were drilled to intersect the extremely permeable Ginyu fault zone.

e.6 Effect of Borehole Diameter on Discharge Capacity Production characteristics of a geothermal well are principally determined by (1) pipe friction and heat losses in the wellbore, and by (2) pressure losses associated with flow in the reservoir rocks. As discussed by Pritchett²⁵, both frictional pressure gradient and heat loss effects are more significant for the small-diameter slim holes than for the large-diameter wells. The difference in heat loss effects is probably responsible, at least in some cases, for the difficulty encountered in inducing deep slim holes (depths $\gg 300$ meters) to discharge.

Pritchett has investigated the fluid-carrying capacity of boreholes of varying size, assuming that pressure losses in the formation are negligible and that the feedzone contains single-phase liquid. The simplest method of comparing flow rates in different-sized boreholes is to introduce the “area-scaled discharge rate” M^* as follows:

$$M^* = M_O(d/d_O)^2$$

where M_O is the actual borehole discharge rate; and d and d_O are the internal borehole diameters; that is, flow rate is proportional to wellbore cross-section. Based on numerical simulation of fluid flow in boreholes of varying diameters, however, Pritchett²⁵ suggests that the “scaled maximum discharge rate” M_{\max} , will increase at a rate somewhat greater than the square of diameter (or area).

$$M_{\max} = M_O(d/d_O)^{2+n}, \quad n \geq 0$$

The exact value of n will depend on the downhole conditions (*e.g.*, feedzone depth, flowing pressure and enthalpy, and gas content of the fluid). For the conditions assumed by Pritchett (feedzone depth = 1500 meters, feedzone pressure = 80 bars, feedzone temperature = 250°C, single-phase liquid-water at feedzone, uniform wellbore diameter), n is equal to 0.56. Hadgu, *et al.*²⁶ have considered single-phase (liquid) adiabatic flow (no heat loss) up a wellbore, and suggest that n equals 0.62. The importance of boiling in the borehole and of heat loss to the formation cannot be overstressed.

Oguni -- With the exception of two boreholes in the high pressure zone of the reservoir, all of the Oguni boreholes have single-phase liquid conditions at their principal feedzones. At Oguni, the formation permeability is sufficiently high that the pressure losses in the reservoir are insignificant compared to pressure losses in the borehole, so the discharge behavior of Oguni boreholes is principally determined by pipe friction and heat losses in the wellbore. On average, the Oguni feedzones are shallower and the feedzone temperatures are somewhat lower than that assumed by Pritchett for his computations.

Both the “area-scaled” and “scaled maximum ($n = 0.56$)” discharge rates for the Oguni boreholes are presented by Garg, *et al.*^{14, 15, 22}. For the low-pressure zone, large-diameter (216 mm) wells, the average measured maximum discharge rate is 311 tons/hour. This is bracketed by the averaged “area-scaled” (194 tons/hour) and averaged “scaled maximum” (338 tons/hour) discharge rates calculated from slimhole data.

Furthermore, using the slim hole data, the predicted M^* and M_{\max} for GH-10 (159 mm diameter) are 105 tons/hour and 155 tons/hour, respectively, compared to the measured discharge rate of 164 tons/hour. Despite differences between the conditions assumed by Pritchett and the actual conditions existing in the Oguni boreholes, it appears that the “scaled maximum discharge rate” provides a reasonable prediction of the discharge performance of large-diameter geothermal wells.

The above analyses of the Oguni borehole data are thus consistent with the premise that it should be possible to forecast the discharge performance of large-diameter production wells using production data from slim holes. This conclusion, however, had to be tested with discharge data from a statistically significant collection of slim holes and large-diameter wells from a number of geothermal fields. Ideally, the set of geothermal fields should include both large and moderate transmissivity geothermal fields; a wide range of reservoir permeabilities is needed to characterize the effect of pressure losses in the reservoir on the discharge characteristics of both slim holes and large-diameter wells.

Sumikawa -- Pressure losses in the reservoir constitute the bulk of pressure losses in boreholes for which discharge is accompanied by *in situ* boiling. Even for boreholes with liquid conditions at the feedzone depth, the pressure loss in the formation exceeds 10 bars, so the conditions assumed in Pritchett’s work do not hold for Sumikawa boreholes with *in situ* boiling.

The discharge rates for Sumikawa boreholes (either actual discharge from nominal 216 mm diameter production wells or discharge from slimholes scaled to that size) with little or no *in situ* boiling range from 100 tons/hour to 490 tons/hour. The comparable range for Oguni wells

extends from 227 ton/hour to 488 ton/hour. The upper limit for the discharge rates is about the same for both the Sumikawa and Oguni boreholes, but the Sumikawa boreholes display considerably more variability in discharge rates than the Oguni boreholes. In any event, the above-discussed data for Sumikawa boreholes, taken in conjunction with Oguni data¹⁴, imply that the “scaled maximum discharge rate” provides a reasonable first prediction of the discharge performance of large-diameter geothermal wells with little or no *in situ* boiling.

Based upon the available data from Oguni and Sumikawa boreholes (four slim holes, four large-diameter wells) with extensive *in situ* boiling, it appears that the “scaled maximum discharge rate” over-predicts the discharge rate of large-diameter wells. In all likelihood, the scaling rule ($n = 0.56$) derived for boreholes with liquid feeds and with little or no pressure loss in the formation, is not applicable to boreholes with two-phase feeds.

Takigami -- The average discharge rate for large-diameter wells at Takigami is significantly greater than the average “scaled maximum discharge rate” computed from slim hole data. The latter result is at variance with the data for Oguni, Sumikawa and Steamboat Hills Geothermal Fields, where “scaled maximum discharge rate” provides an upper bound on the average measured discharge rate for large-diameter wells.

Most large-diameter wells at Oguni and at Sumikawa Geothermal Fields are completed with a 9-5/8” (internal diameter ~224 mm) cemented casing and a 8-1/2” (~216 mm) open hole, although in some cases, the open hole is lined with a 7-inch uncemented liner. Thus, most Oguni and Sumikawa large-diameter wells have a more or less uniform internal diameter (~ 220 mm), satisfying one of the key assumptions made by Pritchett in his analysis.

In contrast, most large-diameter production wells at Takigami are completed with 13-3/8” cemented casing (ID ~ 318 mm) in the upper part, 9-5/8” cemented liner (ID ~ 224 mm) in the middle part, and 8-1/2” open hole (ID ~ 216 mm) in the lower part of the borehole. For well TT-7, the diameter of the cemented casing in the upper part of the borehole is 16” (internal diameter ~ 381 mm). Because Takigami production wells do not have uniform internal diameters we do not expect Pritchett’s scaling rule to apply to the boreholes. For a discussion of Takigami wells, see Section e.7.

Kirishima -- A total of ten slim holes and sixteen large-diameter wells have been discharged at the Kirishima Geothermal Field^{19, 23}. The discharge data are required to determine the characteristics output curves (i.e., mass and enthalpy versus wellhead pressure). Downhole pressure/temperature surveys and wellhead enthalpy measurements indicate that discharge from five slim holes and four large-diameter wells is accompanied by *in situ* boiling; the remaining boreholes at Kirishima produce from liquid feedzones. Slim holes that were discharged for only brief periods did not attain a stable discharge rate during the test period and are not considered in the following discussion.

With the single exception of slim hole KE1-3, all of the boreholes with liquid feedzones in the Kirishima Geothermal Field have a more or less uniform internal diameter. The “area-scaled” and “scaled maximum ($n = 0.56$)” discharge rates for the Kirishima slim holes (liquid feedzones) were compared with measured discharge rates for large-diameter wells at Kirishima and the “scaled maximum discharge” rate, obtained from slim hole data provides a reasonable

estimate of the maximum discharge rate for large-diameter Kirishima wells with liquid feedzones. The latter result is in agreement with data from other geothermal fields (Oguni, Sumikawa, Takigami, and Steamboat Hills in Nevada, USA) analyzed and discussed by Garg and Combs²⁴.

e.7 Mathematical Modeling of Fluid Flow in Takigami Boreholes To explore the relationship between the discharge capacity of slim holes and large-diameter Takigami wells, it is necessary to numerically simulate the production characteristics of non-uniform, large-diameter, wells. Numerical parameters can be varied to fit actual production data (for non-uniform wells) and can then be used to calculate the probable discharge rate for a uniform-diameter (*i.e.*, an “Oguni/Sumikawa type”) well.

The flow characteristics of Takigami boreholes were modeled using the wellbore computer simulation program WELBOR²⁷. The code treats the steady flow of water and/or steam up a borehole. The user provides parameters describing the well geometry, *i.e.*, inside diameter and angle of deviation with respect to vertical along the hole length, a stable formation temperature distribution with depth, and an “effective thermal conductivity” representing the effects of conductive heat transfer between the fluid in the wellbore and the surrounding rock formation. Values must also be specified for the flowing feedpoint pressure (or alternately stable feedpoint pressure and productivity index) and enthalpy (or alternately temperature for wells producing from a single-phase liquid zone).

Since all the Takigami boreholes produce from liquid feedzones, the feedzone fluid state can be prescribed by pressure, productivity index, and temperature. The frictional pressure gradient was treated using Dukler’s correlation²⁸ and a user-prescribed roughness factor. The relative slip between the liquid and gas phases was simulated using the Hughmark liquid holdup correlation²⁹.

Given the downhole (usually at feedzone depth) values for mass flow, pressure and temperature, the WELBOR code was used to compute the conditions along the wellbore and at the wellhead (pressure, flowing enthalpy, *etc.*). The principal parameters that were varied to match the measured conditions in the wellbore and at the wellhead are (1) effective thermal conductivity and (2) interior roughness factor. For both the slim holes and large-diameter production wells at Takigami, WELBOR was used to match the downhole pressure/temperature profiles and the results of characteristic tests. The model parameters derived from fits to actual discharge test data (for both the slim holes and large-diameter production wells) were used to calculate the discharge characteristics of an “Oguni/Sumikawa type” (OST) well (244 mm cemented casing with an internal diameter of 224 mm, and a 216 mm open-hole section).

To illustrate the computational procedure, it is instructive to consider the large-diameter well TT-7. Its principal feedzone is at 1,070 m TVD (True Vertical Depth). The stable feedzone pressure is ~64.5 bars. During the preliminary discharge test of TT-7 (29 August 1986), a pressure/temperature survey was run to a depth of ~699 m TVD. Extrapolating the measured pressure profile, the flowing feedzone pressure is ~59.6 bars; with a discharge rate of 129 kg/s, the productivity index (PI) is computed as 26 kg/s-bar. Detailed numerical simulations with WELBOR (presented below) imply that the productivity index (PI) for TT-7 is ~30 kg/s-bar. In

addition to the preliminary discharge test, characteristic test data are also available from the 1991–1992 long-term discharge test. The feedzone temperature during the preliminary discharge test is estimated to be $\sim 208^{\circ}\text{C}$. For the long-term test, the flowing feedzone temperature may be slightly higher ($\sim 208.8^{\circ}\text{C}$).

The well geometry for TT-7 is as follows:

Measured Depth (m)	Vertical Depth (m)	Angle With Vertical ($^{\circ}$)	Internal Diameter (mm)
0.0 – 752.4	0.0 – 751.0	3.49	381
752.4– 942.5	751.0– 949.4	7.47	224
952.5 – 1075.4	949.4	11.10	216

The upper section of TT-7 has the largest diameter (ID = 381 mm) of all the Takigami production wells. The large-diameter of the upper section is directly responsible for TT-7 being the most prolific producer at Takigami. The casing program for TT-7 was designed based on the drilling and discharge/injection test data for slim hole NE-5. TT-7 was directionally drilled so as to intercept the same fracture system as that encountered by NE-5. Boreholes TT-7 and NE-5 thus constitute a good example of the use of slim holes to drill and complete offset large-diameter production wells.

The stable formation temperature was specified based on measurements in the borehole. The characteristic test data and downhole temperature/pressure surveys taken during the preliminary discharge test on 29 August 1986 were simulated using the following model parameters:

Productivity Index,	$PI = 30 \text{ kg/s-bar}$
Flowing Feedzone Temperature,	$T_f = 208^{\circ}\text{C}$
Effective Thermal Conductivity,	$K = 25 \text{ W/m-}^{\circ}\text{C}$
Friction Factor,	$e = 0.29 \text{ mm}$

The large value of K ($25 \text{ W/m-}^{\circ}\text{C}$) needed for matching characteristic data implies that heat losses were high during the preliminary flow test. Characteristic test data (discharge rate versus wellhead pressure) and downhole temperature/pressure surveys are compared with computed results in Figs IV-11 to IV-13; and the agreement is quite good. The characteristic test data from the long-term discharge test of TT-7 were simulated using the following values for T_f and K :

Flowing Feedzone Temperature,	$T_f = 208.8^{\circ}\text{C}$
Effective Thermal Conductivity,	$K = 4 \text{ W/m-}^{\circ}\text{C}$

All other parameters were assumed to be identical with those for the preliminary discharge test simulation. For the long-term test, the effective thermal conductivity (and hence the heat loss) is a small fraction of that for the preliminary discharge test because conductive heat loss declines with increased production time. The test data from the long-

term test are in good agreement with the simulated characteristic curve (Fig. IV-14).

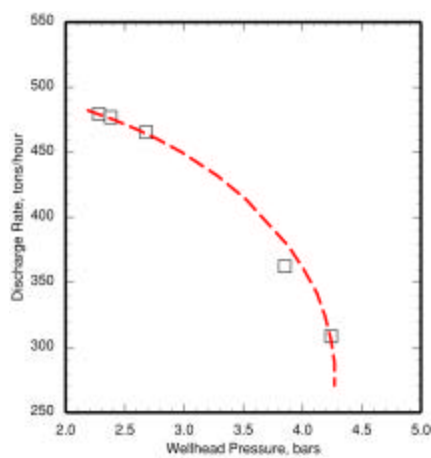


Figure IV-11 - Discharge vs WH Pressure TT-7

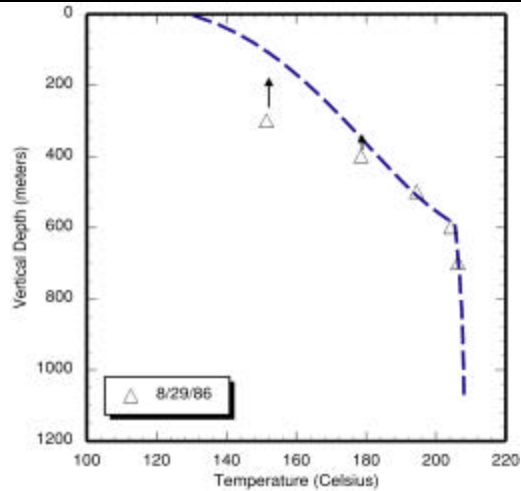


Figure IV-12 – Temperature vs depth, TT-7

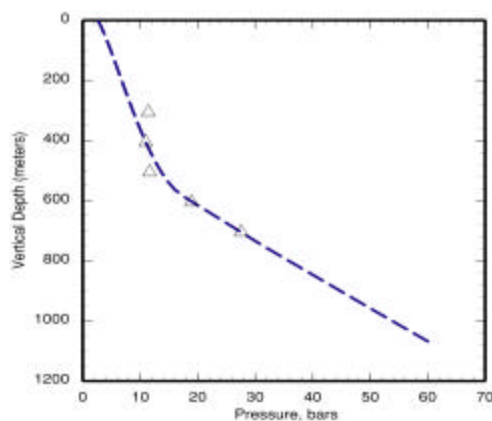


Figure IV-13 – Pressure vs depth, TT-7

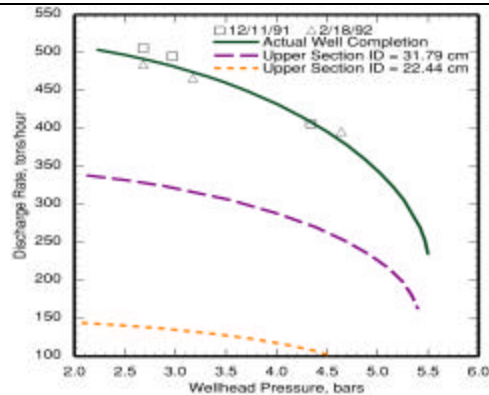


Figure IV-14 – Discharge vs WH pressure, long-term test, TT-7

To assess the effect of the diameter of the upper section of the borehole on the discharge behavior of TT-7, two calculations were run (using the same parameters as employed for the long-term test simulation) assuming that the inside diameter of the upper section equals (1) 318 mm and (2) 224 mm. It should be noted that most of the Takigami production wells were completed with a 318-mm upper section. The upper section diameter of 224 mm defines the hypothetical OST well. The computed discharge characteristics for these two cases are shown in Fig. IV-14. It is apparent that discharge rate is a strong function of upper section diameter. For the 318-mm case, the maximum discharge rate is ~338 tons/hour. The maximum discharge

rate for the OST well is only ~144 tons/hour, but the measured maximum discharge rate for TT-7 is almost 500 tons/hour.

e.8 Comparison of Discharge Rate Predictions for “Oguni-Sumikawa Type” Wells

Takigami -- Several interesting conclusions were drawn from the mathematical models of Takigami boreholes¹⁸. For boreholes with poor injectivity and productivity (*e.g.*, slim hole NE-4), the pressure loss in the formation cannot be neglected, and detailed models of fluid flow in the borehole are needed to make useful predictions. As an example, the predicted discharge rate (18 tons/hour) for an OST well using the detailed mathematical model for slim hole NE-4 is only a small fraction of the scaled maximum discharge rate of 144 tons/hour. As remarked elsewhere in this handbook, Pritchett invoked three key assumptions (*i.e.*, (1) liquid feedzone, (2) uniform wellbore diameter, and (3) large productivity index) in deriving his scaling rule. Clearly, the scaling rule should not be expected to apply in situations where one or more of the key assumptions do not hold.

Mathematical modeling of large-diameter production wells implies that the diameter of the upper section has a large influence on the discharge capacity of a borehole. As an example, a reduction in the diameter of the upper section from 381 mm to 224 mm for well TT-7 results in an almost 70 percent decrease in the discharge capacity, *i.e.*, from 490 tons/hour to 144 tons/hour. For the existing large-diameter Takigami wells, the two-phase part of the flow column is contained entirely within the upper cased interval. Since the pressure drop in the two-phase flow regime is a strong function of well diameter, the large diameter for the upper section is primarily responsible for the large discharge capacity of wells at the Takigami Geothermal Field, relative to OST wells.

Takigami Borehole Name	Open-hole Diameter (mm)	Measured Discharge Rate at Takigami (t/h)	Predicted Discharge Rate for OST well (t/h)
NE-3	101	23	168
NE-4	79	11	18
NE-5(i1)	98	36	210
NE-5(i2)	98	31	188
NE-6(i1)	100	26	118
NE-6(i2)	100	25	116
NE-11	100	20	60
NE-11R	100	12	103
Predicted Average using slim holes		=	123
TT-2	216	260	135
TT-7	216	490	144
TT-8S3	216	180	130
TT-13S	216	200	131
TT-14R	216	280	178
TT-16S	216	90	111
Predicted Average using production wells		=	138

To emphasize this point, calculated maximum discharge rates for hypothetical OST wells (cased interval of 224 mm and 216 mm ID open hole interval) in the Takigami field are provided in the table below. The predicted average maximum discharge rate, obtained using data from the eight Takigami slim holes, is 123 tons/hour, but one of the slim holes was drilled in an unproductive part of the Takigami Geothermal Field. Excluding that slim hole, the predicted average maximum discharge rate for OST wells, using slim hole data, is 138 tons/hour, exactly the same as the predicted average discharge rate obtained from modeling of large-diameter Takigami wells. Although the exact agreement is somewhat coincidental, it can be safely concluded that the Takigami discharge data are consistent with the premise that it is possible to predict the discharge characteristics of large-diameter geothermal wells with liquid feedzones based on discharge data for slim holes with liquid feedzones.

e.9 Mathematical Modeling of Fluid Flow in Boreholes with Two-Phase Feedzones

Reliable data in the Kirishima data set includes only one slim hole and three large-diameter wells. Because of the sparseness of the Kirishima data set for boreholes with two-phase feeds, Garg, *et al.*¹⁹ decided to also simulate, using WELBOR (described above), the discharge characteristics of one slim hole and one large-diameter well each at Oguni and Sumikawa.

This version of WELBOR differs from the previous one in that the relative slip between liquid and gas phases is treated using a modified version of the Hughmark liquid hold up correlation. This allows the slippage rate to vary between the value given by the Hughmark correlation and no slip at all, according to the value of a user-supplied holdup parameter, h , which varies between zero (no slip) and unity (Hughmark). Numerical experimentation has shown that for a given mass flow rate the minimum pressure drop along the wellbore is obtained for an intermediate value of the holdup parameter ($0 < h < 1$). In most of the calculations for boreholes with two-phase feeds, it was necessary to choose h close to the value that gave minimum pressure drop.

Most geothermal wells are completed with an uncemented slotted (or perforated) liner in the open hole section of the borehole. Garg and Combs used the WELBOR²⁴ code to model fluid flow in both slim holes and large-diameter wells at the Takigami Geothermal Field. All of the Takigami boreholes produce from single-phase (all liquid) feedzones. Apparently, the presence of slotted/perforated liner in single-phase Takigami boreholes has little influence on fluid transport.

The situation is quite different for two-phase flow. An examination of downhole pressure profiles for boreholes with two-phase feedzones shows that the pressure gradient is significantly higher in the slotted/perforated liner portion of the borehole than in the cemented and cased part of the borehole. To correctly reproduce the observed pressure gradient in the slotted/perforated liner, it was necessary in most cases to assume that the inside diameter of the wellbore is equal to that of the slotted/perforated liner. In addition, a non-zero pipe roughness factor for the slotted/perforated liner portion of the wellbore was used in most of the calculations presented below.

Given the downhole values (usually at the uppermost feedzone) for mass flow, pressure and enthalpy, the wellbore code can be used to compute the conditions (pressure, temperature)

along the wellbore and at the wellhead (pressure, flowing enthalpy, etc.) We can then vary the following parameters to match the measured conditions in the wellbore and at the wellhead:

- holdup parameter h ,
- effective thermal conductivity K , and
- interior roughness factor e .

In two-phase water/steam flow, pressure and temperature are not independent variables. For any given effective thermal conductivity K , downhole flowing enthalpy may be adjusted to yield the appropriate pressure, and hence temperature, distribution in the wellbore, and flowing wellhead enthalpy.

Because the two-phase mixture can vary in quality (ratio of vapor to total mass) the pressure/temperature distribution in the wellbore does not define the flowing feedzone enthalpy and heat loss. Since the flowing feedzone enthalpy is not a measured quantity, it is difficult to determine a precise value for heat loss. The latter problem does not arise for single-phase liquid feedzones since the flowing feedzone enthalpy can be determined using the measured temperature and the steam tables. For these reasons, effective thermal conductivity K was eliminated as a parameter in the calculations described below, and was taken to be a constant ($= 4 \text{ W/m}^\circ\text{C}$).

For both the slim holes and large-diameter wells with two-phase feedzones, WELBOR was used to match the downhole pressure/temperature profiles. The model parameters (roughness factor, holdup parameter) derived from fits to downhole data were then employed to match the results of characteristic tests by varying feedzone pressure and enthalpy. Finally the discharge characteristics of a “standard” large-diameter well were predicted using model parameters (roughness factor, holdup parameter, productivity index) for slim holes.

To illustrate the computational procedure, slim hole KE1-6 was examined^{19, 23}. The principal feedzone for Kirishima slim hole KE1-6 is located at 1235 m TVD. The stable feedzone pressure and temperature are estimated to be 73.2 bars and $\sim 220^\circ\text{C}$, respectively. The borehole is completed with a 114 mm (103 mm ID) diameter casing cemented to a depth of 1001.2 m TVD; a 83 mm (76 mm ID) diameter uncemented liner in a 98 mm diameter hole is present from 992.3 m TVD to 1514.5 m TVD. After considerable numerical experimentation, the following well geometry was assumed for the Kirishima slim hole:

Measured Depth (m)	Vertical Depth (m)	Angle With Vertical ($^\circ$)	Internal Diameter (mm)
0.0 – 992.3	0.0 – 992.3	0.0	103
992.3 – 1235.0	992.3 – 1235.0	0.0	76

A characteristic discharge test was performed from July 4 to July 8, 1983. The borehole discharged a mixture of water and steam with wellhead enthalpies ranging from 937 kJ/kg to 1009 kJ/kg. The measured wellhead enthalpies imply that discharge from KE1-6 was accompanied by *in situ* boiling. Because of the brief duration of the characteristic test, it is unlikely that stable discharge conditions were realized during the test (see below).

Following the characteristic test, a downhole pressure survey was run in the discharging well on July 11, 1983. The reported discharge rate at the time of the downhole pressure surveys was considerably lower than that reported for the July 4-8, 1983 period. The measured feedzone and wellhead pressures on July 11, 1983 were 16.54 bars and 1.52 bars, respectively. Using the second order polynomial fit (see below) to the characteristic discharge data, the wellhead enthalpy corresponding to a wellhead pressure of 1.52 bars is 1009 kJ/kg.

The stable formation temperature in the vicinity of slim hole KE1-6 was specified based on measurements in the borehole. Despite considerable experimentation²³ involving well geometry and other model parameters, it proved impossible to match the downhole pressure profile of July 11, 1983 using the reported discharge rate (10.07 tons/hour = 2.80 kg/s). Simply stated, a discharge rate of 2.80 kg/s is inconsistent with the measured pressure profile in the cased part of the borehole (*i.e.*, above ~1000 meters). Accordingly, the discharge rate was reduced to 2.50 kg/s (*i.e.*, by about 10 percent). With a discharge rate of 2.50 kg/s, the best fit was obtained using the following model parameters:

Thermal Conductivity,	K	=	4 W/m°C
Holdup Parameter,	h	=	0.18
Roughness Factor,	e	=	0 for depths <992.3 m = 0.28 mm for depths >992.3 m
Feedzone Enthalpy,	h _f	=	1102 kJ/kg.

The computed pressure profile, Figure IV-15, is in good agreement with the measurements. A discharge rate of 2.5 kg/s together with a feedzone pressure of 16.54 bars yields a productivity index of 0.044 kg/s-bar for KE1-6. The characteristic discharge data for KE1-6 were fit using the following second order polynomials (Figure IV-16):

$$\begin{aligned}
 M(\text{tons/hour}) &= 17.92 - 2.928 p_w + 0.109 p_w^2 \\
 h_w (\text{kJ/kg}) &= 937.4 + 85.52 p_w - 25.38 p_w^2
 \end{aligned}$$

Model parameters (K, e, h) obtained by fitting the downhole pressure profile were used to simulate the characteristic discharge data (indicated by a * in Figure IV-16). The feedzone pressure and enthalpy were varied to match the wellhead pressure and enthalpy.

The results of these calculations are summarized in the table below.

Wellhead Pressure (bars)	Discharge Rate (kg/s)	Wellhead Enthalpy (kJ/kg)	Flowing Feedzone Pressure (bars)	Feedzone Enthalpy (kJ/kg)	Productivity Index (kg/s-bar)
1.60	3.76	1009	24.10	1112	0.077
2.07	3.47	1007	22.54	1110	0.069
2.39	3.20	996	20.99	1100	0.061
2.80	2.94	978	19.59	1085	0.055

3.20	2.69	951	18.43	1063	0.049
------	------	-----	-------	------	-------

The calculated results indicate that the flowing feedzone pressure increases with the discharge rate. This phenomenon is contrary to general experience and implies that stable discharge conditions were not attained during the characteristic test of slim hole KE1-6.

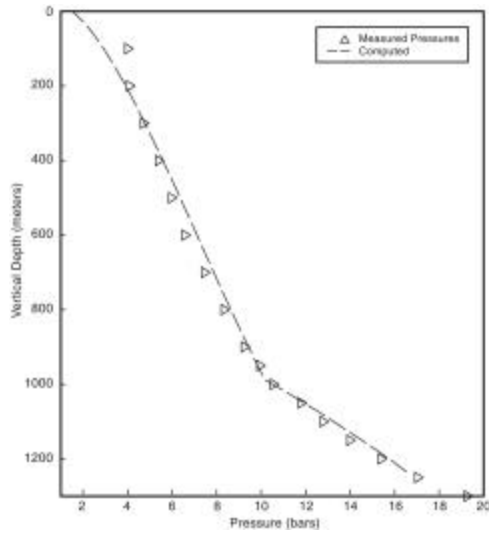


Figure IV-15 – Pressure vs depth, KE1-6

The model parameters (K, e, h) for KE1-6 were also utilized to estimate the maximum discharge rate for a typical large-diameter geothermal well with a 224 mm ID cased interval and a 159 mm ID uncemented liner in 216 mm open hole section. The following geometry is assumed for the large-diameter well:

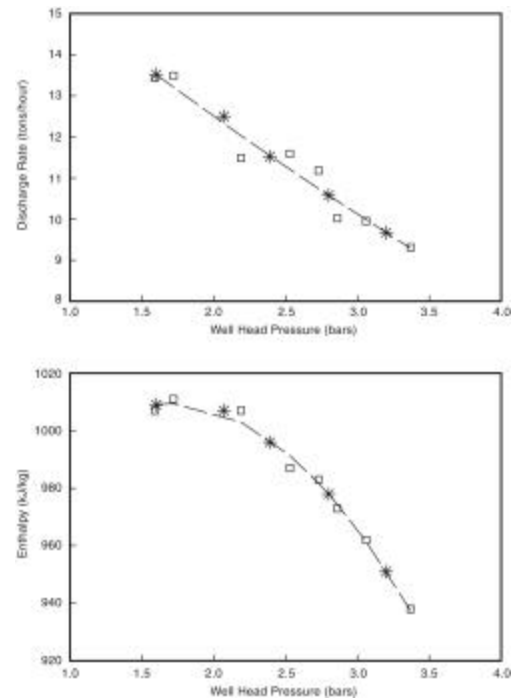


Figure IV-16 – Discharge and enthalpy vs WH pressure, KE1-6

Measured Depth (m)	Vertical Depth (m)	Angle With Vertical (°)	Internal Diameter (mm)
0.0 – 992.3	0.0 – 992.3	0.0	224
992.3 – 1235.0	992.3 – 1235.0	0.0	159

The productivity index and flowing feedzone enthalpy are taken to be 0.06 kg/s-bar and 1110 kJ/kg, respectively. Since stable discharge conditions were not obtained during the characteristic test, the productivity index (PI) for KE1-6 is poorly known. The selected value (PI = 0.06 kg/s-bar) is the median value in the table above obtained from the simulation of characteristic data. The choice for feedzone enthalpy (1110 kJ/kg) is about the highest value inferred from the KE1-6 discharge data. With the preceding parameter values (K, e, h, PI, h_f) the maximum discharge rate for the large-diameter well was computed to be ~4.1 kg/s (*i.e.*, 14.8 tons/hour).

The calculated maximum discharge rate for the large-diameter well is not much greater than that for the slimhole. Because of the very small productivity index, most of the pressure drop takes place in the formation, and increasing the well diameter does not result in a commensurate increase in the discharge rate.

The currently available data set are not well suited for examining the effect of borehole diameter on the discharge rate. Of the five large-diameter wells, four wells have productivity indices ranging from 0.2 kg/s-bar to 0.6 kg/s-bar. The maximum discharge rate for these wells

varies from ~36 tons/hour to ~69 tons/hour. Large-diameter well KE1-21 has a productivity index of 0.06 kg/s-bar; the maximum discharge rate for this well is 17 tons/hour.

Slim hole KE1-6 has a productivity index (~0.06 kg/s-bar) similar to that for large-diameter well KE1-21. Using model parameters for KE1-6, the maximum discharge rate of a hypothetical large-diameter well of a design similar to KE1-21 is predicted to be ~15 tons/hour, which is in substantial agreement with the maximum discharge rate for well KE1-21. The productivity indices for the remaining two slim holes are extremely small (~0.03 kg/s-bar) and the predicted maximum discharge rates for a hypothetical large-diameter well using model parameters for those slimholes are only 6 tons/hour and 5 tons/hour.

e.10 Conclusions and Recommendations from Analysis of Japanese Data

Production and injection test data from Kirishima boreholes with liquid feedzones support the conclusions previously derived from analyses of similar data from Oguni, Sumikawa, Takigami and Steamboat Hills Geothermal Fields²⁴. More specifically, available data from boreholes with liquid feedzones imply that:

- productivity and injectivity indices are more or less equal
- discharge rate of large-diameter wells may be predicted based on test data from slim holes.

Analysis of injection and production data from boreholes with two-phase feedzones from the Oguni, Sumikawa and Kirishima Geothermal Fields indicates that the two-phase productivity index is about an order of magnitude smaller than the injectivity index. Because of the sparseness of the data set (three slim holes and four large-diameter wells), this conclusion must be confirmed by additional data.

The detailed modeling of downhole pressure/temperature measurements and characteristic discharge data from two-phase geothermal boreholes has provided several interesting and useful insights. The pressure profile in most of the two-phase boreholes can be divided into two parts, *i.e.*, (1) cased hole, and (2) open hole or hole with a slotted liner. In most cases, the pressure gradient in the slotted liner/open hole section of the borehole is significantly greater than that in the cased part of the borehole. To model the pressure drop in the slotted liner/open hole, it is usually necessary to assume that the hole diameter is equal to the inside diameter of the liner. In addition, a non-zero roughness factor is required.

Pressure data from high enthalpy wells at Sumikawa suggest that the difference in gradient between the cased and open hole/slotted liner sections of the borehole declines (or even disappears) as the flow approaches single-phase steam. The latter observation is also consistent with the modeling of single-phase liquid flow in Takigami boreholes (Garg and Combs, 1997). For Takigami boreholes, the presence (or absence) of slotted liner was seen to have little influence on mass and heat transport in the wellbore.

Both the Hughmark slip correlation and the no-slip assumption give too large a pressure drop in the wellbore. Best fits to the downhole pressure and temperature data were obtained by taking a slip correlation between the Hughmark and no-slip assumptions. These calculations suggest that the Hughmark correlation should be modified.

Examination of characteristic data from two boreholes at Kirishima and one at Oguni indicates that it may take several days for discharge conditions to stabilize in geothermal wells

with two-phase feedzones. Thus, great care must be taken to obtain valid characteristic data from two-phase geothermal wells. It is simply not satisfactory to change discharge rates every few hours and expect to obtain valid characteristic data.

Simulation of characteristic data from large-diameter wells shows that both the productivity index and feedzone enthalpy undergo changes with variations in feedzone pressure and discharge rate. Lowering the feedzone pressures results in enhanced boiling and hence greater steam phase mobility. The variations in productivity index and feedzone enthalpy are, however, modest (~10 percent), and suggest that the productivity index and feedzone enthalpy corresponding to maximum discharge rate (and lowest feedzone pressure) from slim holes should be used to estimate the discharge capacity of large-diameter wells.

For boreholes with a poor productivity index, almost all of the pressure drop takes place in the formation, and increasing borehole diameter has little or no influence on the discharge capacity of the borehole. The discharge capacity for these boreholes is limited by the formation, and not by the borehole size.

From the data analyzed to date, it appears that a productivity index of the order of 0.3 kg/s-bar is needed to obtain economically significant discharge rates. Data from slim hole KE1-6 and large-diameter well KE1-21 do suggest that barring variations in the productivity index with borehole diameter, it should be possible to deduce the discharge characteristics of large-diameter wells using test data from slim holes with two-phase feeds. The latter conclusion must, of course, be confirmed by data from a statistically significant number of boreholes with two-phase feedzones from different geothermal reservoirs.

References:

1. R. E. Collins; "Flow of Fluids Through Porous Materials", PennWell Books, PennWell Publishing Co., Tulsa OK, pp. 71-73, 1961.
2. H. S. Carslaw and J. C. Jaeger; "Conduction of Heat in Solids", Second Ed., Clarendon Press, Oxford, UK.
3. C. V. Theis; "The relationship between the lowering of piezometric surface and the rate and duration of discharge using ground-water storage", Trans. AGU, 1935, pp. 519-524.
4. J. W. Pritchett; "Preliminary Study of Discharge Characteristics of Slim Holes Compared to Production Wells in Liquid-Dominated Geothermal Reservoirs"; Sandia National Laboratories Contractor Report, SAND93-7028, June 1993.
5. M. A. Grant, I. G. Donaldson, and P. F. Bixley, "Geothermal Reservoir Engineering", Academic Press, New York, NY, 1982, pp. 116-125
6. Teklu Hadgu, et. al., "Preliminary Report on Recent Injection and Flow Tests in Well SNLG 87-29 Steamboat Hills Geothermal Field, Nevada," Draft, Lawrence Berkeley Laboratory, Berkeley, CA, Dec. 1993
7. G. de Marsily, "Quantitative Hydrogeology", Academic Press, Orlando, FL, 1986, pp. 147-149
8. R. C. Dykhuizen and R. R. Eaton, "Modeling of Geothermal Wells With GEM", Memo to J. C. Dunn and J. T. Finger, dtd. 1/8/93, Sandia National Laboratories, Albuquerque, NM

9. H. Orkiszewski, "Predicting Two-Phase Pressure Drops in Vertical Pipe," J. Petr. Tech. 1980, pp. 829-838.
10. G. A. Hughmark, "Holdup in Gas-Liquid Flow," Chem., Engr. Prog., 58(4), 1962, pp. 62-65.
11. T. Hadgu, "Vertical Two-Phase Flow Studies and Modelling of Flow in Geothermal Wells", Ph.D. Thesis, Univ. of Auckland, New Zealand, 1989
12. L. A. Mondy and L. E. Duda, "Advanced Wellbore Thermal Simulator GEOTEMP2 User Manual," Report SAND84-0857, Sandia National Laboratories, Albuquerque, NM, Nov 1984
13. Garg, S. K., J. W. Pritchett, T. G. Barker, L. A. Owusu, J. Haizlip and A. Truesdell (1993), "Reservoir Engineering Studies of the Oguni Geothermal Field (Phase 3)", S-Cubed, La Jolla, California, Report Number SSS-FR-92-13899.
14. Garg, S. K., J. Combs and M. Abe (1994a), "A Study of Production/Injection Data from Slim Holes and Production Wells at the Oguni Geothermal Field, Japan", *Proceedings Nineteenth Workshop on Geothermal Reservoir Engineering*, Stanford University, Stanford, California, January 18–20, pp. 75–82.
15. Garg, S. K., J. Combs and M. Abe (1994b), "A Study of Production/Injection Data from Slim Holes and Production Wells at the Oguni Geothermal Field, Japan", Report No. SSS-TR-94-14464, S-Cubed, La Jolla, California, June.
16. Garg, S. K., Combs, J. and Goranson, C. (1995b), "Use of Slim Holes for Geothermal Reservoir Assessment: An Update", *Proceedings 17th New Zealand Geothermal Workshop*, The University of Auckland, Auckland, New Zealand, November 8–10, pp. 151-156.
17. Garg, S. K., and J. Combs (1995), "Production/Injection Characteristics of Slim Holes and Large-Diameter Wells at the Sumikawa Geothermal Field, Japan", *Proceedings, Twentieth Workshop on Geothermal Reservoir Engineering*, Stanford University, Stanford, California, January 24–26, pp. 31-39.
18. Garg, S. K., J. Combs, F. Ozawa and H. Gotoh (1996a), "A Study of the Production/Injection Data from Slim Holes and Large-Diameter Wells at the Takigami Geothermal Field, Kyushu, Japan", Report No. SSS-DTR-95-15179, S-Cubed, La Jolla, California, April.
- 18alt. Garg, S. K., J. Combs, F. Ozawa and H. Gotoh (1996b), "A Study of the Production/Injection Data from Slim Holes and Large-Diameter Wells at the Takigami Geothermal Field, Kyushu, Japan", *Geothermal Resources Council Transactions*, Vol. 20, pp. 491-502.
19. Garg, S.K., J. Combs, M. Kodama and K. Gokou (1998), "Analysis of Production/Injection Data from Slim Holes and Large-Diameter Wells at the Kirishima Geothermal Field, Japan", *Proceedings, Twenty-Third Workshop on Geothermal Reservoir Engineering*, Stanford University, Stanford, California, January 26–28, in press.
20. Garg, S. K., and J. W. Pritchett (1990), "Cold Water Injection Into Single- and Two-Phase Geothermal Reservoirs", *Water Resources Research*, Vol. 26, pp. 331–338.
21. Grant, M. A. I. G. Donaldson and P. F. Bixley (1982), Geothermal Reservoir Engineering, Academic Press, New York, 369pp.

22. Garg, S. K., J. Combs and M. Abe (1995a), "A Study of Production/Injection Data from Slim Holes and Large-Diameter Production Wells at the Oguni Geothermal Field, Japan", *Proceedings World Geothermal Congress*, Florence, Italy, May 18–31, pp. 1861–1868.
23. Garg, S. K., and J. Combs (1998),), "A Study of the Production/Injection Data from Slim Holes and Large-Diameter Wells at the Kirishima Geothermal Field, Kyushu, Japan", Technical Report Number MFD-DTR-97-15818, Maxwell Technologies Federal Division, San Diego, January.
24. Garg, S.K., and J. Combs (1997), "Use of Slim Holes with Liquid Feedzones for Geothermal Reservoir Assessment", *Geothermics*, Vol. 26, No. 2, pp. 153-178.
25. Pritchett, J. W. (1993), "Preliminary Study of Discharge Characteristics of Slim Holes Compared to Production Wells in Liquid-Dominated Geothermal Reservoirs," *Proceedings Eighteenth Workshop on Geothermal Reservoir Engineering*, Stanford University, Stanford, California, January 26–28, pp. 181–187.
26. Hadgu, T., R. W. Zimmermann and G. S. Bodvarsson (1994), "Comparison of Output from Slim Holes and Production-Size Wells," paper presented at *Nineteenth Workshop on Geothermal Reservoir Engineering*, Stanford University, Stanford, California, January 18–20, pp. 253-260.
27. Pritchett, J. W. (1985), "WELBOR: A Computer Program for Calculating Flow in a Producing Geothermal Well," Report No. SSS-R-85-7283, S-Cubed, La Jolla, California.
28. Dukler, A. E., M. Wicks III, and R. G. Cleveland (1964), "Frictional Pressure Drop in Two-Phase Flow—B. An Approach Through Similarity Analysis", *A.I.Ch.E. Journal*, Vol. 10, pp. 44–51.
29. Hughmark, G. A. (1962), "Holdup in Gas-Liquid Flow," *Chemical Engineering Progress*, Vol. 53, pp. 62–65.

V. GUIDELINES

a. Typical Slimhole Problems

Problems described in this section are not unique to slimholes, but their frequency and relative importance may be different from rotary drilling. Three general situations are described: fluid-related effects, unplanned reduction in hole size, and pressure control.

Fluid-related effects: Drilling fluids are especially important in slimholes, specifically wireline cored holes, for two principal reasons: the percentage of very fine cuttings in diamond drilling is much higher than in rotary drilling, and the small hole/annulus means that both flow rate and total circulating volume of fluid are much smaller than with big rigs. Because of the fine cuttings and small volume, it is critical to keep close control over the solids content of the mud. Failure to do so can lead to differential sticking, mud rings in the drill pipe, and accelerated wear in the pumps.

The drilling fluid must also provide enough lubricity to the drill string to avoid high friction and the consequent downhole vibration. This vibration is not only detrimental to the drilling assembly, but often requires the drill string to be turned at abnormally low rotary speeds, reducing rate of penetration.

Finally, because cement is often the treatment of choice for lost circulation, the mud can quickly become loaded with drilled cement, which thickens the fluid. In many cases, the only remedy for this is to replace the mud with a fresh batch. All these effects are discussed in much more detail in Section V-d below.

Unexpected reduction in hole size: The casing program for any borehole is typically designed from the bottom up. That is, final hole diameter is chosen and the upper casing sizes are then determined from the number of strings that have to be set to reach target depth. The number of strings is usually based on: 1) the best estimate of setting depths which can be reached with assumed conditions of hole stability at that location, 2) aquifers which need to be sealed, and 3) regulatory requirements.

In planning a conventional rotary drilling project, many engineers routinely make the upper hole large enough for a "contingency" casing string, so that if hole problems require setting an unplanned string, the required final hole diameter can still be achieved. If it turns out that the contingency string isn't needed, casing and cement costs are higher than they should have been because the upper casing strings are bigger than they would have been otherwise, but some operators feel that this is an acceptable risk.

In most slimholes, there is much less chance of a contingency string, because the range of possible casing sizes is smaller. In wireline coring, drill rods and bits are sized so that a given size rod will just pass the next smaller size bit. [For example an "H" size drilling assembly has a 3.85" bit with rods that are 3.5" OD by 3.060" ID; the next smaller size is "N", which has a 2.97" bit.] For a typical geothermal exploratory slimhole, hole size at target depth is usually designed to be "H", so if there is a problem which requires leaving a string of H-rods in the hole as casing, drilling can continue with "N" size (or composite N/CHD76) equipment. At that point, the hole is still usable because injection tests are possible (see Section IV-d for a

discussion of hole size on flow tests) and it will pass most logging tools which would have fit into H-rod. Further reduction, however, is usually not practical because the hole is becoming too small to be useful and "B" equipment (the next-smaller size below N) is not available in composite rods and thus doesn't have the depth capability of N-size tools.

It is not clear, however, that inability to reduce size is a common problem. In oil and gas exploration, it is estimated¹ that a contingency string is only used in about 5% of the wells, so if slimholes reduce cost by significant amounts, they will readily pay for the occasional times when lack of the size-reduction option results in loss of a borehole.

Pressure control: An essential part of any drilling operation is control of wellbore pressure. There is a major difference, however, between exploring for geothermal resources and for oil and gas. With hydrocarbons, high downhole pressures are almost always the result of formation geometries which trap fluids under some portion of the lithostatic burden. These pressures are controlled either by closing the annulus with a rotating head (a rotary seal around the drillpipe) or by increasing the mud weight to raise the static head in the wellbore higher than the fluid's pore pressure.

In geothermal drilling, formations are normally under-pressured (pore pressure is less than hydrostatic) and high downhole pressures are the result of high temperature causing either formation fluids or drilling fluids to flash into steam. If the hole is in a production zone which shouldn't be cooled, drilling can continue with heavier fluid (usually brine, because small annulus isn't good for barite-weighted mud) or a rotating head, but higher in the hole a simpler and more common practice is to use cooler drilling fluid or to "kill" the well by pumping cold water into it. These methods usually serve to control pressure, but the driller must always have available geothermal blow-out prevention equipment (BOPE), which is essentially identical to conventional oil and gas equipment but with high-temperature elastomers and seals, in case control of the well is lost. BOPE for geothermal slimholes is also smaller and less expensive than in conventional drilling.

Detection of a "kick" (formation fluid influx to the wellbore) has been detected in large-diameter wells, in the past, by monitoring pit volume for gain. Although this is still done, flow measurements on the inflow and outflow lines are much more accurate and give much quicker identification of the kick -- because of the smaller wellbore volumes, this is even more important in slimholes. Sandia has developed in- and out-flow meters for immediate detection of lost circulation (see Section II-d), but they serve just as well for identification of kicks.

If uncontrolled flow up the wellbore does begin, the narrow annulus has both negative and positive effects. It means that, for equal volumes of gas or steam introduced into the hole, the effect is seen at the surface more quickly than with conventional drilling, but the smaller clearance does have a self-choking effect on the flow. An analysis² of slimhole well-control for oil and gas describes a dynamic process of pumping more fluid to increase the pressure drop in the annulus and thus raise the bottomhole pressure. This may not be a viable option in geothermal drilling, but it is still true that flush-joint drillpipe which has a diameter close to the hole diameter will retard flow.

Another aspect of pressure control is potential flow inside the drill pipe; because the area inside the pipe is greater than the annulus, this is actually a more important problem. The times of greatest risk are those when the hole is "swabbed", that is, either the drill pipe or the core

barrel is being rapidly withdrawn from the hole, which tends to reduce the weight of the fluid column and thus the bottomhole pressure. In addition to controlling the speed with which the pipe or barrel is withdrawn, the core-driller can use a wireline pack-off and a loading chamber (similar to a lubricator) when retrieving the core barrel, and can use a pump-down latch-head with inverted check-valve (which fits in the top of the core barrel and lets fluid flow down, draining the pipe, but not up) when tripping pipe.

In summary, even though a slimhole's small annulus means that pressure effects are felt more quickly at the surface than in conventional drilling, currently available technology, including flow-measuring equipment, is completely adequate to handle pressure control for geothermal slimholes.

b. Recommendations on Well Design

Introduction: Even though many slimholes are drilled with minerals-type core rigs, the hole design for a geothermal exploratory well is considerably different than for a minerals-exploration hole or a temperature-gradient hole. In general, well design will follow these steps: determine final hole diameter, decide whether directional drilling will be required, and design the casing program. Each of these is described in more detail below.

Hole diameter: Assuming that a variety of drilling equipment is available, hole diameter is driven by the following considerations:

- Logging tools - Typical temperature-pressure-spinner logging tools will fit into almost any reasonable size hole, but if more exotic tools, especially imaging tools such as a formation micro-scanner or a borehole televiewer are to be used, the heat-shielding they require at high temperature sometimes defines a minimum hole size. If these tools are under consideration for the slimhole, the tool's manufacturer should be consulted for its operating conditions.
- Core size - Core is generally used to validate a geologic model of the reservoir or to assess the fracture dip, density, and aperture. Diameter is not too important for this data, but sometimes a rock mechanics evaluation will need a minimum core diameter. Larger diameter core also gives better recovery in highly fractured or unconsolidated formation.
- Depth - Each type of core rod has a maximum rated depth, so if a hole's projected TD goes beyond the depth capability of, say, HQ core rods, then NQ rods (and the corresponding hole diameter) will be the largest hole available at that depth. The depth limit is sometimes determined by the drill rig, but more often is a function of the drill pipe. Drill pipe depth limitation comes from its suspended weight, so for a given size pipe, the depth capability can be increased by making up a "composite" string with stronger, heavier pipe (e.g., CHD101) at the top and lighter weight (e.g., HQ) pipe at the bottom. There is some disparity among the depth capabilities quoted by various drilling

CORE ROD TYPE	Max. Depth, Feet
CHD134	7,500
CHD101	10,000
HMCQ	6,000
101/HMCQ composite	12,300
CHD76	10,000
NCQ	6,000
76/NCQ composite	11,200

contractors, but approximate guidelines are shown in the table:

- Packers - Inflatable packers are sometimes used to isolate a specific section of the wellbore for injection tests, fluid sampling, or other diagnostics. In general, this means that some kind of logging or sampling tool must be run through the packer into the zone below it, and the size of this tool will determine the minimum size of the packer and thus the hole. Based just on the diameter of the cable head for most logging cables, it would be very difficult to run a pass-through packer in a hole smaller than HQ (approximately 3.8" diameter).
- Flow test - If a flow test is expected after drilling, there are two advantages to keeping the hole diameter as large as possible: scaling up for predicted flow in a large-diameter well will be more accurate, and if the combination of depth, pressure, and temperature means that the well's ability to produce is marginal, a larger diameter hole is more likely to flow. The larger-diameter wellbore is particularly important where the flow turns two-phase. See Section IV-d.

Directional Drilling: There are a number of reasons for directional drilling in exploration: it may be necessary to correct an inadvertent change in hole direction; surface geographic features or institutional boundaries may prevent the rig from being above the target; or reservoir evaluation criteria may require that the hole intercept as many high-angle fractures as possible. If either of the latter two situations exists, the direction of the hole can be controlled by drilling a slant hole from the surface, or by causing the hole to deviate from vertical at some depth. Many minerals-type coring rigs can drill slant holes, which offer some advantages – it isn't necessary to use expensive downhole tools to change hole trajectory; there is less drillstring fatigue in the straight (but non-vertical) hole; and the hole can be at a high inclination, at shallow depth, without building trajectory change at an excessive rate. Slant holes do encounter more complications with the BOP stack, the casing is more difficult to centralize, and the fact that the drill string is always lying against the side of the hole can cause more friction than in a vertical hole, but this technique usually deserves consideration, especially when shallow, high-angle directional drilling is required.

If more conventional directional drilling is planned, the principal decisions are choice of kick-off point, steering method, and determination of angle-building rate. Kick-off point is affected by many variables, including formation, casing points, and temperature, but it is usually fairly high in the hole for geothermal drilling, because the downhole motors and steering tools are limited by the temperatures they can withstand. Also, if a specific lateral displacement is needed, then building angle at shallower depth means that less angle is required. Finally, if the upper part of the hole is rotary-drilled, then the option of using oilfield directional tools and service companies exists. These are not inherently better than minerals-industry tools and companies, and are not made in small sizes, but they are more readily available in many locations.

Minerals exploration has used wedges (a mechanical device, analogous to a whipstock, which forces the bit off the centerline of the borehole) to control direction for many years, but it is time-consuming to set the wedge, and using one means reducing hole size. Once a wedge has deviated the hole, there is no further control without setting another wedge, because there is little that can be done with BHA design in core drilling to affect angle-building or -dropping. Wedges are still used to get around junk and to mill out of casing, but the availability of slimhole

motors and steering tools now means that wedges and their limitations can usually be abandoned.

Once a steering method has kicked the hole off vertical, angle-build rate should be controlled carefully. Various service companies with different tools have different practices on maximum build rate, but a conservative limit is $1.5^{\circ}/100'$. Oil and gas drilling often builds angle at far greater rates, but that is usually deep in the hole, near the producing horizon.

Casing design: General principles of casing design are described in a number of textbooks³, and casing-design software is commercially available⁴, so this discussion will only touch on a few points specific to exploratory slimholes. In these holes, the casing configuration is usually not complex, but the most significant point is the necessity for competent cement around at least the surface casing, required not only by regulatory agencies in most areas, but by the prospect of producing hot brine or steam during a flow test. For this reason, exploratory slimholes are larger in diameter than common temperature-gradient holes. It is often cost-effective to have the conductor or mud riser hole collared-in by the local earth-moving contractor who builds the location, or even by a local water-well driller. This is even more likely to be true if a substantial hybrid rig is not contracted for the job.

Regulatory requirements in the drilling permit will determine other aspects of the casing design and blow-out prevention equipment (BOPE). A typical stipulation is that surface casing be at least 10% of the total depth and that one-third of the hole be behind casing at any given time, but this and many other details can be found in the Geothermal Resources Operating Orders⁵. Once the minimum required depth is reached, casing will normally be run unless the formation is particularly fractured and broken. It's important to have competent rock at the casing shoe, because it is normally required to do a pressure test by drilling out the shoe and into new formation, then applying a pressure gradient above hydrostatic to the wellbore. This procedure evaluates the well's ability to withstand high pressures without breaking down the formation or the cement around the casing, and is the basis for establishing the temperature to which the well can be drilled without setting another string of casing. Clearly, if there is not competent rock around the shoe, the wellbore will not be able to withstand a high pressure gradient and the ability to advance the well to the desired depth/temperature will be compromised. If the minimum casing depth is reached and there is no competent rock, it is often desirable or necessary to continue drilling in hopes of finding a better formation. The extent to which this is done is often limited by availability of more casing, geological estimates of whether more competent rock may lie below, or temperature increase, but it is, unfortunately, always an uncertain process.

If directional drilling is to be done fairly high in the hole, the directional interval should be cased if that is consistent with other criteria for the casing design. In that way, tight spots, key seats, or other trouble spots encountered in the directional work will be behind casing and will not interfere with drilling the lower section of the hole.

c. Recommendations on Drilling Practice

Drill pipe, tools, and handling: An individual piece of rotary drillpipe is approximately 30' long and has "tool joints" at each end. For added strength, the tool joints are larger in outside diameter than the body of the pipe and are cut with API (American Petroleum Institute) standard threads. These threads are sharply tapered, so that few turns are required to make or break a connection, but to avoid fatigue it is extremely important for the threads' shoulders to be in tight contact, and this requires large make-up and break-out torques (several thousand foot-pounds.) Because of this, rotary rigs use power tongs or tongs with a line from the drawworks to make and break the drill string connections.

Core rods are uniform in length within a given size (most are exactly 10' long, although some are 6 m and other, bigger strings have 5' rods) and have a uniform outside diameter. Length of rods is usually dependent on the size rig chosen. The thread on these rods is much less tapered than an API thread, with smaller torques for connections, and the rods are often made up with pipe wrenches. If a core rig is to be used extensively for drilling with full rotary BHAs, then be sure when planning the job that the rig and crew will be able to apply the proper torques to the drill string. This can usually be done by rigging a line through some sort of snatch block on the rig floor and using either a rented load-cell or the rig's pressure gauges to measure torque. It's also essential to have the proper bit breaker for the rotary bit, and, equally important, a way to anchor the bit breaker to the rig.

Drill collar length can also present a problem on core rigs. If a core-drill rig is large enough for hybrid drilling, it will probably pull 40' stands of pipe, so conventional 30' rotary drill collars can not be stood back in the derrick and the mast is not tall enough to accept a 60' stand of two collars. Therefore, the collars must be laid down for each trip, which is time-consuming and, therefore, expensive. The best solution for this is 20' drill collars, which some core drills already have, but an alternative is to use a combination of "lead" collars (which are about 9' long) and conventional collars to form an assembly which is about the length of a stand of core rods and can be more easily handled. Lead collars, which are normally run just behind the bit, are often in short supply from rental companies, so if this method is to be used the collars must be ordered early. When rotary drilling, the neutral point in the drill string should always be in the collars, because the core rod threads should not be in compression when drilling a hole with enough annulus to allow them considerable side play. Using a composite string with light core rods should be avoided when rotary drilling. CHD 134 (5" OD, 14 lb/ft) or CHD 101 (3.7" OD, 8.8 lb/ft) rods are preferred.

Since core-rod threads don't make up to rotary tools, there will be (usually several) cross-overs in the drill string; check inside and outside dimensions of these to make sure that they can be fished in the size hole that will be drilled. Check the outside diameters on drill collars, too; it may be necessary to machine fishing necks on them if the drill collar OD is too large to be fished in the planned hole size. It is also important that the rig crew keeps records of the dimensions (length, inside diameter, outside diameter, thread sizes) on every tool that goes into the hole. This is normal practice in rotary drilling, but may require some training for coring crews. The project planner should get as many of these dimensions as possible in advance so that an inventory of fishing tools can be specified. Core rigs will usually have spears or swages to go

inside core rods or barrels, but will not have overshots or grapples. If a drill site is remote from a fishing service-company, and if a reasonable price can be negotiated, it is probably prudent to specify fishing tools for all parts of the drillstring and to have them on standby at the rig.

When doing rotary drilling with a top-drive rig such as a UDR5000, it is also possible to use rotary-type drillpipe with tool joints. This will eliminate many of the problems with crossovers and possible thread fatigue, but few coring rigs can pull a string of rotary drill pipe off the shelf, and there is still the handling problem with nominal 30 foot lengths of pipe.

Yet another possibility is the use of a conventional rotary rig modified or retrofitted to use coring tools. Top-drive conventional rigs can turn a string of core rods and, with the proper wireline, can retrieve the core tubes. These rigs would need a drive system which turns the drill string fast enough for effective drilling with the diamond tools, and would probably need a mud system designed for the smaller application. It is also possible to set a minerals-type, chuck-driven drilling unit into a conventional rig so that the coring unit rotates the drill string and controls weight-on-bit, while the rotary rig's draw-works are used to trip pipe. This method was used successfully during Phase II core-drilling at the Long Valley Exploratory Well⁶ and a similar system (but with a top-drive) is being used in overseas geothermal exploration.

Casing and cement: When it is time to run and cement casing, some of this work can usually be done by the drill rig and its crew without calling in service companies. Much of this will depend on the rig's pipe-handling and cement mixing capabilities.

Rotary rigs use elevators for tripping drill pipe, but because core rods are a uniform OD, they can not be directly tripped with this method. Generally, core rigs either raise the drill string by screwing a fitting from the main line into the upper end of the string or, if the core rig does have elevators, by screwing larger-OD lifting plugs into the end of the rods. If the core rig has its own elevators and casing slips, it will not be necessary to rent them, and if the rig has power tongs which can be used to make up the casing couplings, then a tong service will not be required. The tongs must not only be able to apply the proper torque to the connections, but must be able to measure the torque to assure proper make-up.

Casing length is also important, since Range 3 casing (the most common designation) is often more than 40' long and these lengths cannot be handled by many core rigs. The project planner should get definite information from the drilling contractor on the maximum pipe length which the core rig can handle, and then order casing accordingly.

For conductor or shallow surface casing (down to ~150'), the small volumes allow rig pumps to be used to cement the casing. Rig pumps will almost always have adequate pressure capability, but if it is planned to use them for cementing casing, make sure that the flow rate and mix tank volumes are sufficient for the casing job. These capabilities will also bear on the ability to pump cement for sealing lost-circulation zones. For casing, it will also be necessary to have a cementing head and plug, or some other method for displacing the cement from inside the casing.

Mud systems: Although drilling fluids are used, and for basically the same purposes, in both types of drilling, the priorities and practices are somewhat different between core and rotary rigs. In an oversimplified distinction, the most important function of drilling fluid in rotary drilling is to clean the hole bottom (improving penetration rate) and stabilize the wellbore, while

in core drilling it is crucial for the fluid to lubricate the drill string and bit, thus preventing vibration, overheating, and excessive bit wear.

Flow rates are much lower in core drilling than in rotary drilling; e.g., 12-15 gpm in coring a 4" hole compared to hundreds of gallons per minute in rotary drilling an 8" hole. In addition to the smaller hole size, there are three other reasons for this: (1) the annulus is very small in core drilling (typically 3.5" drill pipe in 3.78" hole) so low flow rates give enough annular velocity for hole cleaning, (2) the cuttings are much finer in core drilling, so little velocity is required to lift them, and (3) a large part of the drilled-hole volume is removed in the form of core. This means that a rig normally used only for coring will not have large enough pump capacity for rotary drilling. If a core rig is to be used for hybrid drilling, make sure that its mud system has adequate flow rate, pressure capability, and solids handling. Most core rigs do not have shakers, which are necessary for the larger cuttings and the lost-circulation material generally used in geothermal rotary drilling.

Because of the smaller flow rates and smaller system volume, errors in maintaining the mud are frequently more serious in core drilling. One of the most important criteria for the mud in a core drilling job is to contain a low solids-fraction. The high rotary speed (300+ rpm) of the drill pipe can cause "mud rings", where the solids are centrifuged out of the mud onto the inside of the drill pipe. These rings can then prevent retrieval of the core tube.

The smaller flow rates also mean that, in high temperature formations, the mud in a core hole will reach higher temperature than in a rotary hole at the same depth in that formation. If there are components in the drilling fluid which break down at some threshold temperature, then it is quite possible for that to happen in a core hole but not in a subsequent rotary hole. These unique mud requirements mean that it is extremely useful to have a mud engineer who is experienced in both core and rotary drilling at high temperatures. Return mud temperatures while coring a hot hole are often surprisingly cool, and are therefore not useful as an indicator of formation temperature. See Section V-d for a detailed discussion of drilling fluids for slimholes.

Directional drilling: Core rigs are often set up for drilling angle holes from the surface, but the hole can also be turned from vertical at depth. Inclination in minerals coreholes is usually referenced to horizontal; a vertical hole is a 90° hole to a core driller. Motors, bits, and directional drillers are available from minerals service companies to steer the core hole, and it is highly preferable to use these tools and personnel in core holes, rather than service companies who normally do conventional-rotary directional drilling. Once a core-hole is deviated with a directional motor run (core cannot be taken during the motor run), little can be done with the core-drilling BHA to control direction.

If a hybrid drill rig is used to rotary-drill a 6" or larger hole, conventional-rotary motors and BHAs are used for directional drilling. Build rates for core holes should not exceed 1.5⁰/100 ft, to reduce fatigue on core rods and to minimize inner core-tube retrieval problems.

Supervision: Rotary drilling projects are usually managed by consultants or drilling engineers hired by the operator to direct the operation. The consultant will, in general, give directions to the driller, specifying bottom-hole-assemblies, desired mud properties, bit selection, and drilling parameters such as rotary speed and weight-on-bit. There are also usually a mud-logger, who analyzes the rock cuttings to identify the formation being drilled and who frequently provides required safety equipment for the rig, such as H₂S detectors and pit-level indicators, and a mud

engineer, who advises the consultant on mud properties and is in charge of mixing the mud to obtain those qualities. In addition, the drilling contractor will provide a tool pusher to supervise the operation and maintenance of the rig itself. Some of these responsibilities overlap, and many decisions are made in consultation among these individuals.

In contrast, the driller on a core rig makes most of the decisions that a consultant would make on a rotary job. Bottom-hole-assembly is usually just the core barrel and two stabilizers, so there is no need for designing the complex BHAs of rotary drilling, and there are also fewer choices in bit selection. There may still be need for a mud engineer, especially at high temperatures, but most of the mud-logger's rock identification function is served by having core available. If a mud logger is not used, however, make sure to have all the safety equipment required by regulations and the drilling permit.

In a hybrid drilling job, it is probably appropriate to have a consultant who will design BHAs and suggest drilling parameters (bit hydraulics, rotary speed, weight-on-bit, mud properties, etc.) for the rotary part of the job. In some cases, it is also useful to have a mud-logger for the rotary part of the hole, but not for the cored section. In general, a core-drilling contractor can supply a full-time supervisor on site and he, in consultation with the driller, will provide acceptable management of the job.

d. Recommendations on Drilling Fluids

Introduction: Wireline coring is a very special field that until recently has been used almost exclusively by the mineral exploration industry, and mud systems for that application are well understood. Much has also been written about drilling techniques and mud systems for successful mud rotary drilling.

There are some major differences, however, that must be considered when planning a drilling fluids system for a geothermal wireline coring program⁷⁻¹⁰. Lower overall costs, reduced environmental impact, and excellent geothermal information make wireline coring an attractive alternative to rotary drilling.

Some of the important parameters that have a direct correlation to complete core recovery, reduced costs, and minimal downhole problems are described; they are based upon information gathered during millions of feet of continuous coring in the mineral exploration and geothermal industries.

Drilling fluid functions: A driller who knows about drilling fluids, and has the skills to make them work, has access to a very powerful drilling tool. The functions of a drilling fluid are:

- Clean the hole
- Cool and clean the bit
- Lubricate the drill string
- Maintain the stability of the borehole
- Allow for the collection of geological information
- Form a semi-permeable filter cake to seal the pore spaces in the formations penetrated
- Control formation pressures
- Protect the production zones from damage
- Protect the surface and subsurface environments from contamination.

In coring, the drilling fluid has the following specific tasks related to the recovery and preservation of the complete core. The fluid should:

- Lubricate the rods, barrel, inner tube and the core itself to eliminate vibration or shaking of the core
- Lubricate the inner tube and the core itself so that the tube will slide smoothly over the core
- “Encapsulate” sensitive cores and be chemically suited to stabilize the core to prevent swelling or breaking up.

Planning the mud program: Clearly the purpose and objective of the coring program should be understood by everyone associated with the project. A pre-spud meeting of all operating, drilling, environmental and service company personnel is highly recommended. Discussions of the drilling plan and contingencies may eliminate trouble later in the program. Once there is agreement on the drilling plan, then the mud program should be planned around the following factors.

1. Water: Since water is basic to the mud system, it is important to know the quality, quantity and cost involved with the make-up water. Poor quality make-up water may require chemical treatment prior to its use.
2. Type and thickness of the geologic strata: This is not always known before drilling, but fluid properties must be planned with the best available information about downhole conditions, i.e., the reactions between drilling mud and formation.
3. Site Accessibility: Make sure that supply trucks have reasonable access to the site and that rig placement in relation to pits, bulk storage, etc. is convenient to reduce handling.
4. Climate: Extremes of heat, cold, and precipitation can affect the mud system and products.
5. Drilling equipment: Make sure that the surface equipment, such as: pumps, mixing and circulating tanks, mixing equipment, and solids control capabilities are adequate for the core hole size, downhole tools, etc.
6. Environmental considerations: If at all possible, use non-toxic, easily disposed drilling fluids. All personnel should know local and Federal regulations pertaining to the job.
7. Manpower: The experience, skill, supervision, and attitude of the rig crews is of paramount importance to a successful coring program.

Successful mud systems need at least these three attributes:

- **STABILITY:** The desired properties of the fluid, once established, should be stable under normal drilling conditions.
- **EASY TREATMENT:** If the desired properties are lost, treatment should be available to restore them.
- **PROPERTY TESTING:** Tests and testing equipment should be available to identify fluid properties and indicate any treatment required.

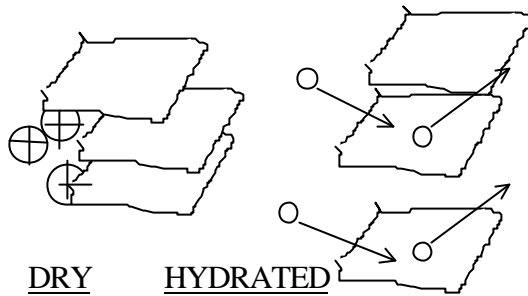
These attributes can be achieved by the following principles.

1. Formula: Have the proper mixture of products to satisfy anticipated downhole conditions.

2. Application: Have the mud properties as needed BEFORE drilling into known or anticipated problems. Don't wait until you have a problem and try to fix it. Use preventive maintenance.
3. Flexibility: Always maintain a system in which the properties may be adjusted without drastic changes in the mud. Don't SHOCK holes by rapidly changing properties.
4. Monitor and Maintain: Monitoring is analyzing certain parameters of the mud (viscosity, weight, filtrate, chemical composition, pH, etc.) on a regular basis (every tour). Maintaining is continually adding the necessary products to maintain the required fluid properties. Drilling mud is continuously being "used up." Polymers are adhering to solids and dissipating, water added for volume needs to be treated. The mud at the beginning of the shift is not the same mud at the end of the shift unless it has been monitored and maintained on a regular basis. At crew changes, do NOT discard the mud and prepare a new batch with different properties.
5. Pumps: Have pumps with adequate pressure and volume capacity to circulate and mix mud.
6. Mixing capacity: The rig should be able to mix bentonite, polymers and other additives through a high-shear hopper mixer, a high-speed hydraulic Thiessen type mixer, or similar adequate mixers.
7. Adequate pits and solids control: Letting solids build up in a core fluid is an ***absolute*** prohibition. Solids build-up can cause differential-pressure sticking, mud rings that prevent the overshot from latching to the inner tube, wear on pump parts, induced loss of returns, and numerous other problems. Pits should be designed to baffle the mud flow, change direction of flow, and cause the mud to flow from one pit to the other. General Rule - Pit volumes should be three times the hole volume at total depth.

Components of mud systems: Drilling mud is made up of three principal components:

- Base liquid: Oil, fresh water, or salt water can be used as a base liquid in drilling muds. Oil and salt water are almost totally restricted to hydrocarbon drilling. Fresh water muds are used for geothermal slimhole drilling. Oil muds should not be used for geothermal drilling.
- Active Solids: Active solids are those bentonites and polymers which are added to the base liquid to produce a colloidal suspension. They determine the viscosity of the mud and are known as viscosifiers.
- Inert Solids: Inert Solids are substances added to the mud either by drilled solids such as sand, limestone, igneous rock, and shale, or by barite added as a weighting material. These solids increase the density of the mud without appreciably affecting the viscosity.



When water gets between the plates, the clay swells.

Figure V-1 -- Clay hydration
drilled formations and become dissolved in the mud system. Some water sources may contain too many undesirable ions to treat out, and thereby require locating a better source of water. Under some circumstances of severe clay swelling, potassium chloride ions may be used to an advantage as an inhibitor. Core-drilling fluids must be designed with simplicity in mind. Exotic and numerous products are generally not necessary. Low solids, low filtrate, and reduced torque must be maintained.

There are also many drilling fluid products sold by mud companies. These are generally classified in the following categories, although some products function in more than one category.

Viscosifiers: According to the American Petroleum Institute, the “yield” of bentonite is the number of barrels of 15 centipoise mud (a measure of viscosity) that can be produced from one ton (2000 pounds) of dry bentonite. Extra High Yield (200 bbl/ton yield) sodium bentonite is recommended for slimhole coring because it minimizes solids content, reduces freight costs, and has the shortest mixing time.

Some clays, like pottery clays, do not expand when they are placed in water. Others, like bentonite are made up of stacks of platelets.

BUYERS BEWARE: There is a definite difference in clays on the market. Laboratory and field experience shows that some bentonites do not produce the viscosity they should, because they contain an abnormal quantity of sand. Know the source or test the product.

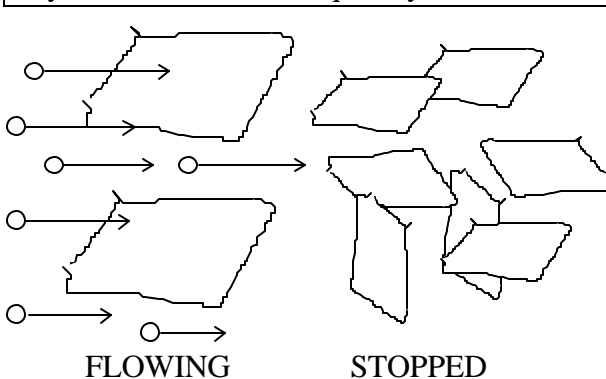


Figure V-2 -- Platelet alignment

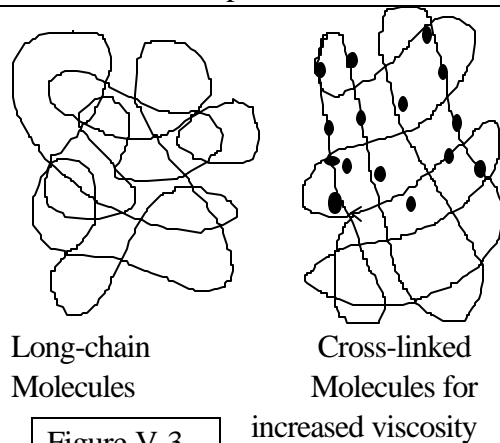


Figure V-3

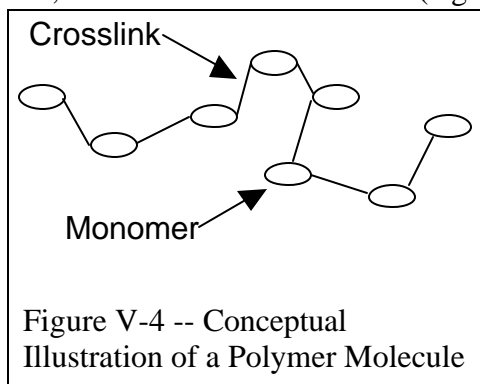
When they get wet, (become hydrated) they expand to many times their former size. When clay platelets are dispersed in water, the increased solids content causes an increase in viscosity.

While the mud is flowing, the platelets become lined up and move freely, thus giving a lower viscosity. When flow stops, the platelets become “disorganized” and form a structure which traps the water. This structure supports cuttings.

With increase in temperature (200°F) and increase in percentage of bentonite (over 8%), the drilling fluid will begin to thicken, resulting in high gel strength, high filtrate volume, and thick wall cakes. Sepiolite and Attapulgite clays do not show this increase in gel structure. Due to their match-stick-like particle structure, however, they tend to build mud rings inside the drill rods.

The organic polymers used in drilling consist of various length and molecular weight “chain” (Figure V-3) molecules. It is these molecules that provide viscosity when the polymer is mixed with water. However, the polymer **MUST** be mixed with a small amount of bentonite to form a filter cake. Drillers working without the assistance of mud engineers often find that the more costly polymer muds turn out cheaper in the long run. There is, however, a temperature limitation: most polymers begin to become ineffective at 300°F, but there are some polymer products which are temperature stable to over 500°F. Driscall D™, a dry powder anionic polymer, manufactured by Drilling Specialties Company (DSC), has been used in the field to 500°F. Alcomer 120L, from Allied Colloids, is a water soluble polymer emulsion that has a temperature stability over 500°F.

Drilling fluid polymers are 10 - 20 times as powerful as bentonite; they are large molecules consisting of repeating groups called monomers. The monomers are chemically aligned end-to-end, similar to the links of a chain (Figure V-4), to form a single molecule.

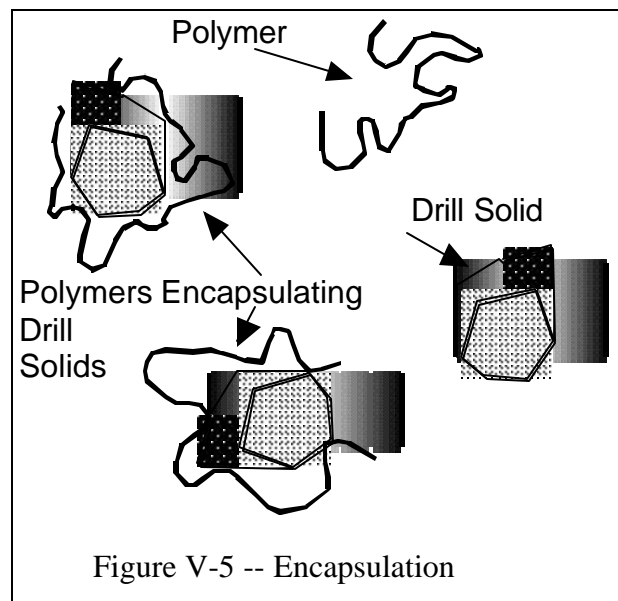


polymer’s ability to wrap around drilled particles and coat them in a manner to prevent water from further disintegrating them. Polymers are generally classified as anionic, cationic, or non-ionic. Most polymers currently being used are anionic.

Filtrate reducers: The reduction of filtrate volume (which in turn results in a thinner filter cake) is one of the most critical parameters to control in wireline coring. Minimizing filtrate volume reduces downhole torque, prevents differential pressure sticking, aids in core

Polymers restrict the hydration of clays and thus polymer muds require less treatment. Polymers provide greater change in viscosity between their flowing state and their still state. Pumping pressures are low. Polymers can be weighted with salt to provide a low solids weighted fluid.

“Encapsulation” is a term referring to some



recovery, helps stabilize water-sensitive clays and gouge zones, and helps eliminate mud rings. To reduce filtrate, polymers are used in conjunction with small amounts of extra-high yield bentonite.

Thinners and dispersants: Sometimes water is the best thinner for a drilling fluid, but the volume increase may be a problem because water additions require more products to restore desired properties. Polymeric deflocculants and lignin-type dispersants will reduce gel strength and improve flow properties. Alcomer 72L and 74L, products of Allied Colloids, are temperature-stable polymeric deflocculants. Lignites are also temperature-stable (450°F) thinners. (Ligno-sulfonates are not recommended due to their decomposition to H₂S and CO₂.) Phosphate-based thinners are not recommended in temperatures over 130°F as they begin to revert to orthophosphates.

Friction reducers: Torque due to friction can be a fatal problem in wireline coring. This friction can be from several sources, such as crooked hole, abrasive formation, swelling clays or gouge, temperature degradation of polymers, or lost circulation leaving no lubrication above the loss zone.

High downhole temperatures (+250°F) can rapidly degrade some lubricating polymers. One of the best friction reducers is a non-hydrocarbon derivative of potassium stearate. This product, called “TORKease” is manufactured by DSC, Inc. in both liquid and dry powder forms. It is stable to 500°F and has been used in Hawaii at temperatures approaching 600°F. Increased concentrations of temperature-stable polymers can also aid in torque reductions. Huskey produces a temperature-stable, synthetic-oil rod grease (Lube-O-Seal) that has been successfully used with TORKease to minimize torque. When coring without returns, torque can be minimized by pumping friction reducers down the annulus.

Surfactants: Surface tension reducers are recommended in sticky or bit-balling clay formations. These drilling detergents produce a “smoother flowing” mud, help reduce torque, and improve wall cake characteristics.

Special Note: All these additives may interact with each other, so it is important to have the advice of an experienced mud engineer, or at least the product’s manufacturer, before combining additives.

Lost circulation materials (LCM): Because of the tight clearances in downhole wireline coring assemblies, the types of LCM which can be used are more restricted than in rotary drilling. It is imperative to be aware of particle sizes in the material, relative to downhole clearances. Also placement technique needs to be addressed, i.e., pulling the tube before spotting LCM or pouring LCM and/or granular bentonite down the hole. Some choices of lost circulation materials are:

1. EZ-SEAL CLASSIC: Blended extra fine LCM. Can be pumped through face discharge bits.
2. Ground Paper: Finely ground paper products.
3. Magma Fiber: An organic, inert, non-toxic, acid-soluble LCM.
4. Multi/Maxi Seal: A special blend of LCMs formulated from granules, flakes and fibers.

5. Mica: Finely ground mica flakes. (CAUTION - mica is found in igneous rock and may contain particles of granite, which can stick the core tube, or even the bit, if circulated through the system.)

Lost circulation can be minimized by reducing pump pressure, pulling the tube at slower speeds, running rods slowly in and out of the hole, and reducing the mud density. In several cases, hundreds of feet have been successfully cored without returns, but if casing is set through these unhealed zones, an inadequate cement job may result and high temperatures can cause the casing to collapse. When other LCMs do not solve lost circulation problems, cement is frequently used to plug loss zones. W-120 and W-60 grades are fast-setting cement media for sealing loss zones and cementing casing in place.

Water treatment: The following treatments are frequently used to adjust the water chemistry.

- Soda Ash: Sodium carbonate to treat out calcium contamination and increase the pH to the alkaline side. This also aids in corrosion control
- Sodium Bicarbonate: Used to pre-treat the drilling mud prior to drilling cement. (Cement will destroy the qualities of a good mud unless it is treated out.)
- Potassium Chloride: Used to inhibit clay matrix. **Caution-** KCl may be corrosive with elevated temperatures and the presence of oxygen.

Solids control: Ninety-eight percent of solids generated by a diamond bit are below 74 microns. Low solids content in a recirculated fluid is important for all drillers, but for diamond core-drillers IT IS ESSENTIAL.

Low viscosity polymer muds will provide the best cleaning. When drilling deeper holes, recirculation offers considerable cost savings. Mud cleaning (by allowing cuttings to settle) can be improved by adding detergents to the low solids mud or water circulation. Always add detergents at the flowline. Only small quantities (one gallon detergent to 500 gallons mud) are

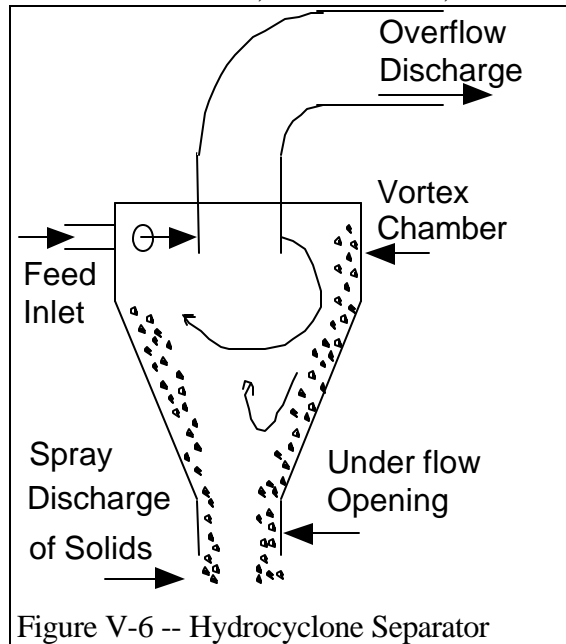


Figure V-6 -- Hydrocyclone Separator

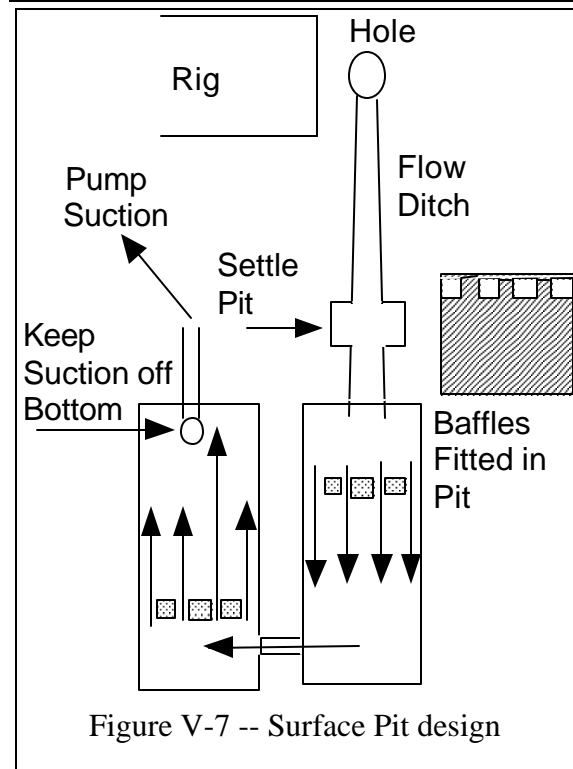


Figure V-7 -- Surface Pit design

required, but detergents are taken out of circulation with the cuttings and must be replaced continuously.

Mechanical solids control for core drilling is usually done with a hydrocyclone (Figure V-6). The mud feed enters the hydrocyclone tangentially causing a high speed spinning of the fluid. The rotation separates the heavier solids from the lighter liquids and the solids fall out the bottom of the separator.

Pit design: Surface pit design (Figure V-7) should allow the mud to change direction often by using baffles in the tanks and having more than one circulating tank. A good settling pit will force the mud to flow in a shallow stream with the flow occupying the full width of the pit. In this way, the flow can be slow while the cuttings have only a short distance to settle before they drop out of the flow path.

Because of the very fine cuttings produced by a diamond drill, the settling time will be proportionately slower. Much of the fine material in suspension has virtually zero settling velocity in muds with any measurable viscosity. To remove fine material, a hydrocyclone must be used. Pits of the design illustrated can only be cleaned when drilling is shut down. Any fluid agitation prevents settling.

Mud mixing: Adequate facilities for mixing, adequate pits, pit configuration, and following recommended product formula mixes per tank are vital parts of maintaining hole stability and minimizing costs.

REMEMBER- Treat The Down Hole Situation. Know what you are adding, and why. Know the proper amount to mix, and how to mix it, and in what sequence the products should be added. Work with your drilling fluids engineer to maintain the right mud for your project. In the pre-spud meeting decide what products may be needed and maintain an adequate stock on location. Keep products covered and maintain good housekeeping at the mud stock. *Don't waste money with broken and unused bags.*

General comments on mud mixing:

- Treat the make up water first, use soda ash for removing calcium ions.
- Use jet mixer or high-shear stirrer.
- Add bentonite slowly; adding bentonite too fast will cause it to lump and settle to bottom.
- Use liquid polymers or easily mixed polymers; add polymer after adding bentonite.
- Current state-of-the-art dry powder polymers do not require pre-mixing the polymer in an oil base to prevent “fish eyes” (unyielded particles of polymer). Driscal D[®] or 110 RD[®], for example, mix easily through a high shear hopper.
- Liquid polymers are rated by the percentage of “active” ingredients in the slurry. Alcomer 120L is a 50% active liquid polymer and performs well at high temperatures. Most liquid polymers are in a 30-35% active range. Liquid polymers should be mixed slowly in shear conditions to prevent setting to the bottom of the pits. Some polymer emulsions in storage tend to settle active ingredients slowly to the bottom of the container. (Frequently rotate containers top-to-bottom.) Do not attempt to wash out

bottom sediments with water. *Polymers by themselves do not build filter cakes.*

They need the presence of active solids (bentonite) in small quantities.

- Add dissolved thinners at the flow line. Detergent, polymeric deflocculants, and any other dispersants such as lignite should be added at the flow line.
- Follow mixing instructions. All crews should follow the mud program as recommended. The mud system is just as important for the night shift as for the day shift.

Typical mud properties: Mud properties should always be adjusted to downhole situations. Generally the following parameters are maintained for core fluids:

- Density: as low as possible, 8.4-8.8 lb./gal measured with a standard API mud balance
- Viscosity: 30-40 seconds per quart measured with a Marsh funnel
- Filtrate volume: 10-15 cc, measured with a full area or half area standard filter press.
- Cake thickness: Film to 1/32" measured with a cake thickness ruler. Cake should be slick and tough indicating adequate polymer content.
- Sand content: Nil or less than 1%, measured with API sand content test kit.
- pH: 8.5-9.5 measured with litmus paper or standard pH meter.
- Plastic viscosity: Below 10 centipoise
- Yield point: Below 10 pounds per 100 square feet. Plastic viscosity and yield point values should be fairly close to each other.
- Gel strength: Measured in pounds per 100 square feet. At 10 seconds = 1 to 3, at 10 minutes = 3 to 5. Gel strengths, plastic viscosity, and yield points are measured with a variable speed rheometer.

Hydraulics: One of the major differences between wire-line coring and mud rotary drilling involves the hydraulics of the mud system. Up-hole velocities and rotary speed of the rods are much higher in wire-line coring than mud rotary. In general, try for the following:

1. Minimize solids
2. Minimize concentrations of ultra fine cuttings in mud
3. Use high yield viscosifiers
4. Use polymers with small amounts of clay
5. Fluid flow patterns can be turbulent or laminar (Figure V-8a-c). High turbulence can cause hole erosion, loss of core and induced lost circulation
6. Maintain low weight, low plastic viscosity, and low yield point

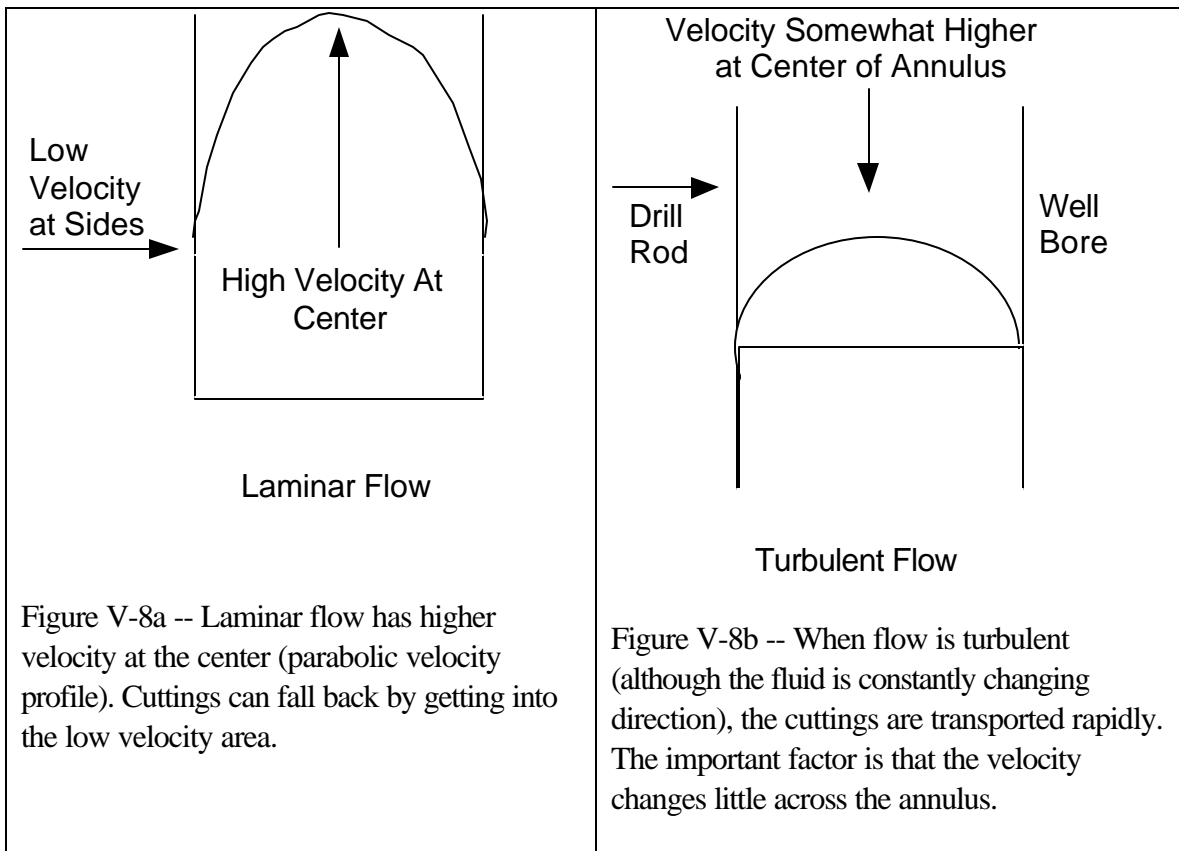
Differential sticking: This phenomenon occurs when collars, pipe or rods are held against the wall of the hole by hydrostatic pressure (Figure V-9). Differential sticking typically occurs when all the following conditions are met:

1. Hydrostatic pressure in the hole is greater than the formation pore pressure and the formation is permeable.
2. A thick, poor quality filter cake has built up over the permeable formation as a result of a slow, continuing mud filtrate loss.
3. The rod, pipe or casing is allowed to lie stationary for several minutes against the wall of the hole.

When tools are held by differential pressure sticking, the fluid circulation in the hole is not affected in any way; however, the drill string cannot be raised, lowered or rotated. To reduce the tendency for differential sticking, pay attention to the following points:

1. Maintain good quality muds with low solids content, low water loss and thin, tough filter cakes.
2. Minimize the pressure differential by running low density muds.
3. Keep the drill string moving so that it does not get a chance to “settle into” the mud cake. There is less tendency to “settle in” in vertical holes.

The obvious way to free a drill string held by differential pressure, is to reduce or even remove the pressure differential. In shallow holes, in diamond drill holes, and in some water wells, this is the preferred procedure. Before reducing the hydrostatic head in the hole, the driller must consider the risk of causing collapse or caving which would add to the problem. If possible, bailing or aeration of the mud is a technique that should help. When pressure reduction is not possible, the placement of commercial spotting fluids, detergents, or TORKase may break down the mud seal and release the string. When the pipe comes free, the mud should be reconditioned before coring ahead.



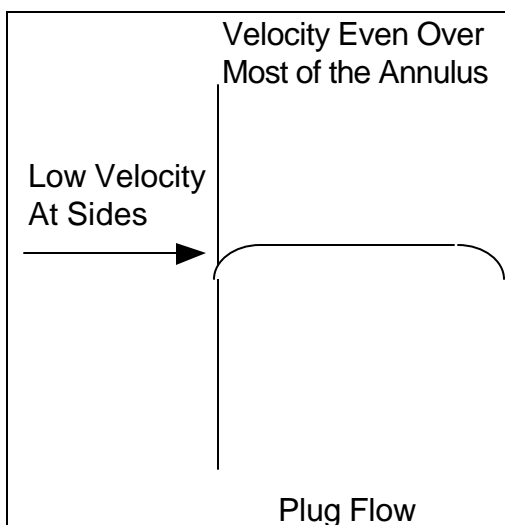


Figure V-8c -- Plug flow, a characteristic of polymer fluids, provides even velocity over most of the flow area.

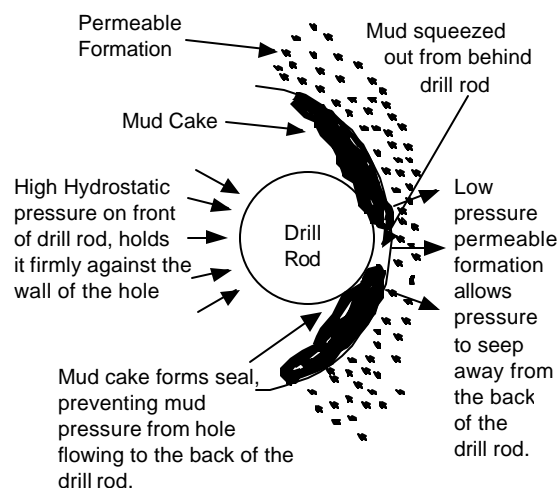


Figure V-9 – Large pressure differential causes large holding force

Downhole heat exchange: Experience on several holes has shown that return fluids are relatively cool even after they have been subjected to extremely high downhole temperatures. After the mud is exposed to these high temperatures, it begins to cool rapidly in the annulus because of heat exchange with the cooler mud inside the rods. Muds exposed to 300°C downhole have returned to the surface only a few degrees warmer than the ambient temperature surface mud (see, for example the temperature log from well VC-2B, Figure V-10.) If the mud is not thermally stable it will become degraded downhole and the returns temperature will give no indication of this degradation.

Case histories:

Trans-Pacific Geothermal 61-10, Vale Oregon. The TGC slim hole at Vale presented an ideal situation for cost comparison of slimhole to rotary-drilled exploration holes. In February 1994, a rotary-drilled exploration hole had been completed less than two miles away, to

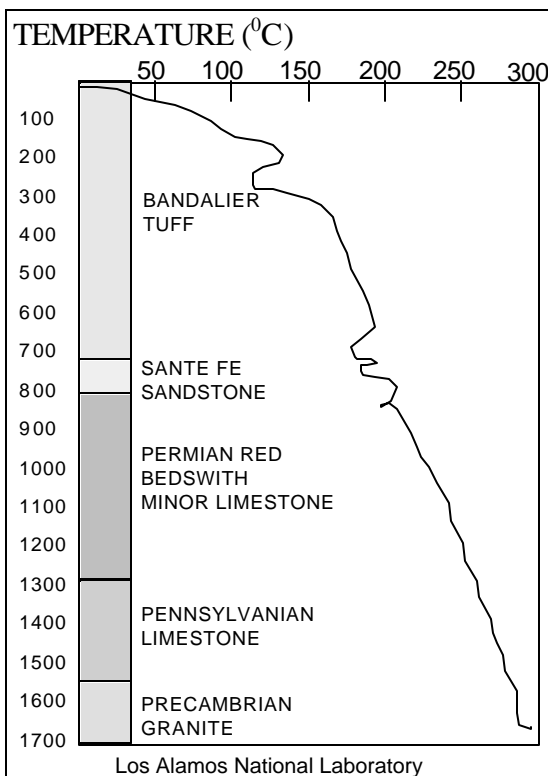


Figure V-10 -- Temperature Log of the VC - 2B Corehole. Return mud temperatures were less than 10°C above inlet temperature.

approximately the same depth. See Section III-b for detailed description of this project.

Drilling fluids costs were \$48,468 (\$8.32/ft) for the TGC slimhole and \$48,421 (\$8.41/ft) for the rotary drilled A-Alt. Although their costs per foot are similar, the slimhole costs were inflated by complete loss of circulation in the lower part of the hole. Mud was being pumped down the hole at 10-15 gpm for the last 20 days of drilling. A slim hole which did not lose total return would have much smaller mud costs than this one. An advantage for slimhole coring in lost circulation zones is that coring can continue with little or no returns (coring blind) in intervals that do not have to be cased. Rotary-drilled holes usually require expensive cementing of lost circulation zones to gain full returns.

CalEnergy/BLM 73-21

Temperature Gradient Hole, Inyo County, California: This hole had 4-1/2" surface casing, with 3.5" (Drill Rods) as intermediate casing and was cored from 405' - 1200'.

Synopsis: The BLM 73-21 Temperature Core Hole was spudded with a 7 7/8" bit and was rotary drilled to 405', where a 4 1/2" casing was set. Coring began at the casing shoe with HQ diamond bit. Drilling proceeded to 560'. The hole began to fall in so the hole was cemented. After sidetracking in the cement and re-cementing, circulation was restored to 90%. Circulation was again lost and the formation again caved. Another cement plug was set and drilled out. Cores were in broken formation to about 620' where solid core was recovered and circulation was restored to 100%. Coring proceeded with few problems to 1254' where about 1500 gallons of fluid was lost and then circulation was restored with an LCM pill. Coring continued to 4000' with no problems. At TD, 2-3/8" tubing was run and the rig moved off.

MUD Cost Per Foot \$4.43

CalEnergy Temperature Gradient Hole 34-10

Inyo County, California: Mud riser was 9.625" conduit at 7', then 4.5" surface casing at 410', and cored HQ (3.875") HQ rods (3.5")

Synopsis: Used the following products - soda ash, Kwik Ben (extra high yield bentonite), Drispac (dry powder polymer), IDAFLO (Starch), and Intervis (liquid polymer). Increased polymer addition improved core recovery and stabilized clay zones. Lost circulation was the major contributor to mud costs. Substantial torque was eliminated with 1% additions of TORKease. Core recovery was excellent.

Mud cost \$9.63 per foot

Summary: Slimhole wireline coring has proven to be a viable method for geothermal exploration. The drilling fluid program should be carefully planned prior to commencing drilling. Solids content must be maintained at an absolute minimum to eliminate mud rings, differential pressure sticking, loss of core, and hole instability. Usually a low-solids polymer system will be efficient and cost effective.

Temperature stable polymers in conjunction with small amounts of extra high yield bentonite will minimize downhole problems. Torque can be negated with the use of temperature stable non-hydrocarbon friction reducers such as TORKease. The services of a drilling fluids engineer experienced in wireline coring technology can help reduce costs and maintain hole integrity.

e. Recommendations on Lost Circulation

Introduction: The effects, costs, and remedies for lost circulation have been extensively studied at Sandia, but most of that work has been directed at large-diameter holes. Early in Sandia's program, considerable effort was focused on identifying lost-circulation materials (LCMs) which could be circulated in drilling fluid to plug up relatively small (~0.1-0.2" aperture) matrix permeability in high-temperature formations. Although several materials which would survive moderate (<150°C) temperatures were found, field experience showed that these LCMs were ineffective in the fracture-dominated loss zones which are common in geothermal fields.

More recent projects have included: flow instrumentation to give quicker indication of lost circulation on-set, a drillable straddle packer for more accurate cement placement, an expert system for lost circulation control, evaluation of cementitious drilling fluid, and an Engineered Lithology Test Facility (ELTF) for improved diagnostics on lost-circulation treatments¹¹. The flow instrumentation has been useful in slimhole drilling (e. g., Section III-d), but the other technologies have either not reached maturity or have not yet been applicable.

When loss zones need repair: The point has been made repeatedly that one of the advantages of slimhole drilling is its ability to drill "blind", that is, with complete lost circulation. There are, however, at least three situations in which it is important to repair loss zones:

- **Cementing casing** - As described in Section V-b, it is essential to get a good cement job on casing, especially when there is a prospect of the slimhole being used for flow testing. If there is persistent drilling-fluid loss in the interval to be cased, then there is little chance that the much heavier cement can be lifted to the surface. The most common remedy for this situation is to cement the loss zones as they are encountered in drilling. Although this is time-consuming, the cost is significantly reduced by the fact that most core drilling companies are accustomed to mixing their own cement and pumping it with rig pumps, avoiding the necessity of bringing in a cementing contractor. This method also enables the drilling team to easily try different accelerated cements and various LCMs mixed into the cement as plugging agents.
- **Reducing drilling fluid cost** - If the slimhole is using a relatively cheap and simple water/bentonite drilling fluid, it is usually not cost-effective to treat loss zones simply to preserve the mud. In some high-temperature holes, however, it is necessary to use very expensive additives (e. g., friction reducers) or costly polymer drilling fluids. Even though flow rates are low (12-15 gpm), long-term complete loss can cost tens of thousands of dollars. This cost is aggravated by the fact that, with total lost circulation, it is usually necessary to pump fluid (5-10 gpm) down the annulus between the drillpipe and wellbore to provide lubricity. In this case, the cost of cementing or otherwise treating a loss zone may well be worthwhile.
- **Well control** - Although geothermal wells are usually underpressured (inherently-high formation pressures are rarely seen), the fluid column is often needed in hot holes to keep both the drilling and formation fluids from flashing to steam. Even this requirement is not always enough to compel repairing a loss zone, because if the zone is high in the hole, the remaining fluid below the loss zone in the wellbore may have enough static

head to maintain the fluids in liquid phase. Some geothermal production wells (and an increasing number of oil and gas wells) are drilled underbalanced, or with pressurized wellbores, but this is probably not a realistic option for a slim, exploration hole.

Even though these various loss conditions are not uncommon, they do not usually become so critical that successful completion of the borehole is jeopardized. In the Fort Bliss drilling project (Section III-d), for example, 2462' of the total 10,810 feet drilled were cased, and lost circulation was severe to total for all the uncased intervals, but this did not seriously affect the drilling progress.

Lost circulation treatment: If one of the lost-circulation situations described above requires treatment, there are three principal methods, listed here in order of increasing cost and effectiveness.

- **Lost circulation material (LCM)** - Fibrous, flaky, or granular materials are used, in great variety, to seal off lost-circulation zones. LCMs are available to withstand ordinary geothermal temperatures, but most losses occur at natural fractures in the formation, and most of the fractures have apertures which are significantly larger than the LCM dimensions. This is especially true for wireline coring, because the narrow passages -- through the core barrel, bit, and annulus -- limit the LCM size which can be circulated in the mud. Still, it is almost always useful to try LCMs because they are sometimes effective, the costs and risks are low, and they avoid the problems with casing and cement which are described below.
- **Cement** - Cement is most often the treatment of choice in slimhole lost circulation because it is relatively cheap (in terms of material), it usually patches a loss zone with enough strength to survive drilling circulation or cementing casing, and it can be placed fairly accurately in small-diameter wellbores. There are, however, serious drawbacks: The wait-on-cement (WOC) time is usually six or more hours (and may be repeated more than once for a given loss zone); the cement has to be drilled out of the wellbore after it sets; and drilling cement is highly detrimental to the drilling fluid (see Section V-d.) In addition to the WOC time, cementing usually requires a trip to remove the bit for placing cement through open-ended drill pipe, and improper procedure when drilling green cement can stick the string.
- **Casing** - Casing is rarely set solely to control lost circulation, unless experience in an area indicates that it will be needed and it can therefore be incorporated into the well design. This is the method of last resort, not only because it is the most expensive, but because it limits the options for continuing the well. Because boreholes are designed "from the bottom up", that is, the desired hole diameter at TD is chosen and then casing and hole sizes in the upper part of the well are selected to yield that diameter, an unplanned reduction in hole size may be very serious in its effect on the ability to test or log the well. Nevertheless, running another casing string (or liner) may sometimes be required because of other hole conditions, and will, at the same time, solve any lost circulation problems. (See the discussion of reducing hole size at Newberry, Section III-c.) In wireline coring, there are two additional problems when reducing from H-size to N-size drill rods (which is the most common way of "running casing" in this kind of drilling.) First, because the H rods left in the hole are high-quality drill pipe, they are

often expensive, and secondly, because of the small annulus around the H rods (3.5" diameter pipe in a 3.8" diameter hole), it is very difficult to get much cement around the rods if drilling conditions require it.

In addition to the conventional methods described above, two concepts have potential for an impact on lost circulation treatment in slimholes: foam cement and cementitious LCM.

- Aerating cement with gas is not a new idea, but lightweight foam cement would be beneficial both for lost circulation and for cementing casing where persistent loss zones occurred during drilling. This cement has been tried a number of times in large-diameter wells¹², but not, to the authors' knowledge, in slimholes.
- Cementitious LCM is a concept being developed by Halliburton with cooperation and assistance from Sandia, wherein a proprietary substitute for Portland cement is used to plug loss zones. This material is reported to set faster (2-4 hours), be less sensitive to temperature, and be more compatible with drilling mud.

Both of these technologies seem to have promise for application in slimholes.

f. Recommendations on Flow Testing Procedures and Equipment

Introduction: Unless simple temperature measurements in a hole have shown that it is too cool for any reasonable geothermal development, then once it has been drilled and completed it must be tested to fulfill its predictive purpose.

There are a number of methods which can be used to infer productivity of a production-size well from slimhole data in the same location. If the combination of depth, temperature, and permeability in the slimhole is such that it can be induced to flow, a *production flow test* is by far the best predictor of productivity. Results from Steamboat Hills, Nevada (Section III-a) and from Japanese data (Section III-f) are convincing that a discharge test in a slimhole can be scaled to a production well. Scaling discharge rates can be done by wellbore modeling, using the wellbore simulators discussed in Section IV-c, or if sufficient local experience exists, by a simple scale factor applied to the wellbore diameters¹³ in the form

$$Q_{\text{prod}} = Q_{\text{slim}} \left(\frac{\text{Diameter}_{\text{prod}}}{\text{Diameter}_{\text{slim}}} \right)^n, \text{ where the exponent } n \text{ is approximately } 2.5. \text{ To do this, of}$$

course, it is necessary to measure the slimhole's flow rate, which can be done in a variety of ways.

Measuring flow rate: The flow-rate measurement method used at the Steamboat Hills exploratory slimhole is described below in some detail. The Steamboat Hills drilling location layout, shown in Figure V-11, allows testing to be performed without large-scale modifications to the location or to the wellhead piping configuration. Slimhole discharge and injection testing methods are similar to those used for large-diameter wells, but the size and cost of the surface flow test equipment are reduced. The smaller surface flow-test equipment also reduces the set-up equipment (cranes, etc.) and personnel requirements.

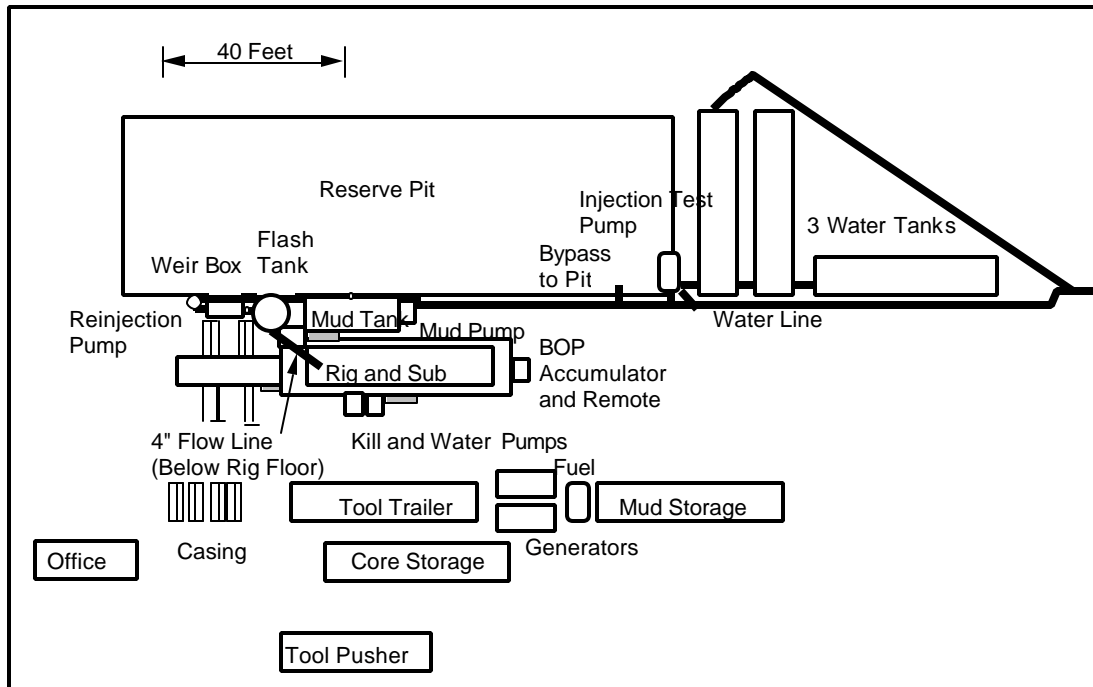


Figure V-11 -- Location layout at Steamboat Hills

Details of the wellhead and flow test piping and measurement equipment are shown in Figure V-12. This equipment is designed so that flow testing can be done during pauses in

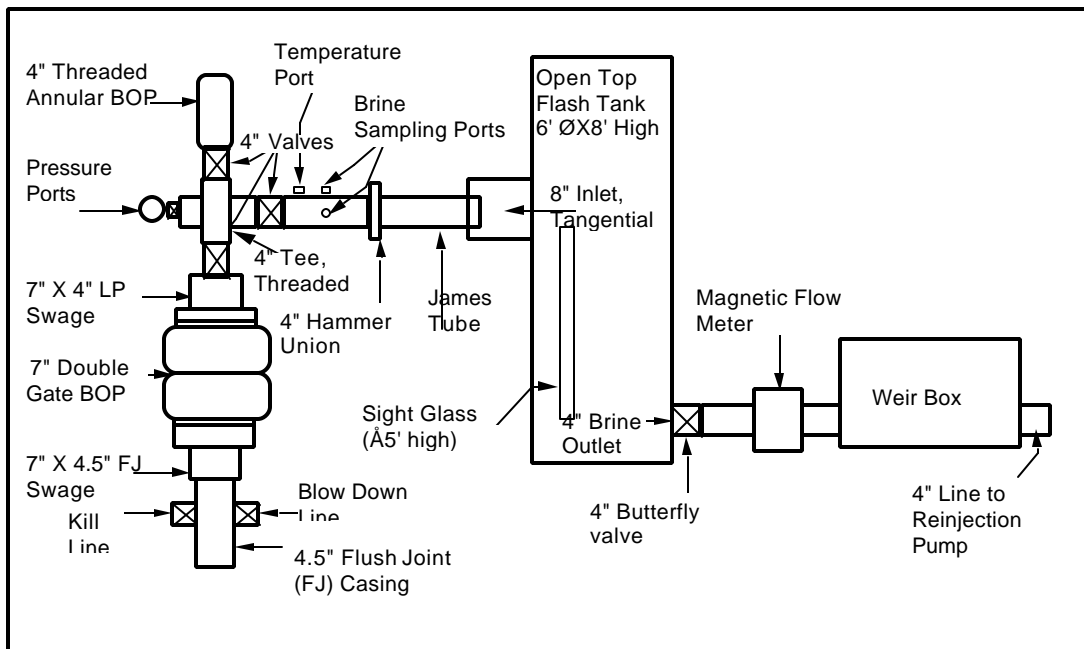


Figure V-12 -- Flow test equipment at Steamboat Hills (typical)

drilling operations without changing the piping configuration. The 4" hammer union on the flow test line allows for readily switching between discharge (production) testing, injection testing,

and drilling operations. The 4" tee in this configuration does mean, however, that more clearance is required under the drill rig for the BOP. Ports for pressure and temperature measurements and chemical sampling are also available for both drilling and testing activities.

Two methods of measuring the liquid discharge rate were used in this system: a weir box indicates flow rate by the height of the water level above the bottom of the weir notch, and a magnetic

flow meter measured flow continuously and directly between the flash tank and weir box. The magnetic meter provides an electrical signal for continuous flow recording, while the weir box maintains a small static head (preserving liquid conditions) through the magnetic flow meter and allows direct measurements of the water flow rate. Total mass flow rate was measured by a James tube as described below.

An atmospheric flash tank design for slimholes is shown in Figure V-13. Flash tanks are often made from surplus fuel tanks and so have those diameters (typically 6-10 feet). Larger diameters would be difficult to position at the test site and inconvenient (because of highway regulations) to transport to other locations. Tank heights are usually determined by the expected flow rates and enthalpy of the produced fluid, but there is considerable variability in this. Principal design criteria for a flash tank are these:

- The inlet pipe around the James tube, and the opening at the top of the tank, should be sized to eliminate any back-pressure during flow. This is required because the lip pressure reading in the James tube is often quite small and is very sensitive to back pressure. Size of the inlet pipe does not usually require a precise calculation, because making it oversize is not detrimental, subject to the other criteria below.
- Design height of brine inside the flash tank must be coordinated with liquid height in the weir box. Because of small pressure losses in the pipe connecting the two, liquid height

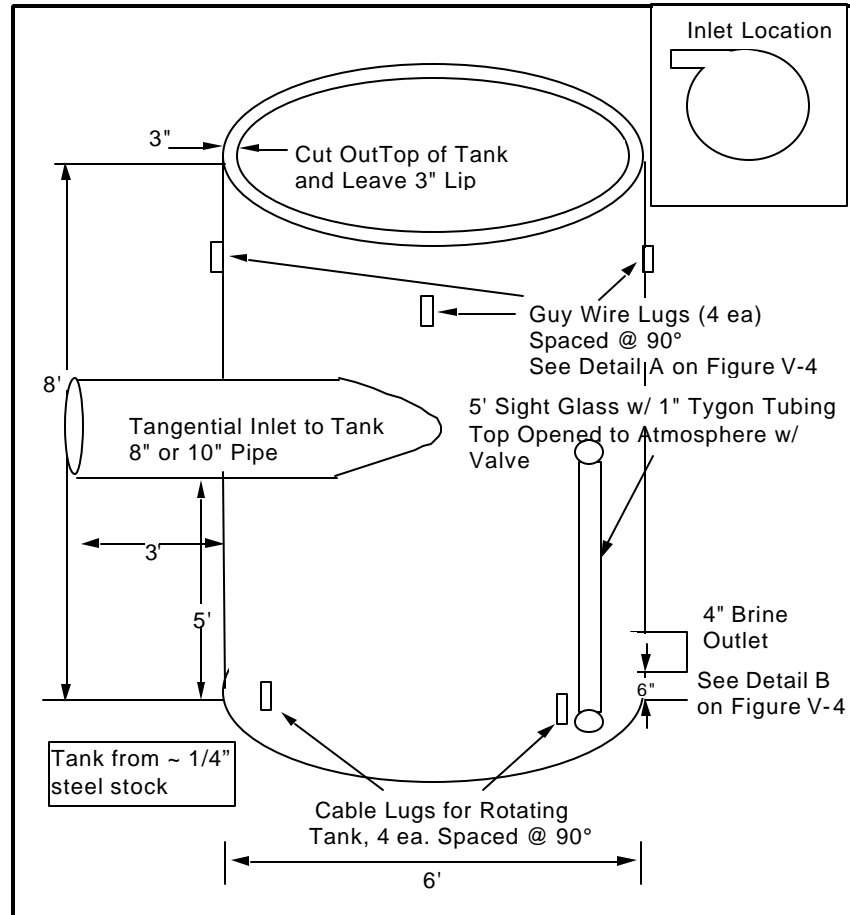


Figure V-13 -- Flash Tank for discharge testing of slimholes

in the tank will be slightly higher, but the pipe size should be chosen to minimize these losses.

- Inlet height to the flash tank should be well above the design liquid height so that brine will not flow back out of the tank through this pipe. The inlet should also be canted up at 2-5° to avoid this kind of flow. Inlet height should also allow for rotation of fluid in the tank, caused by the tangential entry. Equations for this are in most fluid mechanics texts¹⁴, but for slimholes the effect is probably small [at Steamboat, frictionless rotation of the fluid with inlet velocity at the outside radius would have raised the liquid level at the tank wall by less than 6"]. Baffles can also be added to the flash tank to reduce the fluid's angular velocity.

A sight glass, normally made of clear Tygon tubing, can be used in conjunction with the flash tank discharge shut-off valve shown in Figure V-12. The rate at which the water level rises in the flash tank allows for an additional measurement of liquid flow rate.

Several details for the design of the flash tank are shown in Figure V-14 . Using an elbow inside the flash tank on the liquid discharge line reduces surging and water level fluctuations in the weir box and also smoothes the flow through any other liquid metering devices.

The James tube design details are shown in Figure V-15. The location of the pressure port is critical. An

example of calculations necessary to size the James tube are shown in Figure V-16, which is just a graphical representation of the equation shown on the chart.

Wellbore modeling,

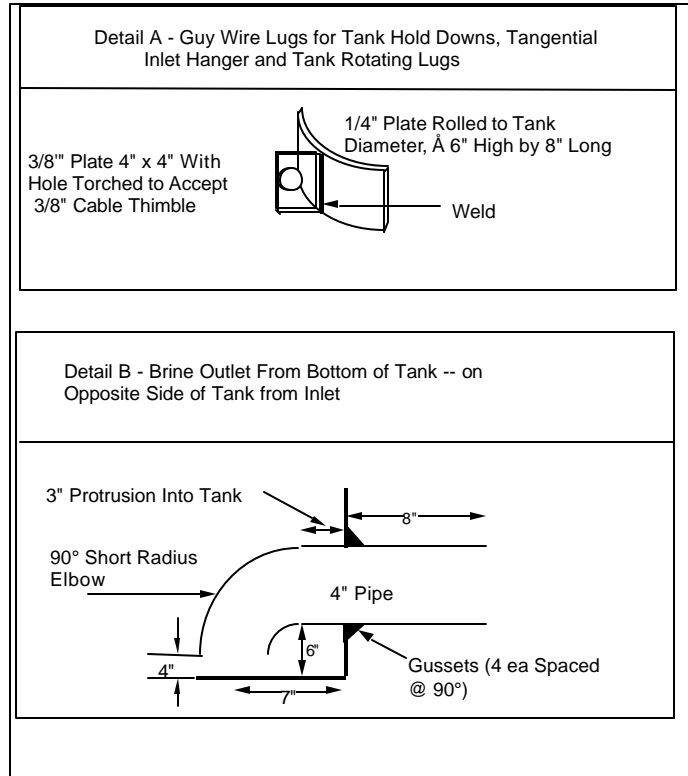


Figure V-14 -- Flash Tank Details

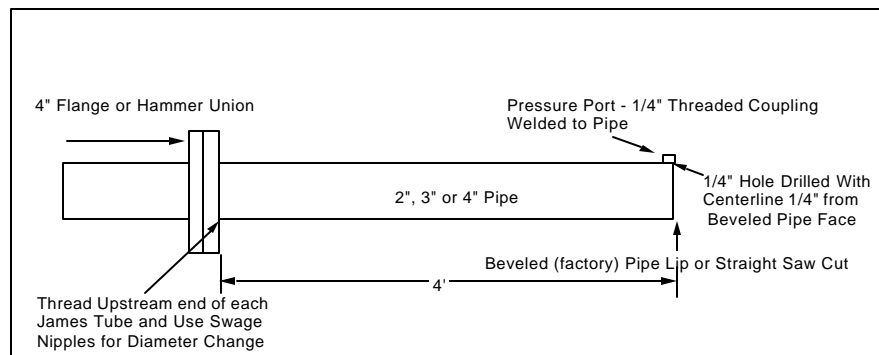


Figure V-15 -- James Tube design details

along with assumptions of reservoir permeability, enthalpy, and static reservoir pressure will help determine the proper James tube size, but it is still useful to have various James tube diameters available, on-site, during discharge test operations. Note that the solution to the equation in Figure V-16 is dependent on local atmospheric pressure; this example is for Steamboat Hills, where ambient pressure is 12.5 psia.

The James tube lip pressure measurement is used to calculate total mass flow rate and energy production rate as described in Section II-d; details of the monitoring equipment are shown in Figure

V-17. This equipment is an important aspect of measuring the energy production rate, and, therefore the discharge rate, of the slimhole. The 2" capped nipple (liquid accumulator), located on the James tube, is filled with water or antifreeze (depending on ambient weather conditions). The valving shown in this diagram allows the James tube pressure port to be closed. When the James tube port is closed, the valve located on the top of the liquid accumulator can be opened. This allows the pressure gage to exhibit ambient pressure conditions plus the pressure due to the height of the water between the pressure gage and liquid accumulator [the pressure due to the vertical water leg must be subtracted from the pressure reading to give the lip pressure].

This equipment allows the pressure gage to be checked periodically for proper operation and prevents condensed steam and water from developing in the tubing between the James tube pressure port and the pressure gage, which would give inaccurate James tube pressure readings, and, therefore, inaccurate discharge rate calculations.

Weir box design details are shown in Figure V-18. A sight glass on the outside of the box allows reading the height of the fluid within the weir box, and thus the height above the bottom of the weir notch, and thus the flow rate. Flow through a weir notch is given by an equation of the general form $Q = Kg^{\frac{1}{2}}H^{\frac{5}{2}}$, where Q is the liquid flow, g is the acceleration of gravity, H is the height of the flowing liquid above the bottom of the weir

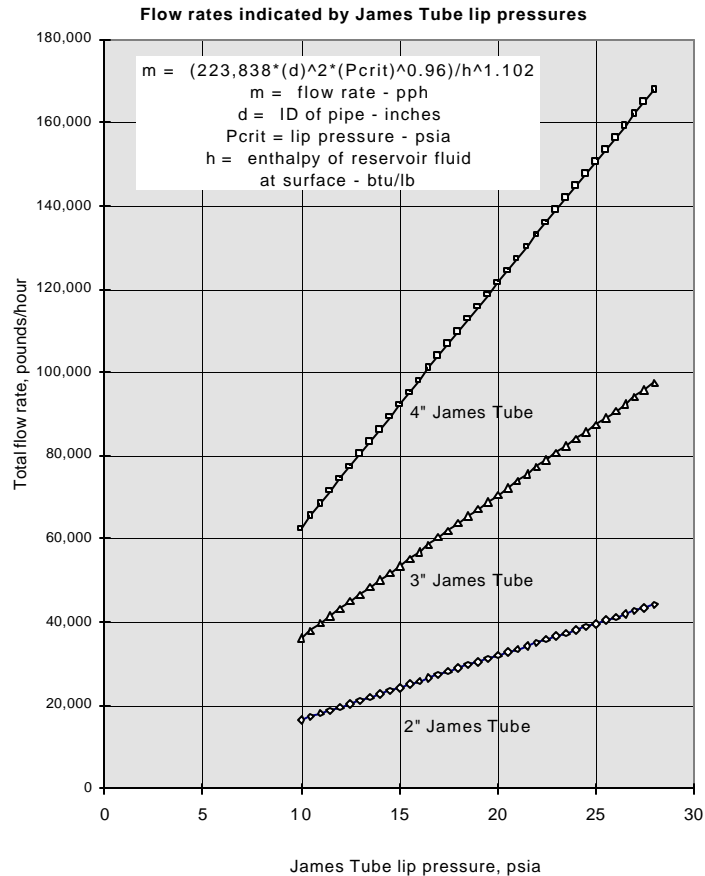


Figure V-16 -- Sample James Tube data

notch, and K is a dimensionless constant which depends on the shape of the notch and the density, viscosity, and surface tension of the fluid. For water, and the notch dimensions shown in the figure, liquid flow is $Q = 2.276H^{\frac{5}{2}}$, where Q is in gallons/minute and H is in inches. The hole in the box's side which feeds the sight glass has a stilling well around it (Figure V-19) to reduce water level fluctuations at the measurement point. The solid plate and discharge pipe located at the discharge end of the weir box allow for liquid conditions to be maintained at the pump used to transfer fluid to storage areas or the injection facility.

Initiating flow: If wellbore conditions (pressure, temperature, permeability, water level) are adequate, there are several methods to start the well flowing. In some cases, pressure and temperature are high enough that just opening the wellhead will produce flow and no stimulation is necessary.

In the next simplest case, the well has high temperature at relatively shallow depth so that injecting compressed air into the wellhead will force the free surface of the brine down into a zone where the wellbore temperature is above boiling. If the pressure is held long enough for the brine to heat up, and then the pressure is released, the liquid at the free surface will flash to steam, unloading pressure on the hot liquid below it and creating a self-sustaining process in which steam and brine flow up the hole.

Finally, if the high temperatures are deeper in the well, or if the wellbore has been cooled by drilling fluid, it may be necessary to pull some of the cooler brine off the top of the fluid column, which will bring hotter liquid up from the production zone, heat the wellbore, and start a self-supporting flow. Liquid can be removed by air-lift (pumping

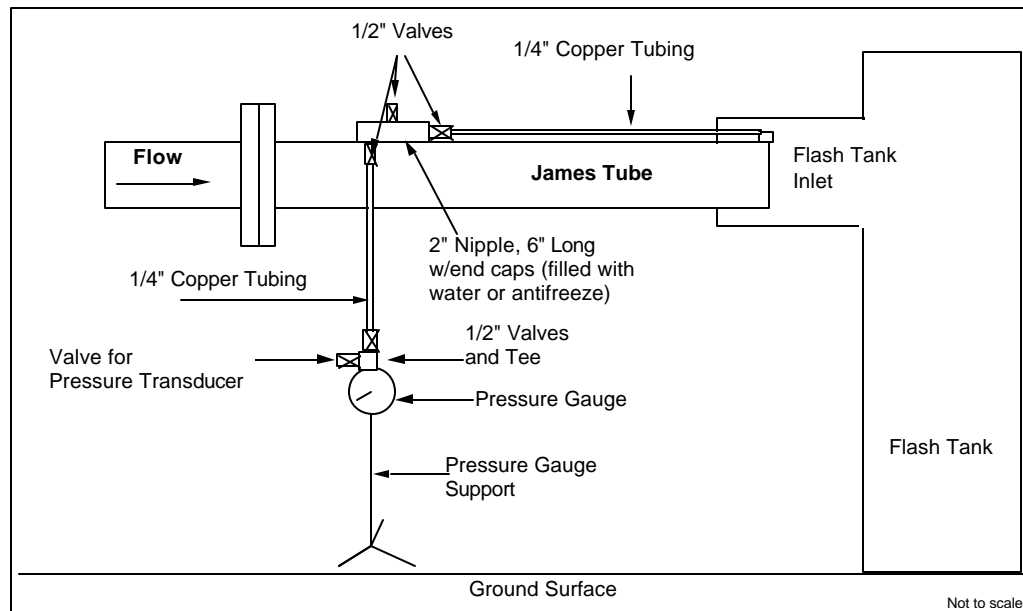


Figure V-17 James Tube installation details

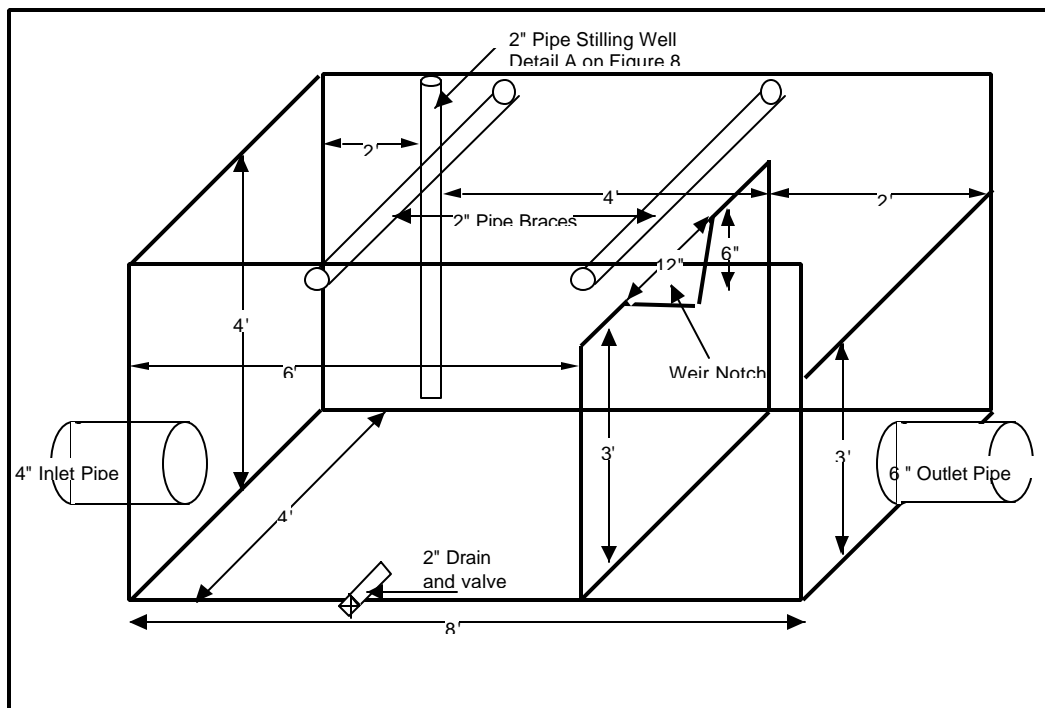


Figure V-18 -- Weir box (typical dimensions for slimhole testing)

compressed air down a string of drill pipe in the hole), by injecting nitrogen through drill pipe or coiled tubing, or by swabbing (pulling a tight-fitting plug, usually on a wireline, rapidly up the wellbore). Once flow is started, the drill pipe or tubing is removed from the hole.

Any time that hot water and steam are produced from a wellbore, there are inherent safety issues related to the high temperature (and possibly high pressure). Safety procedures should be prepared by someone familiar with geothermal well testing and should be thoroughly understood by all personnel involved in the test.

Duration of flow test:

The primary objectives of a discharge test are to assess the reservoir's transmissivity and to predict the productivity of a large-diameter well in the same location. Once the slimhole has flowed long enough to clean up any drilling mud, loose cuttings, or

unconsolidated formation fallen into the hole, the

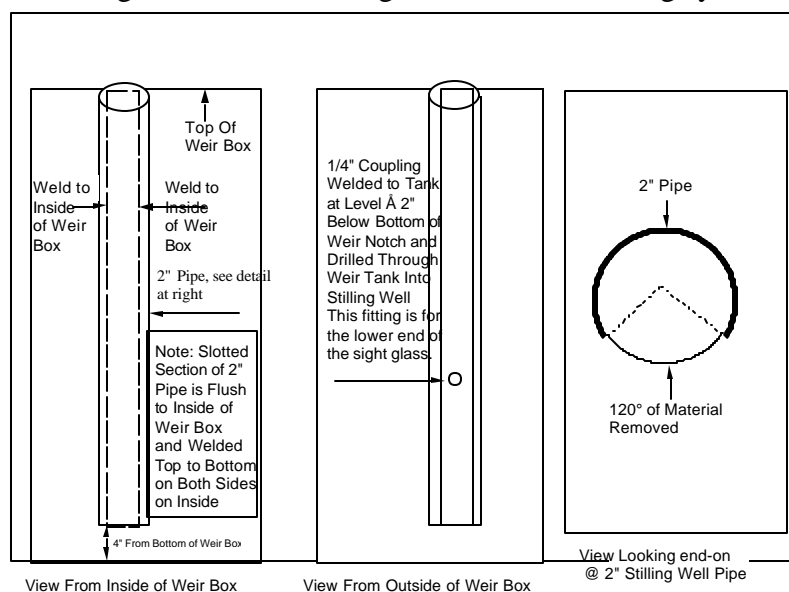


Figure V-19 -- Stilling well for weir box

question arises as to how long the discharge test should last.

Transmissivity is usually estimated by using transient downhole pressure measurements (preferably at the feedzone) to establish build-up and/or fall-off curves, as described briefly in Section IV-a and in detail in Grant¹⁴. The discharge test should then last long enough for the downhole data to form a useful Horner plot. If the pressure transducer has surface readout, the data can be plotted on the fly and the point where the semi-log plot becomes linear is easily identified.

Productivity index, PI, is usually given in the form $PI = \frac{\dot{M}}{P_n - P_f}$, where \dot{M} is total mass

flow rate, P_n is the static reservoir pressure at the feedzone, and P_f is the flowing pressure at the feedzone. This is inherently a measure of the reservoir's flow resistance, and data from Japanese wells (Section III-f) show that PI is generally well correlated between slimholes and production wells. Downhole pressure measurements during the flow test, especially if the well is discharged at several different flow rates, can be used to derive the productivity index.

It is theoretically possible for pressure test analysis to indicate the volume of a reservoir, but the amount of fluid withdrawn in a slimhole flow test is substantially less than in a test of a production well, and it would probably take an inordinate length of discharge time for a slimhole to give useful information about reservoir size. Other logistical factors, such as the difficulty of disposing of produced brine, may affect the length of a flow test, but in general there is little likelihood that a slimhole discharge test should last more than a few days.

g. Recommendations on Data Analysis

The quantity and quality of the data collected from slim holes during drilling, logging, and testing, including any core analyses, temperature-depth surveys, heatup surveys, discharge tests, injection tests, PTS logging, etc., will determine the extent to which the data can be analyzed and used for delineating the areal extent of the geothermal reservoir, obtaining the characteristics of the geothermal reservoir, and predicting the performance of large-diameter production and injection wells. In other words, the goals for the analysis of data from slimhole drilling, logging and testing are to (i) define rock types, fractures, geological structure and stratigraphy; (ii) determine the fluid state of the geothermal reservoir, i.e., temperature, pressure, salinity and gas content; (iii) determine formation properties such as productivity/injectivity indices, transmissivity, storage, boundaries, etc.; and (iv) predict the potential discharge performance of large-diameter production wells. This last goal for the analysis of data from slimhole drilling, logging and testing is a nontrivial one requiring rather sophisticated computer codes. In order to accomplish the goal, it may require obtaining expert consulting assistance.

The initial data analysis for any slim hole should be a careful scrutiny of the drilling history and core recovered from the hole. Many times the drilling history of a slim hole, or even a large-diameter geothermal well, will be ignored as unimportant; however, careful examination of the drilling history can provide information and data about the open fractures and/or fracture zones (i.e., permeability) in the subsurface based on the occurrence of lost circulation during the drilling of the borehole. The location of these fractures and/or fracture zones can be confirmed

by examination of the core. In addition, any temperature-depth logs or heatup surveys can be used to further confirm and document the extent and type of fluid flow through these identified fractures and/or fracture zones.

Heatup surveys are repetitive surveys of downhole temperature and standing water level which are usually carried out for at least several days after a period of cold-water injection into a slim hole is terminated. These heatup surveys permit the estimation of reservoir pressure and temperature. Feedzone pressures for the boreholes can then be determined and plotted versus elevation as in Figure III-21 for the Oguni boreholes. The resulting vertical pressure gradient and the corresponding hydrostatic gradient can be used to analyze the temperature distribution and flow patterns in the geothermal reservoir.

Earlier, the conventional wisdom had been that slim holes could not be discharged; however, as documented in the case histories presented in Section III, slim holes can be discharged in order to define the characteristics of geothermal reservoirs. As noted above, the data collected during the logging and testing phases of an exploration program will determine the extent of the data analysis. First, the logging tools and gauges must be calibrated properly in order to provide the resolution and accuracy that are needed for appropriate data analysis. Secondly, the actual logging and testing data must be carefully considered. For example, during a discharge or injection test, the pressure gauge must be located at the same depth in the borehole as the feedzone, otherwise, the data will not be reliable for determining the productivity or injectivity index.

During injection testing of a borehole, the downhole pressure gauge should be located as near as possible to the principal feedzone. A static pressure should be recorded at the gauge depth prior to the start of cold water injection. The pressure measurements taken at the end of each injection interval can then be used to compute the injectivity index as presented in Section IV.e.3. After start of injection in a borehole, the pressure at first rapidly rises and then slowly falls. As soon as injection is terminated, the pressure begins to decline very rapidly. The rapid fall-off at shutin is not unusual. The fall-off data from injection tests may be analyzed to obtain estimates of the formation transmissivity, i.e., permeability times the effective formation thickness.

Consider the case that during an injection (discharge) test, the downhole pressure tool is placed substantially above the feedzone depth. Because of wellbore cooling due to injection of cold fluid (heating due to discharge of hot fluids), the measured change in pressure, i.e., = flowing pressure - static pressure prior to injection (discharge), at the gauge depth (gauge depth \ll feedzone depth) will underestimate (overestimate) the change in pressure at the feedzone depth. The discrepancy in rates of pressure change at the gauge and feedzone depths will decline with continued injection (discharge). After the injection (discharge) of a few wellbore volumes (say 2 or 3), the temperature in the depth interval between the gauge and feedzone depths should approach a stable value; hence, the rates of pressure change at the two depths will be similar. Unfortunately, most injection (discharge) tests on slim holes are not carried out for long enough period of time for a few wellbore volumes to be injected (discharged), thus, the need for accurate location of the pressure gauge next to the feedzone.

From the logging and wellhead data obtained during a discharge test, it is important to accurately determine the flowrate, enthalpy, water/steam ratio, wellhead pressure, wellhead

temperature, feedzone pressure, feedzone temperature and fluid composition. As noted in Section IV.e.3, these data can be used to calculate a value for the productivity index (PI) of the slim hole. The PI will provide for the calculation of the pressure drop in the formation and with the use of a wellbore flow simulator to calculate the pressure drop in the wellbore, the slimhole discharge data can be used to predict the discharge capacity of a large-diameter geothermal production well. Furthermore, the discharge performance and results of the pressure-temperature logging of the slim hole will provide the information needed to determine whether the feedzone is a liquid feed or a two-phase feed.

In Section IV.e.6, it has been shown that if both the slim holes and large-diameter geothermal wells have liquid feedzones and more or less uniform internal diameter, the “scaled maximum discharge rate” of Pritchett provides a reasonable estimate of the maximum production rate of large-diameter wells based on discharge data from slim holes. Furthermore, it is possible to numerically simulate the production characteristics of non-uniform, large-diameter wells using slim hole discharge data and a wellbore flow simulator. The analyst must provide parameters describing the well geometry, i.e., inside diameter and angle of deviation with respect to vertical along the hole length, a stable formation temperature distribution with depth, and an “effective thermal conductivity” representing the effects of conductive heat transfer between the geothermal fluid in the wellbore and the surrounding rock formation. Values must also be specified for the flowing feedzone pressure (or alternatively stable feedzone pressure and productivity index) and enthalpy (or alternatively temperature for boreholes producing from a single-phase liquid feedzone).

If a slim hole with a liquid feedzone cannot be discharged, it is possible to use injection data to make useful predictions regarding the discharge performance of large-diameter wells. The significant volume of data presented in Figure IV-9 indicates that the productivity and injectivity indices are equal to first order. Therefore, in the absence of discharge testing, the injectivity index may be used to compute the flow resistance of naturally fractured geothermal formations to liquid production, and to compute, in conjunction with a wellbore flow simulator, the probable discharge characteristics of large-diameter geothermal wells.

As noted in Section IV.e.4, based on the data from four Japanese boreholes including both slim holes and large-diameter wells with two-phase feedzones, the productivity index is equal to about one-tenth the injectivity index. However, as pointed out by Garg and co-workers¹⁶, additional studies and statistically significant amounts of data are required to draw firm conclusions regarding the relationship between injectivity index and two-phase productivity index. Some other preliminary conclusions are that the two-phase PI must be greater than 0.3kg/s-bar in order to obtain economically significant discharge rates. Finally, it appears to be possible to use a numerical wellbore flow simulator to predict the discharge characteristics of large-diameter wells with two-phase feedzones utilizing test data from slim holes with two-phase feedzones.

-
1. "Slim Holes, Slimmer Prospects"; Journal of Petroleum Technology; November, 1995; p. 951

2. D. J. Bode, R. B. Noffke, H. V. Nickens; "Well Control Methods and Practices in Small-Diameter Wellbores"; SPE Paper 19526; October, 1989
3. (a) A. T. Burgoyne, M. E. Chenevert, K. K. Millheim, F. S. Young; "Applied Drilling Engineering"; Society of Petroleum Engineers; 1991, pp. 301-350 (b) S. S. Rahman, G. V. Chilingarian; "Casing Design: Theory and Practice"; Elsevier Science Publishing Co.; Apr. 1995; 388 pp. (c) H. Rabia; "Fundamentals of Casing Design"; Kluwer Boston Inc.; 1987; 256 pp.
4. Casing-design software packages include: "StressCheck™" by EnerTech (5847 San Felipe, Suite 1000, Houston TX 77057) and "Windows Casing Design Program" from Lone Star Steel (PO Box 803546, Dallas TX 75380-3546). The EnerTech program is the more sophisticated, and more expensive, of these two.
5. U. S. Department of Interior, Geological Survey, Conservation Division, "Geothermal Resources Operational Orders", January 1976
6. J. T. Finger, R. D. Jacobson; "Phase II Drilling Operations at the Long Valley Exploratory Well (LVF 51-20)"; Sandia Report SAND92-0531, Sandia National Laboratories, June, 1992
7. P. Armstrong, B. Brown, G. Polk; "Drilling Fluids as Applied to Slimhole Exploration at Vale, Oregon, A Case History - a Success story"; Geothermal Resources Council, Reno, NV, Oct. 1995
8. G. Polk, B. Brown; "Differences in Mud Systems for Geothermal Production and Wireline Coring Rigs"; Geothermal Resources Council, Reno, NV, Oct. 1991
9. G. Polk; "Geothermal Drilling Fluids - Developments for Exploration and Production"; ASME Energy Resources Technology Conference, New Orleans, LA, Jan. 1988
10. R. K. Brown; "The Important Role of Drilling Fluids in Core Recovery for Scientific Drilling (Exploration) a Case History"; Northwest Mining Conference, Spokane, WA, Dec. 1995
11. D. A. Glowka, G. E. Staller, A. R. Sattler; "DOE Lost Circulation Technology Development"; Presented at Fall Meeting, Solution Mining Research Institute, Cleveland, Ohio, 20-23 Oct, 1996
12. R. Montman, D Sutton, W. Harms, B. Mody; "Low density foam cements solve many oil field problems"; World Oil magazine, June, 1982
13. J. W. Pritchett; "Preliminary Study of Discharge Characteristics of Slim Holes Compared to Production Wells in Liquid-Dominated Geothermal Reservoirs"; Sandia National Laboratories Contractor Report, SAND93-7028, June 1993.
14. W. Kaufmann; "Fluid Mechanics"; McGraw-Hill, 1963, p. 13
15. M. A. Grant, I. G. Donaldson, and P. F. Bixley, "Geothermal Reservoir Engineering", Academic Press, New York, NY, 1982, pp. 116-125
16. Garg, S.K., J. Combs, M. Kodama and K. Gokou (1998), "Analysis of Production/Injection Data from Slim Holes and Large-Diameter Wells at the Kirishima Geothermal Field, Japan", *Proceedings Twenty-Third Workshop on Geothermal Reservoir Engineering*, Stanford University, Stanford, California, January 26-28, pp. 64-76

VI. GLOSSARY

The following terms are common in drilling practice; many of them are used in this report:

annular preventer - part of the BOP stack; an inflatable bladder which seals around drillpipe, casing, drill collars, or irregularly shaped components of the drillstring.

annulus - Drilling: the space between outside of drill string and inside of casing or wellbore.
Casing: the space between outside of casing and the hole.

backside - annulus between drillpipe and surface casing

balling, bit balling - lumps or balls of clay which form around a bit's cutting structure when drilling soft formations. Balling prevents the bit from cutting effectively.

block, or blocked run - a core run is blocked when fractured rock wedges into the core tube and prevents further drilling before the tube is full.

blow out - uncontrolled flow of fluids from a wellhead or wellbore.

Bowen spear - a fishing tool which expands inside a fish when the drillstring is pulled up

BOP - blow out preventer; one or more devices used to seal the well at the wellhead, preventing uncontrolled escape of gases, liquids, or steam. Also BOPE - blow-out prevention equipment. See *annular preventer, rams*.

boot, booting - forming a plug of drilled material or fill above the bit, usually caused by inadequate hole cleaning or swelling clays.

bottom hole assembly (BHA) - the assembly of heavy drilling tools at the bottom of the drill string; normally includes bit, reamers, stabilizers, drill collars, heavy-weight drill pipe, jars, and other miscellaneous tools.

bridge - a downhole obstruction, usually caused by part of the wellbore wall falling into the hole.

button bit - see tri-cone bit

cave - debris that falls off the wellbore walls and accumulates in the bottom of the hole.

CIP - cement in place

Dewar, Dewared - a Dewar is a double-walled container or heat shield, similar to a vacuum flask, which insulates a piece of equipment from high temperature.

drawworks - the large winch on the rig floor which takes up and pays out the drilling line, thus controlling the movement of the hoist or traveling block.

drilling break - an occasion during drilling when the rate of penetration suddenly increases.

fish - any part of the drillstring, or other tools, accidentally left in the hole

fishing - trying to retrieve a fish

float - essentially a check valve, used in the drillstring to keep liquid from flowing back up the drillpipe or casing

float collar - a coupling with built-in float; placed near the bottom of a casing string to prevent the heavy cement column in the annulus from flowing back into the casing. After displacing the cement in the casing with mud, the casing between the float collar and the shoe will be full of cement

float shoe - a casing shoe with built-in float; used like a float collar, except there won't be cement inside the casing

Geoset - a type of synthetic diamond cutter used in impregnated bits

H or HQ - designation of a coring tool size; rod outside diameter is 3.5", bit is approximately 3.9" OD and 2.5" ID

H₂S - hydrogen sulfide; a poisonous gas sometimes found in geothermal drilling

jars - tools which apply an impulse force to the bottom of the drillstring when the string is pulled up; usually used for fishing, but sometimes included in the string for normal drilling

kerf – width of the circumferential cut made by a core bit; e.g., a bit that drills a 4" diameter hole with a 3" core thus has a ½" kerf

lay down - to take a piece of equipment out of service; e.g., to lay down a worn core rod

LCM - lost circulation material; any material used for plugging formation fractures to avoid loss of drilling fluid

lubricator - sealing element attached to the wellhead which allows a wireline to pass up and down, or which allows a logging tool to be transferred into or out of the wellbore, while there is pressure in the wellbore

matrix - the hard metal portion of a bit which holds the diamond cutting elements in place

mill tooth bit - see tri-cone bit

mislatch - the condition when the core tube, or inner barrel, is not latched into the outer rotating barrel, sometimes caused by core dropped out of the core tube. If the core tube can't be worked down over the core in the barrel, then the drillstring must be tripped to clear it.

MRT - maximum reading thermometer; a mercury thermometer which retains the reading of the highest temperature it has seen (which may not be at the bottom of the hole)

N or NQ - coring tool size; rod OD is 2.75", bit is approximately 2.98" OD and 1.875" ID (N fits inside H)

nipple up (down) - to assemble (disassemble) something; usually the wellhead or BOP stack

OEDP - open ended drill pipe; drillpipe without a bit or other bottomhole assembly, generally used to place cement at a specific point in the wellbore.

overshot - in general, any tool that latches around the outside top of another tool; usually refers to the assembly which retrieves the core tube with the wireline, or to a fishing tool which extracts a fish by gripping it around the top

PTS - pressure-temperature-spinner tool; downhole instrumentation to measure these quantities (spinner output is an indication of velocity or flow rate)

pick up - to put any piece of equipment into use; e.g., to pick up a new bit

pitcher nipple - the vertical tube around the top of the blow-out preventer; it collects the drilling mud returns and empties them back into the mud tanks

POOH - pull out of hole; bringing the drill string and tools out of the hole

possum belly - manifold which connects the return line to the shale shaker

rams, pipe or blind - rams are part of the blow-out preventer; pipe rams seal around the drill pipe if it is in the hole, blind rams seal against each other if the pipe is not in the hole

rathole - either additional hole drilled below the target depth to give room for debris, fill, etc. or, on a rotary rig, where the kelly is stored while tripping pipe

RIH - run in hole; inserting the drillstring and tools into the hole

shoe - a heavy, tapered cap that attaches to the bottom of the casing string and protects it as the casing is lowered into the hole

spud - to begin drilling a well

squeeze - to deliberately apply pressure to the wellbore, usually by closing the BOP and pumping into the well. Often done to force cement into the formation at the casing shoe or into the annulus through perforations in the casing

stab(s) *n.* - stabilizer, or stabilizers; bottom-hole-assembly components which are almost hole diameter, used to keep the drill pipe relatively centered in the hole above the bit.

stab *v.* - to insert the pin-end of a drillstring component into the upward-looking box.

stand - more than one joint of drill pipe screwed together; when tripping, pipe is handled in stands to avoid making and breaking every connection - for a coring rig, a typical stand is four ten-foot joints (40 ft), but for a large rotary rig, a stand is three thirty-foot joints (90 ft).

strip - to wear away the matrix in an impregnated diamond bit; the bit must strip to expose the diamond cutting surfaces; also, to pull out of the hole under pressure, with the annular preventer closed around the drill pipe

swage, inside or outside - a fishing tool which grabs the inside or outside of a fish by forcing an interference fit

TOC - top of cement

top job - casing cement which is placed from the top, rather than being displaced through the casing shoe. It is either pumped directly into the top of the annulus, or pumped through a tremie line to get a deeper placement in the annulus.

tremie line - a small-diameter pipe or tube run down the annulus outside of casing

tri-cone bit - a bit having three toothed, conical rollers which rotate as the bit turns and crush the rock at the bottom of the hole. The teeth can be either steel, milled into the cones (mill tooth), or tungsten carbide buttons set into the steel cones (button bit, insert bit, TCI bit)

trip - any event of pulling the drillstring or core barrel out of the hole and returning it

wash - to run in the hole with circulation, usually required to get back to the bottom of a previously drilled hole when there is fill or cave in the hole

washout - a leak in the flow path through the drillstring, usually at a threaded connection in the drillpipe or drill collars. The hole is enlarged by high-pressure drilling fluid passing through it, and frequently causes the drillstring to fail and separate.

wet pull – pulling the drill string out of the hole with something plugging the bit or drill pipe that keeps it full of mud, rather than having it drain out as normally happens.

wiper trip - running the drill string, with a bit, to the bottom of the hole to make sure there are no obstructions in the hole

WOC - wait on cement, time spent waiting for cement to cure

WOO - wait on orders, time spent waiting for directions

xover or xo - crossover; a coupling used to adapt from one thread size to another